

Bai, Xueying (2025) *Investigating the role of gap junction protein and novel genes in renal function*. PhD thesis.

https://theses.gla.ac.uk/85525/

Copyright and moral rights for this work are retained by the author

A copy can be downloaded for personal non-commercial research or study, without prior permission or charge

This work cannot be reproduced or quoted extensively from without first obtaining permission from the author

The content must not be changed in any way or sold commercially in any format or medium without the formal permission of the author

When referring to this work, full bibliographic details including the author, title, awarding institution and date of the thesis must be given

Enlighten: Theses
https://theses.gla.ac.uk/
research-enlighten@glasgow.ac.uk

Investigating the Role of Gap Junction Protein and Novel Genes in Renal Function

Xueying Bai

Submitted in fulfilment of the requirements for the Degree of Doctor of Philosophy

School of Molecular Biosciences

College of Medical, Veterinary and Life Sciences

University of Glasgow

Glasgow G12 8QQ

UK

November 2024

Abstract

This thesis investigates the roles of genes with enriched expression in particular cells or regions of the *Drosophila* melanogaster Malpighian tubules in renal function and cellular homeostasis. Using reverse genetic, transcriptomic and metabolomic techniques, this study characterises the physiological role of Innexin 2, Innexin 7, the octopamine receptor $Oct\alpha 2R$ and the novel gene *CG6602*. These findings highlight the power of the Malpighian tubules as a model system for studying gene function in relation to osmoregulation, ion transport, and responses to stress.

Initial studies characterised the gap junction proteins Innexin 2 and Innexin 7 to the principal cells of the tubules but found no strong impact of fluid secretion after RNAi knockdown. By contrast, $Oct\alpha 2R$ analysis revealed a specific role in secretion: reductions of Octa 2R in stellate cells decreased the rate of secretion, and tubule secretion was found to be especially sensitive to octopamine compared with other biogenic amines.

Further studies focused on *CG6602*, which is tubule-specific and might contribute to stress response pathways. Collectively, the knockdown of *CG6602* resulted in altered expression of stress response genes, which implies possible involvement of *CG6602* in pathways related to the maintenance of homeostasis of the cell. Metabolomic profiling confirmed this view, detecting changes in metabolites including those associated with oxidative stress defence, suggesting that CG6602's regulatory role in managing metabolic and environmental stress in the tubule cells.

This study highlights the power of performing renal physiology studies in the fruit fly and begin to shed light on the molecular players responsible for maintaining tubule homeostasis. Due to the limitations of the analytical methods applied in this study, a more detailed exploration of the metabolomic data was not possible but the study provides a framework to connect state-of-the-art metabolomics with multi-omics approaches in future. It also adds to knowledge

about the roles of gap junction proteins and the unique gene *CG6602* in the renal system, and the genetic and metabolic networks involved in supporting renal function and stress responses.

Table of Contents

Abstract	i
Table of Contents	iii
List of Tables and Figures	ix
Acknowledgement	xii
Author's declaration	. xiii
Abbreviations	. xiv
Chapter 1 Introduction	1
1.1 Summary	1
1.2 Drosophila melanogaster	2
1.2.1 A History of <i>Drosophila</i> as a genetic model system	2
1.2.2 Genetics of <i>Drosophila</i>	4
1.2.2.1 Classical genetics	4
1.2.2.2 Modern genetics	7
1.2.3 Reasons to use <i>Drosophila</i>	13
1.2.3.1 Life cycle	13
1.2.3.2 Relative inexpensive	14
1.2.3.3 Simple genome	14
1.2.4 Resources	15
1.2.4.1 Fly Base	15
1.2.4.2 FlyAtlas and FlyAtlas 2	15
1.2.4.3 Fly Cell Atlas	17
1.2.4.4 Stock centre	18
1.3 <i>Drosophila</i> Malpighian tubules	19
1.3.1 History	19
1.3.2 Epithelial tissues	19
1.3.3 Morphology	20
1.3.3.1 The development of the Malpighian tubules during Embryogenesi	s 20
1.3.3.2 Larval and adult	21
1.3.3.3 Structure and Function	21
1.3.4 Principal cell and stellate cell	24
1.3.5 Ion transport and osmoregulation	24
1.4 Cell-cell junction	27
1.4.1 Physiological and Morphological Study	27
1.4.2 Gap Junction	29

1.4.3 Innexin Gene Family	31
1.4.3.1 ogre	32
1.4.3.2 Innexin 2	32
1.4.3.3 Innexin 3	33
1.4.3.4 Innexin 5	33
1.4.4.5 Innexin 6	33
1.4.3.6 Innexin 7	34
1.4.3.7 shakB	34
1.5 Bioamines and their receptor	34
1.5.1 Overview of Bioamines	34
1.5.2 Key Biogenic Amines in <i>Drosophila</i>	35
1.5.2.1 Octopamine	35
1.5.2.2 Dopamine	36
1.5.2.3 Tyramine	36
1.5.2.4 Serotonin	37
1.5.2.5 Tryptamine	38
1.5.3 Biogenic Amine Receptors in <i>Drosophila</i>	38
1.5.3.1 Overview of Biogenic Amine Receptors	38
1.5.3.2 Octopamine Receptor	38
1.5.3.3 Dopamine receptors	39
1.5.3.4 Tyramine Receptors	39
1.5.3.5 Serotonin Receptors	39
Chapter 2 Materials and Methods	42
2.1 Drosophila melanogaster Stock & Maintenance	42
2.1.1 Fruit Fly Stocks	42
2.1.2 Fruit Fly Maintenance	43
2.1.3 Drosophila Crossing and Rearing Crosses	43
2.1.4 Drosophila Diet	44
2.2 Fluid Secretion Assay	45
2.2.1 Fruit Fly Tissue Dissection and Preparation for Fluid Secretion Assay	45
2.2.2 Data Analysis for Fluid Secretion Assay	47
2.3 Wet and Dry Weight Measurements	47
2.4 RNA Extraction	48
2.4.1 Whole-Fly RNA Extraction	48
2.4.2 Malpighian Tubules RNA Extraction	48
2.5 Complementary DNA synthesis (cDNA)	49

2.6 Primer Design
2.7 The Polymerase Chain Reaction (PCR)
2.8 Agarose Gel Electrophoresis
2.9 SYBR Green-based Quantitative Real-time PCR(qPCR)
2.10 Transcriptomics
2.10.1 Sample Preparation and Dissection
2.10.1.1 Malpighian tubules
2.10.1.2 Whole-fly RNA Preparation
2.10.2 RNA sequencing (RNA-seq)
2.11 Metabolomics
2.11.1 Sample Preparation
2.11.2 Liquid Chromatography-Mass Spectrometry
2.11.3 LC-MS Data Processing and Analysis
Chapter 3 Functional Roles of the Gap Junction Genes Innexin 2 and Innexin 7 in <i>Drosophila</i> Malpighian Tubules
3.1 Summary 58
3.2 Identification of Innexin Gene Specifically and Highly Expressed in Malpighian Tubules
3.2.1 Introduction
3.2.2 Innexin 2 Expressed in Proventriculus
3.2.3 Gap Junctions Play a Key Role in The Circadian Circuit
3.2.4 Innexin 7 and Innexin 2 Role in The Nervous System
3.2.5 Innexin Protein Play an Important Role During Early Oogenesis 69
3.2.6 The Role of Innexins in The Development of Eye Imaginal Disc 71
3.3 Results
3.3.1 Innexin Gene Family73
3.3.2 Inx2 is Mainly Expressed in The Principal Cells of The Tubules 82
3.3.3 Inx2 Does Not Affect Fluid Secretion of The Tubules
3.3.4 <i>Inx7</i> is Mainly Expressed in The Principal Cells of The Tubule 92
3.3.5 Inx7 Does Not Affect Fluid Secretion of The Tubules
3.3.6 Protein Interactions and Structure96
3.3.6.1 Innexin 2 Protein Structure and Interaction Network96
3.3.6.2 Innexin 7 Protein Structure and Interaction Network
3.4 Discussion
3.5 Conclusion

Chapter 4 Drosophila α 2-adrenergic-like octopamine receptor	106
4.1 Summary	106
4.2 Identification of Octa2R genes expressed in Malpighian tubules and o	
4.2.4 June di cation	
4.2.1 Introduction	
4.2.2 Role in Biogenic Amines	
4.2.3 Expression Patterns and Functional Role	
4.2.4 Characterisation of Octα2R Isoforms	
4.2.5 Possible Role in Malpighian Tubules	
4.2.6 Human Orthologs	
4.2.7 Comparative Analysis with Other Insect Models	
4.3 Results	
4.3.1 Octopamine Receptor family	
4.3.2 Octa2R is expressed in the stellate cells of the tubule	
4.3.3 <i>Octa2R</i> affects fluid secretion of the tubules	
4.3.3.1 <i>Octa2R</i> ⁵⁰⁶⁷⁸ lines	
4.3.3.2 Biogenic Amines	
4.4 Discussion	
Chapter 5 Characterisation of the <i>Drosophila</i> Novel Gene CG6602	
5.1 Summary	
5.2 Introduction	
5.3 Result	
5.3.1 <i>CG6602</i> is mainly expressed in the stellate cells of the tubule	
5.3.2 Knockdown of <i>CG6602</i> i ¹⁸⁹⁰⁰ does affect the fluid secretion of the	
5.3.3 <i>CG6602i</i> ¹⁰⁶¹⁵² (KK 106152) does not affect the fluid secretion of t	
tubules	
5.4 Discussion	159
Chapter 6 Transcriptomics of CG6602	164
6.1 Summary	164
6.2 Introduction	165
6.3 Results	168
6.3.1 Up-regulated gene in the CG6602	168
6.3.2 Down-regulated gene in tubules	176
6.4 Discussion	180
Chapter 7 Metabolomics Analysis in CG6602	187
7.1 summary	187

7.2 Introduction	188
7.3 Results	190
7.3.1 Glutathione metabolism	192
7.3.2 Amino acid metabolism	195
7.3.3 Purine metabolism	198
7.4 Discussion	201
Chapter 8 Conclusion and Future Work	206
8.1 Summary	206
8.2 Introduction	207
8.3 Results	208
8.3.1 Gap junction	208
8.3.2 Drosophila α 2-adrenergic-like octopamine receptor	209
8.3.3 Characterisation of the <i>Drosophila</i> Novel Gene <i>CG6602</i>	210
8.3.4 Transcriptomic Analysis of CG6602	211
8.3.5 Metabolomics analysis in CG6602	212
8.4 Future Work	213
8.4.1 Gap junction	213
8.4.2 Drosophila α 2-adrenergic-like octopamine receptor	214
8.4.3 Characterisation of the <i>Drosophila</i> Novel Gene <i>CG6602</i>	214
8.4.4 Transcriptomic Analysis of CG6602	215
8.4.5 Metabolomics analysis in CG6602	215
8.5 General Discussion	216
8.6 Final conclusion	217
Appendices	218
Appendix 1: The composition of Schneider's medium	218
Appendix 2: Calculation formula of fluid secretion rate	219
Appendix 3 List of additional primers Octα2R	220
Appendix 4 5X TBE buffer recipe	221
Appendix 5 10X PBS Buffer	222
Appendix 6 Fluid secretion assay using the UAS-Octα2R RNAi (#10214)	line223
Appendix 7 Fluid secretion assay using the UAS-Octα2R RNAi (#10215)	line224
Appendix 8 Wet and Dry Weight of CG6602 line	225
Appendix 9: KEGG map of <i>Drosophila melanogaster</i> and biochemical of identified metabolites in Glycerophospholipid metabolism	
Appendix 10: KEGG map of <i>Drosophila melanogaster</i> and biochemical of identified metabolites in Cysteine and methionine metabolism	

	Appendix 11: KEGG map of Drosophila melanogaster and biochemical re	actions
	of identified Cysteine and Pyrimidine metabolism metabolites	229
	Appendix 12: KEGG map of Drosophila melanogaster and biochemical re	eactions
	of identified in Starch and sucrose metabolism	230
L	List of references:	231

List of Tables and Figures

Figure 1.1 Balancer chromosomes	5
Figure 1.2 Principle of enhancer trapping using P-elements in Drosophila	8
Figure 1.3 The GAL4/UAS system	. 10
Figure 1.4 Schematic representation of transgenic RNAi in Drosophila	. 11
Figure 1.5 CRISPR/Cas9-based gene targeting and genome editing in Drosophila	12
Figure 1.6 The life cycle of <i>Drosophila</i> melanogaster	. 13
Figure 1.7 Tissue-specific expression profile of the tsh gene in Drosophila	. 16
Figure 1.8 Data visualisation using Scope	. 17
Figure 1.9 The Malpighian tubules were first described in 1669	. 19
Figure 1.10 D. melanogaster Malpighian tubules	23
Figure 1.11 Views of principal cell and stellate cell in Malpighian	24
Figure 1.12 Schematic diagram summarising ion transport by the Malpighian tubules	. 26
Figure 1.13 Intercellular junctions in vertebrates and insects (Drosophila)	28
Figure 1.14 General structure of channels formed by connexin innexins and pannexins	30
Table 1.15 <i>Drosophila</i> melanogaster innexin families	. 31
Table 2.1 Fly lines were used during this study	. 42
Table 2.2 Recipe of standard <i>Drosophila</i> medium	. 44
Figure 2.3 The dissection and preparation of the tubules for fluid secretion assays	46
Table 2.4 Primers used for quantitative PCR	. 50
Table 2.5 PCR cycling conditions using Taq DNA polymerase	. 51
Table 2.6 SYBR Green master mix qPCR cycling parameters	. 52
Figure 3.1 Localisation of Innexin 2 and junctional proteins in wild-type and Inx2-defic	
Figure 3.2 Schematic illustration of glial structure in Drosophila	67
Figure 3.3 Tissue expression profile of ogre in <i>Drosophila</i>	74
Figure 3.4 Tissue expression profile of Innexin 2 in Drosophila	75
Figure 3.5 Tissue expression profile of Innexin 3 in Drosophila	76
Figure 3.6 Tissue expression profile of Innexin 5 in Drosophila	77
Figure 3.7 Tissue expression profile of Innexin 6 in Drosophila	. 78
Figure 3.8 Tissue expression profile of Innexin 7 in Drosophila	79
Figure 3.9 Tissue expression profile of shaking B in Drosophila	. 80
Figure 3.10 Innexin family gene expression in Malpighian tubules	81
Figure 3.11 RNAi knockdown of UAS-Inx2 ⁴²⁶⁴⁵ in MTs	. 83
Figure 3.12 The RNAi-mediated knockdown of Inx2 using the other UAS-Inx2 line	84
Figure 3.13 Results of the knockdown of Inx2 in the tubules	. 85

Figure 3.14 Fly Cell Atlas: A single-nucleus transcriptomic atlas of the adult fruit fly tubule
Figure 3.15 Scope representation of the <i>Inx2</i> and CapaR single-cell data for the adult tubules from the Fly Cell Atlas
Figure 3.16 Secretion assay for CapaR-Gal4>UAS-Inx2 compared with parental line90
Figure 3.17 The percentage increase in fluid secretion after stimulation by kinin in Inx2 knockdown flies91
Figure 3.18 RNAi knockdown of Inx7 ²²⁹⁴⁸ in MTs at different temperatures92
Figure 3.19 Scope represents the <i>Inx7</i> and CapaR single-cell data for the Fly Cell Atlas adult tubules93
Figure 3.20 Secretion assay for CapaR-Gal4>UAS-Inx7 compared with parental line94
Figure 3.21 The percentage increase in fluid secretion after stimulation by kinin in the Inxi knockdown flies95
Figure 3.22 The predicted protein structure for Inx2
Figure 3.23 Summary of Inx2 protein interaction97
Figure 3.24 The predicted protein structure for Inx7 98
Figure 3.25 Summary of Inx7 protein interaction network99
Figure 4.1 Alternative splicing of the Octa2R gene generates two transcript variants108
Figure 4.2 Structural difference between Octa2R isoforms111
Figure 4.3 Octopamine receptor subtypes in Apis mellifera115
Figure 4.4 Tissue expression of the Oamb receptor in <i>Drosophila</i> melanogaster117
Figure 4.5 Tissue expression of the Octα2R receptor in <i>Drosophila</i> melanogaster118
Figure 4.6 Tissue expression of the OctB1R receptor in Drosophila melanogaster119
Figure 4.7 Tissue expression of the OctB2R receptor in Drosophila melanogaster120
Figure 4.8 Tissue expression of the OctB3R receptor in Drosophila melanogaster121
Figure 4.9 Tissue expression of the Oct-TyrR receptor in <i>Drosophila</i> melanogaster122
Figure 4.10 Expression and enrichment of octopamine receptor family members in <i>Drosophila</i> melanogaster Malpighian tubules123
Figure 4.11 Expression of Octa2R in Malpighian tubules of Drosophila melanogaster124
Figure 4.12 Validation of <i>Octa2R</i> knockdown using two independent RNAi lines in Malpighian tubules126
Figure 4.13 Knockdown of <i>Octa2R</i> in Malpighian tubules using the UAS-Octα2R RNAi (#50678) line
Figure 4.14 Percentage reduction of <i>Octa2R</i> expression in Malpighian tubules following knockdown with the UAS-Octα2R RNAi (#50678) line128
Figure 4.15 Fluid secretion assay for tsh-GAL4>UAS-Octα2R ⁵⁰⁶⁷⁸ compared with parental line131
Figure 4.16 Effect of different dopamine concentrations on the fluid secretion rate of Canton S (CS) tubules
Figure 4.17 The effect of various octopamine concentrations on the rate of fluid secretion of Canton S tubules

Figure 4.18 Effect of different concentrations of tryptamine on the fluid secretion rate of Canton S tubules
Figure 4.19 The effect of various concentrations of tyramine on the rate of fluid secretion of Canton S tubules
Figure 4.20 Fluid secretion responses of Canton S tubules to biogenic amines139
Figure 4.21 Effect of tyramine on the fluid secretion rate of Octa2R knockdown tubules140
Figure 4.22 Secretion assay for tsh-Gal4>UAS-Oct α 2R ⁵⁰⁶⁷⁸ compared with the parental RNAi line141
Figure 5.1 Tissue expression of CG6602 in Drosophila150
Figure 5.2 Single-cell expression profile of CG6602 in adult Malpighian tubules151
Figure 5.3 Validation of knockdown of CG6602 GD and CG6602 KK expression in MTs153
Figure 5.4 Secretion assay for tsh-Gal4>UAS-CG6602i compared with parental line <i>CG6602i</i> ¹⁸⁹⁰⁰ (GD 18900)
Figure 5.5 Secretion assay for tsh-Gal4>UAS-CG6602i compared with parental line CG6602i ¹⁰⁶¹⁵² (KK 106152)158
Figure 6.1 Significantly up-regulated genes in the CG6602
Figure 6.2 These are the up-regulated genes in the CG6602
Figure 6.3 Expression and interaction information of <i>Ugt35C1</i>
Figure 6.4 Expression and interaction information of Cyp6a8
Figure 6.5 Expression and interaction information of Slc45-1
Figure 6.6 Expression and interaction information of MFS12
Figure 6.7 Down-regulated genes in <i>Drosophila</i> tubules following <i>CG6602</i> knockdown177
Figure 6.8 Highly expressed tubule genes with reduced expression after <i>CG6602</i> knockdown
Figure 6.9 Expression and interaction information of Mat
Figure 7.1 Drosophila tubules metabolomics analysis of CG6602
Figure 7.2 Changes in glutathione metabolism in <i>Drosophila</i> tubules caused by the knockdown of <i>CG6602</i>
Figure 7.3 Biochemical pathway of glutathione metabolism in <i>Drosophila</i> following knockdown of <i>CG6602</i> 194
Figure 7.4 Changes in D-amino acid metabolism in the tubules caused by the knockdown of CG6602
Figure 7.5 Biochemical reactions of identified metabolites in D-amino acid metabolism following knockdown of CG6602197
Figure 7.6 Changes in purine metabolism in the tubules caused by the knockdown of CG6602
Figure 7.7 Biochemical reactions of identified metabolites in purine metabolism
Table 7.8 Table of known genes for each enzyme

Acknowledgement

I would like to express my deepest gratitude to my supervisors, Professor Julian Dow and Professor Shireen Davies, for their support and guidance throughout my PhD journey. Julian provided me with the opportunity to pursue a PhD, and as his student, I not only gained invaluable knowledge and learnt how to conduct high-quality research but also developed the courage to face any challenges with confidence, believing in my ability to succeed.

I would also like to thank all members of the Dow/Davies group for their help and support over the past four years. A big thank you goes to Dr Sue Krause, who, at the start of my PhD, helped me integrate quickly and provided me with a thorough introduction to various aspects of *Drosophila* research. During the COVID-19 pandemic, she went above and beyond to compensate for the lack of university seminars by preparing one-on-one article discussions. She provided me with technical support throughout my experiments and offered invaluable writing suggestions during my final year. I am also deeply grateful to Dr Anthony Dornan for his guidance and advice at various stages of my PhD. Many thanks to Dr Andrew Gillen and Dr Karen McCluskey for their assistance with data analysis, as well as to Dr Liyuan Zhuang, Dr Mehwish Akram, Miss Shannon Keenan, and Mr Keqin Li for their support in both my studies and personal life.

A big thank you to my family, including my wonderful parents (Mr Qian Xiao and Ms Xiuping Guo); I will always be grateful for their support during these years. I am also especially grateful to my husband, Mr Junhan Kim, who has provided financial support throughout these four years, for the incredible patience he has shown. He never bothered me with anything during my PhD studies and took on all the household responsibilities. Last but certainly not least, I would also like to thank my daughter Miss Hannah Kim, who supported my work and studies during the weekdays. Their love, encouragement, and tremendous support have been instrumental in helping me complete my PhD.

Author's declaration

The research reported within this thesis is my own work except where otherwise stated and has not been submitted for any other degree. All sources of information used in the preparation of this thesis are indicated by reference.

Abbreviations

°C Degree Celsius

μg Microgram

μl Microliter

μM Micromolar

5-HT 5-hydroxytryptamine

5-HTP 5-hydroxytryptophan

AADC L-amino acid decarboxylase

AMP Adenosine monophosphate

ANOVA Analysis of Variance

APL Anterior paired lateral

ARM Anesthesia-resistant memory

ASM Anesthesia-sensitive memory

BDSC Bloomington *Drosophila* Stock Centre

BLAST Basic local alignment search tool

CapaR Capa receptor

cDNA Complementary DNA

cAMP cyclic adenosine monophosphate

cGMP cyclic guanosine monophosphate

cm Centi-meter

CNS Central nervous system

CS Canton S

Ct threshold cycle

DPM Dorsal paired medial

DMSO Dimethyl sulfoxide

DNA Deoxyribonucleic acid

DN Dorsal neurons

dNTP Deoxyribonucleotide triphosphate

Dpp Decapentaplegic

DTT dithiothreitol

EB Ellipsoid body

EMS ethyl methanesulfonate

EtBr ethidium bromide

FCA Fly Cell Atlas

FPKM Fragments Per Kilobase of transcript per

Million mapped reads

g Gram

GCF Graticule conversion factor

GC-MS Gas chromatography-mass spectrometry

GFP Green fluorescent protein

GFS Giant fiber system

GPCRs G-protein coupled receptors

GSK3B Glycogen synthase kinase 3 beta

InR Insulin receptor

kb Kilobases

LC Liquid Chromatography

LC-MS Liquid chromatography-mass spectrometry

LN Lateral neurons

LNvs The ventral lateral neurons

M Molar

MB Mushroom body

mL Millilitre

mm Millimetre

mRNA Messenger RNA

mM Millimolar

NMR Nuclear magnetic resonanc

MTs Malpighian tubules

MS Mass Spectrometry

m/z mass-to-charge ratio

ng Nanogram

PBS Phosphate-buffered saline

PCR Polymerase chain reaction

PI Pars intercerebralis

PNS Peripheral nervous system

QC Quality control

qRT-PCR Quantitative reverse transcriptase PCR

RNA Ribonucleic acid

RNAi RNA interference

RNA-seq RNA sequencing

ROS neutralizing reactive oxygen species

RT Room temperature

T1-T0 Interval in minutes

Tm Melting temperature

TIM Timeless

TPH Tryptophan hydroxylase

UAS Upstream activating sequence

UV Ultraviolet

 $V\text{-}ATPase \qquad \quad Vacuolar\text{-}type \ H^{\scriptscriptstyle +} \ \text{-}ATPase$

VDRC Vienna *Drosophila* Resource Centre

WT Wild type

Chapter 1 Introduction

1.1 Summary

The introduction chapter outlines the historical and scientific significance of Drosophila melanogaster as a model organism, emphasising its contributions to genetics, developmental biology, and other fields. Beginning with Charles Woodworth's initial breeding of *Drosophila* in the early 20th century, the chapter traces key discoveries, such as gene linkage and the use of Drosophila in Nobel Prize-winning research, particularly those by Thomas Morgan and his students. These discoveries linked specific genes to chromosomes and laid the foundation for modern genetics. The advantages of using Drosophila, including its short life cycle, cost-effectiveness, and well-characterized genome, are thoroughly explained. The chapter also details the structure and function of the Malpighian tubules, analogous to mammalian kidneys, highlighting the roles of principal and stellate cells in ion transport and osmoregulation. Detailed descriptions of principal and stellate cells within the tubules illustrate their distinct roles in ion transport. The discussion extends to cell-cell junctions, particularly gap junctions formed by innexin proteins, indicating their importance in intercellular communication. Finally, the role of biogenic amines and their receptors in regulating *Drosophila*'s physiological processes and behaviours is also explored, providing a foundation for investigating the role of gap junction proteins and novel genes in renal function.

1.2 Drosophila melanogaster

1.2.1 A History of *Drosophila* as a genetic model system

The use of *Drosophila melanogaster* as a laboratory model began more than a century ago. Charles Woodworth, an entomologist at Harvard, was the first to breed *Drosophila* for experimental purposes (Villegas, 2019; Markow, 2015). Although the reasons behind his choice remain uncertain, the short life cycle and high reproductive capacity of *Drosophila* made it attractive to early researchers. Woodworth recommended fruit flies as a system for genetics, and his suggestion was soon taken up by Thomas Hunt Morgan. Morgan identified a white-eyed fly and named the mutant gene white (Morgan, 1910). He later demonstrated that this gene was located on the X chromosome (Villegas, 2019), providing the first evidence of a gene being linked to a specific chromosome (Green, 2010). His work on sex-linked inheritance earned him the Nobel Prize in 1933 and firmly established *Drosophila* as a model for chromosome theory. Unlike Woodworth, whose interest was primarily in rearing, Morgan used the species to investigate inheritance. At a time when the principles of heredity were still unclear, Morgan's studies showed the connection between genes and chromosomes, laying the foundation for modern genetics. His students continued to expand this work, and among them Hermann Joseph Muller demonstrated that X-ray exposure could induce mutations, for which he was awarded the Nobel Prize in 1946 (Stephenson and Metcalfe, 2013).

Later decades brought further landmark discoveries. Edward Lewis, Christiane Nüsslein-Volhard, and Eric Wieschaus identified key developmental genes in *Drosophila*, earning the Nobel Prize in 1995 (Honselmann *et al.*, 2015). Lewis described homeotic genes belonging to the conserved Hox family, which have clear homologues in humans and control body patterning (Lewis, 1978; McGinnis and Krumlauf, 1992; Carroll, 1995). In contrast, many of the segmentation and patterning genes described by Nüsslein-Volhard and Wieschaus are essential for *Drosophila* development but lack direct human counterparts (Nüsslein-Volhard and Wieschaus, 1980; Carroll, 1995; Peel *et al.*, 2005). The use of *Drosophila* was also central to Jules Hoffmann's work on innate immunity, where he showed that the Toll pathway plays a key role in antimicrobial defence, findings that

revealed conserved immune mechanisms and led to the Nobel Prize in 2011 (Lemaitre *et al.*, 1996; Hoffmann, 2003; Lemaitre and Hoffmann, 2007). In 2017, Jeffrey C. Hall, Michael Rosbash, and Michael W. Young were awarded the Nobel Prize for their studies on circadian rhythms. Using *Drosophila*, they identified clock genes such as *period* and *timeless*, and demonstrated how negative feedback loops generate self-sustained circadian oscillations (Hardin *et al.*, 1990; Sehgal *et al.*, 1994; Huang *et al.*, 2018).

Over the past decades, *Drosophila* has become one of the most widely studied organisms, contributing insights across developmental and cell biology, neuroscience (Naddaf, 2023), immunity (Buchon *et al.*, 2014; Davies and Dow, 2009), sex determination (Slee and Bownes, 1990), circadian biology (Parasram *et al.*, 2024), renal physiology (Dow *et al.*, 1994), and neurodegenerative disease research (Marsh and Thompson, 2006). Its continued importance rests on the availability of advanced genetic tools, which enable precise manipulation of gene function and the analysis of pathways underlying diverse biological processes. The ease of generating and studying mutants has ensured that *Drosophila* remains a powerful system for defining the genetic basis of physiology and development.

1.2.2 Genetics of Drosophila

1.2.2.1 Classical genetics

The classical genetics of *Drosophila* include inheritance patterns, gene linkage, recombination, mutation effects, phenotypes, and genetic mapping. Drosophila melanogaster has long been used as an essential model organism for genetics studies (Pandey and Nichols 2011). Morgan's research on chromosome theory confirmed the inheritance of a specific trait with a particular chromosome (Morgan, 1912), leading to the discovery of sex-linked inheritance in fruit flies. Gene linkage revealed that certain traits do not assort independently as predicted by Mendel's laws but are instead linked, with genes located close to each other on the same chromosome tending to be inherited together. Building on Morgan's insights, Alfred Sturtevant developed a genetic linkage map (Gannett and Griesemer, 2004), culminating in the complete sequencing of the Drosophila melanogaster genome in 2000, which contains approximately 14,000 genes spread across four chromosomes (Adams et al., 2000; Kaufman, 2017). The three autosomes are II, III, and IV. Regarding sex chromosomes, males possess one X and one Y chromosome, whereas females have two X chromosomes. The X chromosome is referred to the first chromosome. This chromosomal composition forms the basis of these flies' genetic diversity and inheritance patterns (Kaufman, 2017).

Drosophila melanogaster is notable for its low genetic redundancy (Láruson et al., 2020). Unlike the human genome, which contains multiple gene copies to regulate proteins, the fly genome often shows single copies rather than being part of gene families (Bergman et al., 2017). Low genetic redundancy means a mutation in one gene is more likely to produce a noticeable phenotype, contributing to identifying a direct correlation of phenotypes with specific genetic mutations, meaning mutational analysis to determine gene function. Consequently, the characteristics of Drosophila improve its effectiveness in genetic and genomic research, helping the identification of specific gene and gene family functions using this model organism. In addition to these advantages, researchers have also discovered new genes using mutagenic agents such as chemical mutagenesis and X-ray radiation, altering DNA structure (Bhatia

et al., 2023). As described above (1.2.1), Muller was awarded the Nobel Prize for discovering that X-rays could induce mutagenesis and genetic alterations. By exposing fruit flies to X-rays, he observed a variety of mutations, including lethal mutations that inhibited progeny survival (Komel, 2023), highlighting the roles of essential genes in survival and normal development (Gleason, 2017).

Balancer chromosomes

Balancer chromosomes are essential tools in *Drosophila* genetics for maintaining deleterious mutations in stable stocks (Rubin and Lewis, 2000). They are highly rearranged chromosomes that contain multiple inversions, which suppress recombination during meiosis by preventing proper alignment with their homologous chromosomes. This eliminates crossovers and preserves linked mutations across generations (Miller *et al.*, 2016; Figure 1.1).

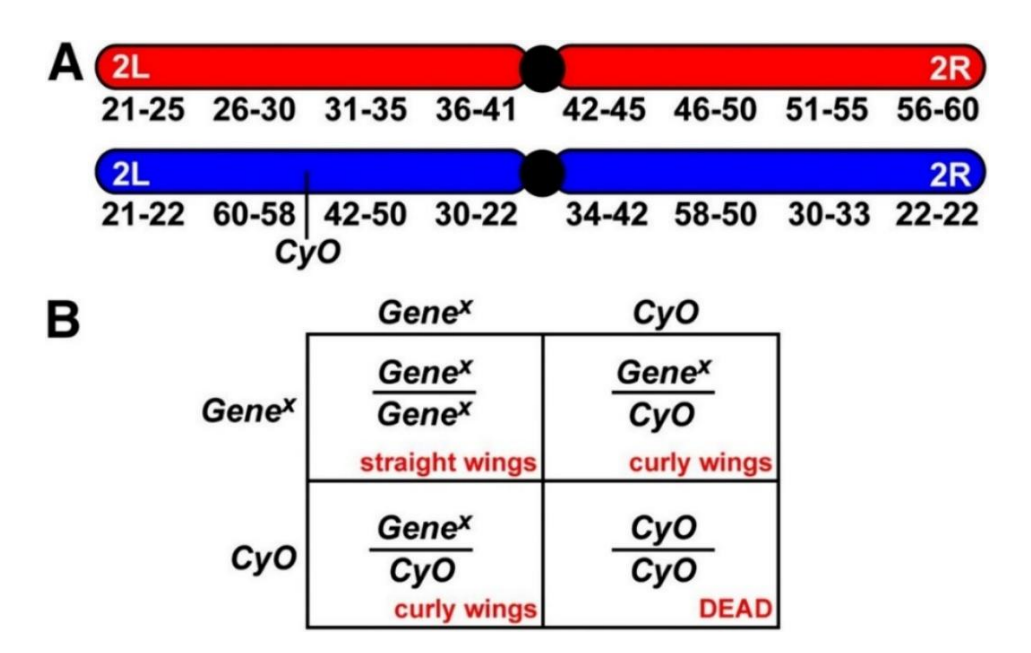


Figure 1.1 Balancer chromosomes. (A) A wild-type chromosome (red) vs a balancer chromosome (blue). Numbers are below wild-type chromosomes to represent ordinal regions of the chromosome. The second chromosome carries a dominant mutation (CyO). (B) Diagram showing the expected progeny from a cross between flies carrying a mutation of interest and the CyO balancer. Offspring include wild-type homozygotes (straight wings), heterozygotes carrying both the mutation and the balancer (curly wings), and homozygous CyO individuals, which are inviable due to the recessive lethal mutation (Ables, 2015).

In addition to inversions, balancer chromosomes typically carry dominant phenotypic marker alleles, such as Curly (CyO) or Stubble (Sb), which produce easily recognisable traits and allow researchers to identify individuals carrying the balancer (Pina and Pignoni, 2012). To ensure genetic stability, balancers also harbour a recessive lethal mutation, meaning that individuals homozygous for the balancer do not survive (Dow and Davies, 2003). This combination of recombination suppression, visible dominant markers, and recessive lethality makes balancer chromosomes a powerful system for preserving deleterious alleles in heterozygous condition and for facilitating controlled genetic crosses.

Mutant screens

Drosophila is a genetic model organism that allows for the efficient and low-cost identification of genes involved in biological processes through large-scale genetic screens (Wolf and Rockman, 2008). Flies of the relevant genotype are exposed to mutagenic agents, such as X-rays or chemical treatments like ethyl methanesulfonate (EMS), which induce random mutations in the genome (Gillmor and Lukowitz, 2020; Kaufman, 2017). Progenies are then screened for alterations in phenotype, which might include developmental abnormalities or unusual behaviours, such as being active at night instead of during the day. Once an interesting phenotype is identified, genetic approaches such as mapping crosses, complementation tests, and molecular characterisation can be applied to determine the gene responsible. Drosophila has been widely used in this way to identify genes associated with development, behaviour, and physiology (Banerjee et al., 2020). While I did not use mutagenesis screens to define gene function in my thesis, they have historically been the basis for identifying many genes and remain an important methodology in genetics.

1.2.2.2 Modern genetics

Transposable elements

Transposable elements, also known as transposons, are semi-autonomous DNA sequences capable of moving within a genome (Pray, 2008). In the late 1940s, Barbara McClintock found in maize that genes could change positions on chromosomes, causing mutations and altering the genome's structure (Ravindran, 2012). Her discovery that specific DNA sequences could move within the genome challenged the original concepts of genes, and in 1983, she was awarded the Nobel Prize in Physiology or Medicine (Ravindran, 2012). McClintock's research on mobile genetic elements in maize provided the foundation for understanding transposon, contributing to the subsequent development of P-elements. In humans, transposable elements contribute to genomic variation and can influence gene expression and regulation (Gebrie, 2023). In *Drosophila*, by carrying marker genes, researchers can track the insertion of these elements and study the resulting mutations (Wang *et al.*, 2023).

Naturally occurring P-elements are about 2.9 kb in size and can relocate their short DNA sequences within the genome, disrupting their sequences. They can induce gene mutations through insertional inactivation and alter gene expression by modifying transcript levels (Muñoz and García-Pérez, 2010; Ryder and Russell, 2003).

Among various P-elements, enhancer traps are extensively characterised and help identify genes with specific expression patterns during developmental stages (Wilson *et al.*, 1989). It allows the visualisation of when and where specific genes are active. This method uses modified P-elements, replacing the transposase gene with a reporter gene, such as *GAL4* and integrating a reporter gene, which produces a detectable product, like a fluorescent protein or an enzyme, into the genome at random locations. This allows researchers to identify and characterise enhancers, promoters, and other regulatory sequences that control gene expression. This principle is illustrated in Figure 1.2, which

shows how a P-element carrying a reporter gene can capture enhancer activity and reveal gene-specific expression domains (Choi, 2024).

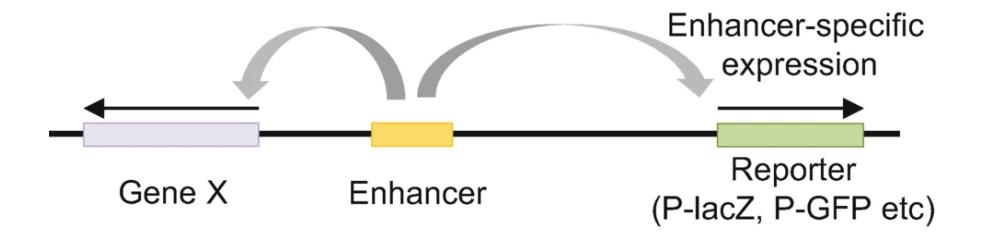


Figure 1.2 Principle of enhancer trapping using P-elements in *Drosophila*. A P-element carrying a minimal promoter and a reporter gene (e.g., lacZ or GFP) is inserted near a genomic enhancer. If the enhancer is active, it drives reporter expression, thereby recapitulating the spatial and temporal expression pattern of the neighbouring endogenous gene (Choi, 2024).

Polytene chromosomes

Polytene chromosomes play an important role in classical genetics research in Drosophila melanogaster. Their large size and distinct banding patterns allow for the creation of cytogenetic maps from the salivary gland chromosomes of fruit fly larvae, contributing to the visual localisation of genes within specific chromosomal regions (Semeshin et al., 2004; Schaeffer et al., 2008). The characteristic banding patterns of polytene chromosomes arise from repeated rounds of DNA replication without subsequent cell division. This process results in expanded chromosomes, which are easily visualised under a microscope (Edgar and Orr-Weaver, 2001). Early observations of polytene chromosomes also uncovered a feature: chromosome puffs. Chromosome puffs in *Drosophila* were first discovered in 1962 by Ritossa (Bonner and Pardue, 1977; De Maio et al., 2012). Researchers exposed flies to heat shock and observed predictable puffing at specific chromosomal regions. It was seen that the DNA changed shape after a heat shock (Bonner and Pardue, 1976). Before these studies, the functional link between chromosomal structure and gene activity was poorly understood. Puffing provided the first cytological evidence that changes in chromosome morphology reflect transcriptional activation of specific genes. Thus, polytene chromosomes serve two purposes: firstly, as cytological markers to visualise transcriptional activity in response to stimuli, and secondly, as genetic markers providing insights into gene flow, regulation, and other genetic parameters (O'Grady et al., 2001).

GAL4/UAS system

The GAL4/UAS system is a second-generation enhancer trapping technique in *Drosophila* melanogaster (Brand and Perrimon, 1993; Caygill and Brand, 2016). This system enables researchers to study gene functions in a tissue-specific manner by directing the expression of target genes in particular tissues. Derived from budding yeast, the transcriptional factor Gal4 binds to an upstream activation sequence (UAS) to activate the transcription of downstream DNA sequences (Traven *et al.*, 2006). This system involves two independent transgenic fly strains: one has the UAS upstream of a transgene of interest (for example GFP, RNAi constructs, or other effectors), while another strain carries the GAL4 gene with a tissue-specific promoter (Elliott and Brand, 2008). When these strains are crossed, the GAL4/UAS system is activated, driving the expression of the UAS-linked transgene.

As described above, the GAL4 and UAS components play distinct roles within the system. Figures 1.3 and 1.4 illustrate different aspects of this system in *Drosophila*. Figure 1.3 provides an overview and demonstrates different applications, including UAS-GFP, UAS-RNAi, and UAS-reaper constructs. UAS-GFP is used to express Green Fluorescent Protein in specific tissues, serving as a fluorescent marker to track gene expression. UAS-RNAi initiates RNA interference for gene knockdown, reducing the expression of specific genes. UAS-reaper induces cell death in specific tissues to analyse gene function. When fruit flies carrying the UAS-reaper construct are crossed with flies expressing GAL4 in specific tissues and under specific conditions, the progeny will express the *reaper* gene in this tissue, leading to targeted cell death. The figure displays the versatility of the GAL4/UAS system in manipulating gene expression for different purposes.

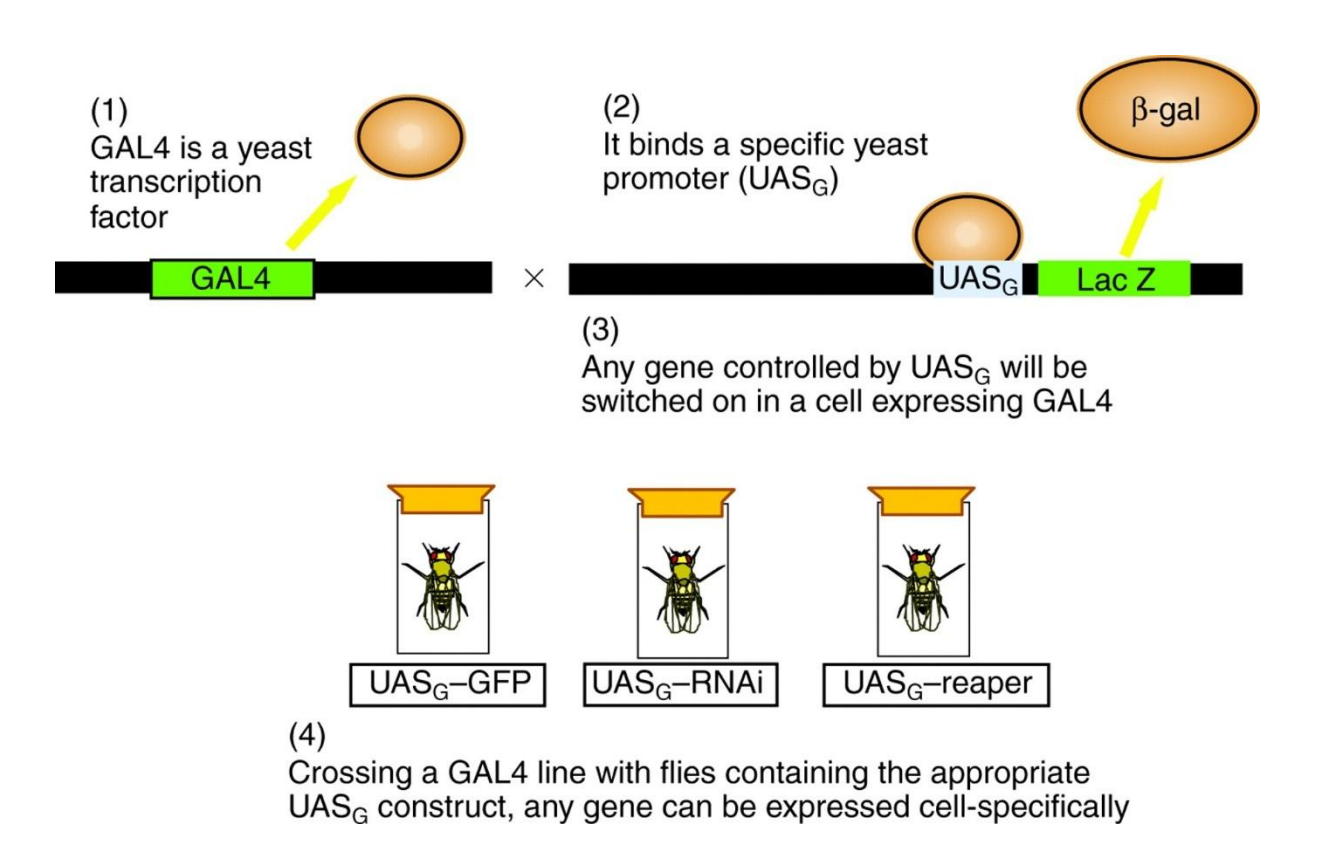


Figure 1.3 The GAL4/UAS system. The transcription factor Gal4 is placed under the control of a tissue-specific enhancer or promoter. It binds to a specific promoter (UASG-GFP). The F1 progeny carrying the UAS construct will express the downstream gene only in cells or tissues where GAL4 is present, which results in the expression of the UAS-linked reporter such as GFP (Dow, 2007).

Transgenic flies carrying RNAi transgenes combined with the GAL4-UAS system allow for gene knockdown. Figure 1.4 illustrates the application of RNAi in *Drosophila*, detailing the gene knockdown mechanism and RNAi pathway activation. The diagram shows how RNAi constructs are expressed and how the RNAi pathway is activated, emphasising the steps involved in this process. This integration of RNAi with the GAL4-UAS system provides a method for gene knockdown. This system and other advanced genetic tools will help to improve the genetic analysis of *Drosophila* genes in the future (Qiao *et al.*, 2018) (Figure 1.4).

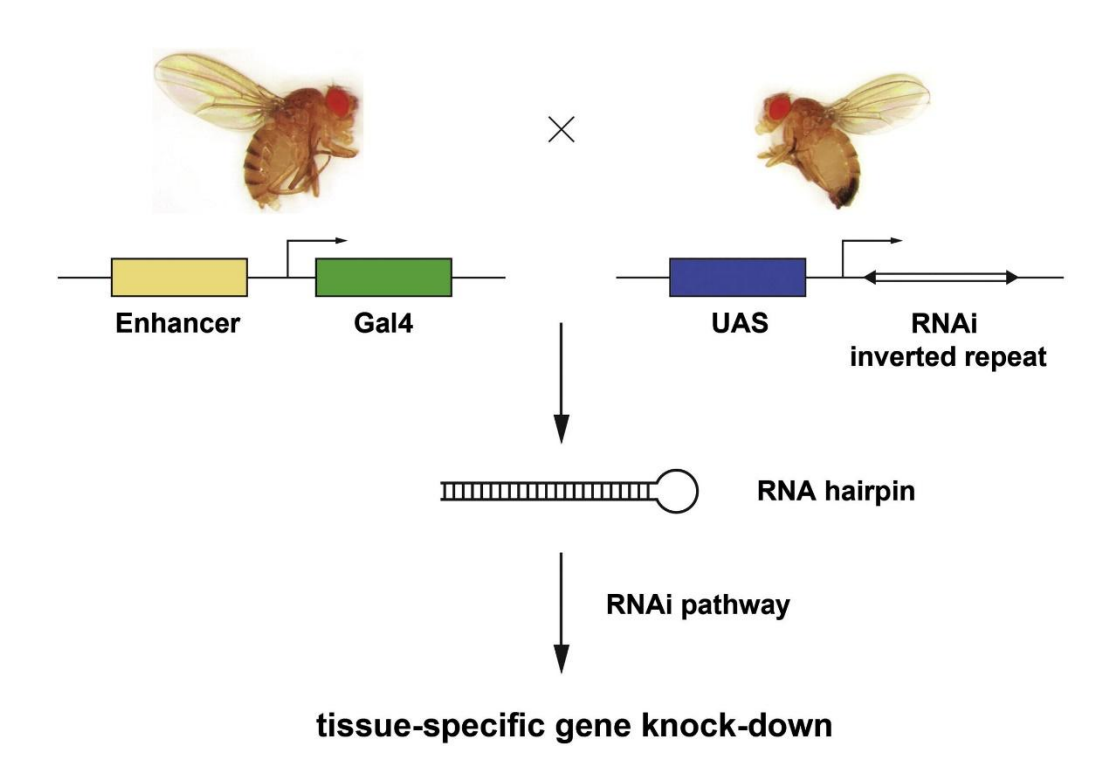


Figure 1.4 Schematic representation of transgenic RNAi in *Drosophila*. The driver line carries the transcription factor Gal4, which is under the control of a specific enhancer. The responder line carries an RNAi construct, which is under the control of UAS. After the two fly lines are crossed, Gal4 binds to UAS and activates the transcription of the RNAi inverted repeat. The functional RNAi molecules are generated and processed through the RNAi pathway, leading to tissue-specific knockdown of target genes (Jiang and Reichert, 2013).

In addition to the GAL4-UAS system, clustered regularly interspaced short palindromic repeats (CRISPR) and their associated protein Cas-9 have become widely used for gene editing and mutation generation in *Drosophila* (Bassett and Liu, 2014). The CRISPR/Cas-9 system involves two key components: guide RNA (gRNA) and Cas-9 proteins. The technique operates through three steps: recognition, cleavage, and repair. The gRNA identifies the target gene sequence by complementary base pairing, while Cas-9 cleaves the DNA at the target site. An overview of the CRISPR/Cas9 system is illustrated in Figure 1.5. This system allows for gene editing, enabling researchers to create targeted mutations and study gene function comprehensively in *Drosophila* (Asmamaw and Zawdie, 2021). These modern genetic tools, including the CRISPR/Cas-9 system, expand the capabilities for genetic research and functional genomics in *Drosophila*, building on the foundational work established by the GAL4-UAS system.

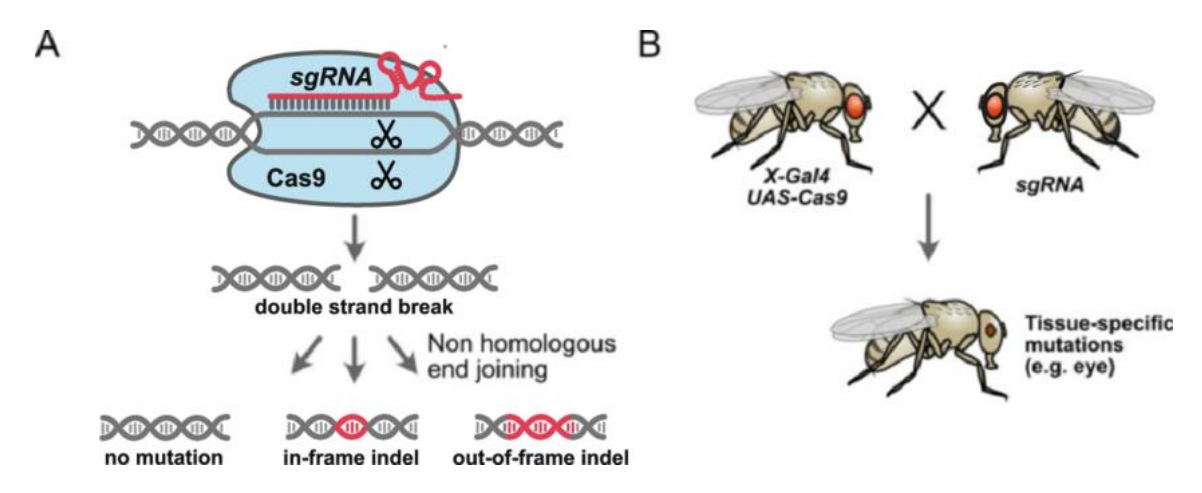


Figure 1.5 CRISPR/Cas9-based gene targeting and genome editing in *Drosophila*. (A) A single guide RNA directs the Cas9 endonuclease to a genomic target site, where Cas9 introduces a double-strand break. DNA repair can occur by non-homologous end joining, resulting in insertions or deletions (indels) that may be in-frame or out-of-frame. (B) Conditional CRISPR mutagenesis in *Drosophila* can be achieved by crossing flies carrying a Gal4-driven UAS-Cas9 transgene with flies expressing a transgenic sgRNA. In the progeny, CRISPR components are expressed in Gal4-positive tissues, leading to targeted mutations and tissue-specific phenotypes (Port and Boutros, 2022).

1.2.3 Reasons to use Drosophila

1.2.3.1 Life cycle

Several advantages of using *Drosophila* as a model organism include its small size, short life cycle, and ease of cultivation, which is easy to maintain in laboratory settings (Taormina *et al.*, 2019). The typical life cycle of *Drosophila melanogaster* is approximately 10-12 days at 25 °C (Ashburner and Roote, 2007). Although developmental timing can vary with temperature, *Drosophila* is generally reared in labs at temperatures between 22 °C and 25 °C. The life cycle comprises four stages: embryo, larva, pupa, and adult (Figure 1.6), allowing for rapid generation turnover and ease of genetic study.

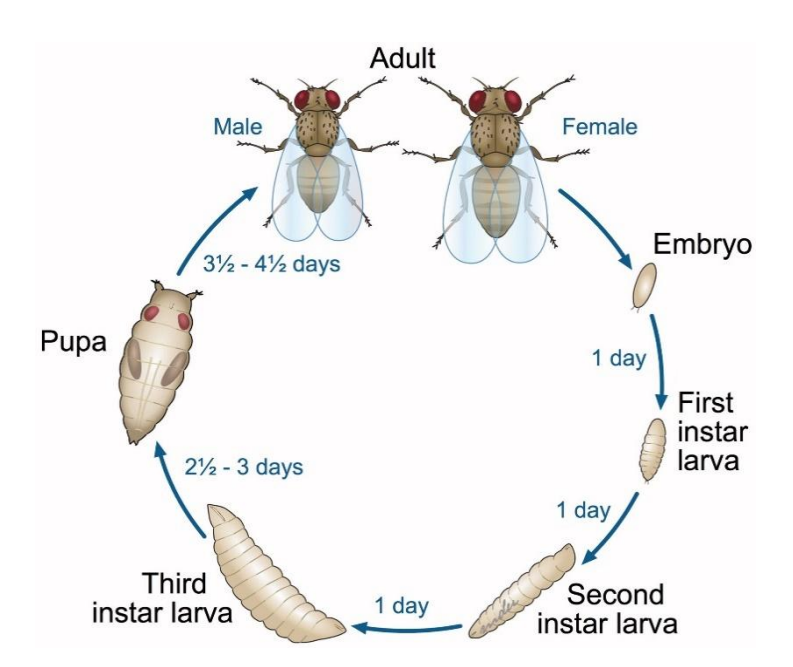


Figure 1.6 The life cycle of *Drosophila* **melanogaster.** The image illustrates the complete life cycle of the fruit fly. Development from the embryo to the adult takes approximately 10-12 days at 25 °C. The cycle comprises six stages: embryo, first instar larva, second instar larva, third instar larva, pupa, and adult (Ong et al., 2015).

Female flies can lay several hundred eggs, with fertilised embryos developing into larvae within 24 hours. The first-instar larva feeds on food at the surface of the vials and then has two moulting stages before forming pupae (Weigmann *et al.*, 2003). Once the larva becomes a pupa, its tissues are degraded. Imaginal discs, which are epithelial structures in the larva, develop into adult organs,

including the head, thorax, wings, limbs, halteres, eyes, and antennae (Fernández-Moreno *et al.*, 2007). Finally, the adult fly emerges from the pupa, completing the life cycle.

1.2.3.2 Relative inexpensive

The cost-effective keeping of fly lines is one of the main advantages of *Drosophila* melanogaster in biological sciences. Fly line maintenance is relatively cheap. For example, producing a single line of transgenic mice requires ethics approval and annual costs in excess of \$10,000 (Malakoff, 2000). In contrast, *Drosophila* can be kept at much lower cost than most other genetic models. It has a more complex genome and anatomy than other widely used model organisms, including *Caenorhabditis elegans* and *Saccharomyces* cerevisiae, and provides better suitability for studies of functions in higher organisms such as mammals (Ogienko *et al.*, 2022). Although *C. elegans* and Saccharomyces *cerevisiae* are less expensive and easier to maintain, they are genetically too straightforward for some research. Therefore, *Drosophila* provides a useful balance between cost and genetic complexity, whereas vertebrate models such as mice and zebrafish are more expensive to maintain and require stricter ethical oversight (National Research Council, 2000).

1.2.3.3 Simple genome

The genome of *Drosophila* melanogaster comprises approximately 180 Mb of DNA distributed across four pairs of chromosomes. In comparison, the human genome is much larger, with around 3.1 billion base pairs organised into 23 pairs of chromosomes (Sharma, 2012). Within the *Drosophila* genome, about 130 Mb consists of gene-rich regions, which encode roughly 13,600 genes (Adams *et al.*, 2000). Despite the evolutionary distance between humans and *Drosophila*, approximately 70% of fly genes have human disease-related orthologs (Davies *et al.*, 2019), highlighting the strong genetic correspondence (Link and Bellen, 2020). Although the complete genome sequence of *Drosophila* melanogaster has been published, many gene functions remain to be characterised.

1.2.4 Resources

A well-annotated genome sequence has made *Drosophila* the system of choice for functional genomics research. Numerous specialised online resources, such as FlyBase and FlyAtlas, are available to identify fly strains, procure reagents, and analyse genomic, transcriptomic, and proteomic data. These resources promote a wide range of genetic and molecular biology studies.

1.2.4.1 Fly Base

FlyBase is an online database that curates all available information about *Drosophila*. It integrates data from various sources, including research literature, genome sequencing projects, and online resources like GenBank (Sayers *et al.*, 2022). FlyBase links to other *Drosophila* and non-Drosophila-specific resources (Öztürk-Çolak *et al.*, 2024). Examples include FlyMet, FlyAtlas2, *Drosophila* stock centres, and research publications

1.2.4.2 FlyAtlas and FlyAtlas 2

FlyAtlas and FlyAtlas 2 are database and web applications which provide tissue-specific transcriptomic information for *Drosophila* and reveal multiple gene expressions of adult flies and larvae (Figure 1.7) (Robinson *et al.*, 2013; Krause *et al.*, 2022; Leader *et al.*, 2018). Moreover, FlyAtlas data show that approximately one-third of *Drosophila* genes are expressed in a tissue-specific manner. This means that many genes may not be detectable if only whole-organism expression is analysed. As a result, reverse genetic approaches become more informative when combined with tissue-level studies, underlining the importance of examining individual tissues rather than relying solely on whole-organism data (Chintapalli et al., 2007; Robinson et al., 2013; Leader et al., 2018).

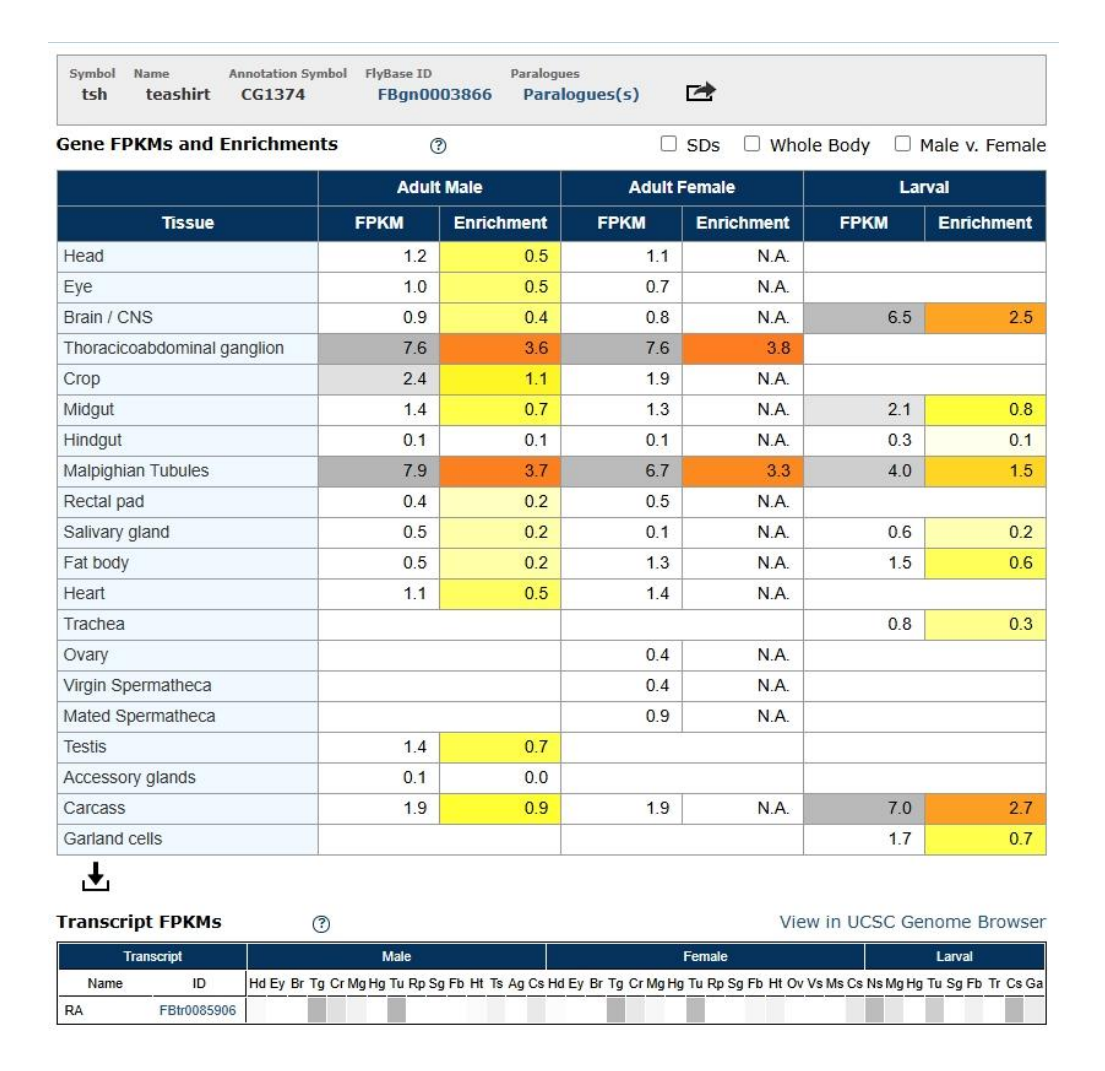


Figure 1.7 Tissue-specific expression profile of the tsh gene in *Drosophila* (FlyAtlas 2 data) Expression profile of the tsh gene in different *Drosophila* tissues according to FlyAtlas 2 data. The table indicates expression levels (FPKM) and enrichment values in adult males, adult females, and larvae, highlighting its expression in the Malpighian tubules (Krause *et al.*, 2022).

FlyAtlas, based on Microarray data, provided initial insights into relative expression levels for known genes through hybridising RNA samples to specific probes on a chip (Liu *et al.*, 2010). Although this method proved effective, microarrays have limitations, such as lower sensitivity, specificity, and potential cross-hybridisation. In contrast, FlyAtlas2 used RNA-Seq technology to generate expression data rather than microarray analysis (Leader et al., 2018). RNA-Seq offers higher sensitivity and specificity, identifies novel transcripts (Vedelek *et al.*, 2018; Daines *et al.*, 2011), detects both high and low-abundance transcripts, and provides absolute quantification of RNA molecules, thus offering detailed gene expression profiles and tissue data (Leader *et al.*, 2018).

1.2.4.3 Fly Cell Atlas

The Fly Cell Atlas (FCA) community comprises researchers focused on single-cell genomics, transcriptomics, and epigenomics. FCA aims to create cell atlases across different developmental stages and disease models, providing references for studying gene function and disease at the single-cell level (Li *et al.*, 2022). Using single-cell sequencing, FCA identified specific gene information in whole adult flies, identifying various fly cell types.

Scope is a visualisation tool for large-scale single-cell RNA sequencing (scRNA-seq) datasets to visualise the annotation and cell types (Figure 1.8). It has links to provide data from the FlyCellAtlas website. This tool can identify cell type, cell stage, and cell-type-specific genes. Cell type-specific markers can compare gene expression in different cells and tissues across the entire head and body (Li et al., 2022).

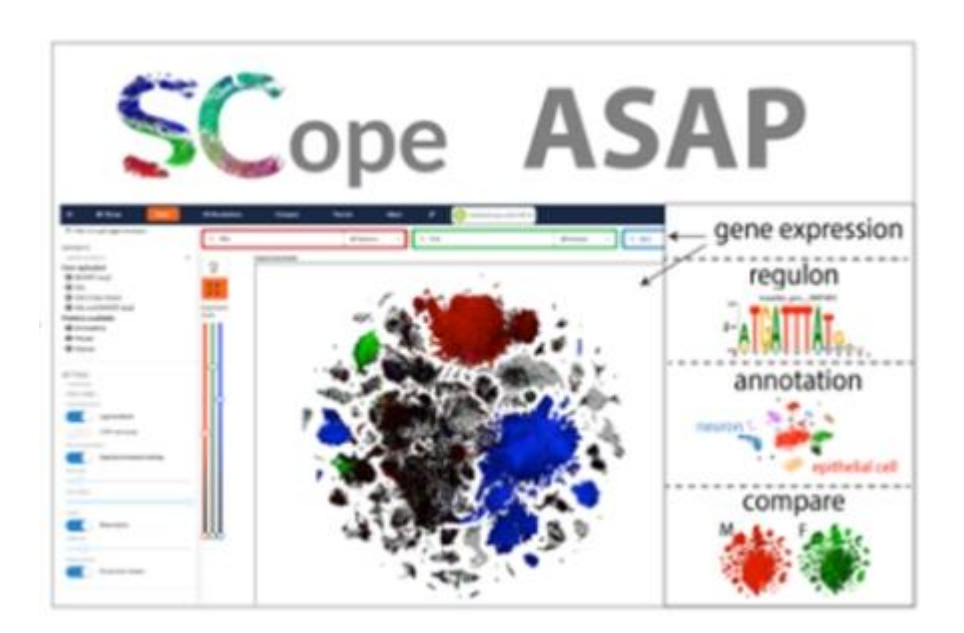


Figure 1.8 Data visualisation using Scope (Li et al., 2022).

1.2.4.4 Stock centre

The *Drosophila* stock centre is an important genetic and developmental research resource, providing well-characterised *Drosophila melanogaster* strains. These centres ensure experimental reliability by providing high-quality fly strains and detailed genetic and phenotypic data. Major *Drosophila* stock centres are located in North America, Europe, and Asia, each maintaining different fly strains. They catalogue strains from researchers and provide them to the global *Drosophila* research groups worldwide, thus supporting a wide range of scientific investigations and ensuring the consistency of genetic research worldwide.

1.3 Drosophila Malpighian tubules

1.3.1 History

The study of Malpighian tubules in *Drosophila melanogaster* has a long history, beginning with Marcelo Malpighi's work in the 17th century (Malpighi, 1666). While exploring insect anatomy, Malpighi discovered these tubules, which were subsequently named after him (Figure 1.9). It was not until the 20th century that the role of Malpighian tubules in urine production was confirmed, leading to research on Malpighian tubule excretory and osmoregulatory functions. Additionally, Malpighian tubules have become an essential model for studying epithelial systems and have been a key target organ in insecticide research (Dow and Romero, 2010).

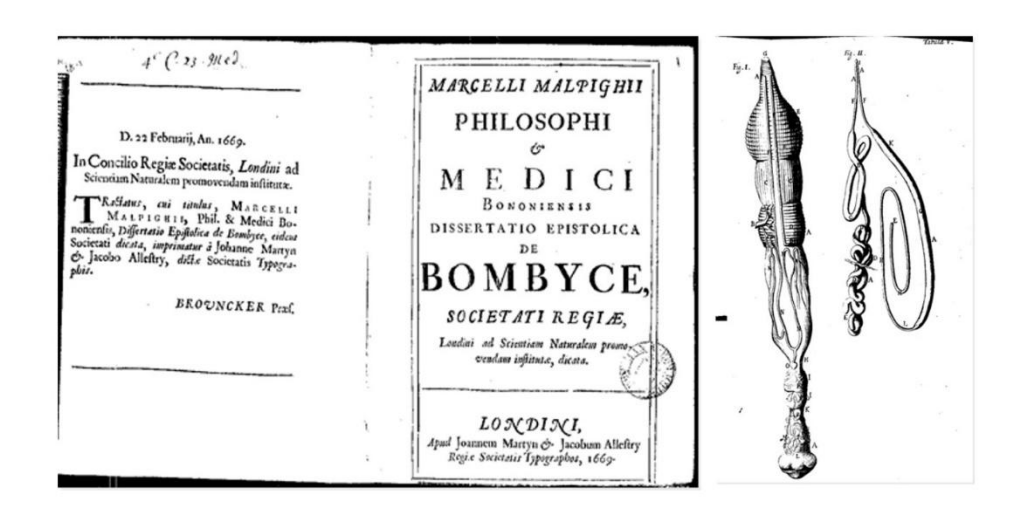


Figure 1.9 The Malpighian tubules were first described in 1669. The structures are represented as Malpighi drew them (Malpighi, M).

1.3.2 Epithelial tissues

Epithelial tissues play an important role in insects and higher organisms. They protect organs by forming single or multiple layers of cells (Guillot and Lecuit, 2013). They also regulate physiological environments by controlling transport processes across the plasma membrane. Epithelia possess two different surfaces: the basolateral membrane and the apical membrane (Lee and Streuli, 2014). The apical membrane faces the lumen or external environment, facilitating direct interaction with fluids or substrates. The basolateral membrane, by contrast,

interfaces with adjacent epithelial cells and the underlying extracellular matrix, enabling exchange with the internal tissue environment (Lee and Streuli, 2014).

Drosophila Malpighian tubules are used as a model for studying epithelial tissue morphogenesis, transport mechanisms, and homeostasis maintenance (Dow et al., 1994; O'Donnell et al., 1996). As a central organ of the excretory system, the Malpighian tubules perform functions analogous to mammalian kidneys (Reynolds et al., 2021). They transport excess fluid and solutes into the hindgut for excretion, maintaining the organism's internal balance. Consequently, Drosophila Malpighian tubules provide a robust model for understanding how epithelial tissues contribute to homeostasis in the renal system.

1.3.3 Morphology

1.3.3.1 The development of the Malpighian tubules during Embryogenesis

The Malpighian tubules in *Drosophila* originate from the evagination of cells at the junction between the hindgut and midgut during embryogenesis (Jack and Myette, 1999). These four tubules develop from the hindgut primordium through a sequence of cellular activities (Denholm *et al.*, 2003) (Figure 1.10). By the end of embryonic development, the tubules are fully formed, comprising two main cell types in the secretory region: principal cells, derived from primordial cells, and stellate cells, which originate from the caudal mesoderm (Cohen *et al.*, 2020). During this stage, the tubules primarily transport organic solutes; however, significant fluid secretion activity does not commence until after hatching (Denholm, 2013). The developmental sequence establishes the structural and cellular organisation of the Malpighian tubules, with principal and stellate cells acquiring distinct identities that underpin later physiological functions. This early specification is crucial, as it provides the foundation for the tubules' role in excretion and osmoregulation following hatching (Denholm, 2013; Cohen *et al.*, 2020).

1.3.3.2 Larval and adult

As detailed earlier, the four Malpighian tubules in *Drosophila* are fully formed by the end of embryogenesis and capable of secreting organic compounds. However, significant changes occur during the larval, pupal, and adult stages. In early larval development, the tubules exhibit a notable increase in fluid secretion capacity (Skaer *et al.*, 1990). This secretion activity is temporarily suspended during the pupal stage (Ryerse, 1978). Additionally, although stellate cells are present from embryogenesis, they do not exhibit their characteristic star shape until several days after the adult fly emerges (Sözen *et al.*, 1997; Ojha and Tapadia, 2020).

1.3.3.3 Structure and Function

As described in section 1.2.3.1, *Drosophila* has four tubules. These are found in pairs, comprising tubular, blind-ended epithelia joined by a short common ureter that connects to the alimentary canal and floats freely in the haemocoel (Wessing and Eichelberg, 1978). Each fly has one pair of anterior and one pair of posterior tubules, contributing equally to tubule function (O'Donnell and Maddrell, 1995) (Figure 1.10). The anterior tubules are located anteriorly in the body cavity, while the posterior tubules extend into the abdomen (Dow and Davies, 2003). The anterior refers to the head end of the embryo. A single Malpighian tubule measures approximately 2 mm in length and has an internal luminal diameter of roughly 17 μ m (Miller *et al.*, 2013).

The anterior and posterior Malpighian tubules are morphologically divided into four distinct segments: the initial segment, the transitional segment, the main segment, and the lower segment, with the latter connecting to the common ureter (Miller *et al.*, 2013) (Figure 1.10). The anterior tubules have larger initial and transitional segments with more cells than those in the posterior tubules. Interestingly, although females have bigger tubules, no significant morphological differences exist between the tubules of males and females.

Malpighian tubules were initially considered simple epithelial tissue, but further research has revealed their complexity (Sözen et al., 1997). Figure 1.10 (D) shows morphologically different regions of tubules. The main segment of the Malpighian tubules comprises two cell types: columnar epithelial principal cells and star-shaped stellate cells. Principal cells have long apical microvilli (Cabrero et al., 2004), whereas stellate cells are smaller and thinner, with shallow basal infoldings and short apical microvilli (Wessing and Eichelberg, 1978). Enhancer trapping has proven highly effective in examining tubule morphology, identifying a distinct 'lower' segment in both the anterior and posterior tubules and finding bar-shaped and tiny cells. Bar-shaped cells are likely equivalent to stellate cells in the initial segment, while tiny cells may function as stem cells or serve a neuroendocrine role (Sözen et al., 1997; Singh et al., 2007).

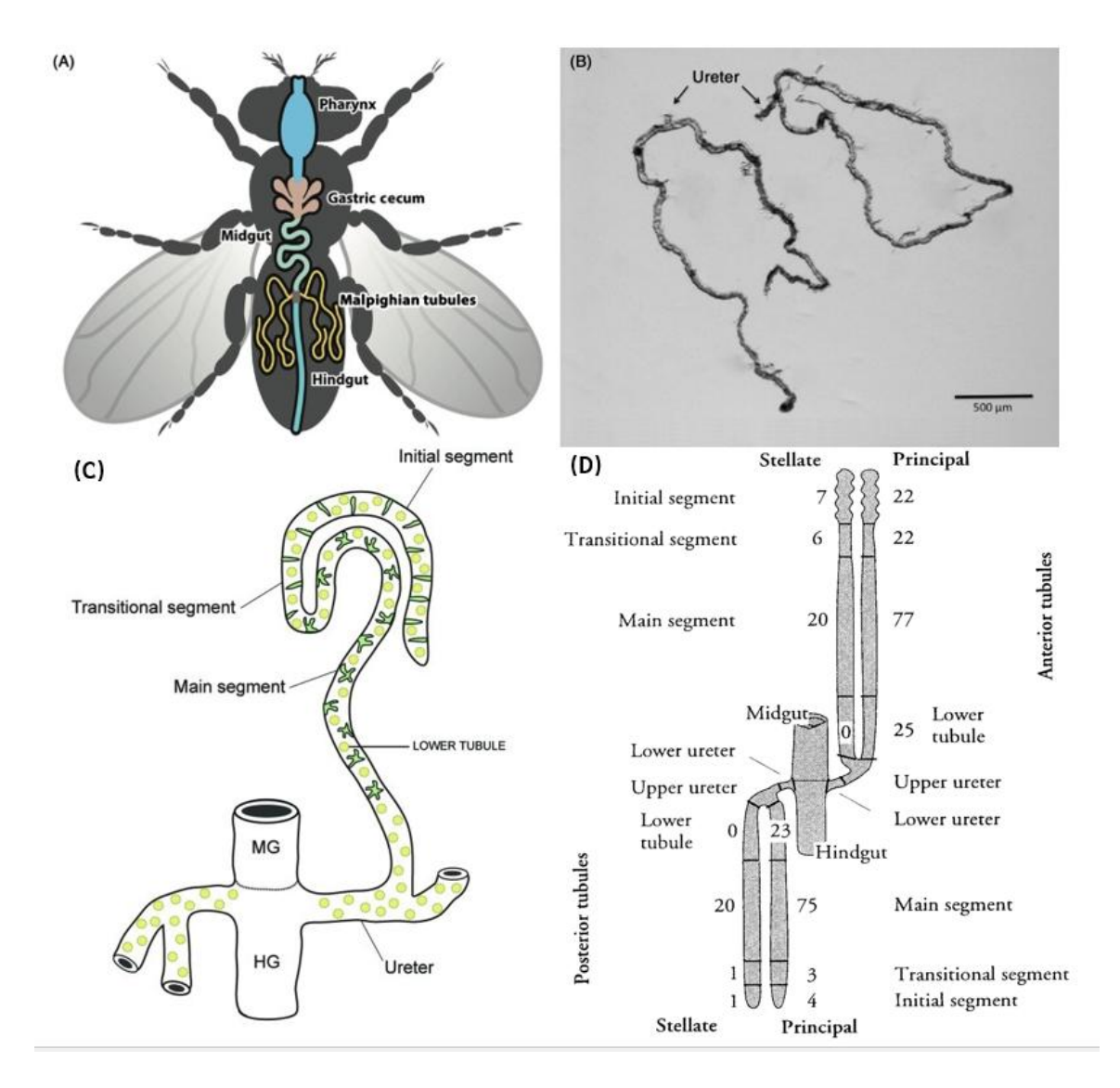


Figure 1.10 D. melanogaster Malpighian tubules. (A) The excretory tract of *Drosophila* melanogaster comprises two pairs of Malpighian tubules, anterior and posterior. Each pair is connected to the hindgut by a common ureter (Miller *et al.*, 2013). (B) Two pairs of Malpighian tubules were dissected from an adult *Drosophila*. The arrows show the common ureter (Tzou *et al.*, 2017). (C) Different morphological regions in the *Drosophila* Malpighian tubules: initial, transitional, and main segments and the ureters, which join each pair of tubules to the hindgut (HG). The green star-shaped patterns in the main segment and the green bar-shaped image in the initial and transitional segments are stellate cells. The yellow pattern in the initial, transitional, and main segments are principal cells (Denholm, 2013). (D): Summary of functionally distinct regions of *Drosophila* tubules. It shows the six domains of the tubule and the number of principal and stellate cells in each, demarcating the initial segment, transitional segments, main segment, and lower tubule from top to bottom (Sozen *et al.*, 1997).

1.3.4 Principal cell and stellate cell

As mentioned in section 1.2.3.3, the Malpighian tubules of *Drosophila* are divided into different segments, each specialising in specific excretion and osmoregulation functions. Figure 1.11 shows several views of these cell types within the tubules. Principal cells, which are more numerous than stellate cells, feature deep basal infoldings and long apical microvilli (Cabrero *et al.*, 2014). Stellate cells, by contrast, are smaller and less abundant, and display distinctive star-shaped morphology that is evident in Figure 1.11 (Davies *et al.*, 2019).

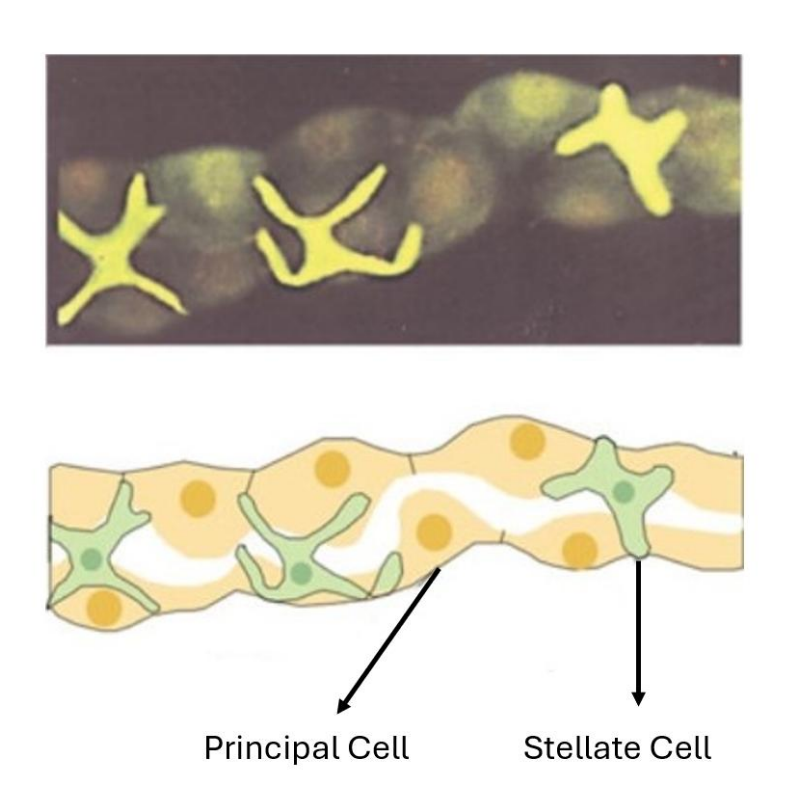


Figure 1.11 Views of principal cell and stellate cell in Malpighian tubule. Top panel: Fluorescence view of *Drosophila* Malpighian tubule. It shows a short region from the main segment of tubules—lower panel: abstraction of the above (Davies *et al.*, 2019).

1.3.5 Ion transport and osmoregulation

Principal cells in the Malpighian tubules are primarily responsible for the active transport of cations, particularly potassium (K⁺) and sodium (Na⁺). They regulate these ions via basolateral cotransporters and contain vacuolar-type H⁺-ATPase proton pumps. These pumps create a pathway for the secondary movement of Na⁺ and K⁺ into the tubules through Na⁺/H⁺ and K⁺/H⁺ exchangers (Wang *et al.*, 2014) (Figure 1.12). In the cation transport, the vacuolar proton pump H⁺-ATPase

mediates the secretion of Na⁺ and K⁺ into the tubule lumen by transporting H⁺ across the membrane from the principal cell cytoplasm to the tubule lumen, generating an electrical gradient (Dow *et al.*, 1994; Wang *et al.*, 2004; Beyenbach *et al.*, 2010). This voltage gradient drives the movement of K⁺ and Na⁺ across the basolateral membrane, subsequently transporting these ions into the lumen (Linton and O'Donnell, 1999).

The main function of the tubules in excretion and osmoregulation involves regulating fluid secretion through second messengers such as cyclic adenosine monophosphate (cAMP), cyclic guanosine monophosphate (cGMP), and calcium. This regulation is complex (Davies *et al.*, 2014) (Figure 1.12 left). Cyclic nucleotide signalling enhances fluid secretion by increasing the membrane potential of the tubules, likely by boosting ATP availability for the V-ATPase. The V-ATPase is also considered the ultimate target of cyclic nucleotide signalling in the tubule (Dow *et al.*, 1994; Davies *et al.*, 2014). Calcium signalling affects various osmoregulation processes in principal cells, including V-ATPase activity, ion transport, and fluid secretion rates (MacPherson *et al.*, 2005; Davies and Terhzaz, 2009). Neuropeptides from the Capa peptide family stimulate fluid secretion in the tubules through cGMP and Ca²⁺ signalling in principal cells (Davies et al., 2014), while the neuropeptides DH44 and calcitonin-like DH31 also active tubules to the secretion of fluid through a cAMP-dependent signalling pathway (Lee *et al.*, 2023).

Stellate cells, characterised by their star-shaped morphology, are crucial for chloride ion transport and water conductance (Cabrero *et al.*, 2014). They are found across the posterior Malpighian tubules, in the initial, transitional and main segments (Figure 1.10 C). In these regions, intracellular calcium (Ca²⁺) regulates chloride shunt conductance by increasing transcellular chloride flux through chloride channels (Blumenthal, 2003; Cabrero et al., 2013). Chloride flux is regulated by kinin and tyramine signalling, which exert their effects through calcium signalling within stellate cells (Radford *et al.*, 2002). Figure 1.12 summarises the proteins, ions, and second messengers involved in tubule

transport, highlighting the intricate coordination required for effective osmoregulation and ion transport in *Drosophila* Malpighian tubules.

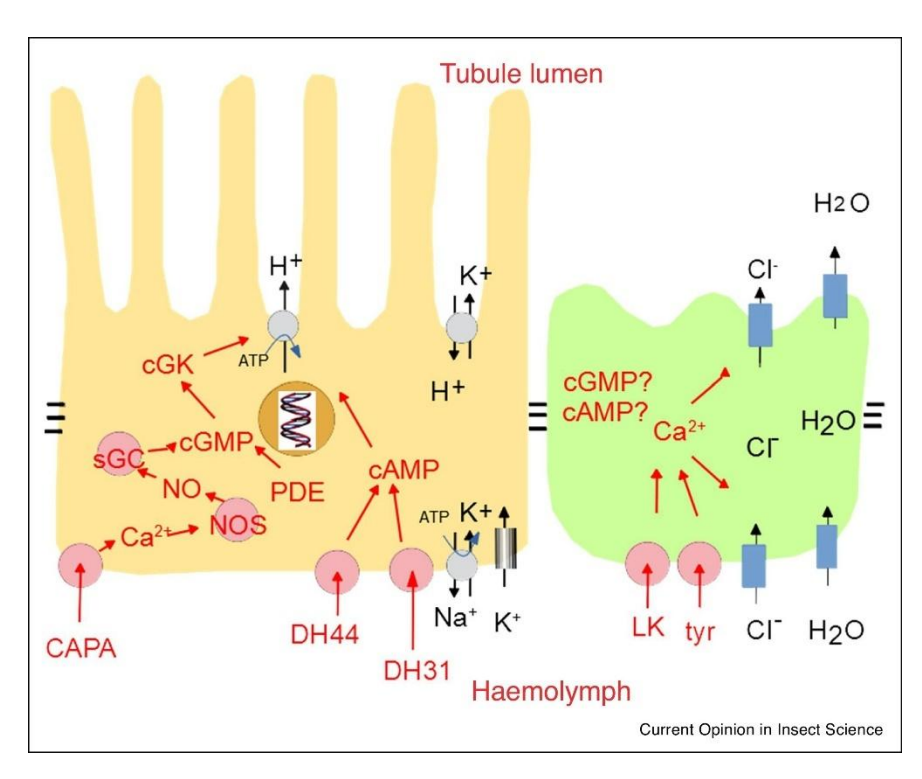


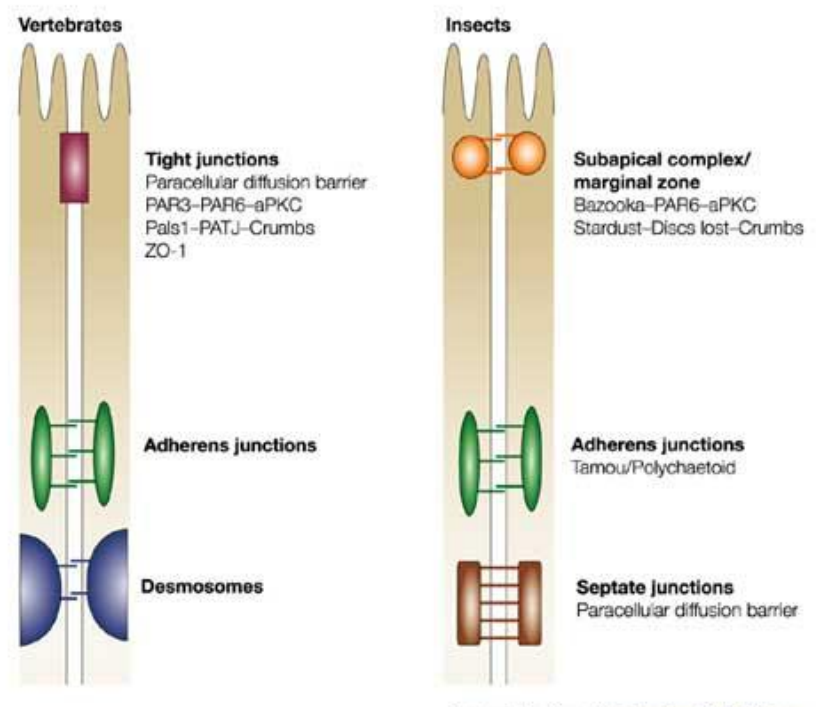
Figure 1.12 Schematic diagram summarising ion transport by the Malpighian tubules. Ion transport pathway in the principal (left) and stellate cells (right) of the main segment Malpighian tubules (Dow et al., 2021).

1.4 Cell-cell junction

1.4.1 Physiological and Morphological Study

Previous studies identified genes with highly specific expression in *Drosophila* tubules (Dow, 2007). We selected gap-junction innexins (*Inx2/Inx7*) and the octopamine receptor Octα2R because they are highly enriched in specific tubule cell types and represent two key control points: cell-to-cell coupling in principal cells and amine-mediated control of secretion in stellate cells. This choice is consistent with our aim to connect enriched genes to tubule function. Our expectation was that these genes would prove important in tubule function. They are described in more detail below.

Cell-cell junctions in *Drosophila* tubules are essential for maintaining the structure and function of these organs. These junctions include adherens junctions, septate junctions, and gap junctions, each serving distinct roles in tissue cohesion and intercellular communication (Tepass and Hartenstein, 1994). Figure 1.13 shows intercellular junctions in vertebrates and insects. Although *Drosophila* gap junctions are formed by innexins rather than connexins, both protein families serve the same role in mediating direct cell-to-cell communication. Innexins and connexins are structurally different but functionally similar, allowing ions and small molecules to pass between neighbouring cells (Skerrett and Williams, 2017; Koval *et al.*, 2014).



Nature Reviews | Molecular Cell Biology

Figure 1.13 Intercellular junctions in vertebrates and insects (*Drosophila*). Diagram showing the main types of epithelial intercellular junctions. In vertebrates, these include tight junctions, adherens junctions, and desmosomes, while in insects (*Drosophila*) they include the subapical complex, adherens junctions, and septate junctions. Adherens junctions are conserved in both groups, while vertebrate tight junctions are considered functionally equivalent to insect septate junctions (Matter and Balda, 2003).

Adherens junctions, composed primarily of E-cadherin and catenin, provide strong adhesive contacts between cells (Mège and Ishiyama, 2017). These junctions ensure mechanical stability and maintain the epithelial layer's structure during different physiological processes.

Septate junctions consist of several proteins, including Neurexin IV, Coracle, and Discs large (Oshima and Fehon, 2011). Their main function is to form a paracellular barrier regulating ions and molecules' movement between cells. This barrier separates the tubule lumen's contents from surrounding tissues, ensuring a stable internal environment (Banerjee *et al.*, 2006; Rouka *et al.*, 2021).

Gap junctions comprise Innexins, allowing communication between adjacent cells by facilitating the passage of ions, small molecules, and signalling compounds (Kapoor *et al.*, 2021). It is described in detail in the following section.

In *Drosophila*, the coordinated interaction of adherens junctions, septate junctions, and gap junctions maintains the structural integrity, barrier function, and communication within the Malpighian tubules (Daniel *et al.*, 2018). This interaction enables the tubules to effectively regulate ion and water balance, respond to environmental changes, and maintain homeostasis.

1.4.2 Gap Junction

Communication between neighbouring cells via gap junctions is essential in developing organs and tissues in multicellular organisms. Gap junctions consist of clusters of hydrophilic membrane channels that link the cytoplasm of adjacent cells (Bauer, Löer *et al.*, 2005). These channels enable direct intercellular communication by exchanging ions, metabolites, and small molecules between principal and stellate cells (Goodenough and Paul, 2009).

Two types of protein families form gap junctions: connexins and innexins. Connexin proteins form these channels in vertebrates, while innexin proteins are responsible in invertebrates such as *Drosophila* (Phelan *et al.*, 1998; Meşe *et al.*, 2007). Although they are structurally distinct and share little sequence homology, connexins and innexins perform the same fundamental role of mediating direct intercellular communication by allowing ions and small molecules to pass between neighbouring cells. Pannexins are related to connexins and innexins and play significant roles in various physiological processes, but there is no evidence that they form gap junctions (Sosinsky *et al.*, 2011).

Despite their different sequences, innexins, connexin, and pannexins have four hydrophobic transmembrane domains, comprising one cytoplasmic and two extracellular loops (Bond and Naus, 2014; Abascal and Zardoya, 2013). Figure 1.14 illustrates the general structures of innexins, connexins and pannexins.

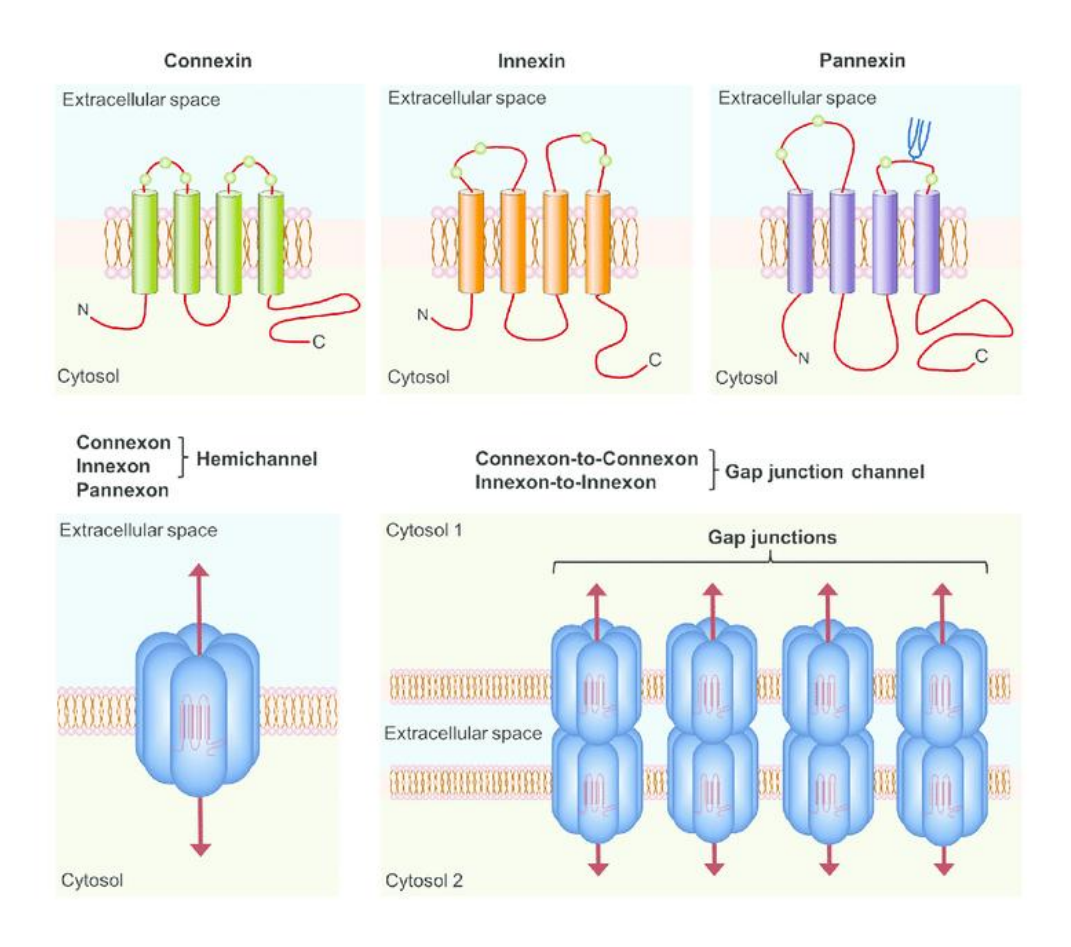


Figure 1.14 General structure of channels formed by connexins, innexins and pannexins.

Connexins contain three cysteine residues in each of their extracellular loops (green balls), whereas Innexins and pannexins each have two cysteines per loop. The blue branches are the extracellular loop cysteines. The connexin, innexin and pannexins structures comprise four transmembrane domains and one cytoplasmic loop and have both NH2 and CO2H terminals in the cytosol. Connexins or innexins, each consisting of six subunits, form connexons or innexons, while Pannexons are single membrane channels composed of six pannexin subunits (Gajardo-Gómez *et al.*, 2016).

Many studies have investigated the functions of pannexins and connexins (Phelan and Starich, 2001; Hervé *et al.*, 2005). Pannexins are involved in cell death, the triggering of inflammasome, and the modulation of Ca²⁺ leakage in the endoplasmic reticulum. Innexins play roles in tissue regeneration, development, and electrical synapse formation, while connexins contribute to cell growth, differentiation, and developmental regulation.

Analysis of the human genome has revealed that more than 20 genes encode different connexin paralogues (Abascal and Zardoya, 2013). Increasingly, studies are focusing on gap junctions to understand cellular activities between adjacent cells and the interactions between cells and the extracellular space (Goodenough and Paul, 2009). Innexins have been confirmed by Güiza *et al*. (2018) to correspond to gap junction formation in non-chordates.

1.4.3 Innexin Gene Family

As discussed earlier, innexins are a family of gap junction proteins (Abascal and Zardoya, 2013; Baranova *et al.*, 2004; Alexopoulos *et al.*, 2004; D'hondt *et al.*, 2009; Goodenough and Paul, 2009). These junctions involve several physiological processes (Güiza *et al.*, 2018), such as the exchange of ions and small molecules between neighbouring cells (Sáez *et al.*, 2003). In *Drosophila melanogaster*, eight innexin family members of gap junction proteins have been found (Stebbings *et al.*, 2002). Their details are provided in Table 1.15.

Gene Symbol	Gene Name	Synonyms	
Inx2	Innexin 2	Prp33, kropf, l(1)G0043, l(1)G0035, l(1)G0118	
Inx3	Innexin 3	Dm-lnx3, inx-3	
Inx5	Innexin 5		
Inx6	Innexin 6	prp6	
Inx7	Innexin 7	prp7	
ogre	Optic ganglion reduced	I(1)ogre, inx1, innexin 1	
shakB	Shaking B	Pas, shak-B, R-9-29, Passover, inx8	
zpg Zero population growth		lnx4, Innexin4	

Table 1.15 *Drosophila* **melanogaster innexin families.** List of innexin genes in *Drosophila* melanogaster, including their gene symbols, names, and known synonyms. Data are modified from FlyBase.

1.4.3.1 ogre

The first gap junction gene described is *ogre*, which is especially important in nervous system development, especially during postembryonic neurogenesis (Watanabe *et al.*, 1992). It interacts with Innexin 2 to form a functional gap junction with unique properties (Holcroft *et al.*, 2013; Curtin *et al.*, 1999). This interaction is essential for the proper functioning of glial cells. Glial cells support and compartmentalise neurons during CNS development (Freeman, 2015). Alterations in *ogre* or *Inx2* expression or function in glial cells can lead to several developmental issues, particularly within the nervous system. For example, it decreases the size of the larval nervous system, resulting in abnormal behaviour in adult *Drosophila* (Holcroft *et al.*, 2013). Ogre and Inx2 cooperatively regulate neurogenesis and neuronal development.

1.4.3.2 Innexin 2

Innexin 2 is a gap junction protein (Bauer *et al.*, 2004) that is essential to facilitate cell communication. This protein is consistently expressed across different developmental stages, with a significant presence in the proventriculus, circadian circuits, nervous system, early oogenesis, eye imaginal disc development, and epithelial tissues (Phelan, 2005; Patop *et al.*, 2023; Ostrowski *et al.*, 2009; Güiza *et al.*, 2018; Richard *et al.*, 2007). During embryonic development, Innexin 2 promotes synchronised cell signalling necessary for tissue development (Sahu *et al.*, 2017). In larval and adult stages, Innexin 2 contributes to the functionality of renal tubules, the development of the nervous system (Ostrowski *et al.*, 2009), and the maintenance of epithelial structure (Tepass *et al.*, 1996). The function and activity of Innexin 2 at different developmental stages highlight its importance in maintaining homeostasis and supporting developmental processes.

1.4.3.3 Innexin 3

Inx3 is another gap junction protein involved in different developmental stages. It interacts with Inx2 to form heteromeric channels, which are essential for preserving epithelial integrity and polarity during embryogenesis (Stebbings *et al.*, 2000). *Inx3* is highly expressed in embryonic tissues such as the hindgut (Lehmann *et al.*, 2006). Furthermore, the absence of *Inx3* function leads to significant defects in dorsal closure, highlighting its critical role in embryonic morphogenesis (Giuliani *et al.*, 2013). In addition to these embryonic roles, *Inx3* also contributes to later development, particularly in the eye imaginal disc, where it interacts with the Decapentaplegic (Dpp) signalling pathway to regulate cell proliferation and thereby control eye disc growth and adult eye size (Richard *et al.*, 2017).

1.4.3.4 Innexin 5

Innexin 5 contributes to intercellular transport (Bauer *et al.*, 2005). It appeared to be associated with consolidated anesthesia-resistant memory (ARM) in mushroom body neurons, specifically in the $\alpha \beta$ neurons. It was preferentially expressed in the somas of MB neurons (Shyu *et al.*, 2019). Functionally, the knockdown of *Inx5* disrupts ARM without affecting the labile anesthesia-sensitive memory (ASM), indicating the role of *Inx5* in memory retrieval.

1.4.4.5 Innexin 6

In contrast to the functional study of Inx5, impairment of Inx6 function results in the disruption of ASM but does not affect ARM, indicating the role of *Inx6* in a particular phase of memory processing (Wu *et al.*, 2011; Shyu *et al.*, 2019). *Inx6* is mostly expressed in DPM neurons (Wu *et al.*, 2011). Together with *Inx7*, it forms heterotypic gap junctions essential for developing ASM in MB neurons (Hughe *et al.*, 2014). These heterotypic junctions develop between the anterior paired lateral (APL) neuron and the dorsal paired medial (DPM) neuron, both important to olfactory associative learning and memory (Shyu *et al.*, 2019; Shih and Wu, 2017).

1.4.3.6 Innexin 7

Innexin 7 is also expressed in the midgut and Malpighian tubules (Leader *et al.*, 2018). As the Malpighian tubules are the main organs for osmoregulation and excretion in *Drosophila* (Dow and Romero, 2010), this expression suggests that Inx7 could play a role in ion transport or fluid balance, although definitive functional tests have not been carried out in Malpighian tubules. *Inx7* has also been linked to roles in the nervous system (Ostrowski et al., 2009) and in eye disc growth (Richard and Hoch, 2015). By contrast, it is not required for the process of cellularisation in *Drosophila* (Bauer et al., 2005; Phelan, 2005; Ostrowski et al., 2008). In *Tribolium*, however, the Innexin 7a ortholog is necessary to stabilise the basal membrane during epithelial morphogenesis (Van Der Zee et al., 2015).

1.4.3.7 shakB

The *shakB* gene in *Drosophila melanogaster* encodes several isoforms important for forming and operating electrical synapses in the giant fiber system (GFS), which participate in the fly's quick escape mechanism (Zhang *et al.*, 1999; Pézier *et al.*, 2016). Additionally, the *shakB* gene generates at least two transcripts, *shakB(N)* and *shakB(N+16)*, with the latter having a 16-amino-acid extension at its N-terminus (Phelan *et al.*, 2017). These isoforms contribute to the relationship between giant fibers and their postsynaptic targets (Pézier *et al.*, 2016).

1.5 Bioamines and their receptor

1.5.1 Overview of Bioamines

Biogenic amines are organic compounds found in vertebrate and invertebrate organisms. They are derived from amino acids through chemical processes. These compounds, neurotransmitters, neuromodulators, and hormones are important in regulating various physiological functions and behaviours. The significance of bioamines is in their ability to facilitate nervous system communication, thereby influencing various biological activities (D'Aniello *et*

al., 2020). By transmitting signals across synapses, they enable swift and efficient communication within the nervous system (Baumann *et al.*, 2009; Malenka, 2010).

To understand how bioamines apply their effects, it is essential to examine their interaction with membrane receptors (Scheiner *et al.*, 2006). These receptors are primarily G-protein coupled receptors (GPCRs), which, once activated, initiate a series of intracellular signalling pathways that culminate in various physiological responses (Gurevich *et al.*, 2019). Moreover, due to biogenic amines' involvement in various neurological activities, the study of biogenic amines extends to exploring human disorders, particularly in the context of neurotransmission and endocrine function (Uçar, 2019).

1.5.2 Key Biogenic Amines in *Drosophila*

In *Drosophila*, these aminergic neuroactive molecules promote neural communication and influence biological activities (Cattabriga *et al.*, 2023). The main types of biogenic amines include octopamine, dopamine, tyramine, tryptamine and serotonin. Each amine interacts with specific receptors, modulating behaviours and physiological responses for the organism's survival and adaptation (Blenau *et al.*, 2001).

1.5.2.1 Octopamine

Octopamine is a biogenic amine synthesised from tyramine, derived from the amino acid tyrosine, through the action of tyramine B-hydroxylase (Roeder, 1999; Roeder, 2005). Functionally and structurally similar to norepinephrine in vertebrates, octopamine plays an important role in the neurophysiology of insects (Blenau and Baumann, 2001). In *Drosophila*, octopamine involves many physiological processes and behaviours, such as regulating aggression, locomotion, feeding, and stress responses (Farooqui, 2012).

The synthesis of octopamine is accomplished in specific groups of neurons within the central nervous system (CNS) and the peripheral nervous system (PNS) (Rosikon *et al.*, 2023). This synthesis involves the enzymatic conversion of tyramine to octopamine (Roeder *et al.*, 2005). Octopamine-expressing neurons in *Drosophila* melanogaster display an extensive distribution in the CNS, experience many developmental transformations, and have different roles in influencing behaviour and neuromuscular function (Farooqui, 2012; Monastirioti *et al.*, 1995). Moreover, these neurons exhibit a stereotypic distribution pattern (Busch *et al.*, 2009), suggesting that the synthesis and release of octopamine are highly regulated processes.

1.5.2.2 Dopamine

Dopamine is another major biogenic amine that regulates various physiological and behavioural processes in *Drosophila*. Produced from the amino acid tyrosine via the enzymes tyrosine hydroxylase and DOPA decarboxylase (Daubner *et al.*, 2011; Friggi-Grelin *et al.*, 2003), dopamine is essential for regulating locomotor activity, learning, and memory (Berry *et al.*, 2012). Dopamine depletion in *Drosophila* leads to decreased movement and impaired coordination (Naz *et al.*, 2020), highlighting its importance in motor control. In addition, dopamine contributes to forming memories, especially those linked to reward (Abraham *et al.*, 2014), and affects feeding behaviour (Eriksson *et al.*, 2017). Moreover, dopamine regulates arousal and sleep, with dopaminergic activity promoting wakefulness (Ueno *et al.*, 2012). Its functions in *Drosophila* show similarities to those in vertebrates, where dopamine affects locomotion, cognition, and development (Mustard *et al.*, 2005).

1.5.2.3 Tyramine

Tyramine, closely related to octopamine biogenic amines, is synthesised from tyrosine by the enzyme action of tyrosine decarboxylase (Marcobal *et al.*, 2012). This synthesis occurs within specific neuronal populations in the CNS (Schützler *et al.*, 2019). It is essential in the neurophysiology of *Drosophila* melanogaster (Roeder, 2020; Cole *et al.*, 2005). Through its interaction with specific

receptors, tyramine regulates neural and physiological processes necessary for survival and adaptation. Tyramine influences locomotion and feeding behaviours similarly to other biogenic amines like octopamine and dopamine (Schützler *et al.*, 2019). Studies indicate that disruptions in tyramine levels can affect motor functions (Pirri *et al.*, 2009). Additionally, tyramine modulates stress responses, allowing *Drosophila* to adapt to environmental changes by adjusting their metabolic and physiological conditions (Chentsova *et al.*, 2002). Its role extends to reproductive behaviours, such as mating (Huang *et al.*, 2016). Although it is less abundant than other biogenic amines like dopamine and octopamine, it performs essential functions as a neuromodulator and a precursor for octopamine (Lange, 2009).

1.5.2.4 Serotonin

Another biogenic amine involved in numerous physiological functions and behaviours is serotonin (5-hydroxytryptamine, 5-HT). It is produced through a series of chemical reactions starting with the amino acid tryptophan (Walther *et al.*, 2003). The enzyme tryptophan hydroxylase (TPH) adds a hydroxyl group to tryptophan, converting it into 5-hydroxytryptophan (5-HTP). Next, 5-HTP is decarboxylated by aromatic L-amino acid decarboxylase (AADC), resulting in the creation of serotonin (Li *et al.*, 2014; Wang *et al.*, 2023; Watanabe *et al.*, 2011).

Serotonin in *Drosophila* participates in circadian rhythm modulation, mood regulation, aggression, sleep, and learning activities (Bacqué-Cazenave *et al.*, 2020). In regulating circadian rhythms, serotonin interacts with the brain's central clock neurons, notably the ventral lateral neurons (LNvs), to maintain circadian rhythm stability (Yuan *et al.*, 2005; Hamasaka *et al.*, 2006). The 5-HT1B receptor affects light sensitivity of the circadian clock via modulating the activity of glycogen synthase kinase 3 beta (GSK3B), which regulates the stability of the timeless (TIM), a critical circadian component (Yuan *et al.*, 2005; Barnard *et al.*, 2008). In addition to these neural roles, serotonin also acts as a diuretic factor in *Drosophila* Malpighian tubules, where it stimulates fluid secretion and contributes to the regulation of renal function (Dow and Davies, 2006; Halberg *et al.*, 2015).

1.5.2.5 Tryptamine

Tryptamine is synthesised in *Drosophila* through the decarboxylation of tryptophan, a process catalysed by tryptophan decarboxylase (Ruddick *et al.*, 2006). It performs as the precursor to serotonin and melatonin in the brains of mammals (Jones, 1982; Kema *et al.*, 2000). In *Drosophila*, it relates to reproduction, olfaction, and behaviour modulation (Blenau and Baumann, 2001).

In influencing reproductive functions, tryptamine primarily impacts oviposition, the process by which female flies lay eggs (Thomas *et al.*, 1998). In olfaction, tryptamine, as an antagonist to odorant responses, modulates olfactory sensitivity by interacting with olfactory receptors (Chen *et al.*, 2014). This modulation potentially influences foraging and mating behaviours. Additionally, tryptamine maintains water and ion balance by controlling the secretion rates of Malpighian tubules (Thomas *et al.*, 1998).

1.5.3 Biogenic Amine Receptors in Drosophila

1.5.3.1 Overview of Biogenic Amine Receptors

Biogenic amine receptors in *Drosophila* regulate different physiological and behavioural processes. They primarily belong to the GPCR family (Baumann *et al.*, 2009). When a biogenic amine binds to its receptor, it induces a conformational change in the receptor, activating intracellular G-proteins and initiating signalling cascades. These cascades alter enzyme activity, ion channel function, and gene expression, thus impacting the fly's physiology and behaviour (Monastirioti, 1999; Rosikon *et al.*, 2023; Baumann *et al.*, 2009).

1.5.3.2 Octopamine Receptor

Octopamine binds to the Octopamine-Tyramine receptor (Oct-TyrR), β-adrenergic-like (OctβR) and α2-adrenergic-like (Octα2R) (Nakagawa *et al.*, 2022). When octopamine binds to these receptors, it triggers intracellular signalling cascades, increasing cAMP levels in different systems and resulting in various physiological responses (Han *et al.*, 1998). The differential expression of

these receptors across various tissues enables octopamine to regulate different physiological processes and behaviours in *Drosophila*.

1.5.3.3 Dopamine receptors

Dopamine influences cellular activity through its binding to dopamine receptors, which are divided into two types of dopamine receptor families in *Drosophila*: D1-like (dDA1, DAMB) and D2-like receptors (DD2R) (Qi and Lee, 2014). These GPCRs mediate different physiological responses by modulating adenylate cyclase activity. Specifically, D1-like receptors activate adenylate cyclase, leading to an increase in cAMP levels, while D2-like receptors inhibit adenylate cyclase, resulting in decreased cAMP levels (Podda *et al.*, 2010; Vonk *et al.*, 2008).

1.5.3.4 Tyramine Receptors

In *Drosophila*, the main receptors for tyramine are TyrR, TyrRII, TyrRIII and Oct-TyrR, which also interact with octopamine (El-Kholy *et al.*, 2015; Huang *et al.*, 2016). These receptors modulate intracellular signalling pathways by inhibiting adenylate cyclase activity, reducing cAMP levels (Bayliss *et al.*, 2013). However, this mechanism contrasts with octopamine's stimulatory effects on cAMP production, as octopamine receptors increase intracellular cAMP levels (Nakagawa *et al.*, 2022). The differential expression of these receptors across various tissues enables tyramine to influence physiological processes and behaviours in *Drosophila*.

1.5.3.5 Serotonin Receptors

Like other biogenic amines, serotonin also affects the physiology and behaviour of *Drosophila* through interactions with specific serotonin receptors. There are four primary serotonin receptors: 5-HT1A, 5-HT1B, 5-HT2, and 5-HT7 in *Drosophila*, each displaying different intracellular pathways and differential expression (Johnson *et al.*, 2009). The 5-HT1A and 5-HT1B receptors inhibit adenylate cyclase, affecting cAMP levels, and contribute to mood and stress

regulation (Sampson *et al.*, 2020; Xiong *et al.*, 2019). The 5-HT2 receptor activates phospholipase C, increasing inositol triphosphate (IP3) and diacylglycerol (DAG) levels. This activation influences muscle contraction and neuronal excitation, illustrating serotonin's broad impact on *Drosophila*'s motor functions and neural activities (Singh *et al.*, 2016; Blenau and Baumann, 2001; Gu and Singh, 1997). Furthermore, the 5-HT7 receptor, mainly found in the central nervous system, modulates circadian rhythms by influencing clock protein stability and gene expression (Yuan *et al.*, 2005; Becnel *et al.*, 2011), indicating that serotonin is involved in maintaining daily biological cycles and adapting to environmental changes.

This thesis describes the identification of genes of interest, the development of genetic resources for these genes, and the assessment of their phenotypic effects on tubule morphology, cellular structure, physiology, transcriptomes and metabolomes. This thesis takes as its starting point the view that genes with high and cell type specific expression in the Malpighian tubules are likely to have important roles in tubule function. This reasoning comes from transcriptomic resources, including FlyAtlas/FlyAtlas2 and single-cell datasets, which consistently show strong enrichment of certain candidates in principal or stellate cells. On this basis, a small number of genes were selected for detailed study, including the gap junction proteins Innexin 2 and Innexin 7, and the octopamine receptor $Oct\alpha 2R$. These genes represent different forms of regulation: local cell-cell communication through gap junctions and hormonal control of secretion.

To test their importance, this work mainly applies reverse genetic approaches, using RNA interference together with cell-type specific expression through the GAL4/UAS system. These tools provide a direct way to assess gene function in selected tissues. Other reverse genetic methods, such as CRISPR/Cas9, are also available in *Drosophila* and offer complementary strengths, but they were not applied in the experiments described here. Reverse genetics depends on prior assumptions from expression data and may miss genes that act redundantly or unexpectedly, whereas forward genetic screens are unbiased and can reveal novel regulators, although they are more time-consuming and often require

extra steps to identify the affected gene. By choosing a reverse genetic strategy, and where possible complementing it with classical tools such as enhancer traps and reporters, the thesis seeks to test predictions from transcriptomic evidence and connect them to functional outcomes.

The overall aim is to find out how genes enriched in the Malpighian tubules contribute to renal function at different levels, from tubule structure to fluid secretion, gene expression, and metabolite patterns. The central hypothesis is that genes expressed in principal cells regulate epithelial coupling and cation transport, while those expressed in stellate cells regulate chloride and water fluxes. Changing the activity of these genes is expected to alter secretion and ion balance, with predictable shifts in gene expression and metabolites, while restoring their activity should reverse these effects. In this way, the thesis aims to explain how a set of tubule-enriched genes shape the physiology of the *Drosophila* renal system, while also recognising that expression alone does not prove function and that genetic methods have both strengths and limitations.

Chapter 2 Materials and Methods

2.1 Drosophila melanogaster Stock & Maintenance

2.1.1 Fruit Fly Stocks

The *Drosophila melanogaster* stocks used are summarised in Table 2.1, which provides detailed information on the fly IDs, genotypes, descriptions, and relevant references. These stocks were sourced from the Bloomington *Drosophila* Stock Centre (BDSC) and the Vienna *Drosophila* Resource Centre (VDRC). The Dow/Davies lab maintained wild-type flies and the driver lines.

Fly ID	Genotype	Description	Reference	
Canton S	W+; +/+; +/+	Wildtype. Used for controls	Dow/Davies lab stock	
W ¹¹¹⁸	W ¹¹¹⁸ ; +/+; +/+	Used for controls	Dow/Davies lab stock	
C724-Gal4	w ⁻ ; +/+; c724-GAL4/c724-GAL4	Gal4 enhancer trap specific to	Dow/Davies lab stock	
		stellate cells of Malpighian tubules	(Sozen et al., 1997)	
CapaR- <i>GAL4</i>	w ⁻ ; +/+; CapaR-GAL4/CapaR-GAL4	Gal4 enhancer trap specific to	Dow/Davies lab stock	
0.00 V 0.00 V 4.00 V 0.00 V	A serie Konse Konse materialismos estados arche	principal cells of Malpighian tubules	(Terhaza et al., 2012)	
UAS-Inx2 RNAi Lines				
42645	y¹ sc*v¹sev²¹; P{TRiP.HMS02481}attP2	Knocks down Inx2 expression	BDSC	
80409	y1 v1; P{TRiP.HMS05974}attP40/CyO	by RNAi	BDSC	
90966	y¹w ⁶⁷ ° ²³ ; P{UAS-Inx2.RR.RFP}attP2	Expresses RNAi-resistant Inx2 with a C-terminal RFP tag under UAS control	BDSC	
V102194	P{KK111067}VIE-260B	Knocks down Inx2 expression by RNAi	VDRC	
UAS-Inx7 RNAi Lines				
10000000000			BDSC	
85083	w ¹¹¹⁸ P{XP}Inx7 ^{d00942}		(Thibault et al., 2004)	
v22948	w ¹¹¹⁸ ; P{GD12738}v22948	Knocks down Inx7 expression by RNAi	VDRC	
v22949	w ¹¹¹⁸ ; P{GD12738}v22949		VDRC	
v103256	P{KK112684}VIE-260B		VDRC	
CG6602				
v18900	w ¹¹¹⁸ ; P{GD6037} v18900	Knocks down CG6602 expression	VDRC	
v106125	P{KK103128}VIE-260B	by RNAi	VDRC	
Octa2R				
50678	y¹ v¹; P{TRiP.HMC03079}attP2	V	BDSC	
v10214	w ¹¹¹⁸ ; P{GD3056}v10214	Knocks down CG18208 expression by RNAi	VDDC	
v10215	w ¹¹¹⁸ ; P{GD3056}v10215/TM3		VDRC	

Table 2.1. Fly lines were used during this study. BDSC: Bloomington *Drosophila* Stock Center, VDRC: Vienna *Drosophila* Research Centre. (TM3 and CyO are balancer chromosomes for the third and second chromosomes, respectively.

2.1.2 Fruit Fly Maintenance

All *Drosophila melanogaster* stocks were maintained on standard fly medium in vials under controlled conditions: a 12-hour light/12-hour dark (L/D) cycle, a constant temperature of 25°C, and 55% atmospheric humidity. Adult flies were transferred to fresh vials every two weeks, except when flies of specific ages were required for experimental purposes. A breeding population of approximately 18 females and 9 males were transferred to fresh vials every three days to ensure consistent egg-laying and progeny production. The progeny was collected on the day of emergence (day 0) to provide age and developmental stage uniformity. These newly emerged flies were then maintained under the same controlled conditions and used in experiments seven days post-emergence. This seven-day period ensured that the flies had reached sexual maturity and were physiologically stable for experimental use.

2.1.3 Drosophila Crossing and Rearing Crosses

The UAS-GAL4 system was utilised to generate gene knockdowns within the Malpighian tubules. The procedure involved crossing virgin female flies from UAS-RNAi lines with males expressing GAL4 or, conversely, crossing virgin females from GAL4 lines with UAS-RNAi males. These crosses were performed using 3-5 virgin females and 6-10 males. These genetic crosses were maintained under controlled conditions at 25°C, with regular transfers to fresh vials every three days to sustain optimal conditions. The transgene expression was confirmed using visual markers and qPCR analysis.

To generate a steady population of virgin flies for subsequent experiments, a group of approximately 30 flies—consisting of 20 females and 10 males—was transferred to fresh vials every 2-3 days to allow for egg laying. Adult progenies were collected as they emerged, and virgin females were isolated for further crossing experiments.

2.1.4 Drosophila Diet

Flies were reared on a standard *Drosophila* medium composed of yeast cornmeal, sucrose, and agar, as detailed in Table 2.3. The food was stored in 50 ml vials at 4°C until used.

Per 1 litre of food recipe

- 1. 10 g agar
- 2. 15 g sucrose
- 3. 30 g glucose
- 4. 35 g dried yeast
- 5. 15 g maize meal
- 6. 10 g wheat germ
- 7. 30 g treacle
- 8. 10 g soy flour
- 10 ml Nipagin (25 g Nipagin M (<u>Tegosept</u> M, p-hydroxybenzoic acid methyl ester) in 250 ml Ethanol]
- 10. 5 ml Propionic acid

Table 2.2. Recipe of standard *Drosophila* medium (Cabrero et al., 2014).

2.2 Fluid Secretion Assay

2.2.1 Fruit Fly Tissue Dissection and Preparation for Fluid Secretion Assay

Schneider's insect culture medium (Thermo Fisher) was used throughout the dissection process. Before dissection, the 7-10 days old adult flies were anesthetised by placing them on ice. Once anesthetised, the flies were carefully transferred to a dissecting dish containing Schneider's liquid medium. The Malpighian tubules were then dissected from the abdomen using fine dissecting forceps (Dumont No. 5 Biology Grade Dissecting Forceps), allowing for carefully isolating the tubules from surrounding tissues.

After dissection, the Malpighian tubules were delicately transferred to prepared secretion plate wells using a 3 mm diameter glass rod pulled to a fine (100 μ m tip). The secretion plate was prepared by filling a petri dish with paraffin wax, allowing it to cool, and then creating 21 small wells arranged in three lanes using a 2 mm bit. Subsequently, 21 entomological 'minuten' pins were inserted adjacent to the wells. Mineral oil was then used to cover the dish, maintaining a stable environment for the assays. (Davies et al., 2019).

Each well was filled with a prepared medium composed of a 1:1 (v/v) mixture of Schneider's insect culture medium (Thermo Fisher)(Appendix 1) and D. *melanogaster* saline (117.5 mM NaCl, 20 mM KCl, 25 mM MgCl₂, 2 mM CaCl₂, 10.2 mM NaHCO₃, 4.5 mM Na₂HPO₄, and 8.6 mM HEPES, and 20 mM Glucose freshly added).

Figure 2.3 illustrates the procedure used to isolate and prepare Malpighian tubules for fluid secretion assays. The diagram shows the dissection of anterior and posterior tubules from the gut, their separation from surrounding tissues, and subsequent transfer into bathing solution for secretion measurements. This schematic helps to visualise the workflow described in this section, from tissue isolation to the setup used for secretion assays.

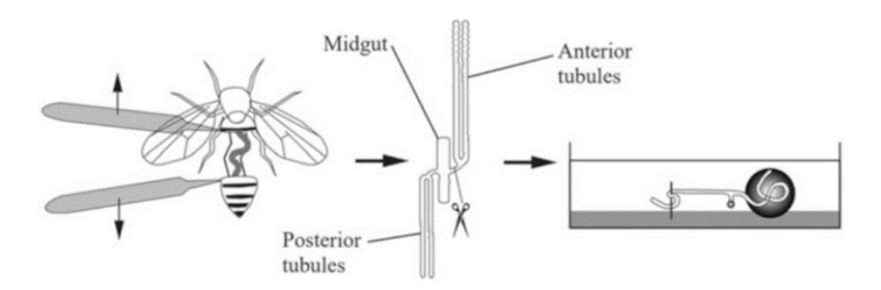


Figure 2.3 The dissection and preparation of the tubules for fluid secretion assays. Schematic showing the isolation of anterior and posterior Malpighian tubules from adult *Drosophila*. After separation from the midgut, the tubules are transferred into a drop of bathing solution for measurement of fluid secretion (Davies *et al.*, 2019).

In the fluid secretion assay, the volume of secreted fluid was measured using a method that assumes the secreted fluid droplet forms a perfect sphere. The diameter of the droplet was measured using an ocular micrometre under a stereo dissecting microscope, and this diameter measurement was then converted into a volume using the formula for the volume of a sphere. Detailed formulas and specific calculation steps are provided in Appendix 2. Then, secretion droplet volumes were used to calculate the secretion rate in nl/min by dividing the volume by the 10-minute interval between measurements for each tubule pair.

2.2.2 Data Analysis for Fluid Secretion Assay

The mean secretion rate and the standard error of the mean (SEM) are calculated at 10-minute intervals to measure changes in fluid secretion over time. A series of formulas are used to compare and calculate the percentage increase in fluid secretion after stimulation. First, the difference between the maximum secretion rate observed after stimulation and the average (mean) secretion rate before stimulation is determined. This difference represents the increase in secretion rate due to stimulation. Next, this difference is divided by the mean basal secretion rate (the average rate before stimulation) to normalise the increase relative to the baseline activity. Finally, the result is multiplied by 100 to convert it into a percentage. This method quantitatively assesses the effect of different stimulations on fluid secretion in a standardised manner. Additionally, to assess if there were significant differences in secretion rates between the three biological groups, one-way ANOVA and independent t-tests were performed for each secretion rate measurement. Multiple comparisons were employed in a typical secretion assay, observing basal secretion rates and those following peptide stimulation to compare each fly line.

2.3 Wet and Dry Weight Measurements

Adult male and female flies were anesthetised with CO₂ separately. Groups of 20 males and 20 females were then placed into Eppendorf tubes, chilled on ice, and immediately weighed using a GR-202 precision balance to determine their wet weight. After recording the wet weight, the flies were frozen at -80°C for 20 minutes, followed by a desiccation process at 60°C for 24 hours. A small hole was made in the lids of the Eppendorf tubes, allowing moisture to escape during the desiccation process. After drying, their dry weight was remeasured. The difference between the wet and dry weights was then calculated to determine the water content of the flies. Total body water weight was calculated by subtracting dry weight from wet weight. To calculate water loss over 24 hours for each genotype, the water content at 24 hours was subtracted from that at 0 hours. Each measurement was repeated in three replicates with 20 flies per line. The data were analysed using GraphPad Prism 10.0 software, and statistical significance was assessed using a one-way ANOVA.

2.4 RNA Extraction

RNA was extracted from *Drosophila* melanogaster samples to provide material for transcriptomic analyses. Both whole-fly samples and dissected Malpighian tubules were processed, allowing comparisons between organism-wide expression and tissue-specific expression. Extractions were performed using Qiazol Lysis Reagent together with the Qiagen miRNeasy Mini Kit, according to the manufacturer's instructions. The procedures for whole-fly and tubule extractions are described in detail in sections 2.4.1 and 2.4.2.

2.4.1 Whole-Fly RNA Extraction

Adult *Drosophila* were first anesthetised on ice for whole-fly RNA extraction. The flies were then collected into 1.5 ml Eppendorf tubes containing 1000 μ l of Qiazol reagent and homogenised using a micropestle. Following homogenisation, 200 μ l of chloroform was added to the solution. The samples were left to stand for 5 minutes at room temperature, vortexed vigorously for 30 seconds, and then allowed to stand for an additional 3 minutes. The solution was centrifuged at 12,000xg for 15 minutes at 4°C and then was carefully transferred to a new 1.5 ml tube. To precipitate the RNA, 1.5 volumes of 100% ethanol were added and mixed thoroughly by pipetting. The RNA extraction was then completed using the Qiagen miRNeasy Mini Kit, and the RNA was eluted in 30 μ l of RNase-free water. The eluted RNA was stored at -80°C.

2.4.2 Malpighian Tubules RNA Extraction

Malpighian tubules were dissected from 7-day-old adult *Drosophila*. Approximately 20-25 adults were anesthetised on ice and then dissected in *Drosophila* Schneider's medium. The dissected tubules were immediately transferred to an Eppendorf tube containing 500 µl of Qiazol Lysis Reagent (Qiagen). After extraction, the concentration of total RNA was measured using a Nanodrop spectrophotometer, with the A260/280 absorbance ratio recorded to assess the purity of the RNA samples.

2.5 Complementary DNA synthesis (cDNA)

Complementary DNA (cDNA) was synthesised from RNA using the SuperScript II reverse transcriptase, following the manufacturer's protocol (Qiagen, UK). The reaction mixture was prepared by combining 500 ng of total RNA, 1 μ l of Oligo(dT)_{12_18} primers (IDT, U.K.), 1 μ l of dNTP mix (10 mM) (Promega), 4 μ l of 5X First Strand Buffer, 2 μ l of DTT (0.1 M), and 1 μ l of RNaseOUT inhibitor (40 units/ μ l, Invitrogen). The total volume of the reaction was adjusted to 19 μ l with RNase-free water. The mixture was incubated at 42 °C for 10 minutes using a PCR block to initiate the reverse transcription process, then chilled on ice for 1 minute. Subsequently, 1 μ l of SuperScript II reverse transcriptase was added to each reaction tube, followed by a quick centrifugation. The samples were then incubated at 42 °C for 50 minutes, followed by a 15-minute incubation at 70 °C. The synthesised cDNA was stored at -20 °C.

2.6 Primer Design

The gene of interest is selected, and the NCBI Primer-BLAST tool is accessed online. The transcript sequence is then input into Primer-BLAST to generate potential primers. Matching primers are selected and documented from the resulting candidates. Quality control (QC) is then performed using IDT's OligoAnalyzer Tool, and the primer sequences are analysed for properties such as hairpin formation, self-dimerisation, and heterodimerisation, with specific thresholds for melting temperature (Tm) and free energy (dG) values guiding the selection process. This QC process is repeated for the reverse primer. The UNAFold software assesses the amplicon sequence for secondary structure formation, with parameters set for DNA folding and magnesium ion concentration. The predicted structures are inspected to ensure they meet the required criteria, specifically that their Tm is lower than the primer annealing temperature.

The primers listed in Table 2.4 were subsequently used in RT-qPCR assays to specifically amplify target cDNAs from Malpighian tubule RNA. Relative transcript levels were determined by analysing Ct values after normalisation to the reference gene RpL32, thereby providing an experimental validation of expression patterns predicted from transcriptomic datasets. Two additional Octα2R primers, designed but not used in this study, are provided in Appendix 3.

Primer	Forward	Reverse
CG6602	ATGTCTGGCGAAATGAGGCA	CACCTCCAACTTCAGAGCGA
Octa2R	ATCATCGTGGTGGGCAACAT	TAGCTCATTGGCCAGCGAAA
lnx2	CAACGAGTGAGGAACCCGAAAG	TGCACACCTGGTCGATCTTCA
lnx7	CCAAAACCGAAGATAACGAAGGC	GAAGAACAGGACAAAGGGCAC

Table 2.4 Primers used for quantitative PCR. Forward and reverse primer sequences for CG6602, Octα2R, Inx2, and Inx7, which were designed and applied in qPCR assays to analyse gene expression in *Drosophila* Malpighian tubules.

2.7 The Polymerase Chain Reaction (PCR)

PCR was carried out to amplify target gene fragments for validation of primer specificity and subsequent analyses. Reactions were set up using the DreamTaq Green PCR Master Mix (Thermo Fisher Scientific), which contains DreamTaq Green buffer, DreamTaq DNA Polymerase, dNTPs (0.4 mM each), and 4 mM MgCl₂. Each 20 µl reaction consisted of 1 µl forward primer, 1 µl reverse primer, 1 µl cDNA template, 10 µl master mix, and 7 µl RNase-free water. Amplifications were performed in 20 µl PCR tubes using the Applied Biosystems StepOne™ Real-Time PCR System. The thermal cycling programme is summarised in Table 2.5. Amplified products were verified by agarose gel electrophoresis to confirm expected fragment sizes and primer specificity.

Step	Temperature	Time	Description	Number of cycles
Initial denaturation	95°C	10 mins	To denature the cDNA	1
Denaturation	95°C	15s	To continually denature cDNA after each synthesis step	
Annealing	58.1~62°C	1 min	Temperature is set depending on the melting temperature of the primers used; typically, ~5°C lower than Tm.	35~40
Extension	72°C	1 min	Extension time is set at the rate of base pairs/sec	
Final Extension	72°C	5 mins	The final extension of incomplete synthesised strands of DNA	1

Table 2.5: PCR cycling conditions using Taq DNA polymerase. Summary of the thermal cycling programme used for amplification, showing the temperatures, times, and number of cycles for each step. Annealing temperatures were adjusted according to the melting temperature (Tm) of the primers.

2.8 Agarose Gel Electrophoresis

The quality and specificity of PCR products or DNA were assessed by running on a 1% agarose TBE gel. The gel was prepared in 0.5x TBE (Appendix 4), containing 0.1 µg/ml ethidium bromide (EtBr), using 0.5x TBE as the electrophoresis buffer. A 1 kb DNA ladder (Invitrogen) was used as a molecular weight marker to determine the size of the samples. Agarose gel electrophoresis was run at 100 V. Following the electrophoresis, the DNA bands were visualised using a high-performance ultraviolet (UV) transilluminator (UVP, UK).

2.9 SYBR Green-based Quantitative Real-time PCR(qPCR)

For the SYBR Green-based quantitative real-time PCR (qPCR) method, cDNA samples, primers, and RNase-free water were prepared in seven mini-Eppendorf tubes. These components were combined with SYBR Green PCR Master Mix (Agilent Technologies) and processed using the Applied Biosystems Real-Time PCR system. Each reaction mixture was composed of 10 μ l of 2X SYBR Green Master Mix, 1 μ l of forward primer, 1 μ l of reverse primer, and 1 μ l of cDNA, with the final volume adjusted to 20 μ l using RNase-free water. The following section describes the qPCR cycling protocol used in this study (Table 2.6).

Step	Temperature	Time	Number of cycles
Denaturation	95°C	10 mins	
Denaturation	95°C	15s	
Annealing	55-60°C	1 min	
Extension	72°C	1 min	40
Absorption reading	76°C	15s	
Incubation	7 2°C	1 min	
Melting curve	60-95°C	Read every 0.3°C	

Table 2.6: SYBR Green master mix qPCR cycling parameters. Thermal cycling profile used for quantitative PCR, including denaturation, annealing, extension, absorption reading, incubation, and melting curve analysis.

All qPCR reactions were triplicated using three biological replicates with target gene primers. The ribosomal protein gene Rpl32, a housekeeping gene, was used as an internal control to standardise the qPCR reactions. After amplification, the threshold cycle (Ct) values for the target genes and Rpl32 were determined for each sample. For the relative quantification of gene expression, the $\Delta\Delta$ Ct method was utilised. This approach involves calculating the difference in ΔCt values between the experimental and control groups ($\Delta\Delta$ Ct = Δ Ct (experimental) - ΔCt (control)). The relative expression of the target gene in the experimental group compared to the control group was determined using the 2^{-4} formula, yielding a fold change value. A fold change greater than one suggests upregulation of the target gene, while a value less than one indicates downregulation of the target gene. Three biological replicates were analysed. The mean Δ Ct values from three replicates were used to calculate the $\Delta\Delta$ Ct values and relative expression levels. The resulting data were analysed and presented as mean ± SEM using GraphPad Prism 10.0 software. For statistical analysis, one-way ANOVA was used to assess the significance of differences among multiple samples. At the same time, a Student's t-test was also applied to compare two paired samples.

2.10 Transcriptomics

2.10.1 Sample Preparation and Dissection

2.10.1.1 Malpighian tubules

Seven-day-old adult flies were selected for transcriptomic analysis of *Drosophila* melanogaster Malpighian tubules. The dissection was done in phosphate-buffered saline (PBS). Tubules were processed in batches and separated from the gut at the lower ureter to avoid contamination from other tissues. Once isolated, the dissected tubules were transferred into Qiazol, and RNA was isolated as described above.

2.10.1.2 Whole-fly RNA Preparation

Seven-day-old *Drosophila* melanogaster was selected for whole-fly preparations. The flies were anesthetised by placing them on ice. Once anesthetised, the flies were quickly collected and put into pre-cooled Eppendorf tubes. Qiazol was added to the flies and stored at -80C. RNA was isolated as described above.

2.10.2 RNA sequencing (RNA-seq)

Isolated RNA was sequenced at the Molecular Analysis Facility within the MVLS Shared Research Facilities at the University of Glasgow. Here, they first checked the quality of the RNA using an Agilent Bioanalyzer. Sequencing was then completed using the NextSeq 2000 system, which provided the capability to generate vast amounts of sequencing data. The high-resolution data produced by NovaSeq 2000 allowed for detailed and accurate transcriptome profiling.

2.11 Metabolomics

2.11.1 Sample Preparation

Flies aged 7 days old were anesthetised on ice. Malpighian tubules were dissected as described in section 2.10.1.1. The tubules were prepared in small groups and carefully detached from the gut at the lower ureter, ensuring

minimal risk of contamination. After separation, the tubules were placed in Qiazol to preserve RNA, which was subsequently extracted following previously outlined protocols.

2.11.2 Liquid Chromatography-Mass Spectrometry

Liquid Chromatography-Mass Spectrometry (LC-MS) was used to separate and identify metabolites in the *Drosophila* samples. LC allows metabolites to be separated according to their chemical properties, such as polarity, while MS provides sensitive detection and quantification. Together, LC-MS is widely applied in metabolomics because it enables the analysis of a broad range of small molecules within complex biological samples.

The samples were analysed using LC-MS in quadruplicate, ensuring reliable and reproducible results. The analysis was completed at Glasgow Polyomics' metabolomics facility (GPMF) using a QExactive Orbitrap mass spectrometer (MS) from Thermo Fisher Scientific, constructed to operate in a mode that alternates between positive and negative mode. The MS was integrated with a highperformance liquid chromatography system (Dionex UltiMate 3000 Rapid Separation LC) to separate metabolites. A zwitterionic column (ZIC-pHILIC, 150 x 4.6 mm, Merck, Sequant, UK) was used, effectively separating polar and hydrophilic metabolites, including carbohydrates, organic acids, amino acids and nucleotides. The samples were maintained at a low temperature (5 °C) to prevent degradation, and 10 µL of each sample was injected into the column for analysis. The column was run at 30 °C. The separation process utilised a linear gradient elution method involving two methods: 20 mM ammonium carbonate (referred to as A) and acetonitrile (referred to as B). The flow rate was set to 0.3 mL per minute. The elution process consisted of several phases: initially increasing A from 20% to 80% (over 30 minutes), followed by a wash step with 92% A for 5 minutes (31-36 min), and finally, a 9-minute re-equilibration at 20% A (37-46).

In addition to analysing the *Drosophila* samples, a standard reference library of approximately 240 metabolites maintained by Glasgow Polyomics was also tested under identical experimental conditions. Except for LC-MS analysis, fragmentation data (LC-MS/MS) was also collected in this mode. The process involved a full MS1 scan and selecting the ten most intense ions. These ions were then transferred to a collision cell, which was fragmented to generate MS/MS data. At the end of these experimental runs, the data obtained in both ionisation modes were converted from the proprietary form into open-format MS data mzXML (MS1 data) and mzML (MS/MS data).

2.11.3 LC-MS Data Processing and Analysis

The initial processing of LC-MS/MS data was carried out using the Glasgow Polyomics integrated Metabolomics Pipeline (GPMP), a specialised platform for metabolomics data processing (Gloaguen et al., 2017). The tissue and aged fly samples were subjected to the same LC-MS analysis method (LC-MS/MS analysis) in separate batches. However, once the LC-MS data was collected, the processing through GPMP was organised into two single runs—one specifically for the tissue samples and the other for the aged fly samples. This approach allowed for a direct comparison of the metabolomic data between individual tissues or different ages of the file.

To process the data obtained from the LC-MS analysis, the information for both positive and negative ionisation modes was loaded into the GPMP (Gloaguen et al., 2017). MS1 data (mzXML files) were uploaded to the GPMP in quadruplicate. Calibration samples were also uploaded, including blanks and pooled quality control (QC) samples. The fragmentation data was loaded in mzML format, and the standard compound library files were uploaded in CSV format.

Data processing within GPMP involves several key steps to extracting and interpreting information from the LC-MS data. First, features are detected and aligned using XCMS, a LC/MS-based data analysis tool (Smith *et al.* 2006). After alignment, batch correction is applied. The following steps involve annotating

and identifying the LC-MS detected peaks using mzMatch (Scheltema *et al.* 2011). MS/MS data is extracted and linked to the features identified in the MS1. This is done using GPMP's Fragmentation Annotation Toolkit using MSPepSearch and the NIST 14 MS/MS spectral library.

The features detected in the LC-MS data are represented as peaks. Each of these peaks can be described by three information: the mass-to-charge ratio (m/z), the retention time (RT) and the signal intensity ((I), relative abundance). For further analysis, the data from all detected peaks, including their respective compound annotations, were exported from GPMP in JSON format.

Chapter 3 Functional Roles of the Gap Junction Genes Innexin 2 and Innexin 7 in *Drosophila*Malpighian Tubules

3.1 Summary

This chapter investigates the roles of the gap junction proteins Innexin 2 and Innexin 7 in the Malpighian tubules of *Drosophila* melanogaster, where they are strongly expressed but their functions are not well understood. Using RNA interference with the GAL4/UAS system, I selectively reduced their expression in principal cells, and confirmed the effectiveness of the knockdown by quantitative PCR. Fluid secretion assays and microscopic examinations were then performed to evaluate how reduced innexin expression influenced tubule function. The results showed that knockdown of *Inx2* and *Inx7* did not significantly alter basal secretion rates, but *Inx2* knockdown flies displayed a modest change in the response to kinin stimulation, suggesting a role in modulating hormonal sensitivity. These findings provide the first functional evidence for innexins in the *Drosophila* renal system, highlighting their contribution to intercellular communication between principal and stellate cells and their importance in maintaining epithelial coordination and homeostasis.

3.2 Identification of Innexin Gene Specifically and Highly Expressed in Malpighian Tubules

3.2.1 Introduction

After Krishnan and collaborators described the first *innexin* gene in 1993 (Krishnan et al., 1993; Güiza et al., 2018), Bauer et al. (2004) showed that *Inx2* is essential for establishing and maintaining cell polarity, epithelial organisation, and morphogenesis in *Drosophila* embryos. They analysed the phenotype of *Inx2* mutants (*kropf*), where loss of *Inx2* leads to large cuticular holes and disrupted epithelial morphogenesis. These mutants exhibit defects in epithelial tissue development, including impaired cell polarity and organisation, and they lack both maternal and zygotic *Inx2* contributions. A combination of maternal and zygotic inputs is required for normal epithelial development, highlighting the critical role of *Inx2* in epithelial morphogenesis.

The interaction of Innexin 2 and other junction proteins was investigated in the embryonic epithelial cells by disrupting the expression of *Inx2* in mutants for *coracle, shotgun,* and *armadillo* (Bauer *et al.*, 2004). Coracle is a septate junction-associated protein required for salivary gland morphogenesis. In *coracle* mutants, the septate junctions are disrupted without affecting cell polarity (Lamb *et al.*, 1998). *Inx2* was observed to be localised to the apical region of these *coracle* cells instead of the baso-lateral region of wild-type embryos (Bauer *et al.*, 2004). In the DE-cadherin mutant *shotgun*, Innexin 2 is also mislocalised, accumulating in the cytoplasm. The mislocalising led to cell polarity and adhesion disruption, resulting in loss of epithelial integrity and cell death, which ultimately disordered epithelial tissues (Uemura *et al.*, 1996). Similarly, in the *armadillo* mutant, an increased level of Innexin 2 protein expression was detected in the cytoplasm rather than the cell membrane (Bauer *et al.*, 2004). Due to the loss of cell-cell adhesion and communication, this mislocalisation causes disordered epithelial structure.

Interaction studies showed a direct interaction between three key junctional proteins, Armadillo, Shotgun and Coracle, and Innexin 2, which was confirmed by immunoprecipitation, in vitro translation and immunohistochemical analysis. These experiments revealed how disruptions in these interactions affect the localisation of Inx2, leading to disordered epithelial structures. Under normal conditions, Inx2 colocalises with Armadillo and Shotgun at the adherens junction, supporting epithelial organisation and maintaining polarity. However, in zygotic kropf mutants, the correct localisation of Coracle, Armadillo and Shotgun was disrupted, resulting in their cytoplasmic accumulation and a loss of epithelial integrity. This highlights that Innexin 2 is required to preserve the structural stability of epithelial tissues.

Figure 3.1 is a diagram that illustrates this by contrasting wildtype epithelial cells with cells that lack Inx2. In wild-type, Inx2 is at the PM with Armadillo and Shotgun for correct adherens junction and cell polarity. In contrast, Inx2-deficient cells, the proteins localise to the cytoplasm, leading to polarity failure and defects in epithelial integrity. This diagram summarises these experimental results and supports for Inx2 having an important function for epithelial integrity.

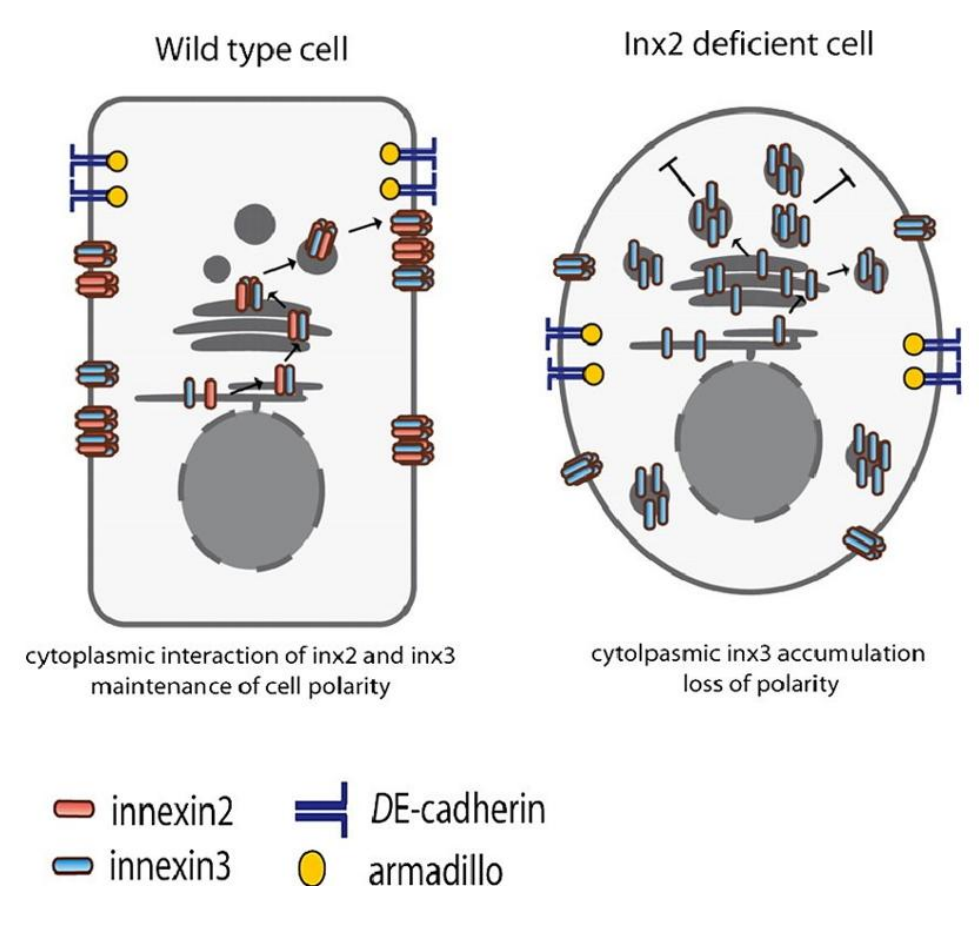


Figure 3.1 Localisation of Innexin 2 and junctional proteins in wild-type and Inx2-deficient epithelial cells. Diagram illustrating the distribution of Innexin 2 and related junctional proteins. In wild-type cells, *Inx2* is found at adherens cell junctions, colocalised with Armadillo and Shotgun proteins, where it contributes to the maintenance of epithelial polarity. In the case of Inx2 loss, both Armadillo and Shotgun become mislocalised, show cytoplasmic accumulation and cause a disruption of the epithelial organisation and polarity. modified from Lehmann et al. (2006).

As shown in Figure 3.1, the disruption of *Inx2* also affects the localisation of *Inx3*, highlighting that these innexins act in a coordinated manner and providing the basis for examining the role of *Inx3* in epithelial organisation during dorsal closure. Further evidence for innexin interactions comes from studies of *Inx1*,

Inx2, and shg (shotgun, which encodes DE-cadherin). The stability of these proteins at the plasma membrane is affected when Inx3 is absent, suggesting that these four proteins can form a functional complex (Giuliani et al., 2013). Dorsal closure is a mid-embryogenesis process in *Drosophila* that seals the epidermal gap at the dorsal side of the embryo by migration of the ectoderm over the extraembryonic amnioserosa, a morphogenetic event comparable to human wound healing and neural tube closure (Hayes and Solon, 2017). Giuliani et al. (2013) demonstrated that Inx3 contributes to dorsal closure by maintaining the stability and localisation of other junctional proteins. The correct localisation of these proteins is interdependent, with Inx3 playing a central role. Localisation to the plasma membrane enables plaque formation, indicating functional gap junctions that are essential for maintaining epithelial integrity during dorsal closure. Importantly, only the loss of *Inx3* causes clear dorsal closure defects, as disruption of Inx3 destabilises the interaction of Inx2 with DEcadherin at the plasma membrane, leading to weakened cell-cell junctions and impaired closure (Giuliani et al., 2013).

3.2.2 Innexin 2 Expressed in Proventriculus

The proventriculus and Malpighian tubules have complementary roles in *Drosophila* physiology. Although the proventriculus belongs to the digestive system and the tubules are components of the excretory system, both organs contribute to homeostasis: the proventriculus regulates the passage and processing of ingested food (Phelan, 2005), while the Malpighian tubules maintain ionic and osmotic balance by excreting waste and regulating fluid composition (Dow and Davies, 2006). Together, these tissues coordinate digestive and excretory functions to stabilise the internal environment.

Phelan's research has highlighted the role of innexin 2 by identifying its specific expression in proventriculus. In the proventriculus, the expression of *Inx2* mRNA was initially discovered in the early evagination stage (Phelan, 2005). After the ectodermal cells invaginate to the proventricular endoderm, the expression of *Inx2* is upregulated. The ectodermal cells fail to invaginate in hedgehog and *wingless* mutants, and in *hedgehog* mutants, gap junction communication is strongly reduced. This data suggests that as a core protein in gap junction channels, *Inx2* mediates the coupling of cells induced in response to hedgehog and wingless activities. This connection is essential in the development of organs in *Drosophila*.

Hedgehog and Wingless are two key developmental signalling pathways in *Drosophila*, both of which intersect with innexin regulation. Hedgehog signalling controls tissue growth and embryonic patterning, while Wingless regulates cell polarity and developmental patterning (Ingham and McMahon, 2001; Swarup and Verheyen, 2012). Their relevance to innexins lies in their regulation of *Inx2* expression and localisation. As shown in proventriculus studies, loss of Hedgehog or Wingless function disrupts epithelial invagination and significantly reduces *Inx2*-mediated gap junction communication (Phelan, 2005). This highlights that these pathways act upstream of *Inx2*, ensuring correct expression and localisation during organogenesis. In this way, Hedgehog and Wingless signalling provide the developmental context for the direct regulation of *Inx2* expression described below (Lechner et al., 2007).

Further, Innexin 2 has been confirmed to be expressed in precursor cells of the proventriculus (cardia) (Lechner et al., 2007). It participates in proventriculus development and could be a target gene for the wingless signalling pathway in the proventriculus. Lechner et al. (2007) also showed that the hedgehog and wingless signalling pathways activate the expression of the Inx2 gene. These signalling pathways also contribute to regulating Inx2 expression in the germarium region of the ovary (Mukai et al., 2011). The Wingless signalling pathway also regulates the localisation of Inx2. This regulation establishes proper cell-cell communication and adhesion. Moreover, Wingless is a target gene of hedgehog signalling. Wingless expression is affected by Hedgehog signalling and vice versa. Disruption of the Wingless signalling pathway can lead to mislocalisation of Inx2 and failure to maintain the structural integrity of epithelial tissues.

3.2.3 Gap Junctions Play a Key Role in The Circadian Circuit

Gap junction protein Inx2 has been reported to participate in the circadian circuit (Ramakrishnan and Sheeba, 2021), facilitating circadian signals. These signals could affect the function of Malpighian tubules (Patop *et al.*, 2023).

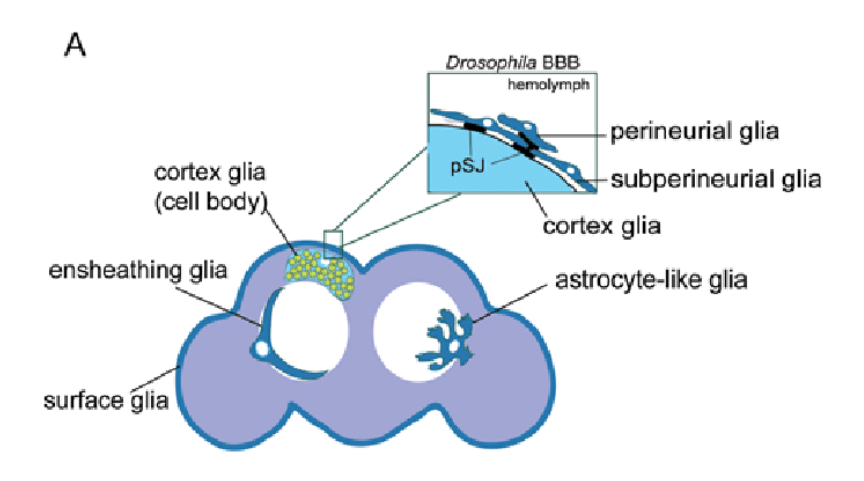
There are 150 neurons distributed in the *Drosophila* brain, which are involved in circadian circuit regulation (Ramakrishnan and Sheeba, 2021). All neurons are divided into lateral neurons (LN) and dorsal neurons (DN) based on their location. Each neuron comprises a self-sustained transcriptional-translational feedback loop (TTFL) (Sheeba, 2008; Hardin, 2005). In the pacemaker circuit of the *Drosophila* brain, the period of circadian rhythmic behaviours is associated with the period of molecular oscillations in mRNA and proteins. Previous studies of the *Drosophila* neuronal network proved that small ventral lateral neurons (s-LNv) participate in maintaining activity-rest rhythms. The s-LNv releases the neuropeptide pigment dispersing factor (PDF) (Park *et al.*, 2000). PDF is also involved in circadian rhythms (Yoshii *et al.*, 2009). A lack of PDF can lead to the failure to display a rhythm or regularity

The *Inx2* regulates activity-rest rhythm and presents functions in the s-LNv and large ventral neuronal (I-LNv) subsets (Ramakrishnan and Sheeba, 2021). *Inx2* in the plasma membrane of LNv can affect the membrane condition of the neurons, resulting in molecular clock alteration and circadian rhythm regulation. Furthermore, *Inx2* is involved in the release of PDF in the dorsal projections (Renn *et al.*, 1999). PDF can lengthen the period of the activity-rest rhythms. *Inx2* not only affects the activity-rest rhythm circuit but also the development of the clock neuronal system. Existing results show that a lack of *Inx2* can lead to circadian rhythms slowing down and can alter the oscillation of the PERIOD coreclock protein (Ramakrishnan and Sheeba, 2021).

3.2.4 Innexin 7 and Innexin 2 Role in The Nervous System

Recent genetic studies have shown that the Innexin gene also plays an important role in the development of the nervous system in addition to its role in the circadian circuit. *Inx7* and *Inx2* contribute to maintaining homeostasis by facilitating efficient communication within the nervous and renal systems. *Inx7* is specifically expressed in midline glial cells, which are associated with the nucleus of neurons in CNS development (Ostrowski *et al.*, 2009). One possible reason for this is that *Inx7* is required for the development of the nervous system (Wu *et al.*, 2011). To explore this possibility, *Inx7* was knocked down, disrupting the embryonic nervous system in *Drosophila*, suggesting that *Inx7* is essential for neural system development.

Inx2 also plays an important role in peripheral glial development. Glial cells support nervous system development and maintain the nervous environment (Das et al., 2023). The primary function of glia is to form the glial sheath around peripheral axons. There are three glial layers, which are perineurial glia (PG), subperineurial glia (SPG) and wrapping glia (WG), that ensheath each peripheral nerve of Drosophila larvae (Das et al., 2023). These layers and their organisation are illustrated in Figure 3.2, which shows the arrangement of PG, SPG and WG around peripheral axons, highlighting their roles in providing structural support and maintaining axonal stability. Das et al. (2023) verified that both Inx1 and Inx2 are expressed in all three glial layers by using the RNAi approach to knock down innexin genes expressed in Drosophila glia (Inx1, Inx2, Inx3 and Inx7). These knockdown experiments resulted in phenotypes such as disruption of glial membranes and defective axonal wrapping, which compromise the protective and supportive roles of glia in the peripheral nervous system. This shows that innexins are required to maintain glial structure and function.



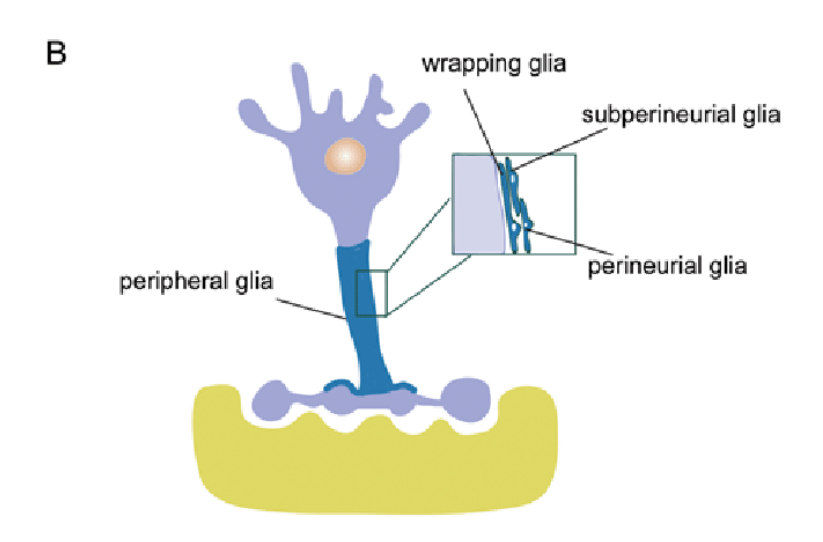


Figure 3.2 Schematic illustration of glial structure in *Drosophila*. (A) Cross-section of the larval central nervous system showing glial subtypes including cortex, astrocyte-like, ensheathing and surface glia. Perineurial glia (PG) and subperineurial glia (SPG) contribute to the blood-brain barrier and provide protection for the nervous system. (B) Organisation of peripheral glia around motor axons. PG, SPG and wrapping glia (WG) are shown surrounding axons, where PG and SPG contribute to barrier functions and WG forms a supporting sheath around axons to maintain stability and communication.

Inx1 and Inx2 colocalised through the glial layers and can identify heteromeric plaques between the SPG and WG membranes (Das et al., 2023). The loss of the Inx1 and Inx2 genes may affect WG, disrupting the glia wrap. However, the phenotypes of the loss of Inx1 function are different from the Inx2 loss-of-function phenotypes. Inx2 loss in the WG could cause glial membrane fragments. WG is also affected when only Inx2 (not Inx1) is knocked down in the SPG. This suggests that Innexin 2 participates in communication between SPG and WG.

Peripheral nerves have revealed two distinct functions of innexins (Guiza et al., 2018; Sánchez et al., 2019). In the SPG, Das et al. (2023) observed that knockdown of Inx2 disrupted normal gap junction activity, even without calcium-dependent signalling, indicating that innexins in this layer help maintain junctional communication independently of Ca²⁺ pulses. In both the SPG and WG, innexins may also support structural roles that do not rely on their channel activity, such as supporting membrane contacts and maintaining glial architecture.

It is well-known that *Inx2* is required in peripheral glia development (Ostrowski *et al.*, 2008), but it needs to be clarified whether *Inx3* and *Inx7* are present in the peripheral glia. *Inx3* and *Inx7* are not required for glial development. Das *et al.* verified this idea by knocking down these genes to be expressed in the glia using the RNAi approach (Das *et al.*, 2023). The loss of *Inx3* and *Inx7* does not affect glial or nerve morphology, indicating that they could form junctions with each other or by themselves.

3.2.5 Innexin Protein Play an Important Role During Early Oogenesis

Gap junctions are involved in the initial stages of egg development and in the interconnection between germline and somatic cells in the *Drosophila* ovary (Güiza et al., 2018). These proteins support the development of oocytes and at the same time protect normal excretory functions in the renal system. Five of the eight known *Drosophila* innexin genes have been identified in the ovary, including Inx1, Inx2, Inx3, Inx4 and Inx7 (Stebbings et al., 2000). To examine whether innexins form functional gap junction channels in the ovary, Bohrmann and Zimmermann (2008) microinjected antisera raised against different innexins into developing follicles and performed dye-coupling assays to trace intercellular transfer. Only antisera against Inx2 produced a marked reduction in dye movement between oocytes and follicle cells, identifying Inx2 as the main innexin responsible for germline-soma communication. Additional analyses localised Inx1, Inx2, Inx3 and Inx4 to distinct domains of follicle and nurse cells, showing complementary patterns of distribution (Bohrmann and Zimmermann, 2008). Together these results indicate that Inx2 provides gap junction channels that mediate the transfer of small signalling molecules, including ions, metabolites and developmental cues, between germline and somatic cells. This exchange is required to coordinate oogenesis and ensure early egg development.

During gametogenesis, germ cells are required to become associated with the surrounding somatic cells. During oogenesis, the communication between germ cells and somatic support cells needs to be mediated by gap junctions (Kidder and Mhawi, 2002). Mukai *et al.* (2011) identified the mechanisms regulating germline development and the requirement of Innexin 2 in oogenesis by isolating a femalesterile mutation in Innexin 2. Innexin 2 is expressed in the somatic support cells and participates in the formation of gap junctions to complete the regulation of germline development (Mukai *et al.*, 2011; Tolkin *et al.*, 2022). It is essential for developmental processes during early oogenesis. Furthermore, in inner germarial sheath (IGS) cells, Innexin 2 is necessary for early germ cells' survival and cyst formation (Bauer *et al.*, 2004). It has been confirmed that Innexin 2 is present in IGS cells and could provide nutrients and signalling molecules to differentiate

early germ cells, supporting their survival and differentiation into cysts (Bohrmann and Zimmermann, 2008). The Cyst formation requires a functional EGFR signalling pathway in escort cells (Schulz *et al.*, 2002). The EGFR pathway could interact with *Inx*2 to promote cyst formation (Mukai *et al.*, 2011). Therefore, another function of Innexin 2 is promoting EGFR signalling in escort cells.

Innexin 2 is necessary to specify the cells' migratory group during oogenesis. Innexin1, Innexin 2, Innexin 3 and Innexin 7 have been detected as expressed in the follicle cells and the border cells of the *Drosophila* egg chamber (Bohrmann and Zimmermann, 2008). In the early stage of the egg chambers, *Inx2* transcripts have been found in the anterior follicle cells (Stebbings *et al.*, 2002). The expression of *Inx2* in this early stage contributes to identifying border cell establishment during the oogenesis of *Drosophila* (Sahu *et al.*, 2017). Increasing the Innexin 2 level in the follicle cells can rescue border cells in Innexin 2-depleted follicle cells, whereas in later stages of development, Innexin 7 is presented in a punctate pattern in the epithelial tissues and cytoplasm (Ostrowski *et al.*, 2009).

3.2.6 The Role of Innexins in The Development of Eye Imaginal Disc

Further, although the eye imaginal disc and Malpighian tubules are different organs and have different biological processes, innexin proteins enable coordination and efficient communication in both biological processes. Interaction between each innexin gene also contributes to eye imaginal disc development. The cooperation between Inx2 and Inx3 promotes the growth of the eye disc. Richard et al. (2017) analysed the function of Innexin genes in controlling eye size. Inx1, Inx2 and Inx3 were colocalised during eye development. The protein levels of *Inx1* and *Inx3* were monitored in the absence of Inx2. The result shows that the expression of Inx1 and Inx3 were dramatically decreased, indicating that their expression levels depend on Inx2 during eye development (Richard et al., 2007). Further research shows that the Inx3 level affects the Inx2 level in larval eye discs. However, the Inx1 level does not affect the level of Inx2 and Inx3 (Richard et al., 2017). Inx2 can regulate eye size during development and control disc cell proliferation and the speed of morphogenetic furrow movement, impacting the number of differentiated photoreceptors. During larval eye development, the loss of Inx3 causes an eye size decrease, while an increase in the Inx3 level can lead to an eye size increase. Furthermore, the expression of the *Inx3* level significantly relies on the Inx2 level, with Inx3 participating in regulating the Inx2 level in the larval eye disc. They cooperate to promote the development of the eye disc.

Richard et al. (2017) have also analysed whether Inx6 and Inx7 contribute to maintaining eye disc growth (Richard and Hoch, 2015). Inx6 and Inx7 can form gap-junction channels in neurons of the mushroom bodies (Wu et al., 2011). The mushroom bodies are important structures in the *Drosophila* brain, contributing to olfactory learning and memory formation (Lee et al., 1999). Stebbings et al. (2002) detected transcripts for inx6 and inx7 in the pupal eye disc, but they did not colocalise with transcripts for inx1, inx2 and inx3. Richard et al. (2017) used antibodies against Inx6 and Inx7 to determine the protein expression level in third instar eye discs. Inx6 and Inx7 are not colocalised with Inx1, Inx2 and Inx3 during eye disc development. Taken together, these data indicate that while

Inx6 and Inx7 are present in eye tissues and form channels in specific neurons, they are unlikely to act in the Inx2-Inx3-dependent growth mechanism of the larval eye disc. Therefore, in the context of this thesis we focus on Inx2 (and Inx3) as the innexins most relevant to epithelial growth, including in the Malpighian tubules.

3.3 Results

This study investigated the role of the Innexin gene family in *Drosophila* Malpighian tubules, with the working hypothesis that Innexin proteins contribute to intercellular communication between tubule cells and thereby influence fluid transport and osmoregulation. To test this, RNAi experiments were performed to suppress Innexin expression specifically in the principal cells of the tubules using the GAL4/UAS system. The efficiency of gene knockdown was validated by quantitative PCR. Subsequent analyses focused on determining whether reduced Innexin expression altered tubule physiology, including fluid secretion rates, assessed through fluid secretion assays, and cellular organisation, examined using microscopy. These experiments were designed to clarify how Innexins may regulate epithelial function in the tubules.

3.3.1 Innexin Gene Family

The innexin family in *Drosophila* consists of eight genes (Bauer et al., 2015), which are expressed across multiple tissues (Stebbings et al., 2002). To investigate their relevance to Malpighian tubule physiology, transcriptomic data from FlyAtlas2 were examined for adult males, adult females, and third instar larvae (Leader et al., 2017). *Inx5* and *Inx6* show predominant expression in the testis (Figure 3.6, Figure 3.7), while *shakB* is mainly expressed in the adult nervous system (Figure 3.9). Ogre, *Inx2*, and *Inx3* are expressed to varying degrees across the body (Figure 3.3-3.5); however, both ogre and *Inx3* display only low transcript levels in the Malpighian tubules. In contrast, *Inx2* and *Inx7* exhibit comparatively higher expression in the tubules (Figure 3.4, Figure 3.8), with *Inx7* also expressed in the midgut.

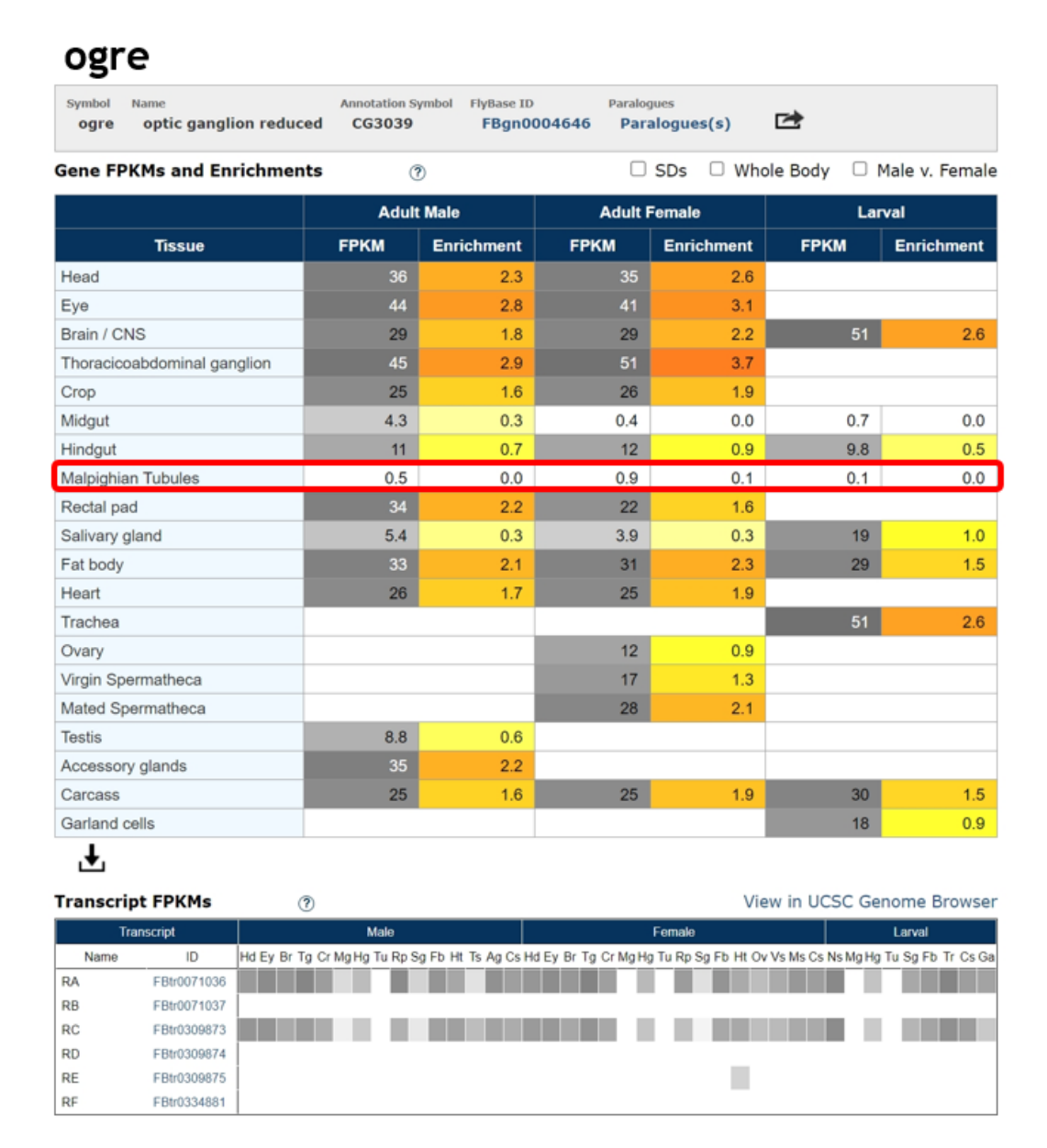


Figure 3.3 Tissue expression profile of ogre in *Drosophila*. Expression levels are shown as FPKM (Fragments Per Kilobase of transcript per Million mapped reads) across 21 adult and larval tissues (18 major tissues plus carcass, mated spermatheca, and unmated spermatheca). Enrichment values represent the relative transcript abundance in each tissue compared to the whole body. The red box highlights transcript levels in Malpighian tubules, where ogre shows very low expression. Data from FlyAtlas2 (Krause et al., 2022).

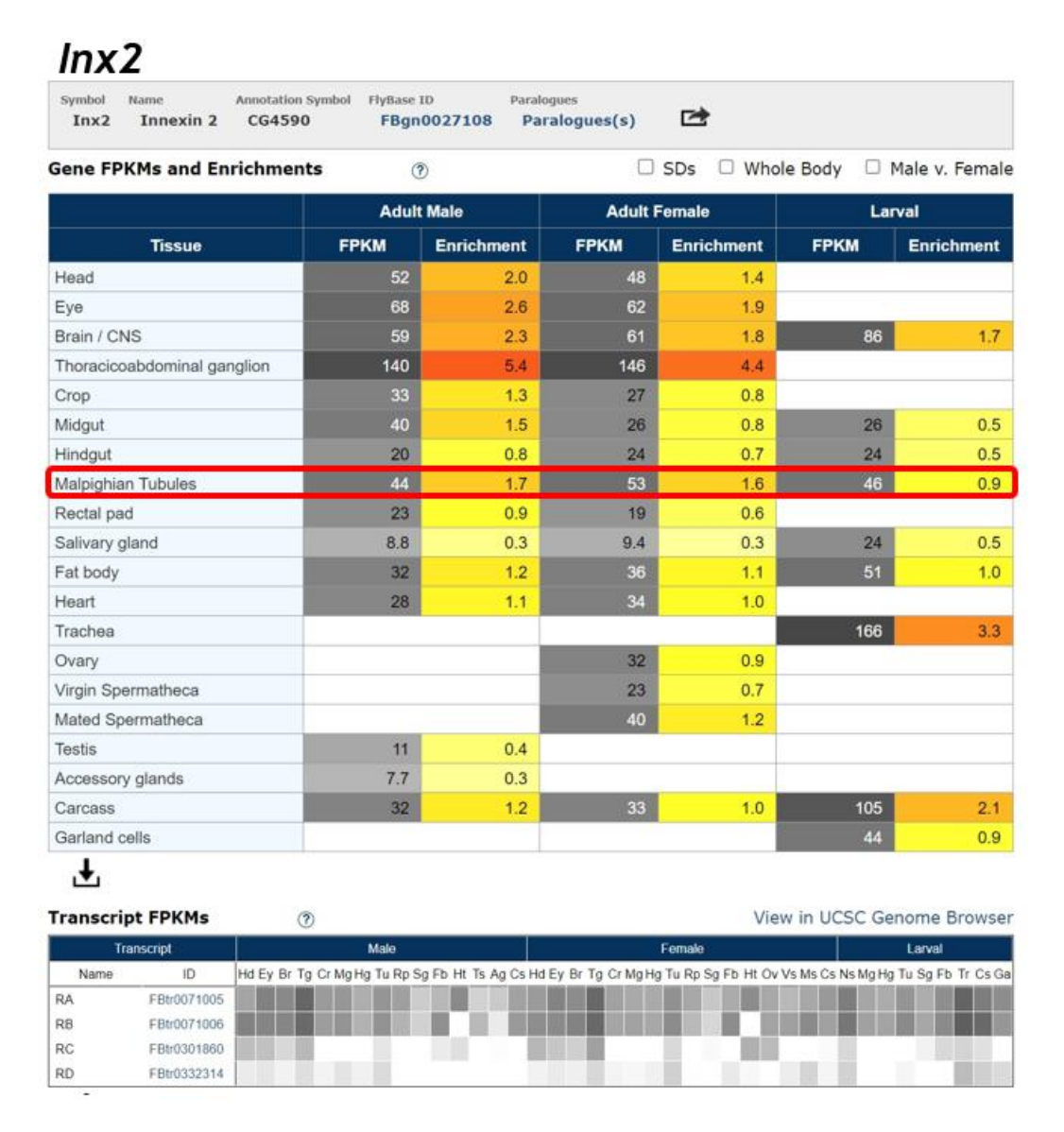


Figure 3.4 Tissue expression profile of *Innexin* **2** in *Drosophila*. FlyAtlas2 data showing transcript levels across adult male, adult female, and larval tissues. In Malpighian tubules (red box), *Inx*2 is expressed at 44, 53, and 46 FPKM, respectively (Krause et al., 2022).

Inx3



Figure 3.5 Tissue expression profile of *Innexin 3* in *Drosophila*. Expression data from FlyAtlas2. *Inx3* is widely detected in several tissues, including hindgut and brain. In Malpighian tubules (red box), expression is comparatively low, ranging from 0.4 to 1.7 FPKM (Krause et al., 2022).

Inx5



Figure 3.6 Tissue expression profile of *Innexin 5* in *Drosophila*. FPKM values obtained from FlyAtlas2. Inx5 shows its highest expression in the testis (18 FPKM), whereas transcript levels in Malpighian tubules (red box) are negligible, between 0.0 and 0.2 FPKM (Krause *et al.*, 2022).

Inx6

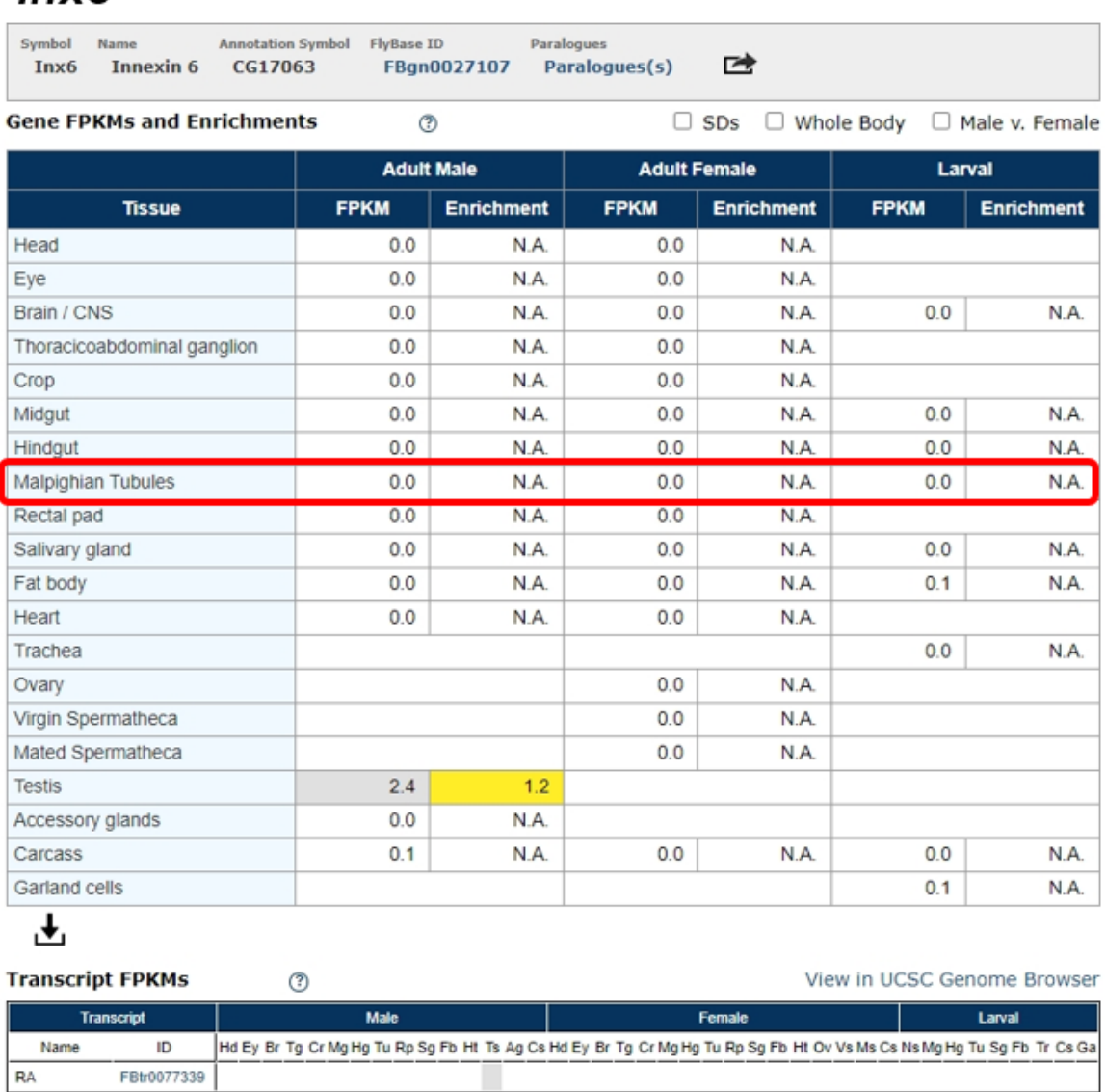


Figure 3.7 Tissue expression profile of *Innexin 6* in *Drosophila*. Data from FlyAtlas2. Inx6 expression is largely restricted to the testis. No transcripts were detected in Malpighian tubules (red box, 0 FPKM across all stages) (Krause et al., 2022).

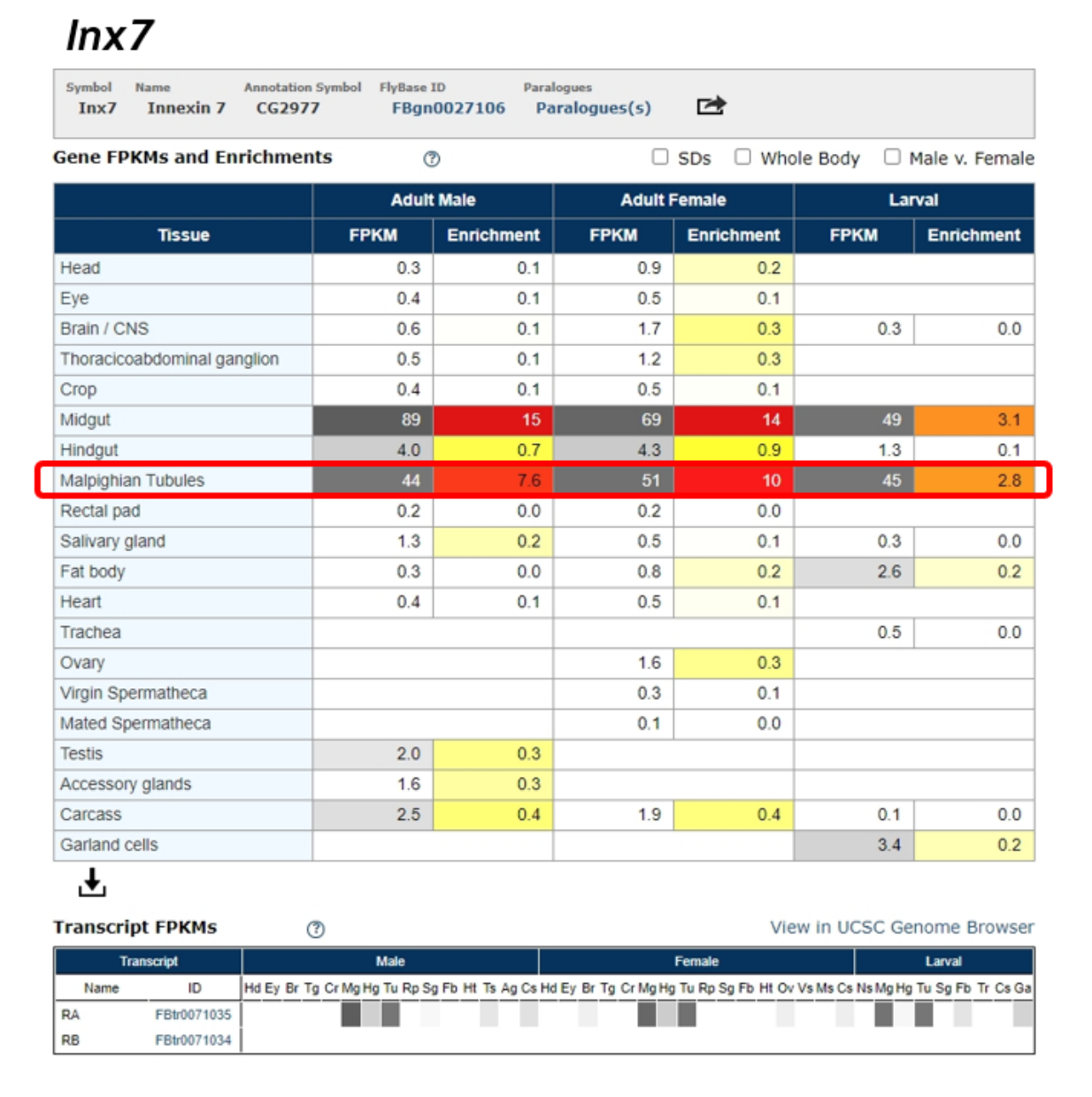


Figure 3.8 Tissue expression profile of *Innexin 7* in *Drosophila*. FlyAtlas2 dataset showing FPKM values across adult and larval tissues. Inx7 is present in both midgut and Malpighian tubules. Transcript levels in tubules (red box) are 44, 51, and 45 FPKM for adult male, adult female, and larval tissues, respectively (Krause et al., 2022).



Figure 3.9 Tissue expression profile of *shaking B* in *Drosophila*. Expression values from FlyAtlas2 are shown across adult male, adult female, and larval tissues. As expected, *shakB* transcripts are predominantly detected in nervous-system tissues. In Malpighian tubules (red box), expression remains at background levels, with values close to 0 FPKM.

Figure 3.10 shows the expression levels and enrichment values of innexin genes in the Malpighian tubules across adult males, adult females, and larvae. These data illustrate the differential expression profiles of the eight innexin genes and highlight that Inx7 displays the highest relative enrichment in the tubules. While such transcriptomic data provide an important indication of which genes may be active in this tissue, gene expression alone cannot be taken as direct evidence of functional importance. Instead, these results identify candidate genes, such as Inx2 and Inx7, for subsequent experimental investigation.

The dataset indicates that the enrichment values of Inx2 and Inx7 are higher than those of other innexins. Specifically, Inx2 shows enrichment values of 1.7, 1.6, and 0.9 in adult male, adult female, and larval tubules, respectively, while Inx7 enrichment reaches 7.6, 10, and 2.8 in the same groups. These values are descriptive outcomes derived from FlyAtlas2 RNA-seq data and are not accompanied by statistical significance testing within the database.

Based on these results, Inx2 and Inx7 were selected for further study. The strategy for subsequent experiments was two-fold. First, the expression of these genes was defined more precisely within Malpighian tubules using cell-type specific GAL4 drivers for principal and stellate cells. Second, knockdown efficiency was validated by RNAi using qPCR, and the functional impact was assessed through fluid secretion assays.

	Adult Male		Adult Female		Larval	
	FRKM	Enrichment	FRKM	Enrichment	FRKM	Enrichment
ogre	0.5	0.0	0.9	0.1	0.1	0.0
lnx2	44	1.7	53	1.6	46	0.9
Inx3	1.1	0.1	1.7	0.2	0.4	0.0
Inx5	0.2	N.A.	0.1	N.A.	0.0	N.A.
lnx6	0.0	N.A.	0.0	N.A.	0.0	N.A.
lnx7	44	7.6	51	10	45	2.8
ShakB	0.1	0.0	0.1	N.A.	0.0	N.A.

Figure 3.10: Innexin family gene expression in Malpighian tubules. FlyAtlas2 indicates innexin family gene expression in tubules at the adult and larval stages. Data from FlyAtlas2 ((Krause *et al.*, 2022). FRKM in the Malpighian tubules are indicated in the figure. Enrichment values are calculated as the ratio of the FPKM value in the Malpighian tubules to the FPKM value in the reference condition. FPKM in Malpighian Tubules: the expression level of the gene in Malpighian tubules. FPKM in Reference: the average expression level of the gene across all other tissues.

3.3.2 Inx2 is Mainly Expressed in The Principal Cells of The Tubules

Several different publicly available UAS-Inx2 RNAi lines can be used to decrease the mRNA level of *Inx2* in tubules. Among these, the line UAS-Inx2 ⁴²⁶⁴⁵ was selected for detailed analysis. Tubules have two main cell types, and this line was used to determine the specific cell type in which *Inx2* is expressed. *Inx2* can be expressed in all cell types. This was done by crossing it to GAL4 lines specific to the principal cells (CapaR-Gal4 line) or the stellate cells (tsh-Gal4 line). I used qPCR to determine the levels of *Inx2* mRNA. I used the parental lines, UAS-Inx2⁴²⁶⁴⁵ and the *GAL4* lines as my controls. For the gene knockdown in the principal cells of the tubules, the CapaR promoter-specific GAL4 line (CapaR-GAL4) was crossed with the UAS-Inx2 target lines. Furthermore, the *tsh* promoter-specific GAL4 line (tsh-GAL4) was crossed with the UAS-Inx2 target lines for the gene knockdown in the stellate cells. Using qPCR, the *Inx2* mRNA levels were determined in the tubules from the control and the knockdown flies. Ribosomal Protein L32 was used as a control gene to validate the analysis of gene expression levels.

Quantitative PCR of dissected Malpighian tubules (Figure 3.11) demonstrated that when knockdown was driven in principal cells (CapaR-Gal4 > UAS-Inx 2^{42645}), Inx2 mRNA levels were reduced relative to the driver control (CapaR-Gal4). In contrast, driving the same RNAi in stellate cells (tsh-Gal4 > UAS-Inx 2^{42645}) did not lead to a reduction in Inx2 mRNA when compared with the stellate-cell driver control (tsh-Gal4). Statistical comparisons were performed separately for the two cell types as indicated in the figure legend. These results confirm that the RNAi construct is effective in principal cells but not in stellate cells.

For this, initially, to calculate relative expression, the expression level of *Inx2* in parental control lines, UAS-Inx2⁴²⁶⁴⁵, was set at 1. The expression level of *Inx2* in CapaR-Gal4> UAS-Inx2⁴²⁶⁴⁵ was compared to this control and other parental control CapaR-Gal4 lines. It was found that the expression of mRNA level of *Inx2* was reduced by 60%, while stellate cells specific knockdown of the *Inx2* gene (tsh-GAL4> UAS-Inx2⁴²⁶⁴⁵) showed marked increases of expression level compared to two parental control lines (UAS-control 150%, tsh-GAL4 200%). Together,

these results show that the expression of Inx2 mRNA is mainly in the principal cells of the tubules but not the stellate cells. Although more spatially resolved approaches, such as in situ hybridisation or immunohistochemistry, could provide additional confirmation of this localisation, these methods were not employed in the present study and are considered further in the Discussion (Section 3.4).

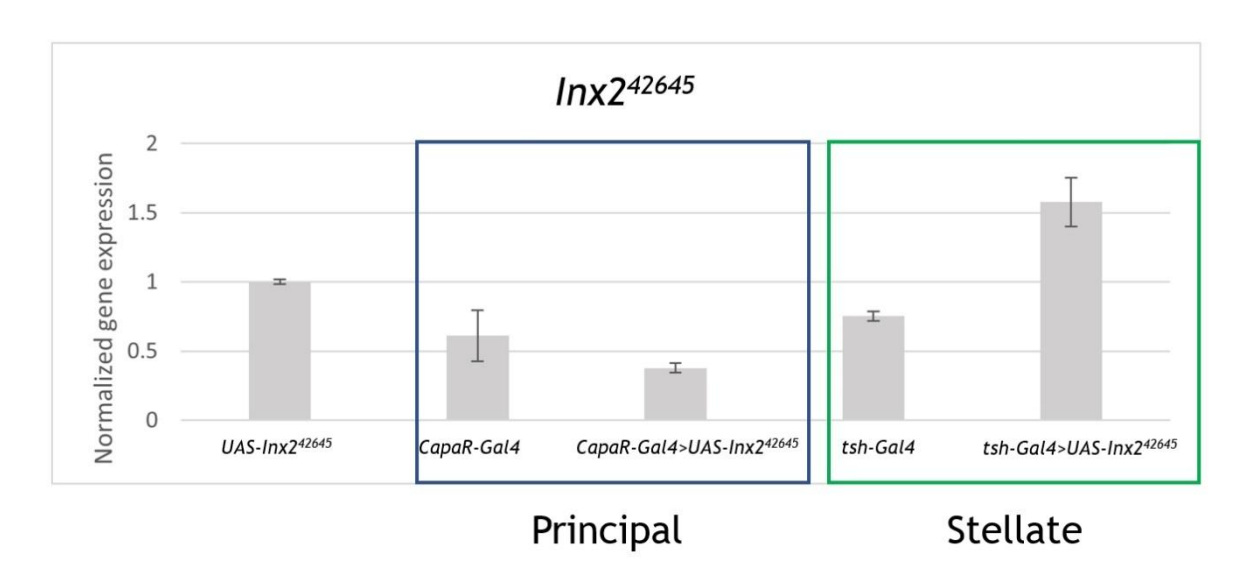


Figure 3.11: RNAi knockdown of UAS-Inx2⁴²⁶⁴⁵ in MTs. *Inx2* mRNA levels were measured by qPCR after RNAi with UAS-Inx2⁴²⁶⁴⁵ driven in principal (CapaR-Gal4) or stellate (tsh-Gal4) cells. Expression was normalised to *RpL32* and to the parental line (UAS-Inx2⁴²⁶⁴⁵, set to 1). Data are mean \pm SEM (N = 5 biological replicates). Two-tailed unpaired Student's t-tests were applied separately for principal- and stellate-cell comparisons; significance is annotated in the figure (p < 0.05; ns, not significant).

These experiments tested three additional publicly available UAS-Inx2 RNAi lines to further assess their effectiveness in reducing *Inx2* mRNA levels (Figure 3.12). The expression level of *Inx2* in UAS- Inx2¹⁰²¹⁹⁴, CapaR-Gal4>UAS-Inx2¹⁰²¹⁹⁴ and tsh-Gal/UAS- Inx2¹⁰²¹⁹⁴ is shown as 0. The other parental control *CapaR-Gal4* line was set at value of 1 to calculate the relative expression (Figure 3.12 A). In the case of the UAS-Inx2⁹⁰⁹⁶⁶ (Figure 3.12 C), only the principal-cell driver (CapaR-Gal4) was tested. The stellate-cell driver (tsh-Gal4) was not used, as *tsh* is expressed in stellate but not principal cells, and earlier experiments (Figure 3.11) had already shown that driving the same RNAi in stellate cells did not reduce *Inx2* mRNA compared with the driver control. The expression levels of *Inx2* in the UAS-Inx2⁹⁰⁹⁶⁶ and CapaR-Gal4>UAS-Inx2⁹⁰⁹⁶⁶ are also shown as 0 in the Figure 3.12 (C).

By contrast, the line UAS-Inx2⁸⁰⁴⁰⁹ showed inconsistent results (Figure 3.12 B). In principal cells, expression did not decrease relative to controls, and in stellate cells expression was increased compared with the driver control. This indicates variability among RNAi stocks, and that not all lines achieve effective knockdown. In some controls, relative expression values exceeded the y-axis scale used in the figure and were therefore normalised to 1 for comparison. Overall, these results highlight the differing efficiencies of independent *UAS-Inx2* RNAi lines in reducing *Inx2* expression.

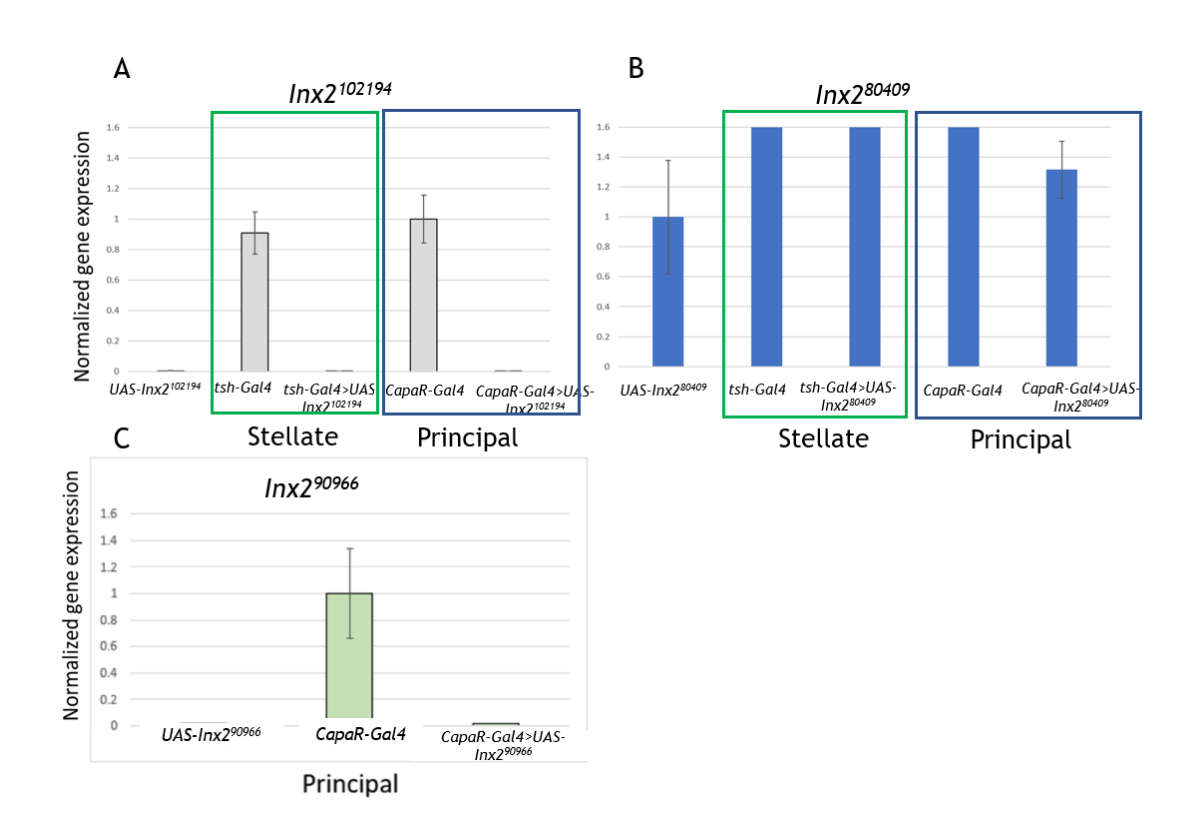


Figure 3.12: The RNAi-mediated knockdown of Inx2 using the other UAS-Inx2 line. A: Three parent lines were tested: $UAS-Inx2^{102194}$, CapaR-Gal4, and tsh-Gal4. $UAS-Inx2^{102194}$ was crossed with both the CapaR-Gal4 (principal-cell driver) and tsh-Gal4 (stellate-cell driver) lines. B: $UAS-Inx2^{80409}$ was also crossed with CapaR and tsh-Gal4 line. C: UAS-Inx2^{90966} was only crossed with the CapaR promoter-specific Gal4 line (CapaR-Gal4). In all parts of the figure, stellate-cell data are shown on the left and principal-cell data on the right. Where only one cell type was analysed (e.g., $Inx2^90966$ in panel C), only principal-cell data are displayed. The experiment was conducted in three biological replicates. Data are expressed as the mean of mRNA relative expression \pm SEM, N=5, p>0.05, Student's t-test. Error bars represent SEM from three biological replicates.

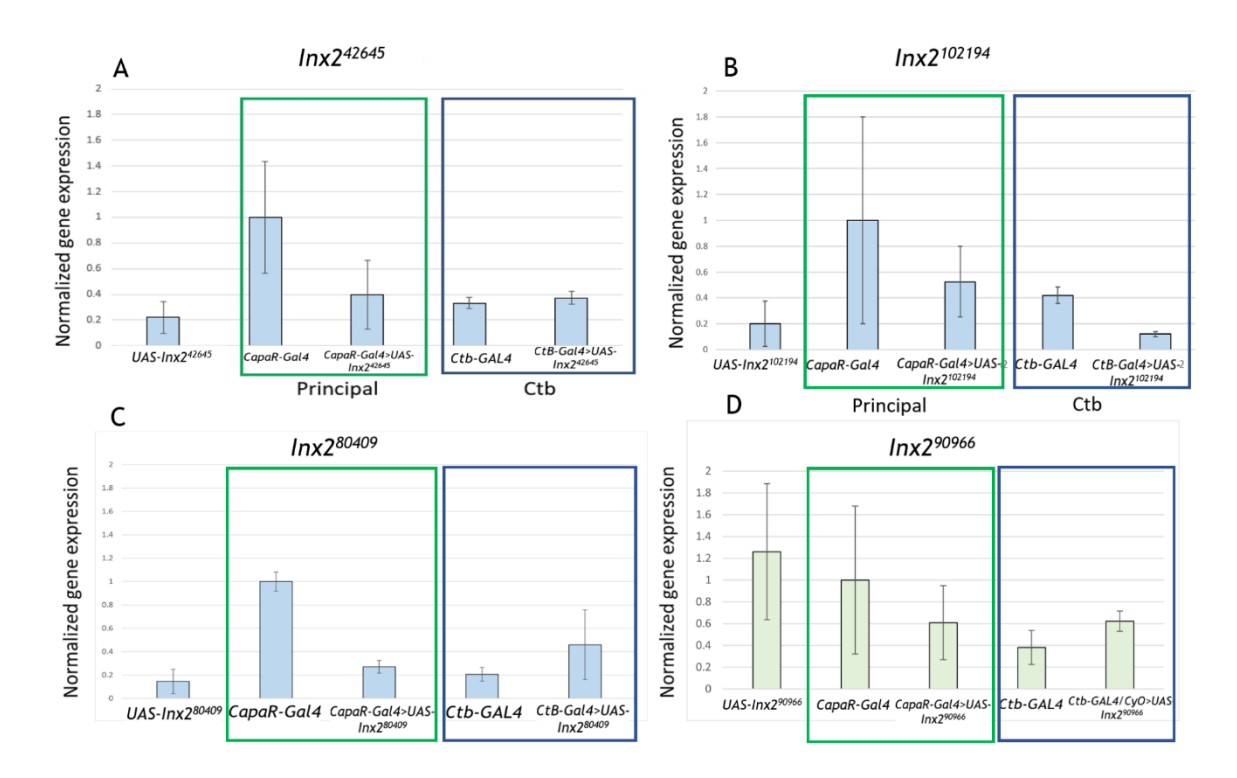


Figure 3.13: Results of the knockdown of *Inx* 2 in the tubules. A. CapaR-Gal4 and Ctb-GAL4 crossed to UAS-Inx2⁴²⁶⁴⁵; B. *CapaR-Gal4* and *Ctb-GAL4* crossed to UAS-Inx2¹⁰²¹⁹⁴; C. CapaR-Gal4 and Ctb-GAL4 crossed to UAS-Inx2⁸⁰⁴⁰⁹ lines; D. UAS-Inx2⁹⁰⁹⁶⁶ crossed with Ctb-GAL4/CyO. Only non-CyO progeny (Ctb-GAL4>UAS-Inx2⁹⁰⁹⁶⁶) were selected for qPCR analysis; the CyO balancer was used solely for stock maintenance and was not included in the assay. Data are expressed as the mean of mRNA relative expression \pm SEM, N=5, p>0.05, Student's t-test.

The Fly Cell Atlas (Li *et al.*, 2022 dataset indicates that the transcription factor *cut (ct)* is expressed primarily in principal cells, but low levels are also detected in stellate cells (Figure 3.15). Based on this information, *Ctb-GAL4* was used as an alternative driver to test whether *Inx2* could be knocked down when driven by a promoter with activity in both cell types. This approach was intended to complement the results obtained with the principal-cell driver (CapaR-GAL4) and the stellate-cell driver (tsh-GAL4), and to provide further validation of cell-type specificity. Accordingly, Ctb-GAL4 and Ctb-GAL4/CyO were crossed to *UAS-Inx2* RNAi lines, and expression was measured by qPCR. In the case of Inx2⁹⁰⁹⁶⁶, the cross Ctb-GAL4/CyO > UAS-Inx2⁹⁰⁹⁶⁶ did not result in detectable reduction of *Inx2* mRNA (Figure 3.13D).

In addition to the line described above, three other UAS-Inx2 RNAi lines were crossed to Ctb-Gal4 (Figure 3.13A-D). Across these crosses (Ctb-Gal4/CyO > UAS-Inx2⁴²⁶⁴⁵, Ctb-Gal4>UAS-Inx2¹⁰²¹⁹⁴, and Ctb-Gal4>UAS-Inx2⁸⁰⁴⁰⁹), qPCR did not show a reduction in Inx2 mRNA relative to the corresponding driver-only controls; in several groups, values were similar to controls. Thus, driving *Inx2* RNAi with Ctb-Gal4 did not achieve an effective transcript-level knockdown in Malpighian tubules. Accordingly, subsequent analyses used the principal cell driver CapaR-Gal4, as validated earlier (Figure 3.11).

The Fly Cell Atlas is a single-cell transcriptomic atlas of the adult fruit fly (Li et al., 2022). The cell cluster data are annotated from the Fly Cell Atlas resource, and the different regions of the tubule from the clusters are defined (Figure 3.14). Within the Malpighian tubules, the Fly Cell Atlas identifies principal cells as distinct regional subtypes, including principal cells of the initial segment, lower segment, and lower ureter. This indicates that principal cells are not a single group of cells but instead consist of region-specific subtypes with distinct transcriptional signatures and functional roles. *Inx2* is expressed across several of these principal-cell clusters, but not in stellate cells (Figure 3.15). According to the Fly Cell Atlas, these principal-cell clusters represent anatomically distinct regions of the tubule, each defined by unique transcriptional features. This highlights that *Inx2* expression is not the same across all principal cells but is consistently absent from stellate cells.

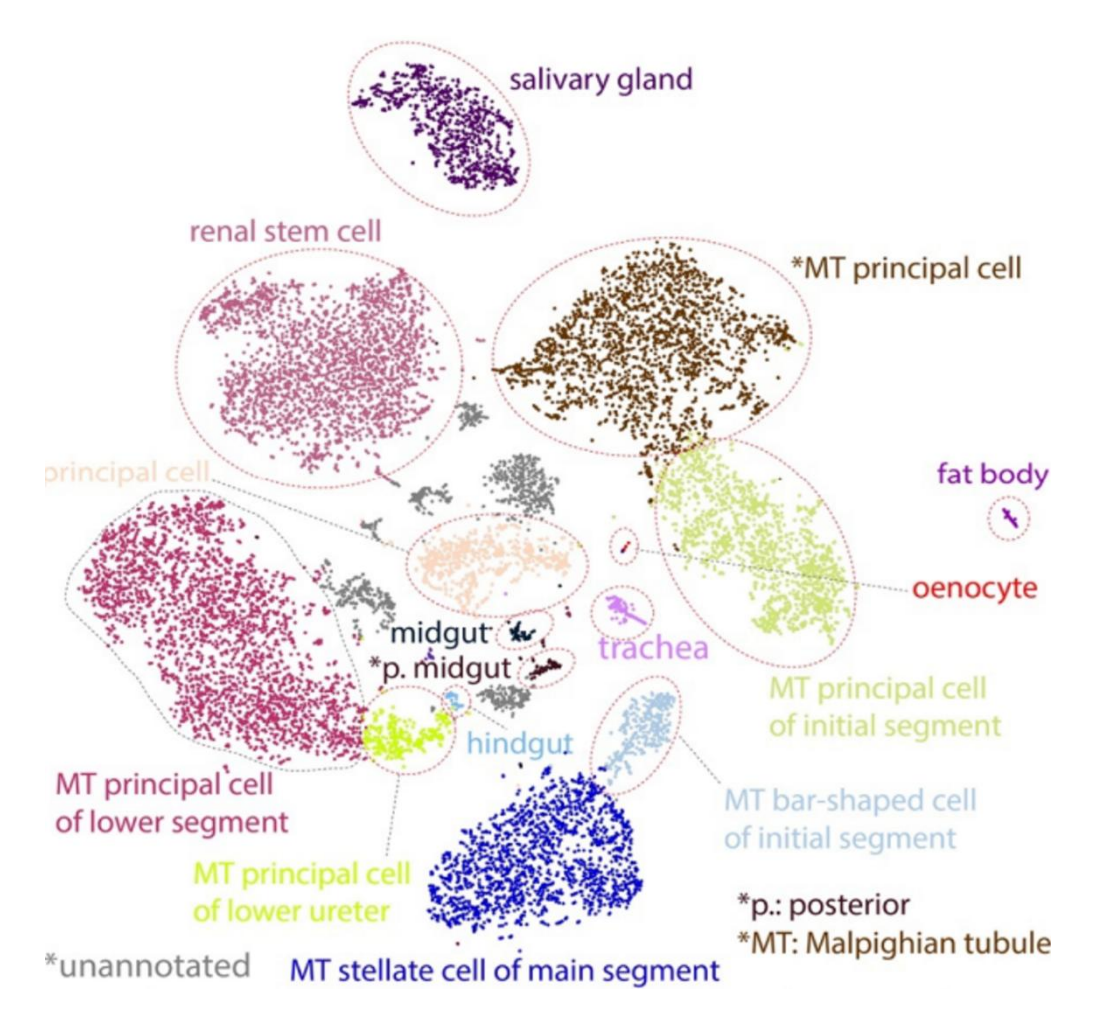


Figure 3.14 Fly Cell Atlas: A single-nucleus transcriptomic atlas of the adult fruit fly tubule. SNE plots of the other 13 tissues from the Stringent 10x dataset (Li *et al.*, 2022). FlyCellAtlas, as a single-cell sequencing technique, provide single-cell sequencing data to identify different cell types in flies' tubules.

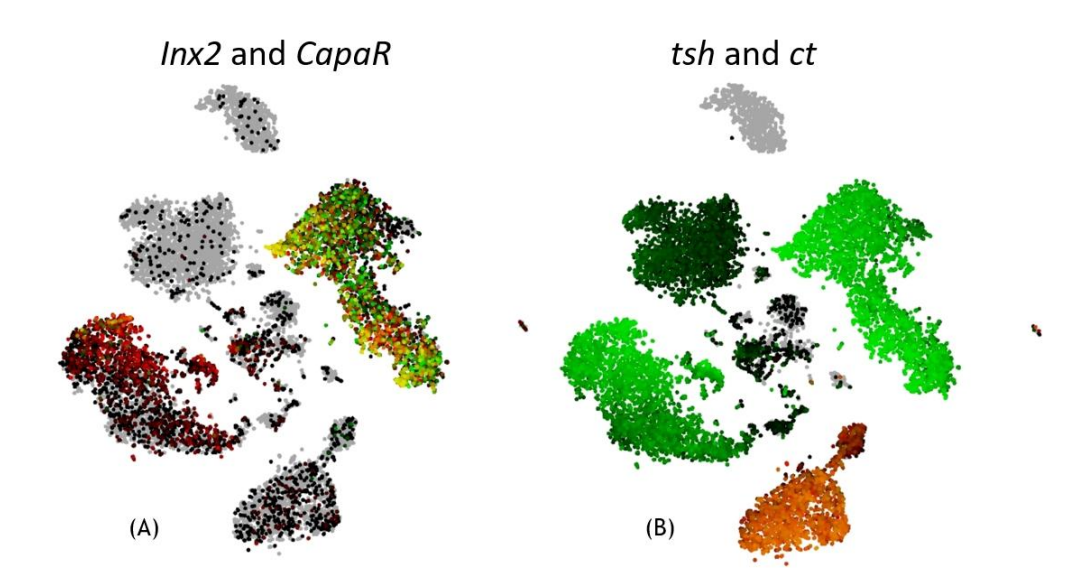


Figure 3.15: Scope representation of the *Inx2* and CapaR single-cell data for the adult tubules from the Fly Cell Atlas. (A) Co-visualization of *Inx2* (red) and *CapaR* (green). Overlap of expression is indicated by yellow/orange points. (B) *Co-visualization of tsh* (red) and ct (green). Each point represents a single nucleus from the Fly Cell Atlas dataset (Li et al., 2022), projected using SCope ((Li and Janssens et al., 2022; Davie et al., 2018). Points are coloured according to the expression of the selected genes, while cells with no detectable expression are shown in black and serve as a background reference. The notation therefore indicates gene-specific expression (red or green), co-expression (yellow/orange), or absence of detectable expression (black). This representation illustrates that Inx2 and CapaR are co-expressed in principal cells, whereas tsh and ct mark stellate cells, with no overlap between the two groups.

3.3.3 Inx2 Does Not Affect Fluid Secretion of The Tubules

The function of the tubules can be analysed by determining the fluid secretion rate through the Ramsay assay (Cabrero *et al.*, 2014; Ramsay, 1954). I dissected five tubules from each fly line and set them up to the secretion plate wells, then measured the size of the secreted bubble every 10 minutes. The bubble from the aperture at the cut end of the common ureter. I obtained the diameter of the spherical droplet. Using the diameter data from all the spherical droplets, I calculated the fluid secretion rate via several formulas (see Materials & Methods). The MEAN and SEM secretion rates (nL/min) were also calculated every 10 minutes (Figure 3.16). Three lines (*CapaR-Gal4*, *UAS-Inx2* and *tsh-Gal4*) were used as parental control lines to compare the *Inx2* knockdown (*CapaR-GAL4>UAS-Inx2* and *tsh-GAL4>UAS-Inx2*) fluid secretion rate. Assays were performed at both 21-22 °C (room temperature) and 25 °C to check that conclusions were consistent across conditions. This design was chosen because GAL4/UAS-driven expression is known to increase with temperature, and theoretically, 25 °C provides higher driver activity than approximately 21 °C.

Kinins are neuropeptide hormones (Lu *et al.*, 2011) that participate in insect diuretic activity (Nachman *et al.*, 2009). In *Drosophila*, they affect fluid secretion via Cl⁻ transport in the stellate cells (O'Donnell *et al.*, 1998). In the fluid secretion assays, I used kinin to stimulate the tubules at 30 minutes (Figure 3.16). The results of Figure 3.16 show that basal secretion rates did not change compared to control MTs, while kinin-stimulated secretion rates in *CapaR-Gal4>UAS-Inx2* RNAi MTs also did not change compared to both controls. Statistical comparisons were made between the knockdown and the corresponding parental controls at each time point using two-tailed Student's t-tests; no significant differences were detected (p > 0.05).

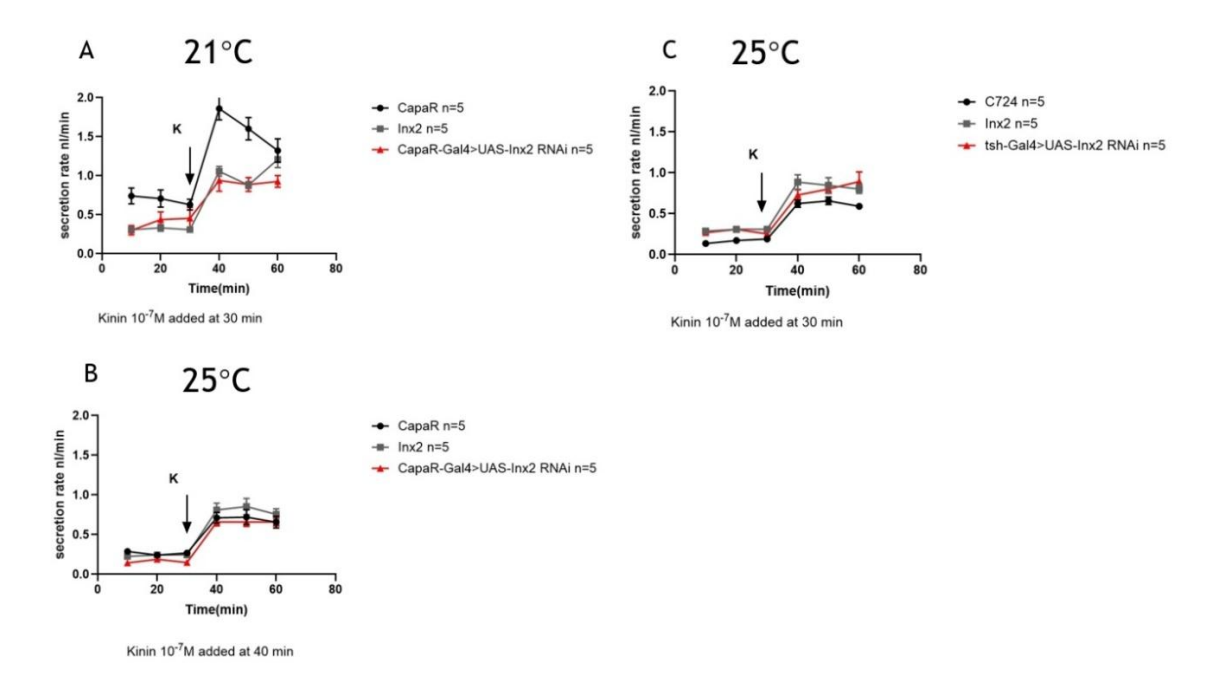


Figure 3.16 Secretion assay for *CapaR-Gal4>UAS-Inx2* compared with parental line. A. Secretion rates at 21-22 °C for CapaR-Gal4 (black circles), UAS-Inx2⁴²⁶⁴⁵ (dark grey squares), and CapaR-Gal4>UAS-Inx2 RNAi (red triangles). B. Secretion rates at 25 °C for the same three genotypes. C. Secretion rates at 25 °C for *C724* (tsh-Gal4), UAS-Inx2⁴²⁶⁴⁵, and tsh-Gal4>UAS-Inx2 RNAi. Kinin (10^{-7} M) was added at 30 or 40 minutes, as indicated by arrows. Data are shown as mean \pm SEM, N = 5 tubules per genotype. Statistical comparisons were performed using two-tailed Student's *t*-tests at each time point (p > 0.05).

I also determined the increase in fluid secretion following kinin stimulation, expressed as the percentage change relative to the basal level (Figure 3.17). Figure 3.17A shows assays performed at room temperature (21-22°C), whereas Figures 3.17B and 3.17C show assays conducted at 25°C. Figure 3.17 shows the percentage increase in fluid secretion at different temperatures compared to the basal fluid secretion calculated from Figure 3.16. There is no significant change between parental and experimental lines in Figure 3.19 (A) and (C), and also no difference between knockdown and RNAi lines (B). However, it shows a change between knockdown and CapaR-Gal4 lines and a difference between RNAi and CapaR-Gal4 lines. Our fluid secretion results cannot conclude a significant difference between knockdown and parental lines. Taken together, the results show that the knockdown had a neutral effect on fluid secretion at room temperature. Although Figure B indicates a positive knockdown impact on fluid secretion at 25°C compared to CapaR-Gal4, the knockdown had a neutral effect on fluid secretion.

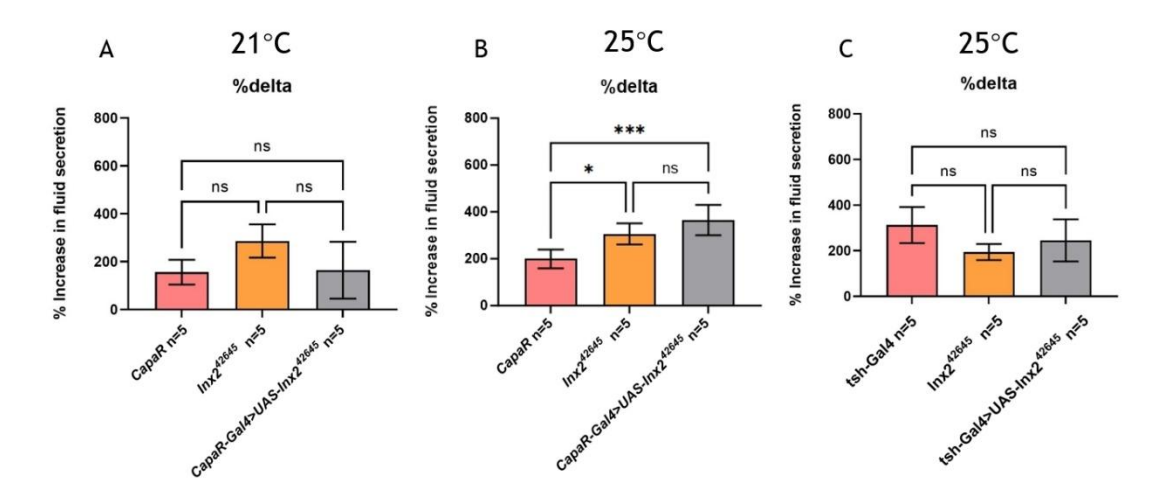


Figure 3.17 The percentage increase in fluid secretion after stimulation by kinin in *Inx2* knockdown flies. The animals were reared, and the assay was performed at room temperature (21°C-22°C) (A) and 25°C (B and C). The mean percentage change from the three biological replicates of the fluid secretion assay is shown and calculated. Formulas are described in the previous chapter. * Indicates a statistically significant difference (p<0.05). All graphs show mean ± SEM. N=5

3.3.4 Inx7 is Mainly Expressed in The Principal Cells of The Tubule

I used *Inx7*²²⁹⁴⁸ to determine its efficiency at decreasing the mRNA levels of *Inx7*. The mRNA levels of *Inx7* were determined using qPCR. The parental UAS-Inx7 and GAL4 lines were used as the controls. Figure 3.18 (A) shows the results of the *Inx7* knockdown experiment at room temperature. There was a statistically significant difference between *Inx7* expression from the CapaR-Gal4>UAS-Inx7 and UAS-Inx7, indicating a 45% decrease in the experimental flies relative to the control flies. Figure 3.18 (B) shows the results of the *Inx7* knockdown experiment at 25°C, but only the UAS-Inx7 line was used as the control. There is also a statistically significant difference between *Inx7* expression from the CapaR-Gal4>UAS-Inx7 and UAS-Inx7, indicating an 80% decrease in the experimental flies relative to the control flies. By contrast, when the knockdown was driven in stellate cells using tsh-Gal4>UAS-Inx7, no reduction in *Inx7* transcript levels was observed compared with the tsh-Gal4 driver control, consistent with the low or absent expression of *Inx7* in stellate cells.

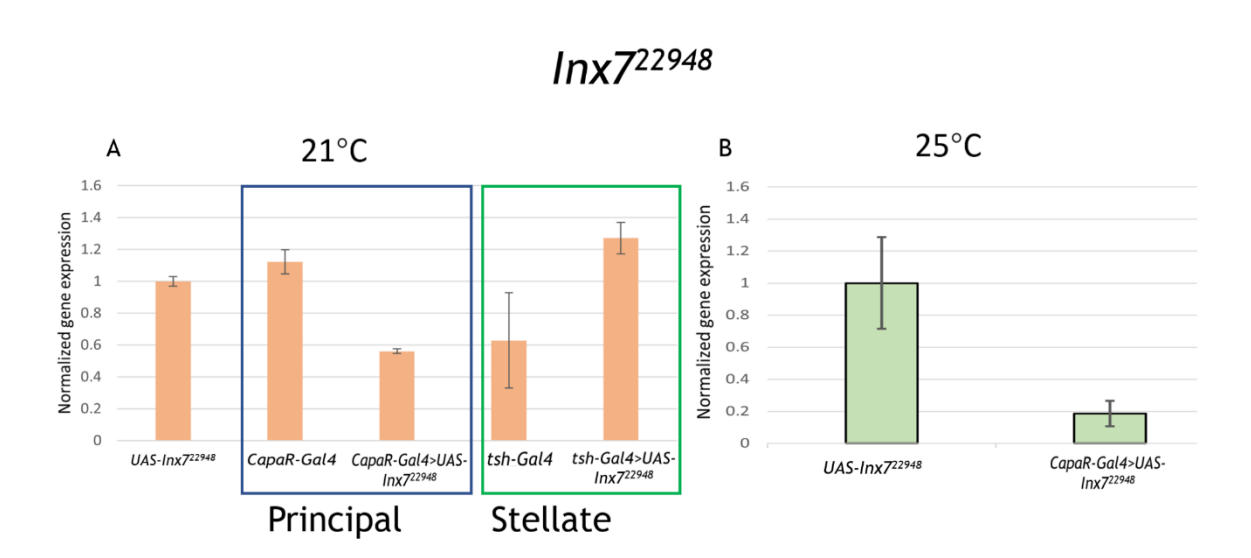


Figure 3.18 RNAi knockdown of $Inx7^{22948}$ in MTs at different temperatures. qPCR experiments show that CapaR-Gal4>UAS-Inx7 exhibits a reduced level of $Inx7^{22948}$ mRNA expression compared to the control at 21°C (A) and 25°C. Data are expressed as the mean of mRNA relative expression \pm SEM, N=5, p>0.05, students t-test.

Fly Cell Atlas data provides supporting evidence for the RNAi knockdown results (Li et al., 2022). Inx7 expression is detected within clusters that partially overlap with the CapaR-positive principal-cell populations, but it is not associated with the tsh clusters that mark stellate cells (see Figure 3.15 and Figure 3.19). However, the overlap between Inx7 and CapaR expression is not complete. This incongruence highlights a limitation of the dataset and suggests that additional spatially resolved methods, such as in situ hybridisation, would be needed to confirm the precise localisation of Inx7.

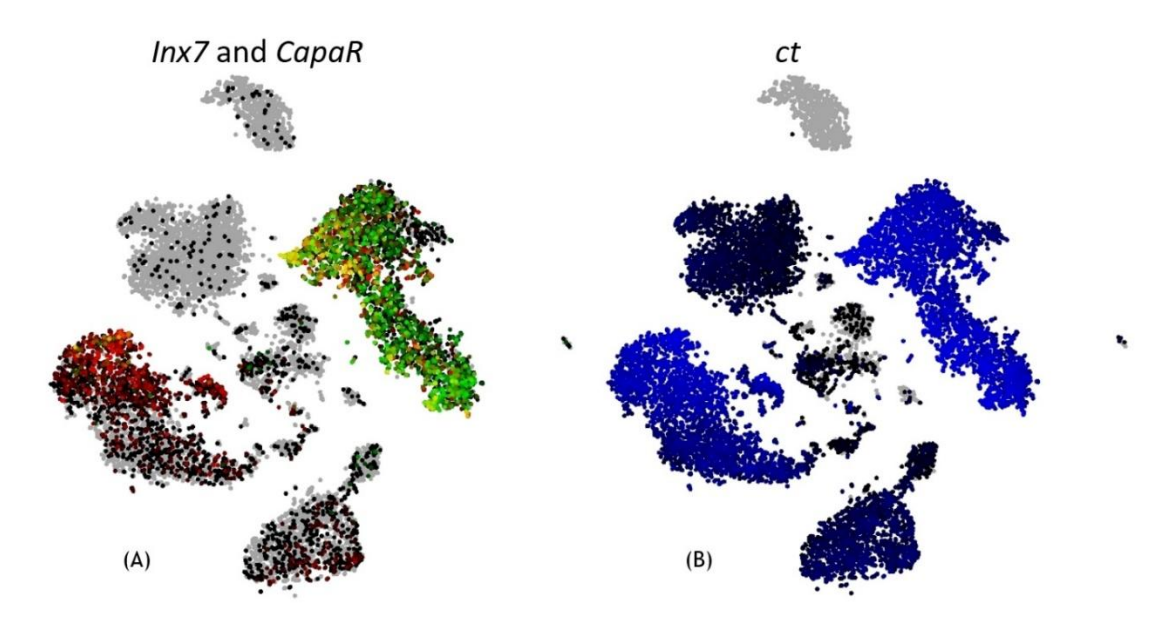


Figure 3.19 Scope represents the *Inx7* and CapaR single-cell data for the Fly Cell Atlas adult tubules. (A) Expression of *Inx7* (red) and *CapaR* (green) in tubule principal-cell clusters. (B) Expression of *ct* (blue), marking a different subset of cells. Black dots indicate cells without detectable expression of the selected genes (unannotated cells). Data are extracted from the Fly Cell Atlas and visualised using the SCope tool (Li and Janssens et al., 2022).

3.3.5 Inx7 Does Not Affect Fluid Secretion of The Tubules

CapaR-Gal4, UAS-Inx7 and tsh-Gal4 were also used as parental control lines to compare *Inx7* knockdown (CapaR-GAL4>UAS-Inx7 and tsh-GAL4>UAS-Inx7) fluid secretion rates in Figure 3.20. Basal secretion rates measured before kinin addition did not differ significantly between knockdown and control lines at either room temperature or 25°C. The response to 10⁻⁷ M kinin was also not reduced in the principal-cell-specific *Inx7* knockdown tubules (red triangles) at room temperature or 25°C (Figure 3.20A, B). The results of Figure 3.20 therefore show that neither basal secretion rates nor kinin-stimulated secretion rates in CapaR-Gal4>UAS-Inx7 RNAi Malpighian tubules changed compared to both parental controls. The knockdown of *Inx7* in the stellate cells similarly did not affect either basal or kinin-stimulated fluid secretion rates (Figure 3.20C). Statistical comparisons were performed at each time point using two-tailed Student's t-tests; no significant differences were detected (p > 0.05).

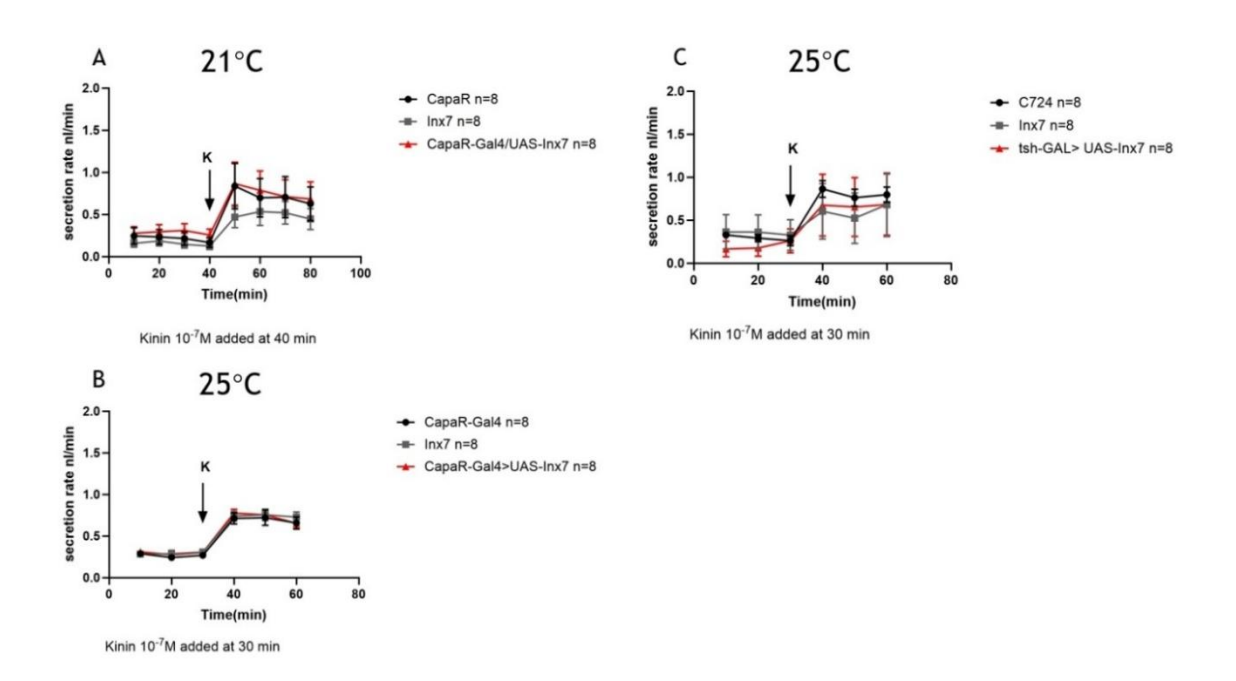


Figure 3.20 Secretion assay for *CapaR-Gal4>UAS-Inx7* compared with parental line. The knockdown of $Inx7^{22948}$ in the principal cells of the Malpighian tubules was tested at room temperature (21-22°C; A) and 25°C (B), as well as in stellate cells at 25°C (C). Basal secretion rates were measured for 40 minutes before kinin addition, and kinin (10^{-7} M; arrow K) was then applied. The secretion rates were monitored every 10 minutes up to 60 minutes. Statistical comparisons between knockdown and corresponding controls were carried out using two-tailed Student's t-tests. No significant differences were found (p > 0.05). Data are expressed as mean \pm SEM, N=8.

Figure 3.21 shows the percentage increase in fluid secretion at different temperatures compared to the basal fluid secretion calculated from Figure 3.20. Figure 3.21 (A and B) shows that the kinin-stimulated percentage increase in fluid secretion at room temperature (21°C to 22°C) and 25°C was similar in CapaR-Gal4, UAS-Inx7 and CapaR-Gal4>UAS-Inx7 RNAi. The percentage increase in the fluid secretion rate was similar in the tsh-Gal4 and tsh-Gal4>UAS-Inx7 RNAi tubules. While Figures 3.21A and B showed no significant difference between knockdown and controls, Figure 3.21C indicated a statistically significant difference when *Inx7* RNAi was driven in stellate cells at 25 °C. However, given the small sample size (n=5) and the absence of consistent effects in the other conditions (Figure 3.20 and Figure 3.21A-B), this result should be interpreted with caution and may reflect variability rather than a consistent knockdown effect.

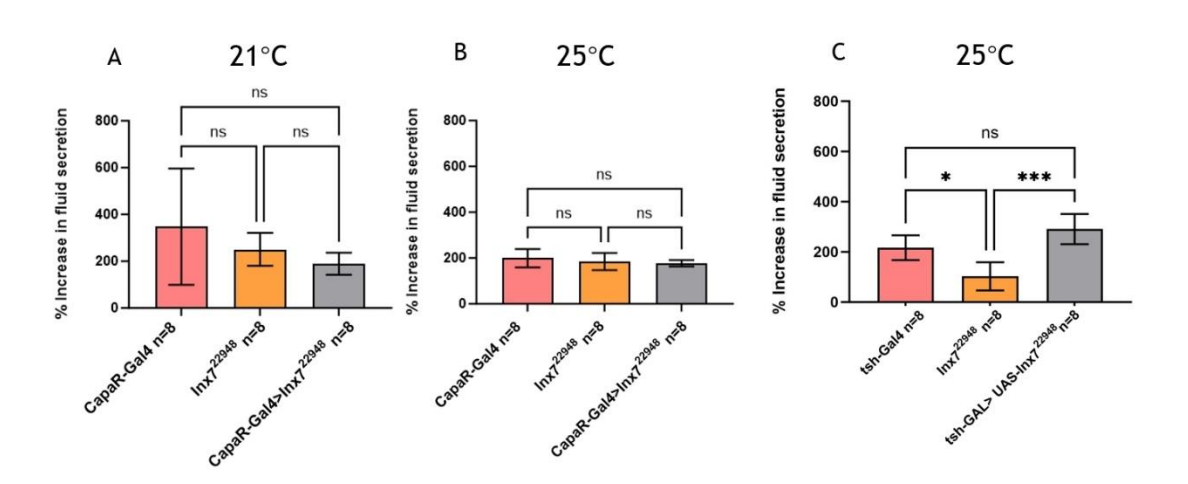


Figure 3.21 The percentage increase in fluid secretion after stimulation by kinin in the Inx7 knockdown flies. Fluid secretion assays were carried out at room temperature (21-22 °C; A) and at 25 °C (B, C). Percentage change was calculated relative to basal secretion shown in Figure 3.20. Panels A and B show data from CapaR-Gal4, UAS-Inx7 and CapaR-Gal4>UAS-Inx7 RNAi lines, while panel C shows data from tsh-Gal4, UAS-Inx7 and tsh-Gal4>UAS-Inx7 RNAi lines. Values represent mean \pm SEM from three biological replicates (N = 5). Statistical analysis was performed using one-way ANOVA. ns, not significant; *p < 0.05; ***p < 0.001.

3.3.6 Protein Interactions and Structure

3.3.6.1 Innexin 2 Protein Structure and Interaction Network

The sequence of Inx2 predicts four hydrophobic transmembrane regions, two extracellular loops, and three cytoplasmic domains that include both termini (Bauer et al., 2005). These are the usual features of innexin proteins and are thought to give them the ability to assemble into gap junction channels. In fact, earlier studies also noted that Inx2 is the smallest of the *Drosophila* innexins, with noticeably shorter cytoplasmic regions than most of the others (Bauer et al., 2005). This difference may have an effect on the way Inx2 interacts with other proteins, and it may also influence how the tubule epithelium is coordinated. A predicted structure from AlphaFold is shown in Figure 3.22. The figure presents the main domains and also marks, with different colours, which parts of the prediction are more reliable and which are predicted with lower confidence.

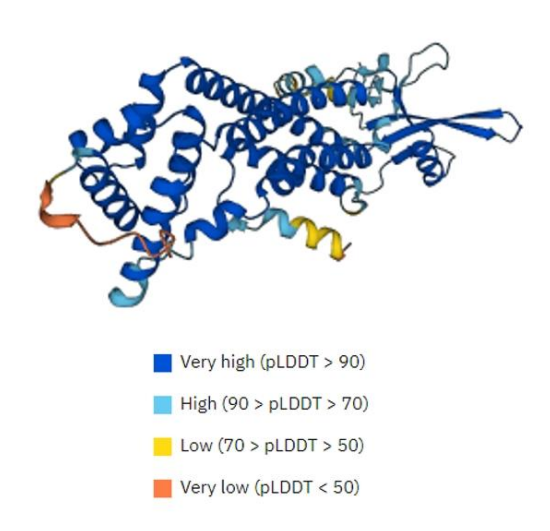


Figure 3.22 The predicted protein structure for Inx2. The structure of Inx2 was predicted using the AlphaFold Protein Structure Database. The model shows four transmembrane domains, extracellular loops, and the N- and C-terminal regions. Colour coding indicates the confidence of prediction using the pLDDT score: dark blue (very high, >90), light blue (high, 70-90), yellow (low, 50-70), and orange (very low, <50) (Varadi et al., 2022; Jumper et al., 2021). Regions in blue are considered reliable, whereas yellow and orange areas represent structural uncertainty.

A protein interaction network can provide insight into the potential functions of Inx2. Table 3.23 lists two proteins, Acam and CG4942, that were identified as interacting partners of Inx2 in the IntAct database (Del Toro et al., 2022). Acam (also known as androcambin) is a testis-expressed protein with proposed roles in male fertility, whereas CG4942 encodes a predicted protein of unknown function. These interactions were identified using the yeast two-hybrid method and classified as physical associations. Although the confidence scores are relatively modest, they suggest potential links between Inx2 and proteins outside the innexin family. The interaction network is summarised in Figure 3.23.

Gene name	Detection Method	Interaction Type		
Acam	2 hybrid	physical association		
CG4942	2 hybrid	physical association		

Table 3.23 Summary of Inx2 protein interaction network. Interactions were retrieved from the IntAct molecular interaction database (Del Toro *et al.*, 2022). The table lists two proteins, Acam and CG4942, identified as physical interactors of Inx2 in two-hybrid assays. Interaction type, experimental method, and confidence score are shown as reported in the IntAct database (Del Toro *et al.*, 2022)

3.3.6.2 Innexin 7 Protein Structure and Interaction Network

The sequence of Inx7 predicts that it has a similar sequence to Inx2. Inx7 also has four hydrophobic transmembrane domains, two extracellular loop domains, and three cytoplasmic domains, including extracellular loops and the intracellular N- and C-terminal domains (Bauer et al., 2005). The structure of Inx7 is slightly different from that of other innexin genes. It has the largest C-terminal domains and displays a cytoplasmic loop of 66 amino acids. Figure 3.24 shows the predicted protein structure for Inx7. Figure 3.25 displays 15 proteins that physically interact with Inx7. Previous results from Curtin et al. (2002) have identified the genetic interaction between two Innexin proteins, Inx7 and shakB.

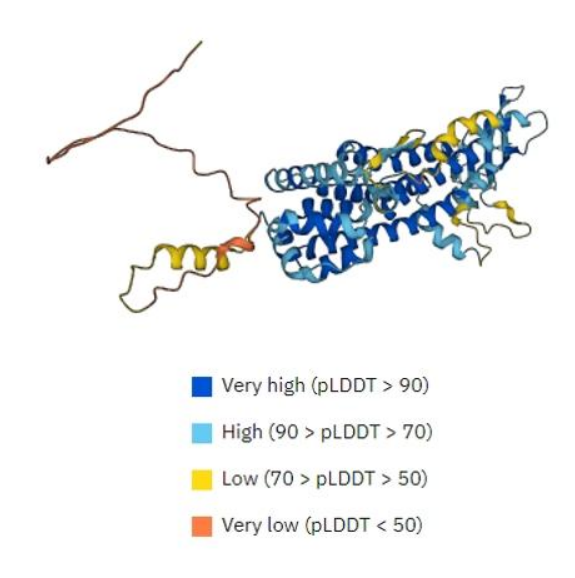


Figure 3.24 The predicted protein structure for Inx7. The output from the AlphaFold protein structure database is shown. Presentation of the prediction of a 3D molecular graph of the Inx 7. pLDDT is an amino acid-level confidence measure (Varadi *et al.*, 2022; Jumper *et al.*, 2021). Residues are colour-coded based on their pLDDT scores, showing prediction confidence ranging from very high, blue, to very low, or red.

Gene name (Interactor)	Detection Method	Interaction Type	
CG17580	two hybrid prey pooling approach	physical association	
	two hybrid array	physical association	
CG31222-RA	two hybrid prey pooling approach	physical association	
	two hybrid array	physical association	
CG14401	two hybrid prey pooling approach	physical association	
	two hybrid array	physical association	
CG17985	two hybrid prey pooling approach	physical association	
	two hybrid array	physical association	
SEC22	two hybrid prey pooling approach	physical association	
	two hybrid array	physical association	
whe	two hybrid prey pooling approach	physical association	
	two hybrid array	physical association	
Atpalpha	2 hybrid	physical association	
CG4835	2 hybrid	physical association	
CG6933	2 hybrid	physical association	
Fcp3C	2 hybrid	physical association	
Hale	2 hybrid	physical association	
Trim9	2 hybrid	physical association	
Knrt	2 hybrid	physical association	
Miro	2 hybrid	physical association	
fax	anti tag coip	association	

Table 3.25 Summary of Inx7 protein interaction network. A table of the interactions of the Inx7 protein and other proteins from IntAct. Edges represent protein-protein associations. Data extracted from IntAct Molecular Interaction Database (Del Toro *et al.*, 2022)

3.4 Discussion

The goal of the experiments described in this chapter was to investigate innexin gene function in the Malpighian tubules. Specifically, we first asked whether RNAi knockdown of *Inx2* and *Inx7* altered their transcript levels in the tubules. For *Inx2*, principal-cell knockdown (CapaR-Gal4>UAS-Inx2⁴²⁶⁴⁵) was compared with both parental controls, the driver-only CapaR-Gal4 line and the UAS-Inx2⁴²⁶⁴⁵ line (Fig. 3.11). Although the mean *Inx2* mRNA in CapaR-Gal4>UAS-Inx2⁴²⁶⁴⁵ appeared lower than in each parental control, statistical testing (two-tailed Student's t-test) gave p > 0.05, so the data do not support our initial expectation that tissue-specific *Inx2* RNAi would lower *Inx2* mRNA abundance in principal cells relative to the parental controls. Consistent with this, additional UAS-Inx2 lines tested in the same way did not show a clear reduction, and some gave mixed results (Fig. 3.12). Together, these qPCR results indicate incomplete or inconsistent knockdown at the transcript level under our conditions.

Although none of the results from the four *Inx2* RNAi lines gave consistent evidence for reduced *Inx2* levels in principal cells, we tested knockdown efficiency directly by qPCR. Both CapaR-Gal4>UAS-Inx2 RNAi and Ctb-Gal4>UAS-*Inx2* RNAi lines were compared with their respective parental controls, but the results did not show significant reductions in transcript abundance. These experiments were designed to evaluate knockdown efficiency, rather than to determine the precise localisation of *Inx2* expression. The data therefore indicate that under our conditions the RNAi knockdowns were incomplete or variable.

In contrast, Fly Cell Atlas data (Li et al., 2022) provide independent evidence that *Inx2* is normally expressed in principal cells. Our own analysis also supports this, showing enrichment of *Inx2* in principal cells of both the initial and lower segments (Fig. 3.15). CapaR expression was detected in the initial and main segments but not in the lower tubules, which may partly explain why knockdown effects were weak. Taken together, while qPCR knockdown assays did not yield clear reductions in transcript levels, the FlyCellAtlas dataset confirms that *Inx2* is expressed in principal cells

To interpret the changes in fluid secretion following *Inx*2 knockdown, it was important to place the assay results in the context of gap junction function in epithelial physiology. Gap junctions, formed by innexins such as Inx2, enable intercellular communication and coordination of secretion. In the secretion assays, three relevant genotypes were compared. The driver-only parental line (CapaR-Gal4 or C724) is shown in black in the figures, the UAS-only parental line (UAS-Inx2) is shown in grey, and the knockdown line (CapaR-Gal4>UAS-Inx2) is shown in red (Figures 3.16-3.17). The knockdown line showed a statistically significant difference when compared with the driver-only control (p < 0.05), but no significant difference when compared with the UAS-only control (p > 0.05). This inconsistency, together with the qPCR data showing incomplete knockdown, indicates that the secretion assay alone cannot establish a functional role for Inx2. Taken together, these assays suggest that Inx2 knockdown did not reproducibly alter basal or stimulated secretion rates, although the possibility remains that compensatory mechanisms within the tubule could buffer against partial loss of Inx2 function. In addition, we tested the effect of kinin peptides, which stimulate secretion through Cl⁻ transport in stellate cells, as a functional probe. The responses of knockdown lines to kinin stimulation were similar to those of both parental controls, reinforcing the conclusion that *Inx*2 knockdown did not impact secretion under these conditions. CAPA peptides were not selected for detailed analysis in this study because their role in tubule physiology is broader and less specific; they can influence other pathways beyond secretion, making them less suitable as a direct probe of gap junction function. For this reason, kinin was used as the principal stimulus to assess whether Inx2 contributed to epithelial coordination of secretion.

These results indicate no differences between each line in terms of fluid secretion. Although Figure 3.19 (B) shows a significant difference between the CapaR-Gal4 and RNAi lines, as well as a slight difference between the CapaR-Gal4 and knockdown lines at 25°C, there is no difference between the RNAi and knockdown lines. Therefore, *Inx2* knockdown did not impact the secretion rate. Figure 3.19 (A) also shows no change between these three lines (CapaR-Gal4, UAS-Inx2, CapaR-GAL4>UAS-Inx2) at 21°C. Gal4 protein can more efficiently bind to Gal4-binding sites at a higher temperature, leading to the CapaR-Gal4 line

having a more severe phenotype at 25°C. This contributes to transcribing the RNAi line more efficiently and explains why a better knockdown result is shown at 25°C.

Following the *Inx2* experiments, the RNAi line *Inx7*²²⁹⁴⁸ was tested by crossing with CapaR-Gal4 and tsh-Gal4 to determine whether transcript levels of *Inx7* were reduced in the Malpighian tubules. Unlike *Inx2*, only one RNAi line was available, so the efficiency of knockdown was assessed under both conditions. qPCR analysis (Figure 3.18) showed that *Inx7* expression was reduced by approximately 45% at room temperature (21-22 °C) and by about 80% at 25 °C when driven with CapaR-Gal4. In contrast, knockdown driven in stellate cells with tsh-Gal4 did not produce a significant reduction in *Inx7* transcript levels compared with the control. These results indicate that knockdown of *Inx7* was effective in principal cells when driven with CapaR-Gal4, particularly at 25 °C, but was ineffective in stellate cells.

Having established that *Inx7* knockdown could be achieved in principal cells at the transcript level, we next examined whether this reduction influenced tubule physiology by measuring basal and kinin-stimulated secretion rates (Figure 3.20). The basal secretion rate was similar across experimental and control groups, and the increase in secretion following stimulation with kinin peptide was also comparable. These results indicate that reducing *Inx7* transcript levels in principal cells did not alter either the basal secretion rate or the responsiveness to kinin stimulation. In other words, the observed knockdown did not lead to measurable functional changes in fluid transport under these conditions.

Figure 3.21 further illustrates that temperature can influence the results. At 25 °C, Gal4-driven expression is generally stronger than at room temperature, which can enhance the efficiency of RNAi knockdown. This may explain why differences between control and knockdown lines were more apparent at 25 °C than at 21 °C. The higher activity of Gal4 at elevated temperature can increase the expression of UAS-linked transgenes, whereas expression driven by the

CapaR promoter may not be similarly temperature-sensitive. Consequently, CapaR function itself may remain relatively constant, but the extent of RNAi-mediated reduction of *Inx7* can vary depending on the rearing temperature. Taken together, these findings suggest that while *Inx7* knockdown was effective at the transcript level, it did not lead to a clear effect on fluid secretion, and any subtle changes may have been masked by compensatory mechanisms in the tubule epithelium.

A further limitation of the present study is that the localisation of *Inx2* and *Inx7* within the Malpighian tubules was inferred indirectly from qPCR results, RNAi knockdown outcomes, and transcriptomic resources, rather than being demonstrated by spatially resolved methods. Techniques such as in situ hybridisation or immunohistochemistry would provide direct cell-level confirmation of innexin expression and clarify whether *Inx2* is confined to principal cells and whether *Inx7* has a broader distribution, as suggested by single-cell datasets. These approaches were not employed here due to practical constraints, but they remain an important priority for future work and would complement the current findings by providing visual evidence of gene expression within specific tubule cell types.

As the expression level of *Inx2* and *Inx7* in the knockdown line is decreased, I expect its knockdown positively affected fluid secretion. However, my fluid secretion results show that the knockdown had a neutral effect on fluid secretion. In future studies, the qPCR primers for *Inx2* and *Inx7* can be redesigned to improve the accuracy of transcript detection. The number of flies in my research (n = 5) may be insufficient. Future experiments can increase the number of flies in fluid secretion. Furthermore, different kinin concentrations can be used in fluid secretion stimulation, and CAPA peptide can also be involved in fluid secretion stimulation. Finally, an experimental approach can be tested in the simultaneous knockdown of *Inx2* and *Inx7* in MTs in future work. It could help to understand the function of *Inx2* and *Inx7* in the secretion process. UAS-RNAi constructs targeting *Inx2* and *Inx7*, driven by tissue-specific Gal4 drivers (e.g., CapaR-Gal4), can be used to knock down both genes

simultaneously in MTs. *Inx2* and *Inx7* expression levels in the knockdown line can be validated using qPCR.

Another limitation of the present study is that localisation of *Inx2* and *Inx7* was assessed only indirectly, based on transcriptomic datasets and qPCR of whole tubules. More spatially resolved methods, such as in situ hybridisation or immunohistochemistry, would allow confirmation of their expression in principal versus stellate cells. These approaches could directly test predictions from FlyAtlas2 and single-cell data and provide stronger evidence for the precise distribution of these innexins. Although not applied here, they represent an important future step that would provide a stronger basis for the conclusions of this work.

The evidence indicates that *Inx2* and *Inx7* expressions are enriched in principal cells of the Malpighian tubules, while additional expressions are also detected in other tissues such as the nervous system (*Inx2*) and the midgut (*Inx7*) (FlyAtlas2). Compared with other innexins, *Inx2* and *Inx7* appear to be the predominant family members in the tubules. Functional assays showed that knockdown of either gene had a neutral effect on basal and kinin-stimulated secretion, suggesting that their roles may not be directly linked to secretion, or that redundancy and compensatory mechanisms mask any effect.

The protein structure predictions and interaction data provide further context. The AlphaFold models of *Inx2* and *Inx7* show the conserved four-transmembrane and two extracellular-loop organisation that supports gap junction channel formation. Interaction network data also identified possible binding partners such as Acam and CG4942 for *Inx2*, and a wider set of interactors for *Inx7*. Together, these results indicate that structural features and protein-protein interactions are likely to contribute to their function in maintaining epithelial coordination in the Malpighian tubules, even though direct effects on secretion were not observed in this study.

3.5 Conclusion

The renal (Malpighian tubule) system has been an attractive and effective genetic model for understanding insect homeostasis regulation. Principal and stellate cells are the two main cell types in the tubules. Between the two cell types, gap junctions play an important role in communication and in the exchange of small ions and molecules (Liu et al., 2011). In this study, Inx2 and Inx7 were found mainly in principal cells based on transcriptomic data and gPCR analysis. Lowering the levels of Inx2 and Inx7 did not lead to clear or consistent changes in fluid secretion. The percentage increase in secretion after kinin stimulation was only slightly different in the *Inx2* knockdown. These results suggest that the contribution of Inx2 and Inx7 to secretion in the adult tubule is uncertain, and any effect may be masked by redundancy between innexins. Further work will be needed to test directly whether gap junctions couple principal and stellate cells, as this could be a key route for intercellular communication in the tubule. It will also be important to confirm the expression of Inx2 and Inx7 using in situ hybridisation or immunohistochemistry, methods that would give stronger evidence for their localisation in specific cell types.

Chapter 4 *Drosophila* α2-adrenergic-like octopamine receptor

4.1 Summary

This chapter investigates the role of the Octα2R octopamine receptor in *Drosophila* Malpighian tubules, with emphasis on its expression, function, and physiological relevance. The results demonstrate that *Octa2R* is specifically expressed in the stellate cells of the tubules, where it plays an important role in regulating fluid secretion. The effects of four biogenic amines, namely dopamine, tyramine, octopamine, and tryptamine, were examined on fluid secretion rates in *Drosophila* tubules in order to determine the optimal concentration for stimulating secretion. Using UAS-driven knockdown of *Octa2R* under the control of *tsh-Gal4*, it was shown that octopamine, more than other biogenic amines, exerts a significant influence on tubule secretion. Knockdown experiments further revealed that reducing *Octa2R* expression in stellate cells decreases the secretion rate and reduces sensitivity to octopamine. These findings highlight a previously undocumented role for octopamine, mediated through Octα2R, in tubule function.

4.2 Identification of *Octa2R* genes expressed in Malpighian tubules and control

4.2.1 Introduction

This Octalpha 2R study will provide an important example of how biogenic amine signals mediate physiological and behavioural responses. In *Drosophila melanogaster*, Oct α 2R, an α 2-adrenergic-like octopamine receptor, is required for physiological and behavioural functions (Nakagawa *et al.*, 2020). The receptor was identified as a GPCR responding to octopamine (Xu *et al.*, 2022). Octopamine is a biogenic amine that functions analogously to norepinephrine in vertebrates. Oct α 2R regulates locomotor activity (Nakagawa *et al.*, 2022), grooming behaviour, and starvation-increased hyperactivity (Yang *et al.*, 2015). Oct α 2R also responds to serotonin, which points to roles in neurotransmission and neuromodulation (Qi *et al.* 2017).

4.2.2 Role in Biogenic Amines

Biogenic amines are essential for regulating insect behaviours and play significant roles in their central nervous system. Octopamine, analogous to noradrenaline in vertebrates, has been identified in insects, including Drosophila. Four octopamine receptors have been identified in Drosophila, with my research focusing on one of these receptors, $Oct\alpha 2R$. The basis for this selection will be discussed in this chapter. Although the detailed mechanisms by which $Oct\alpha 2R$ regulates physiological and behavioural functions remain unclear, recent studies demonstrate that this receptor is actively involved in a variety of behavioural processes, such as locomotion, that is linked to octopamine signalling (Nakagawa $et\ al.$, 2022; El-Kholy $et\ al.$, 2022). While $Oct\alpha 2R$ was initially considered specific to octopamine, recent research has found that it also responds to other biogenic amines, including tyramine and serotonin, suggesting its broader role within the biogenic amine signalling network (Qi $et\ al.$, 2017).

DmOcta2R (CG18208)

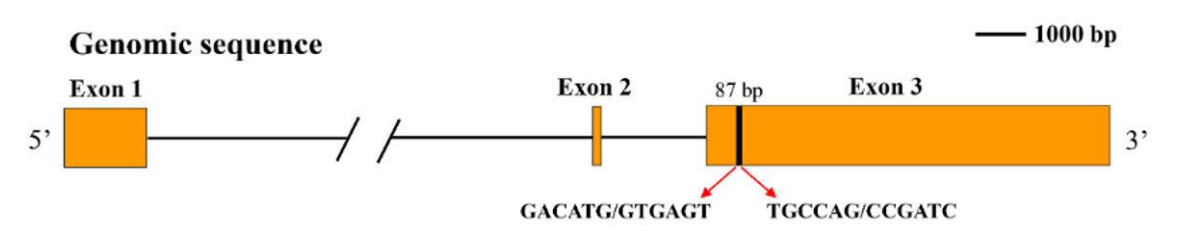


Figure 4.1 Alternative splicing of the *Octa2R* gene generates two transcript variants. Cartoon showing the exon structure of the *Octa2R* locus (CG18208). Exons are drawn as orange boxes. A splice event in exon 3 introduces an 87 bp insertion, giving rise to a long form (Oct α 2R-L) and a short form (Oct α 2R-S) of the receptor (Qi *et al.*, 2017)

The Octa2R gene is alternatively spliced to produce two transcript variants, Oct α 2R-L and Oct α 2R-S, which differ by an 87 bp insertion in exon 3 (Fig. 4.1). This structural diversity is at the basis of generation of long and short forms of the receptor. The cAMP assay data of Qi et al. (2017) demonstrated that Octα2R blocks cAMP, a secondary messenger required for neurotransmitter release, upon activation by biogenic amines (Snyder, 2009). This suggests that Octα2R is capable of regulating intracellular pathways (Qi et al., 2017). Additionally, Nakagawa et al. (2022) reinforce this conclusion by showing that the activation of Oct α 2R leads to reductions in the intracellular levels of cAMP and consequently in behaviour and physiology under the control of octopamine signalling (Nakagawa et al., 2022). Meanwhile, cAMP levels may affect the release and regulation of the neurotransmitters norepinephrine and serotonin. The activation of Octα2R receptors also supports that they are functional receptors subserving in neurotransmission and neuromodulation (Qi et al., 2017). Octa2R does not interact with dopamine (DA) receptors or affect DA release, but it indirectly acts on neural circuits by controlling the cAMP level and neural activity. Besides, dopamine is involved in the modulation of neural circuitry function (Olgún et al., 2016), so there exists an indirect communication pathway between Octα2R and dopamine. According to Qi et al. (2017) and Nakagawa et al. (2022), Octα2R in *Drosophila melanogaster* can be activated not only by octopamine and tyramine but also by serotonin. Serotonin-induced stimulation of Oct α 2R leads to inhibition of adenylate cyclase, resulting in a decrease of intracellular cAMP. In view of the fact that Oct α 2R can be activated by distinct agonists, it serves a complex function in neurotransmission and neuromodulation in the nervous system. This result is in contrast to the previous picture of the specificity of octopamine receptors. Overall, Oct α 2R is crucial for biogenic amine homeostasis. The primary role of this receptor is to bind with octopamine and adjust signalling cascades to control physiological and behavioural processes. It plays a wider role in the biogenic amine signalling system of *Drosophila*.

4.2.3 Expression Patterns and Functional Role

The octopamine receptor Octα2R in *Drosophila melanogaster* displays a specific expression pattern within the central nervous system (CNS). By using T2A-Gal4 and Trojan-Gal4 lines (Deng *et al.*, 2019; Lee *et al.*, 2018), Nakagawa *et al.* have demonstrated that Octα2R is mainly expressed in the pars intercerebralis (PI), the ellipsoid body (EB) of the central complex, and the mushroom body (MB) (Nakagawa *et al.*, 2022). These brain regions are critical for various neurological processes, such as locomotion, memory, and sleep regulation (Belgacem *et al.*, 2002; Yan *et al.*, 2023; Aso *et al.*, 2014).

The PI is a major neuroendocrine centre analogous to the hypothalamus in vertebrates (Hasebe and Shiga, 2021). It processes sensory information and coordinates physiological responses, particularly those related to homeostasis, including feeding and metabolism (Wang et~al., 2019; Wang et~al., 2020). The expression of Oct α 2R in the PI suggests that this receptor may be crucial for regulating neuroendocrine activities and metabolic processes (Nakagawa et~al., 2022). Moreover, octopaminergic neurons in this region demonstrate the Oct α 2R role in integrating octopamine signalling to regulate complex behaviours such as sleep and feeding.

The ellipsoid body (EB) within the central complex coordinates locomotor activity and spatial orientation (Yan *et al.*, 2023). Like the PI, the EB processes sensory information but is primarily known for generating motor outputs

essential for navigation and movement (Pisokas et al., 2020; Heinze *et al.*, 2017). The expression of $Oct\alpha 2R$ in the EB suggests its potential involvement in motor control and ensuring adaptive responses to environmental changes. This role is further supported by altered movement patterns observed in Octa 2R mutants (Nakagawa *et al.*, 2022).

The mushroom body (MB) is integral to associative learning and memory consolidation (Heisenberg *et al.*, 1998), analogous to the hippocampus in vertebrates (Strausfeld and Sayre, 2020). The presence of Octα2R in the MB underscores its importance in cognitive functions. The role of Octα2R in memory processes is particularly significant because its primary ligand, octopamine, improves memory performance by modulating synaptic plasticity and neural circuit activity within the MB.

The differential expression of Oct α 2R across different brain regions suggests a complex role in regulating physiological and behavioural functions. For example, the involvement of the PI in maintaining homeostasis and the function of MB in memory indicates that Oct α 2R could be a key mediator in connecting metabolic states to cognitive performance (Machado *et al.*, 2021). Additionally, the role of EB in motor control corresponds with Oct α 2R's function in regulating movement (Zhao *et al.*, 2021). The supporting evidence is the observed decrease in activity levels in *Octa2R* mutants. These findings suggest that Oct α 2R is crucial not only for specific neurological functions but also for integrating these functions to produce coordinated behavioural responses.

4.2.4 Characterisation of Octq2R Isoforms

DmOcta2R generates two transcripts by alternative splicing: the long isoform Octa2R-L and the short isoform Octa2R-S (Qi et al., 2017). The long isoform differs from the short isoform by the insertion of 29 amino acids within the third intracellular loop (ICL3), located between TM5 and TM6 (Qi et al., 2017). This structural difference is illustrated in Figure 4.2, which shows that Octa2R-L contains the additional 29 amino acids in the third intracellular loop, while

Octa2R-5 lacks this insertion. Pharmacological analyses have shown that both isoforms can be activated by octopamine, tyramine, epinephrine and norepinephrine, leading to inhibition of intracellular cAMP production (Balfanz et al., 2005; Maqueira et al., 2005). Moreover, Qi et al. (2017) reported that DmOcta2R can also be directly activated by serotonin and its agonists. Consistent with its restricted expression in defined brain regions, Octα2R plays an important role in central nervous system regulation. Nakagawa et al. (2022) further demonstrated that hypomorphic mutants of Octa2R display behavioural alterations, including increased grooming duration and reduced starvation-induced hyperactivity, supporting its role in maintaining physiological homeostasis.

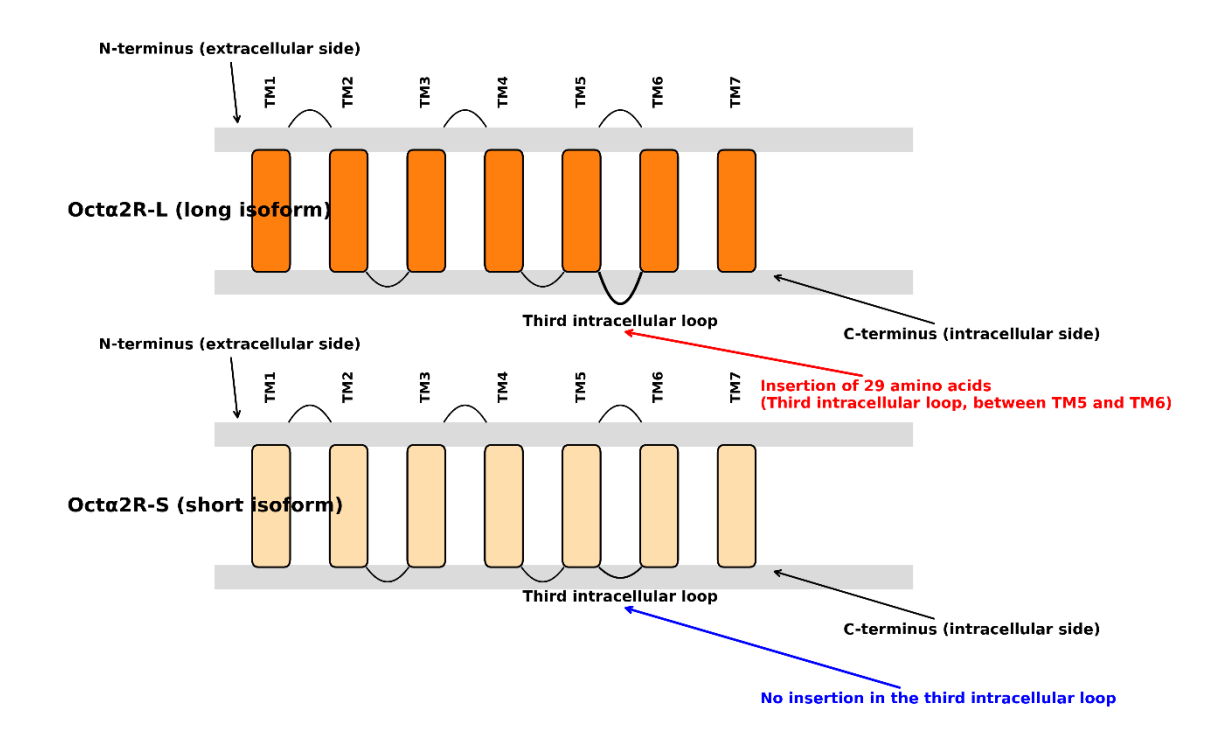


Figure 4.2 Structural difference between Octα2R isoforms. Cartoon representation of the *Drosophila* Octα2R receptor showing seven transmembrane domains (TM1-TM7). The long isoform (Octα2R-L, upper panel) contains an insertion of 29 amino acids within the third intracellular loop, located between TM5 and TM6 (highlighted with a red arrow). The short isoform (Octα2R-S, lower panel) lacks this insertion, as indicated by the blue arrow. This structural difference distinguishes the two isoforms and underlies their functional characterisation (modified from Qi *et al.*, 2017).

4.2.5 Possible Role in Malpighian Tubules

As previously described, octopamine participates in the regulation of many physiological functions. These functions are likely to include excretion and osmoregulation, similar to the norepinephrine function in the kidney in vertebrates. Although direct studies on $Oct\alpha 2R$'s role in these tubules are limited, its involvement in osmoregulatory and metabolic activities implies a potential function in fluid regulation and waste removal. Data from FlyAtlas 2 confirm that $Oct\alpha 2R$ is expressed in Malpighian tubules (Leader et~al., 2017). As Malpighian tubules are essential for maintaining Drosophila's ion balance and waste excretion (Dow et~al., 2021), $Oct\alpha 2R$ may participate in these functions by affecting the activity of epithelial cells in Malpighian tubules. This modulation may alter ion transport mechanisms, affecting fluid secretion rates (Shum et~al., 2023; Orchard et~al., 2021; El-Kholy et~al., 2015). Given $Oct\alpha 2R$'s known roles in locomotor activity and metabolic regulation, similar signalling may also operate in Malpighian tubules, where $Oct\alpha 2R$ contributes to homeostasis by coordinating ion transport, fluid balance and waste removal.

Furthermore, Oct α 2R may interact with other signalling pathways within the Malpighian tubules to improve excretory processes. For example, Octopamine can affect ion channel and transporter activities (Shum *et al.*, 2023). By modulating these factors, Oct α 2R could increase the capacity of tubules to adjust to different physiological conditions, such as those resulting from changing environmental conditions or metabolic states. This adaptive regulation contributes to maintaining internal homeostasis. Additionally, investigating the specific mechanisms by which Oct α 2R affects Malpighian tubule function could affect pest management. Targeting octopamine receptors, including Oct α 2R, could affect pest insects' osmoregulatory and excretory capabilities, leading to novel methods for managing pest populations (Ocampo *et al.*, 2023). This method could provide an alternative to pesticides by utilising the unique roles of these receptors in insects' physiology (Ocampo *et al.*, 2023). Investigating the role of Oct α 2R in Malpighian tubules can help us understand how organisms maintain homeostasis through complex signalling.

4.2.6 Human Orthologs

Human counterparts of the Oct α 2R receptor are the α 2-adrenergic receptors (α 2-ARs), specifically the α 2A, α 2B, and α 2C subtypes (Proudman et~al.,~2022). These receptors regulate neurotransmitter release in the central and peripheral nervous systems, impacting cognition, mood, and cardiovascular function (Hein et~al.,~1999). The α 2A subtype, mainly found in the central nervous system, inhibits sympathetic outflow, thus controlling blood pressure and heart rate (Philipp et~al.,~2002). In contrast, the α 2B and α 2C subtypes are more involved in peripheral functions such as vasoconstriction and blood flow regulation (Hering et~al.,~2020; Brede et~al.,~2004). The ability of these receptors to mediate diverse physiological responses underscores their importance in maintaining systemic balance and responding to stressors.

These $\alpha 2$ -adrenergic receptors are GPCRs that respond to norepinephrine and epinephrine (Wong *et al.*, 2023). They are related to modulating neurotransmitter release, regulating vascular tone, and managing central nervous system functions (Philipp *et al.*, 2002). Like Oct $\alpha 2R$, $\alpha 2$ -adrenergic receptors inhibit cAMP production, leading to various downstream effects on cellular activity (Taylor and Cassagnol, 2023). This functional similarity highlights these receptors' evolutionary conservation and significance in maintaining physiological homeostasis (Angelotti *et al.*, 2010; Proudman *et al.*, 2022).

By comparison, we can observe that the functional roles of Oct α 2R and its human orthologs display similarities. In *Drosophila*, Oct α 2R regulates behaviours such as locomotor activity, grooming, and responses to starvation (Nakagawa *et al.*, 2022). Similarly, human α 2-adrenergic receptors also affect various behaviours and physiological responses (Philipp *et al.*, 2020). For example, these receptors modulate anxiety and feeding behaviours (Perez *et al.*, 2020). Oct α 2R and α 2-adrenergic receptors can inhibit the production of cAMP, leading to reduced neuronal excitability and neurotransmitter release, thereby affecting mood, alertness, and stress responses (Nakagawa *et al.*, 2022; Brown *et al.*, 2023). The functional similarity between *Octa2R* in *Drosophila* and α 2-adrenergic

receptors in humans indicates the conservation of GPCR-mediated signalling pathways. This similarity enables researchers to utilise *Drosophila* as a model organism to investigate the complexities of GPCR signalling, offering insights into human health and disease.

4.2.7 Comparative Analysis with Other Insect Models

Other insect models, such as *Apis mellifera* (honeybee), *Anopheles gambiae* (mosquito) and *Bombyx mori* (silkworm), have shown common features of octopamine signalling pathways (Bertaud *et al.*, 2022; Fuchs *et al.*, 2014; Hayashi *et al.*, 2021). The function of the Octa2R receptor modulates behaviours such as flight, learning, and responses to stress. Octopamine in *Apis mellifera* exhibits complex learning and memory phenomenology related to foraging behaviour (Schulz *et al.*, 2002). Octa2R in *honeybees* display similar functions to those found in *Drosophila*, particularly its role in cAMP pathways (Blenau *et al.*, 2020). This indicates that mechanisms of memory formation exist in different species. In the malaria vector *Anopheles gambiae*, octopamine receptors participate in important physiological responses to environmental stressors, such as temperature and humidity fluctuations (Georgiades *et al.*, 2023). This receptor may mediate responses to different environmental pressures, indicating that the octopamine signalling system has evolved specific adaptations tailored for individual species.

Previous studies on Malpighian tubules have not identified a specific role for the $Oct\alpha 2R$ receptor, and no research paper could be found that directly investigates its function in these tubules. An earlier study also reported no significant effects of biogenic amines on tubule function (Kerr *et al.*, 2004). In this study, 5HT receptors were put into tubule cells in *Drosophila* using the Gal4-UAS system, which led to responses but not complete responses, suggesting that *Drosophila* tubules did not normally respond to 5HT. Similar experiments in other insects, such as *Rhodnius* showed different results. Given the lack of evidence for tubule responsiveness to biogenic amines and the specific expression of $Oct\alpha 2R$ in the tubules, I decided to re-examine and further investigate this finding. To illustrate the conserved signalling mechanisms of

octopamine receptors across insect species, Figure 4.3 shows a cartoon of $\alpha 2$ -adrenergic-like octopamine receptors characterised in *Apis mellifera*. In particular, AmOct $\alpha 2R$ acts via inhibition of cAMP production. Although the cartoon is derived from *Apis mellifera*, this GPCR-mediated reduction in cAMP has also been demonstrated for *Drosophila* Oct $\alpha 2R$, highlighting a conserved mechanism across insect species (El-Kholy *et al.*, 2015; Qi *et al.*, 2017; Nakagawa *et al.*, 2022).

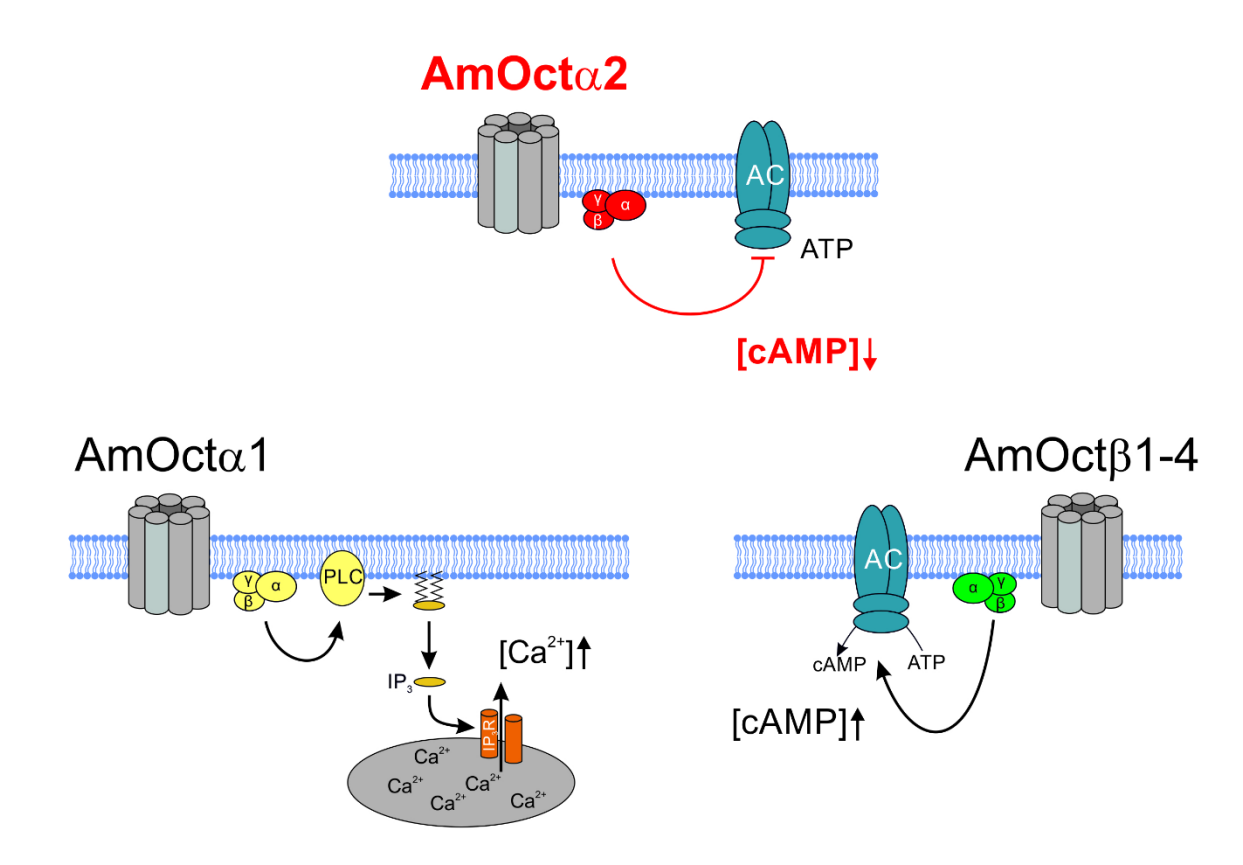


Figure 4.3 Octopamine receptor subtypes in *Apis mellifera*. AmOctα2R couples to G proteins and inhibits adenylyl cyclase, leading to reduced intracellular cAMP levels. AmOctα1 activates the PLC-IP₃ pathway and increases intracellular Ca²⁺, while AmOctβ receptors stimulate adenylyl cyclase and elevate cAMP (Balfanz *et al.*, 2020).

4.3 Results

4.3.1 Octopamine Receptor family

Octopamine exerts its function by binding to octopamine receptors. These receptors show a structural and signalling function similar to vertebrate adrenergic receptors. According to these similarities, insect OA receptors are classified into three subgroups (Zhang *et al.*, 2023): α1-adrenergic-like receptors (*Octa1R*, also referred to as *OAMB*), β-adrenergic-like receptors (*Octa2R*) (Qi *et al.*, 2017; Zhang *et al.*, 2023) (Figure 4.4 to 4.9). *OCTBRs* are further divided into three sub-types (Farooqui, 2012). At the cellular level, α-adrenergic-like receptors expressed in cells lead to an increase in calcium concentration in intracellular storage (Wu *et al.*, 2017). β-adrenergic-like receptors activate adenylyl cyclases, which raise the concentration of intracellular cAMP (Chen *et al.*, 2010; Wu *et al.*, 2012). Both *Octa2R* isoforms can increase calcium concentration, while short isoform can reduce intracellular cAMP levels (Wu *et al.*, 2017)

The *Octa1R* is mainly expressed in the nervous system (Figure 4.4) and is associated with modulating reproductive behaviours, such as ovulation (Lim *et al.*, 2014; Lee *et al.*, 2009), courtship (Fernandez, 2017; Zhou *et al.*, 2012) and appetitive learning (Kim *et al.*, 2013) in *Drosophila melanogaster*. Similar to *Octa1R*, *OctBR* is also mainly expressed in the nervous system (Figure 4.6 to 4.8), including the brain, thoracic, and abdominal ganglia (Farooqui, 2007). It involves many functions, including sleep regulation, feeding behaviour and immune response (Zhao *et al.*, 2021; Zhang *et al.*, 2023; Fernandez, 2012).

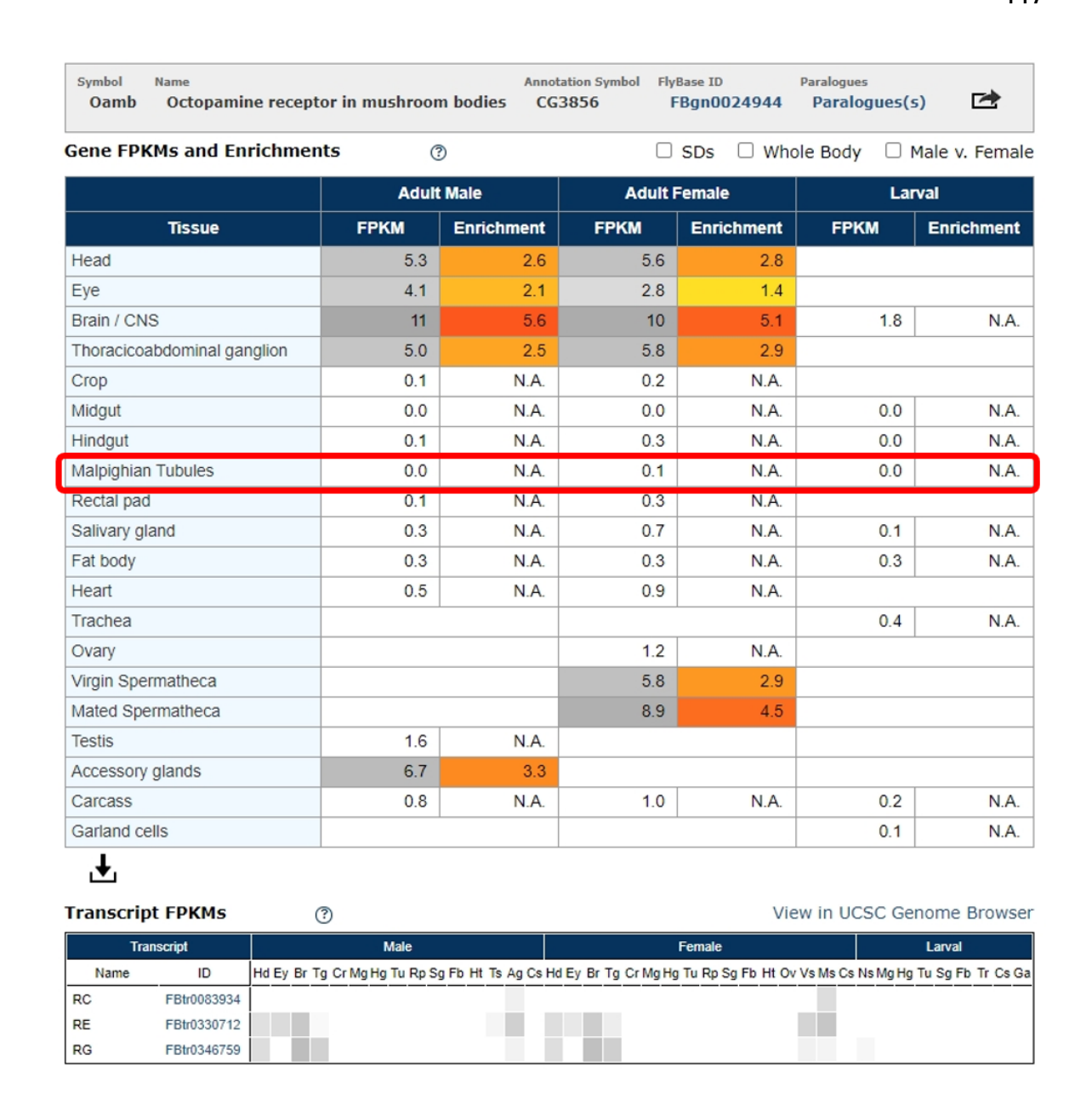


Figure 4.4. Tissue expression of the Oamb receptor in Drosophila melanogaster.

Expression is highest in the central nervous system and associated ganglia. In Malpighian tubules, expression is undetectable in adult males and larvae and barely detectable in adult females (≈ 0.1 FPKM). Red box = Malpighian tubules. Data from FlyAtlas2 (Leader *et al.*, 2018).

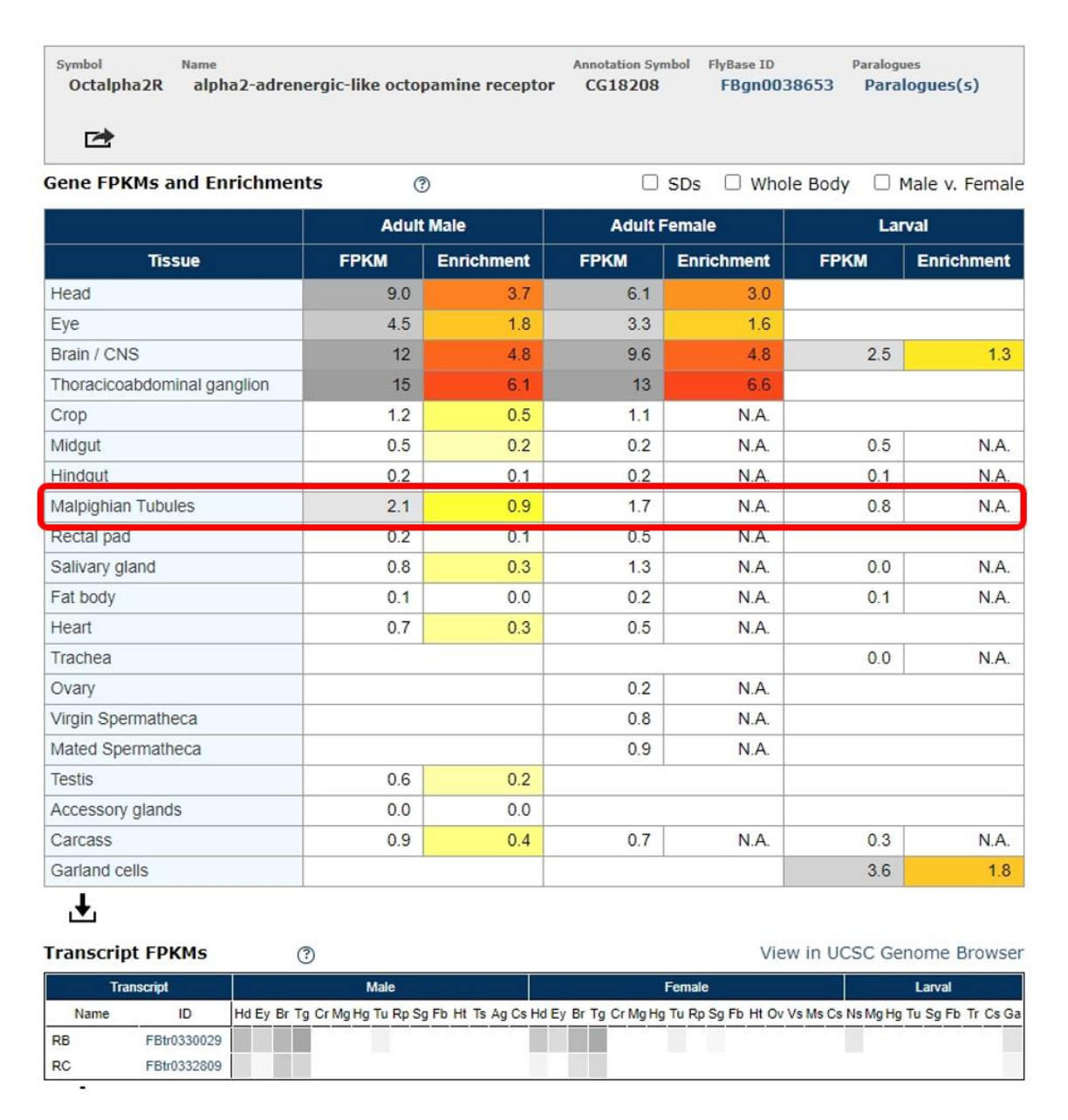


Figure 4.5. Tissue expression of the Octα2R receptor in *Drosophila melanogaster*.

Expression is strongest in neural tissues, including the brain, central nervous system and thoracicoabdominal ganglion, where levels range between approximately 9 and 15 FPKM in adults. Malpighian tubules also show clear expression, with values of about 2.1 FPKM in adult males, 1.7 FPKM in adult females and 0.8 FPKM in larvae. The adult male tubule signal is not tubule-enriched, with an enrichment value of about 0.9. The transcript panel indicates that both annotated isoforms are detected across multiple tissues. Data from FlyAtlas2 (Leader *et al.*, 2018).

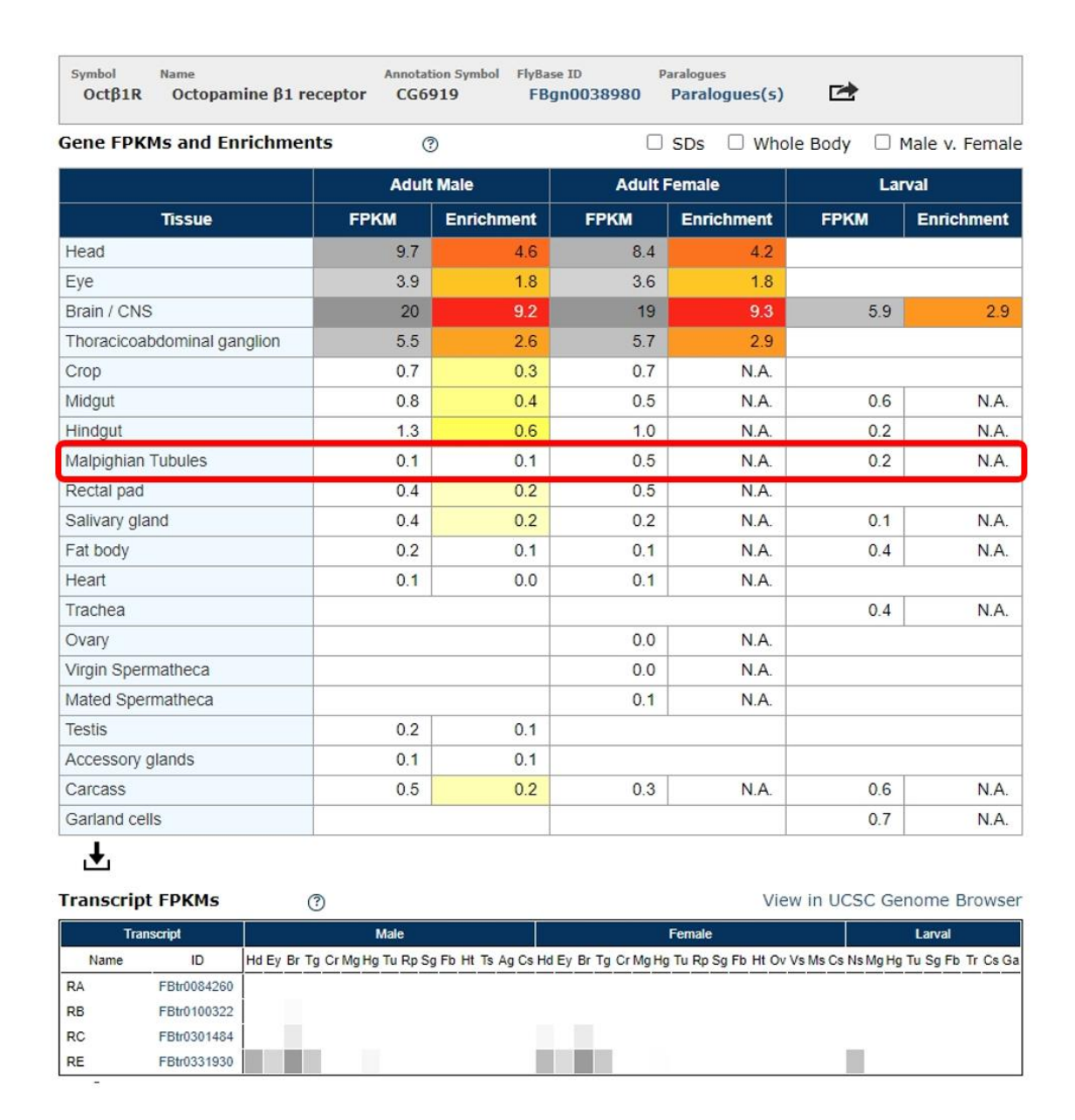


Figure 4.6. Tissue expression of the OctB1R receptor in Drosophila melanogaster.

Expression is highest in neural tissues, including the brain, central nervous system and thoracicoabdominal ganglion. In Malpighian tubules, expression is low, with about 0.1 FPKM in adult males, 0.5 FPKM in adult females and 0.2 FPKM in larvae. Red box = Malpighian tubules. Data from FlyAtlas2 (Leader *et al.*, 2018).

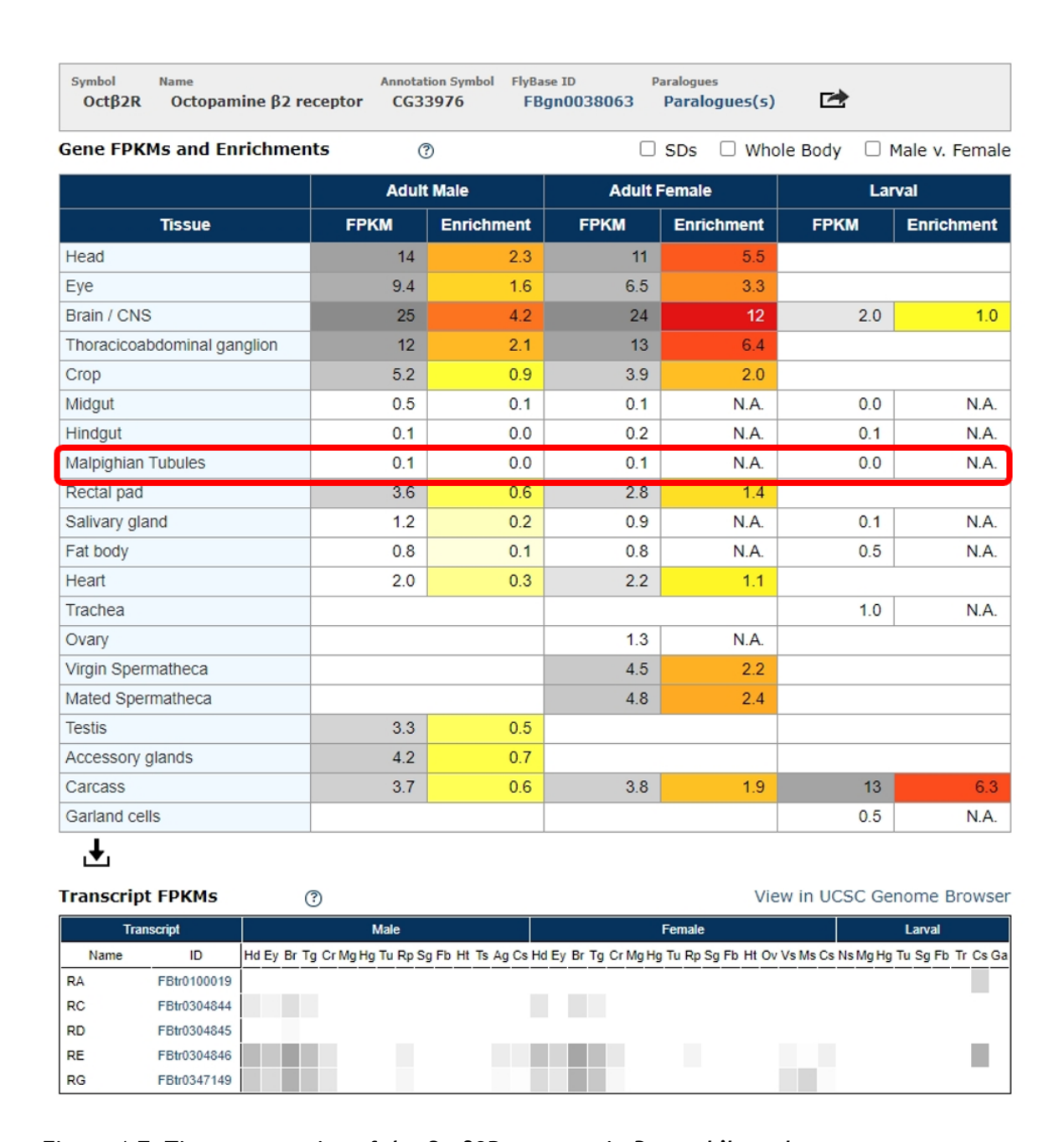


Figure 4.7. Tissue expression of the OctB2R receptor in Drosophila melanogaster.

Expression is enriched in neural tissues. Malpighian tubules show only trace expression in adults, at about 0.1 FPKM in both males and females, and are undetectable in larvae. Red box = Malpighian tubules. Data from FlyAtlas2 (Leader *et al.*, 2018).

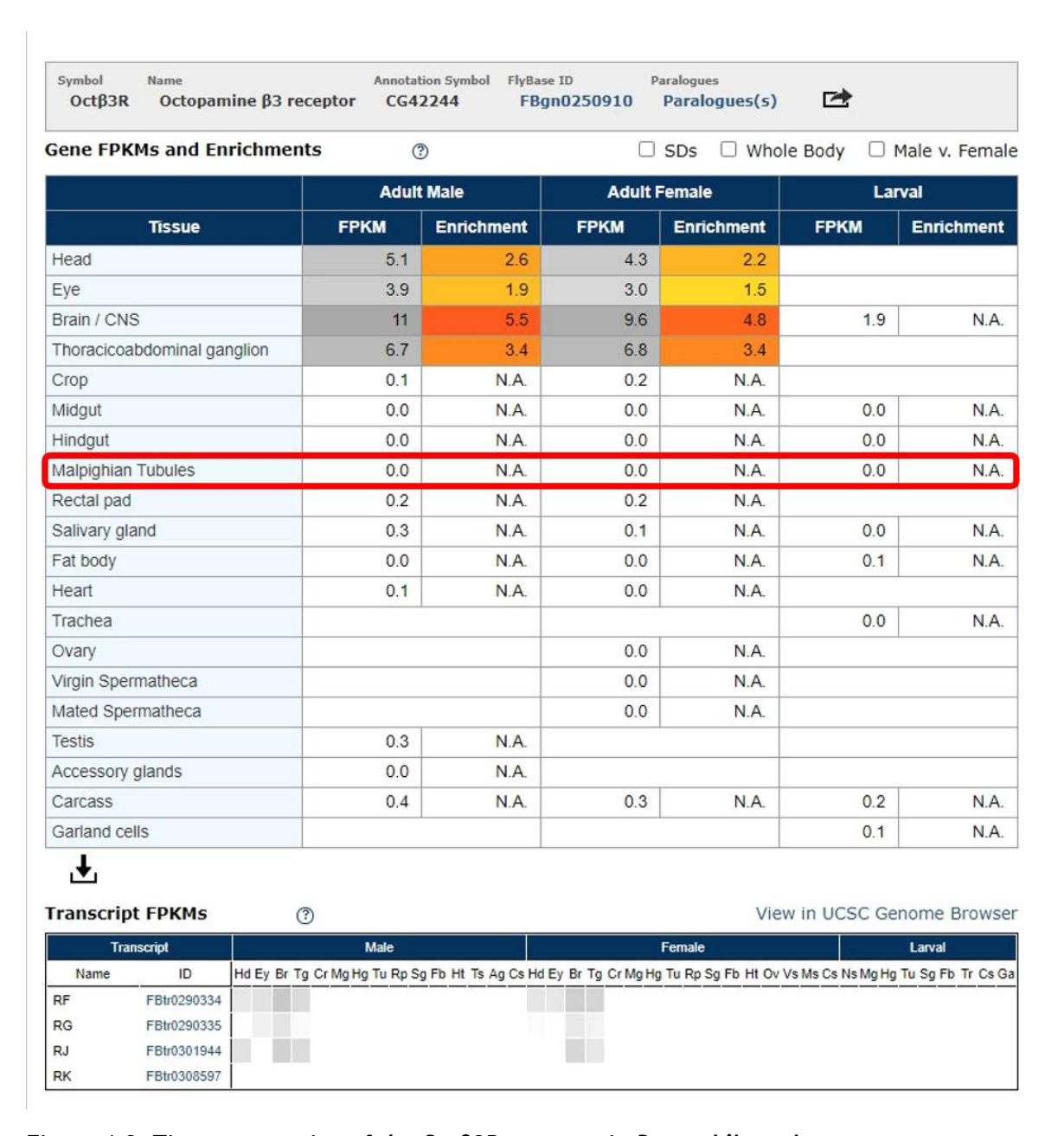


Figure 4.8. Tissue expression of the OctB3R receptor in *Drosophila melanogaster*.

Overall expression is lower than other B-type receptors, and Malpighian tubules show no detectable signal at any stage examined. Red box = Malpighian tubules. Data from FlyAtlas2

(Leader et al., 2018).

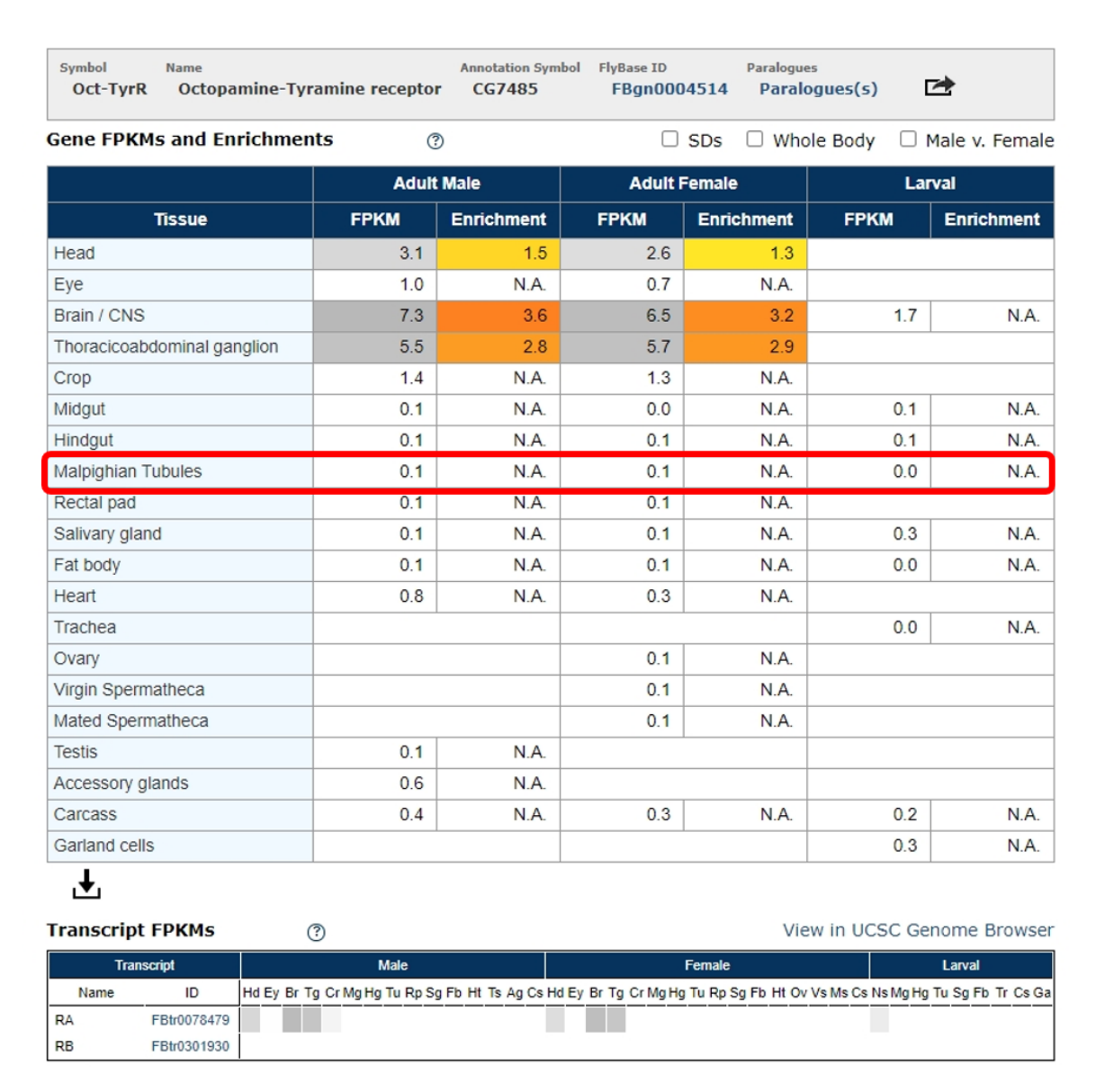


Figure 4.9. Tissue expression of the Oct-TyrR receptor in Drosophila melanogaster.

Expression is mainly neural. Malpighian tubules show very low expression in adults, at about 0.1 FPKM in males and females, and are undetectable in larvae. Red box = Malpighian tubules. Data from FlyAtlas2 (Leader *et al.*, 2018).

Further, the data from Figure 4.10 indicate that the enrichment values of *Octa2R* are higher than those of the other members of the octopamine receptor family. The enrichment values for other octopamine receptor family genes are nearly zero. Specifically, *Octa2R* is enriched up to 0.9 times in adult male MTs. Although the expression level of *Octa2R* in the tubule is low, FlyCellAtlas data show that it is specific to stellate cells, explaining its low expression levels in whole tissue. Figure 4.11 illustrates this cell-type-specific localisation, showing that *Octa2R* expression is restricted to stellate cells of the main segment.

	Adult Male		Adult Female		Larval	
	FRKM	Enrichment	FRKM	Enrichment	FRKM	Enrichment
Oamb	0.0	N.A.	0.1	N.A.	0.0	N.A.
Octa2R	2.1	0.9	1.7	N.A.	0.8	N.A.
OctB1R	0.1	0.1	0.5	N.A.	0.2	N.A.
OctB2R	0.1	0.0	0.1	N.A.	0.0	N.A.
OctB3R	0.0	N.A.	0.0	N.A.	0.0	N.A.
Oct-TyrR	0.1	N.A.	0.1	N.A.	0.0	N.A.

Figure 4.10. Expression and enrichment of octopamine receptor family members in *Drosophila melanogaster* Malpighian tubules. Among the receptors examined, *Octa2R* shows the highest expression in tubules, with enrichment reaching 0.9 in adult males. Other receptor family members, including *Oamb*, *OctB1R*, *OctB2R*, *OctB3R* and *Oct-TyrR*, display little or no detectable enrichment. Data from FlyAtlas2 (Leader *et al.*, 2018).

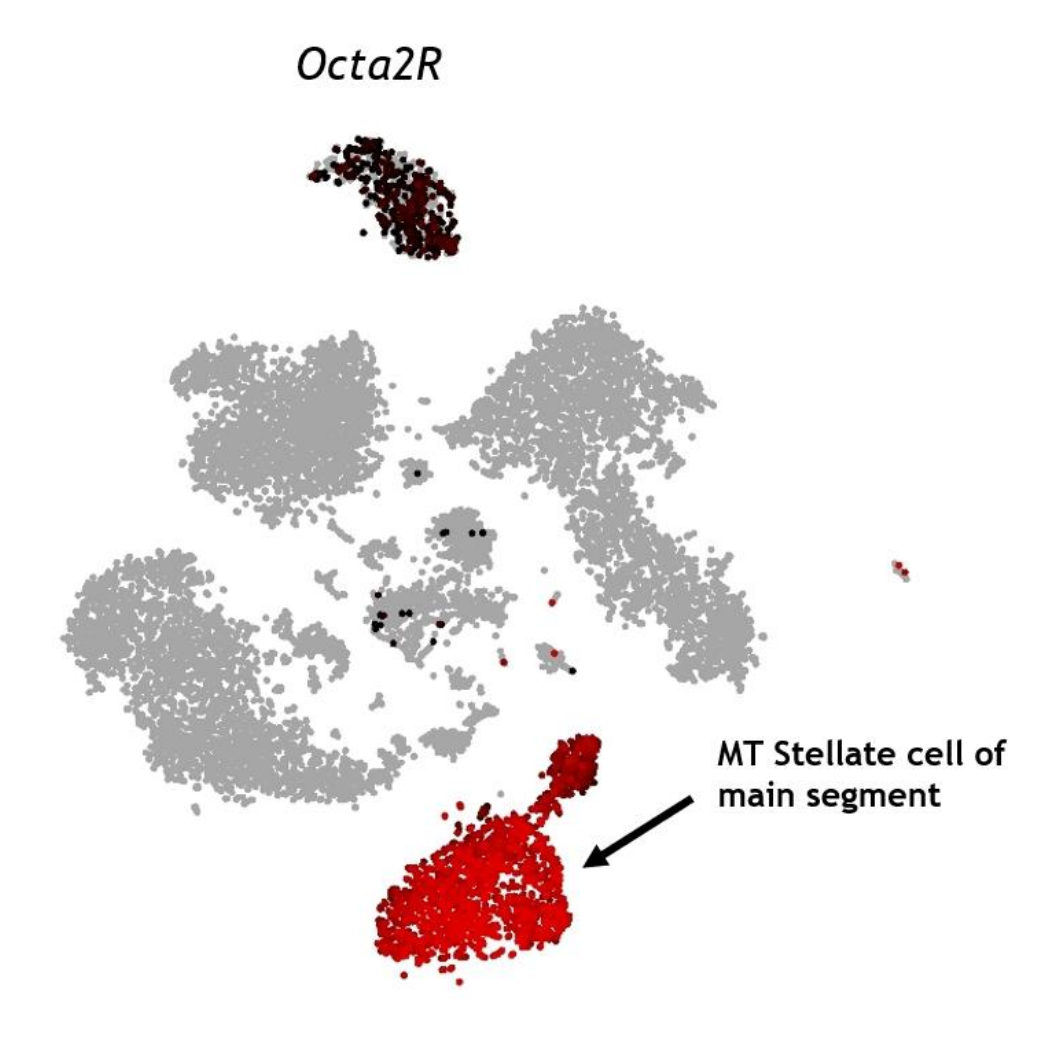


Figure 4.11. Expression of *Octa2R* **in Malpighian tubules of** *Drosophila melanogaster***.** Single-cell RNA-seq data from the FlyCellAtlas show that *Octa2R* expression is restricted to stellate cells of the main segment (red). Grey indicates other cell types with no detectable expression. Data from FlyCellAtlas (Leader *et al.*, 2018) and Scope (Li and Janssens *et al.*, 2022).

4.3.2 Octa2R is expressed in the stellate cells of the tubule.

As the *Octa2R* gene is expressed in the tubules, I conducted gene knockdown experiments to investigate its function. Several publicly available *DmOcta2R* (CG18208) lines can be used to reduce the mRNA level in tubules. The first aim of this experiment is to determine the specific cell types in which *Octa2R* is mainly expressed in tubules by crossing it to GAL4 lines (Capa*R*-Gal4 line and tsh-Gal4 line). I used qPCR to determine the levels of *Octa2R* mRNA. I used the parental lines *Octa2R* and the *tsh*-GAL4 as my controls. For the gene knockdown in the stellate cells of the tubules, the tsh promoter-specific GAL4 line (tsh-GAL4) was crossed with the *Octa2R* target line for the gene knockdown in the stellate cells, and the CapaR promoter-specific GAL4 line (CapaR-GAL4) was crossed with the *Octa2R* target lines. *Octa2R* mRNA levels were determined in the tubules from the control and the knockdown flies. Similar to innexin qPCR experiments in Chapter 3, *RPL32* was used as a control gene to validate the analysis of gene expression levels.

Two independent RNAi lines, UAS-Octa2R RNAi (#10214) and UAS-Octa2R RNAi (#10215) (VDRC), were initially selected for this experiment, with results shown in Figure 4.12A and B. The expression level of Octa2R mRNA in the parental lines was set to a baseline value of 1, and the relative expression in the knockdown flies was compared to this control (tsh-GAL4 line) and the other parental control (CapaR-GAL4 line). In the stellate cell-specific knockdown (tsh-GAL4>UAS-Octa2R RNAi), there was no significant reduction in Octa2R mRNA compared with controls, and in some cases a slight increase was observed (Figure 4.12A and B). By contrast, principal cell-specific knockdown (CapaR-GAL4>UAS-Octa2R RNAi) showed marked decreases in expression relative to both parental controls (tsh-GAL4 and CapaR-GAL4) (Figure 4.12A). However, in Figure 4.12B, the CapaR-GAL4>UAS-Octa2R RNAi cross did not show a change in expression compared to the controls. These inconsistent results may reflect variability in driver line efficiency or compensatory effects, and therefore do not provide a definitive indication of which tubule cell type expresses Octa2R.

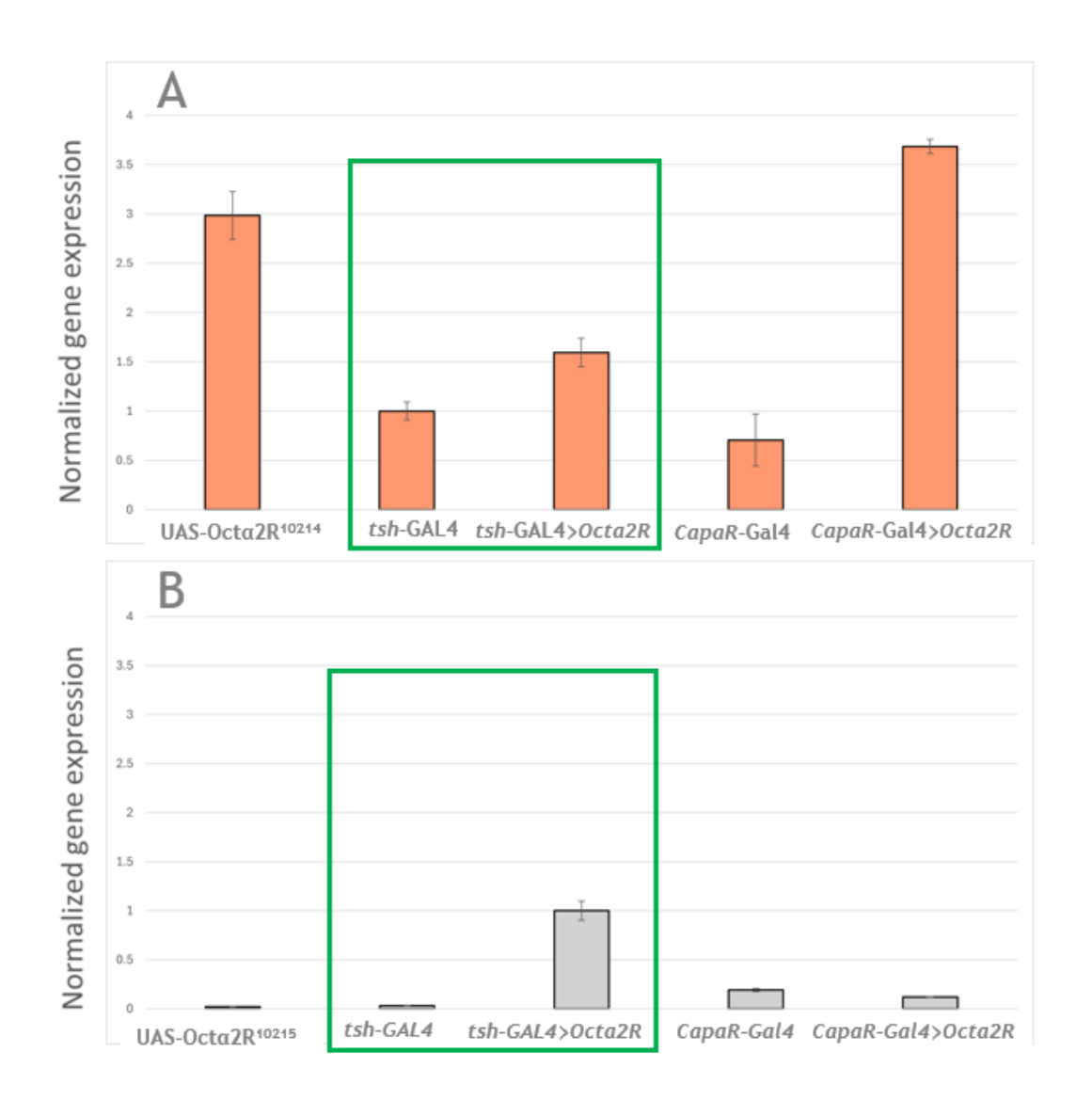


Figure 4.12. Validation of *Octa2R* knockdown using two independent RNAi lines in Malpighian tubules. (A) Expression of *Octa2R* was examined in UAS-Octα2R RNAi (#10214) crossed with the *tsh*-GAL4 and *CapaR*-GAL4 driver lines. Gene expression levels were normalised to the parental control lines (*Octa2R*, *tsh*-GAL4, and *CapaR*-GAL4). Knockdown with the *tsh*-GAL4 driver did not reduce *Octa2R* mRNA in stellate cells, whereas knockdown with the *CapaR*-GAL4 driver decreased expression compared with both parental controls. (B) Analysis of the second RNAi line UAS-Octα2R RNAi (#10215) showed a similar pattern when crossed with the *tsh*-GAL4 driver, with no reduction in *Octa2R* mRNA detected. By contrast, crossing with the *CapaR*-GAL4 driver again did not show a clear change compared with controls. Data are presented as mean ± SEM.

To further explore the role of *Octa2R* in tubules, another UAS-Octα2R RNAi line (#50678) was used for additional knockdown experiments. Subsequent qPCR analyses measured the expression level of *Octa2R* in the knockdown line (*tsh*-GAL4>UAS-Octα2R RNAi) in Figure 4.13. This was done by crossing the RNAi line to the stellate cell-specific driver (tsh-GAL4). The parental RNAi line (*Octa2R* RNAi #50678) and the tsh-GAL4 driver line were used as controls, and the parental line was normalised to 1 to facilitate relative comparisons. It was found that the expression of *Octa2R* mRNA in the knockdown line was dramatically reduced compared with both controls.

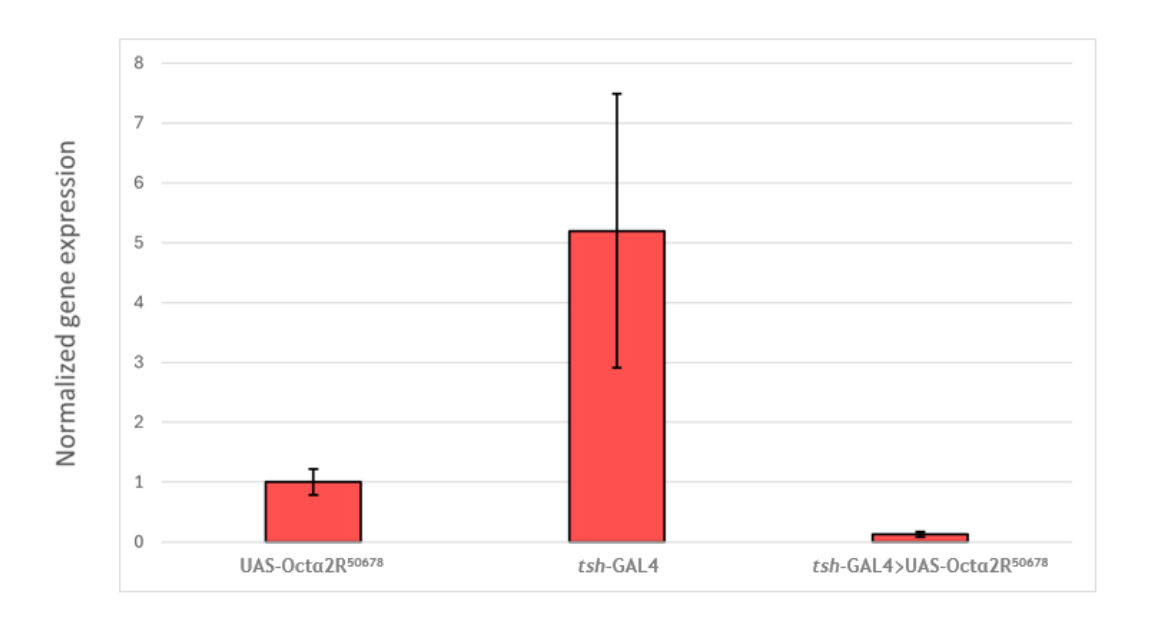


Figure 4.13. Knockdown of Octa2R in Malpighian tubules using the UAS-Octa2R RNAi (#50678) line. qPCR analysis of Octa2R expression in parental RNAi line (UAS-Octa2R⁵⁰⁶⁷⁸), driver line (tsh-GAL4), and knockdown progeny (tsh-GAL4>UAS-Octa2R⁵⁰⁶⁷⁸). Expression in the parental line was set to 1. A clear reduction in Octa2R transcript levels was observed in the knockdown flies compared with both controls. Data are shown as mean \pm SEM, n = 6.

As shown in the previous paragraph (Figure 4.12), there was no significant reduction in the knockdown line (tsh-GAL4>UAS-Octα2R) as compared to the parental line (tsh-GAL4), but it shows a statistically significant difference in *Octa2R*⁵⁰⁶⁷⁸ line knockdown experiments. Figure 4.13 presents the initial qPCR results comparing the UAS-Octα2R RNAi (#50678) parental line and the tsh-GAL4>UAS-Octα2R⁵⁰⁶⁷⁸ knockdown line, showing a marked reduction in *Octa2R* expression. While Figure 4.13 presents relative expression levels compared with parental controls, Figure 4.14 represents the same data recalculated as percentage reduction, providing a clearer view of knockdown efficiency. In contrast, Figure 4.14 shows the same dataset reanalysed to quantify the percentage reduction, highlighting an 87% decrease in expression, and thereby providing a clearer measure of knockdown efficiency. To more clearly observe the specific percentage reduction of *Octa2R* mRNA in the knockdown line, data from the parental *Octa2R* line and the knockdown line were organised and reanalysed using GraphPad, resulting in Figure 4.14.

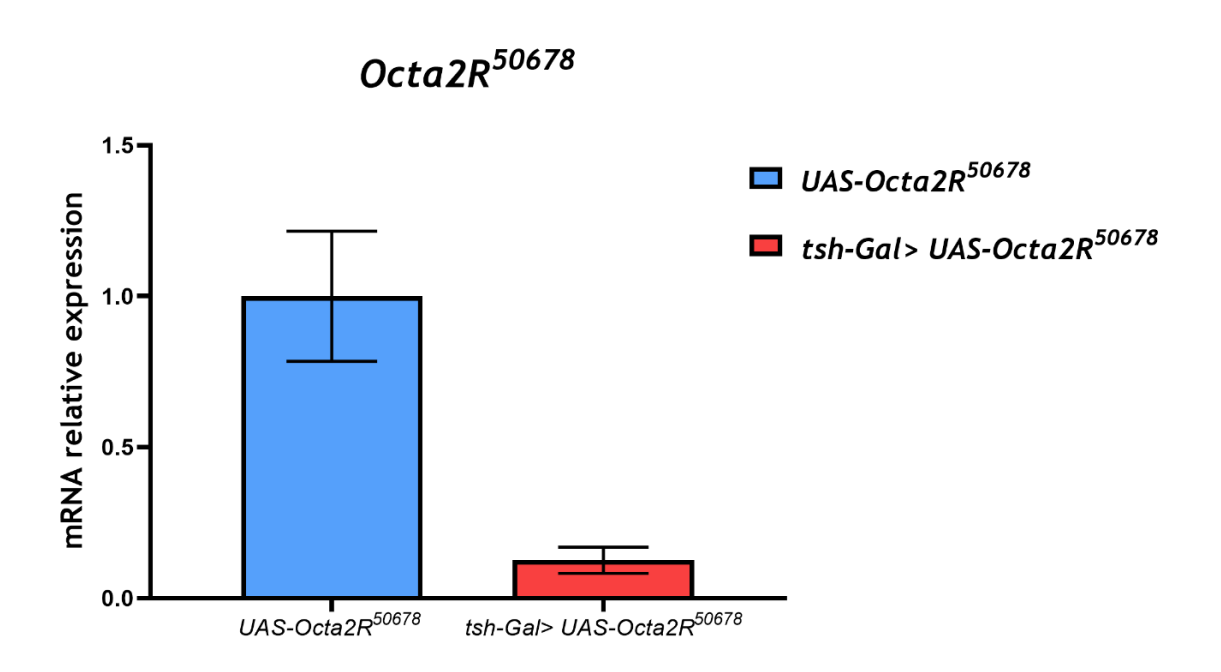


Figure 4.14. Percentage reduction of Oct α 2R expression in Malpighian tubules following knockdown with the UAS-Oct α 2R RNAi (#50678) line. qPCR data were recalculated to show the extent of knockdown as a percentage change relative to parental controls (tsh-GAL4 and UAS-Oct α 2R⁵⁰⁶⁷⁸). Progeny carrying both the driver and the RNAi construct (tsh-GAL4>UAS-Oct α 2R⁵⁰⁶⁷⁸) exhibited an 87% decrease in Oct α 2R transcript levels compared with controls. Data are shown as mean \pm SEM, with statistical comparisons between knockdown and each parental control (P < 0.05).

My result demonstrates that *Octa2R* is expressed in stellate cells and can be knocked down successfully with a *tsh*-Gal4 driver using the *Octa2R*⁵⁰⁶⁷⁸ line. Together, these results validate the previous findings in Figures 4.5 and 4.11 that *Octa2R* are expressed in the stellate cells of MTs. Moreover, the cell cluster data, annotated from the Fly Cell Atlas resource, supports the result. Octα2R expression is detected in clusters corresponding to stellate cells (Figure 4.14). This evidence strongly supports the conclusion that *Octa2R* is mainly expressed in the stellate cells of MTs, highlighting its potential role in regulating fluid secretion in the tubules.

4.3.3 Octa2R affects fluid secretion of the tubules

As described in Chapter 3, the Ramsay assay was used to measure fluid secretion rates in *Drosophila* Malpighian tubules, and the same method was applied here to assess whether knockdown of *Octa2R* affects tubule function. Two independent RNAi lines UAS-Octα2R RNAi (#10214) and UAS-Octα2R RNAi (#10215) were first tested, but neither produced consistent or effective knockdown of *Octa2R* expression; the full secretion assay data for these lines are provided in Appendix 6 and Appendix 7. A third UAS-Octα2R RNAi (#50678), however, showed effective knockdown of *Octa2R* mRNA (see Section 4.3.3.1), and all subsequent fluid secretion experiments in this chapter were therefore performed using this line.

4.3.3.1 Octa2R⁵⁰⁶⁷⁸ lines

The $Octa2R^{50678}$ line was used in the final fluid secretion experiments (Figure 4.15). Following stimulation with kinin at 10^{-7} M, the basal secretion rate of tubules showed a similar increasing trend in both the knockdown (tsh-GAL4>UAS-Oct α 2R⁵⁰⁶⁷⁸) and the parental RNAi control (UAS-Oct α 2R⁵⁰⁶⁷⁸). Statistical comparison using a two-sample t-test indicated a significant difference in secretion rate between these two groups at specific time points (p = 0.0023; Figure 4.15A).

To further evaluate the functional response, the percentage increase in fluid secretion after kinin stimulation was calculated (Figure 4.15B). This analysis did not reveal a statistically significant difference between the knockdown and parental control groups (p = 0.0776). These results suggest that while Octa2R knockdown may influence secretion dynamics at certain time points, the overall kinin-stimulated increase in secretion is not significantly altered.

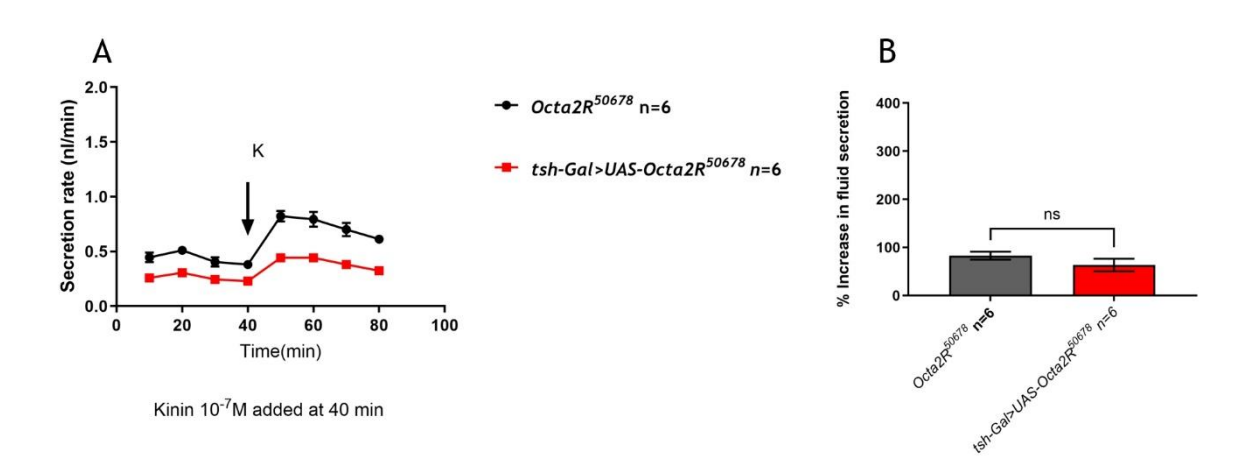


Figure 4.15. Fluid secretion assay for tsh-GAL4>UAS-Oct α 2R⁵⁰⁶⁷⁸ compared with parental line. (A) Basal and kinin-stimulated fluid secretion rates were measured in $Octa2R^{50678}$ parental controls (black circles) and knockdown flies (tsh-GAL4>UAS-Oct α 2R⁵⁰⁶⁷⁸, red triangles). Secretion was recorded at 10-minute intervals, with kinin (10^{-7} M) added at 40 minutes (arrow). (B) Percentage increase in secretion following kinin stimulation is shown for both groups. No consistent or significant reduction was observed in knockdown flies compared with controls. Data are mean \pm SEM, n = 6. Statistical significance was assessed by two-sample t-test.

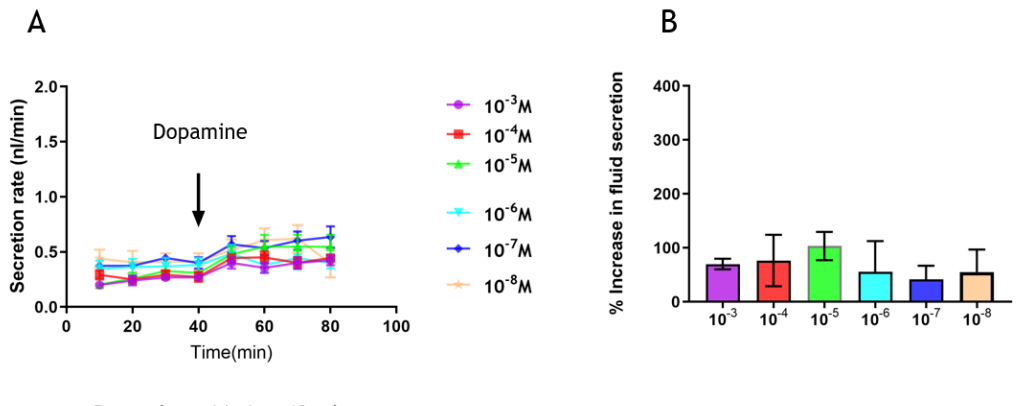
4.3.3.2 Biogenic Amines

Because *Octa2R* is an octopamine receptor that can be activated by other amines, biogenic amines were tested on *Octa2R* to understand its role in fluid secretion. Before doing this, the concentration of each amine needs to be confirmed. The best concentration was determined using Canton S (CS) flies (n=5), using different concentrations of each biogenic amine. This concentration was then used to stimulate the tubules during *Octa2R* fluid secretion assays.

Dopamine

Basal secretion rates are similar among all groups, ranging from 0.27 to 0.41 nl/min (Figure 4.16 C). After dopamine stimulation, the secretion rates increase, ranging from 0.40 to 0.60 nl/min across different concentrations. When comparing the overall basal and stimulated secretion rates, the p-value is 0.0027, suggesting a significant effect of dopamine on tubule secretion.

The p-value for the basal rate and stimulated rate at each concentration are also calculated (Figure 4.16 D). The p-value for 10^{-3} M, 10^{-4} M, 10^{-5} M, and 10^{-7} M concentrations was significantly different, supporting that dopamine at this concentration is a stimulant of fluid secretion. However, the p-values for 10^{-6} M and 10^{-8} M were not significant differences, which indicates that dopamine at these concentrations did not change anything along with secretion other than basal rates.



Dopamine added at 40 min

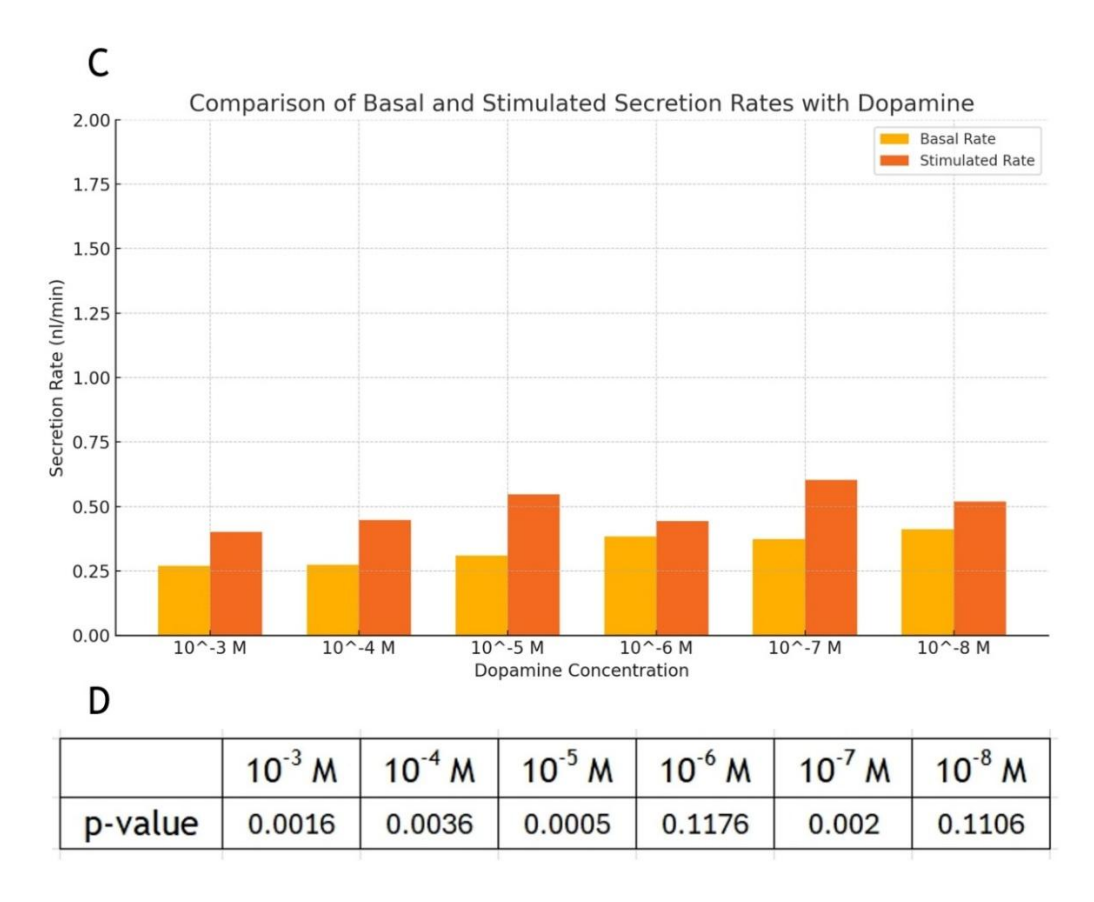
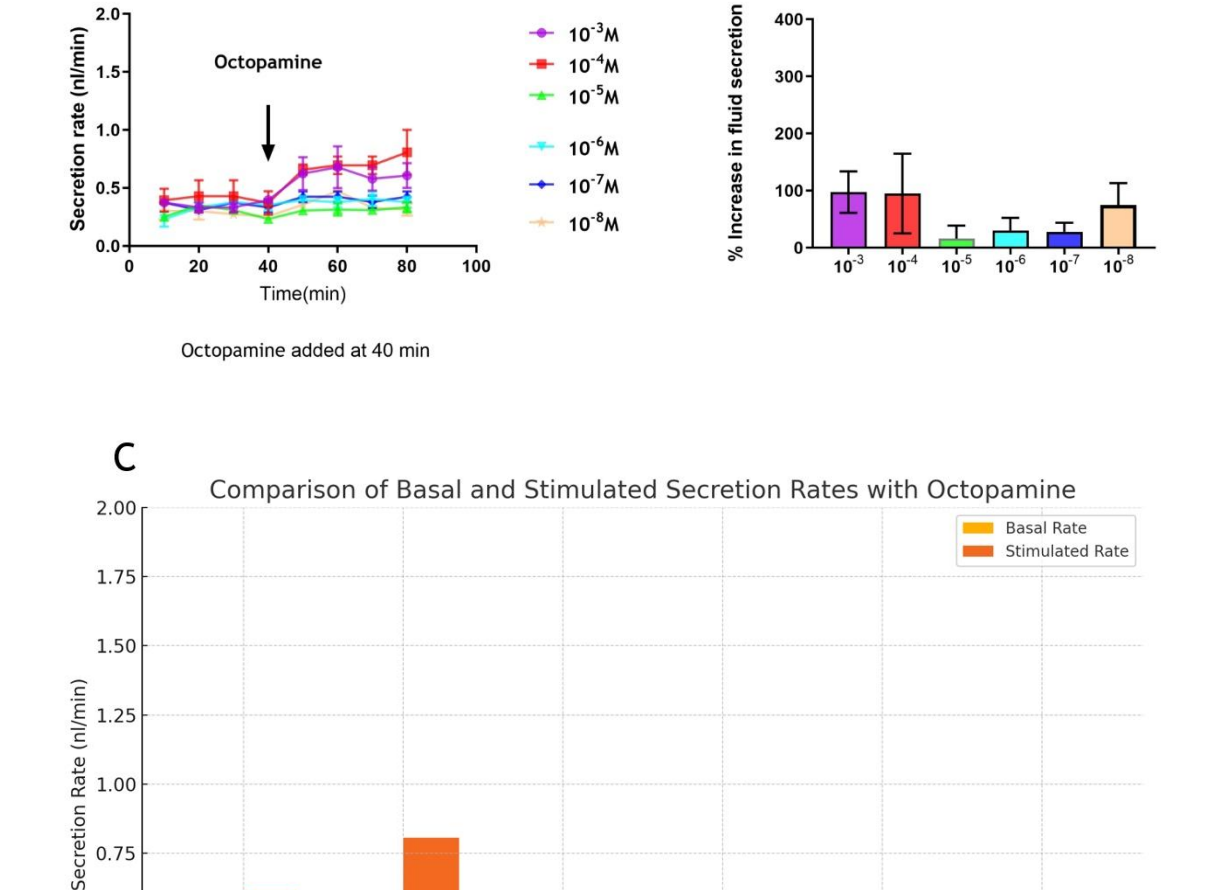


Figure 4.16. Effect of different dopamine concentrations on the fluid secretion rate of Canton S (CS) tubules. Tubules were dissected from 7-day-old CS flies, and basal secretion was recorded for 40 minutes before stimulation with dopamine at 10^{-3} M, 10^{-4} M, 10^{-5} M, 10^{-6} M, 10^{-7} M, or 10^{-8} M. (A) Secretion rate over time before and after dopamine addition (arrow). (B) Percentage increase in secretion after stimulation. (C) Comparison of basal and stimulated secretion across concentrations. (D) Summary of p-values for basal versus stimulated secretion at each concentration. Data are presented as mean \pm SEM, n = 5. Statistical comparisons were performed using one-way ANOVA with Dunnett's test and paired t-tests. The y-axis scales differ across panels because they present distinct types of data (raw secretion rate, percentage change, or statistical outcomes). Scales were selected to optimise clarity and kept consistent with other biogenic amine experiments for comparability.

Octopamine

I used the Canton S line to test which octopamine concentration more effectively affected the fluid secretion rate. Different concentrations of octopamine were applied to Malpighian tubules, and secretion rates were measured. The basal secretion rate across all groups ranged from 0.25 to 0.4 nL/min (Figure 4.17A). A percentage increase in secretion relative to basal levels was then calculated, and comparisons between experimental and control groups were performed using a t-test (Figure 4.17B). Overall, basal and stimulated secretion rates differed significantly (p < 0.05). However, the effect varied depending on concentration (Figure 4.17C, D). At higher concentrations (10⁻³ M and 10⁻⁴ M), octopamine significantly increased secretion. By contrast, at lower concentrations (10⁻⁵ M to 10⁻⁸ M), secretion rates were not significantly different from basal levels. To improve clarity of interpretation, the scales in Figure 4.17 were standardised to match the range of secretion rates observed in these experiments, ensuring consistency across panels.



10⁻³M

A 2.0

0.50

0.25

0.00

10^-3 M

10^-4 M

В

400

D						
	10 ⁻³ M	10 ⁻⁴ M	10 ⁻⁵ M	10 ⁻⁶ M	10 ⁻⁷ M	10 ⁻⁸ M
p-value	0.0028	0.0053	0.3975	0.2733	0.0727	0.1103

Octopamine Concentration

10^-6 M

10^-7 M

10^-8 M

10^-5 M

Figure 4.17 The effect of various octopamine concentrations on the rate of fluid secretion of Canton S tubules. Tubules from 7-day-old Canton S flies were assessed as above, with octopamine added after 40 min at 10^{-3} - 10^{-8} M. (A) Secretion profiles recorded every 10 min before and after stimulation. (B) Percentage change in secretion relative to basal. (C) Basal versus stimulated secretion rates across concentrations. (D) p-values for basal compared with stimulated secretion. Data are mean \pm SEM, n = 5. Statistical comparisons were performed by one-way ANOVA with Dunnett's test.

Tryptamine

Tryptamine was tested to determine whether it influences the fluid secretion rate of Canton S tubules. Basal secretion rates across all concentrations remained stable, indicating consistent baseline fluid transport (Figure 4.18A). After stimulation, no clear increase in secretion was observed. Interestingly, at 10⁻³ M and 10⁻⁵ M, secretion rates showed a small decrease compared with the other concentrations (Figure 4.18B). It should be noted that the y-axis scale in Figure 4.18 differs slightly from that used in the dopamine and octopamine experiments. This wider range was chosen because tryptamine had a weaker overall effect, and the broader scale allowed the small changes to be visualised in a comparable way across all concentrations. Since tryptamine was diluted in DMSO, a DMSO-only control was also included, and no effect on secretion was detected. This confirmed that the observed responses were due to tryptamine itself rather than the DMSO solution.

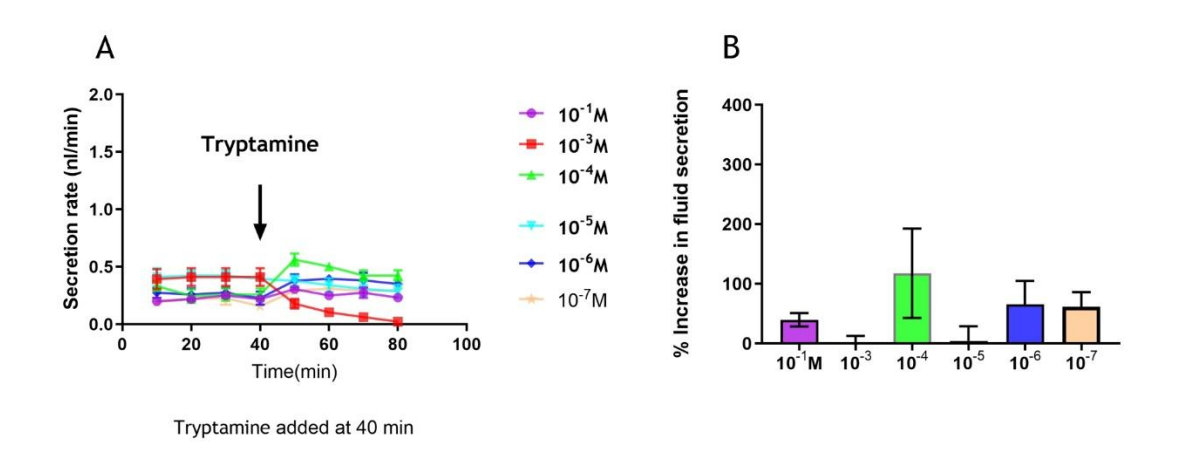


Figure 4.18 Effect of different concentrations of tryptamine on the fluid secretion rate of Canton S tubules. Basal secretion was first measured in 7-day-old Canton S tubules for 40 min, after which tryptamine was applied at 10^{-1} - 10^{-7} M. (A) Mean secretion rates recorded every 10 min before and after addition at 40 min. (B) Secretion shown as percentage change relative to basal. Data are mean \pm SEM, n = 5. A DMSO-only control was included and showed no effect. The y-axis scale was adjusted to allow small changes to be visualised.

Tyramine

Tyramine was also tested at six concentrations ranging from 10^{-3} M to 10^{-8} M. Most concentrations produced an increase in secretion rate after tyramine addition, with the exception of 10^{-7} M. At this concentration, a transient decrease was observed at 40 minutes, followed by a recovery after 50 minutes. By 60 minutes, secretion rates had stabilised (Figure 4.19 A). The percentage change in secretion relative to basal levels is shown in Figure 4.19 B.

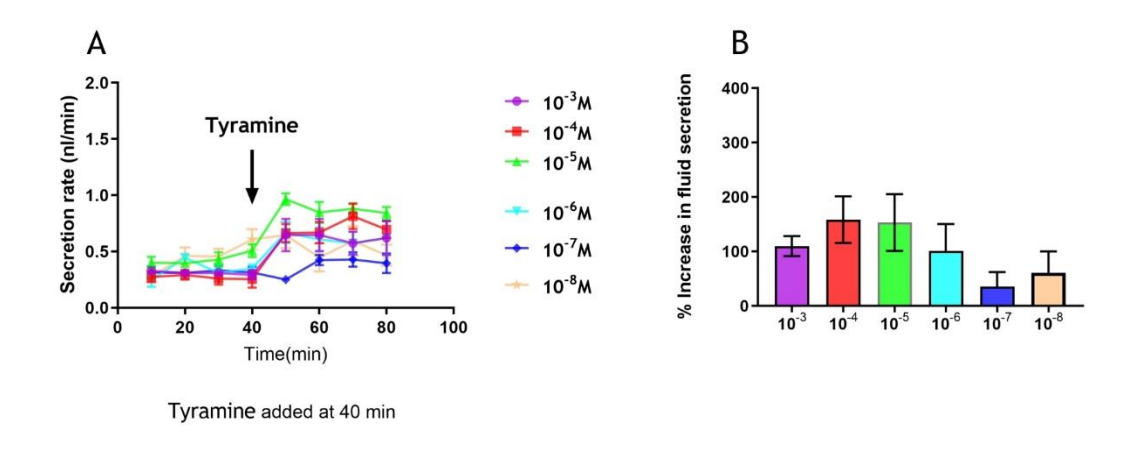


Figure. 4.19 The effect of various concentrations of tyramine on the rate of fluid secretion of Canton-S tubules. Canton S tubules were dissected from 7-day-old flies, and basal secretion was measured for 40 min before tyramine was added at 10^{-3} - 10^{-8} M. (A) Secretion traces averaged at 10-min intervals before and after addition. (B) Secretion expressed as percentage increase over basal levels. Data are mean \pm SEM, n = 5. p < 0.05 was considered significant. The y-axis scale was standardised across figures to permit comparison between amines.

My experiment measured the effects of four different biogenic amine stimulations on fluid secretion at different concentrations in order to find the optimal concentration for each biogenic amine. Figure 4.16 shows the dopamine results. After dopamine stimulation, the secretion rate increases in every group and the different increases through concentrations. For the 10^{-3} M and 10^{-4} M concentrations, the increase in secretion is moderate compared to 10^{-5} M and 10^{-7} M concentrations. There is a noticeable increase in 10^{-5} M and 10^{-7} M concentrations. Moreover, the stimulatory effect is not strictly concentration-dependent, as 10^{-6} M shows a relatively lower response. The basal rates remain consistent across all concentration groups, indicating that

dopamine stimulation is the main reason for changes in secretion rates. The optimal dopamine concentration could be 10^{-3} M or 10^{-4} M concentrations.

Octopamine results are shown in Figure 4.17. The 10⁻⁴ M octopamine concentration appears to be the optimal concentration because it results in a higher percentage increase in fluid secretion than other concentrations. This suggests that 10⁻⁴ M stimulates the Malpighian tubules more effectively, resulting in a better secretion response. Therefore, the 10⁻⁴ M concentration was selected for my further fluid secretion assay.

The results for tryptamine and tyramine showed a decreasing trend in secretion rate after stimulation with a specific concentration of amine. Tryptamine stimulation does not seem to affect the secretion rate. While the 10⁻⁶ M and lower concentrations result in minor increases in fluid secretion, their effects are less than observed by a maximum at 10⁻⁴ M. The 10⁻⁴ M could be a selected concentration. Another decrease in secretion rate after the 40 minutes is 10⁻⁷ M tyramine stimulated based on the secretion curve in the previous Figure 4.19. The slight decrease in secretion rate indicates that a 10⁻⁷ M concentration of tyramine stimulation does not affect fluid secretion. However, a significant increase in the secretion rate is the tyramine of 10⁻⁵ M concentration, and this concentration in Figure 4.19 (B) also shows the highest percentage increase in fluid secretion. p<0.05.

All data were analysed and compared, and the concentration for each biogenic amine was selected, as shown in Figure 4.20. The concentration of each amine is 10^{-3} for dopamine, 10^{-4} M for octopamine, 10^{-4} M for Tryptamine, and 10^{-5} M for Tyramine.

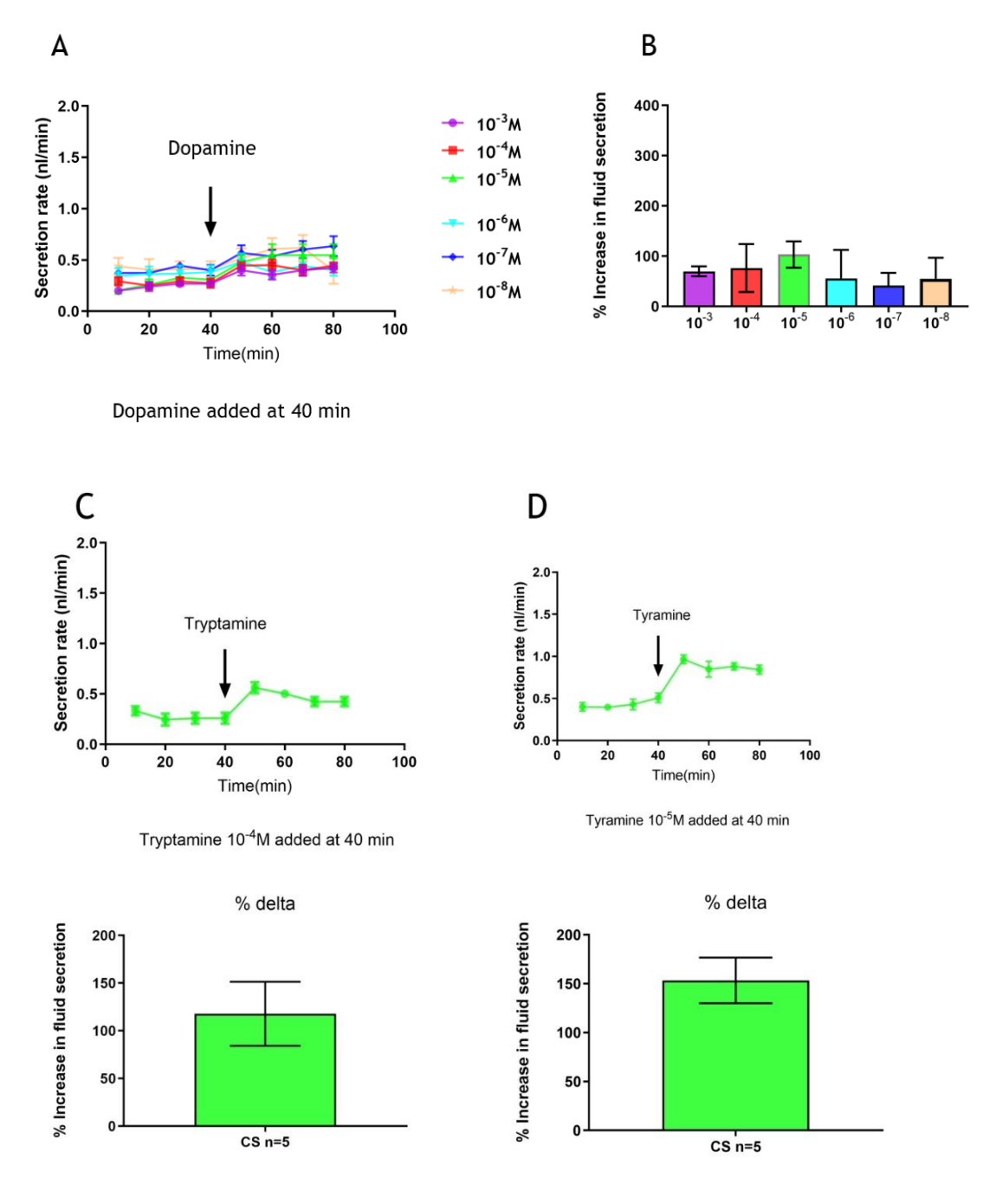


Figure 4.20 Fluid secretion responses of Canton S tubules to biogenic amines.

Panels A-D show secretion rate traces (upper) and the corresponding percentage change relative to basal secretion (lower) for dopamine, octopamine, tryptamine and tyramine. Each panel combines the average secretion profile with the percentage increase following amine stimulation. Data are expressed as mean \pm SEM, n = 5. Y-axes were standardised across panels to allow direct comparison of responses between amines.

Comparative analysis of tyramine and octopamine responses in $Oct\alpha 2R$ knockdown tubules

The effect of tyramine on fluid secretion was examined using the Ramsay assay. Tubules were stimulated with tyramine (10^{-5} M) at 40 minutes (Figure 4.21). Basal secretion rates did not differ significantly between the knockdown and control groups. Following tyramine stimulation, the secretion rate of tsh-Gal4>UAS-Oct α 2R⁵⁰⁶⁷⁸ tubules was not significantly different from that of the $Octa2R^{50678}$ parental line. These findings indicate that knockdown of Octa2R does not alter the response to tyramine, suggesting that tyramine may act through a receptor other than Octa2R. To allow clearer visualisation of these data, the y-axis scale was adjusted to be consistent with Figures 4.17-4.20.

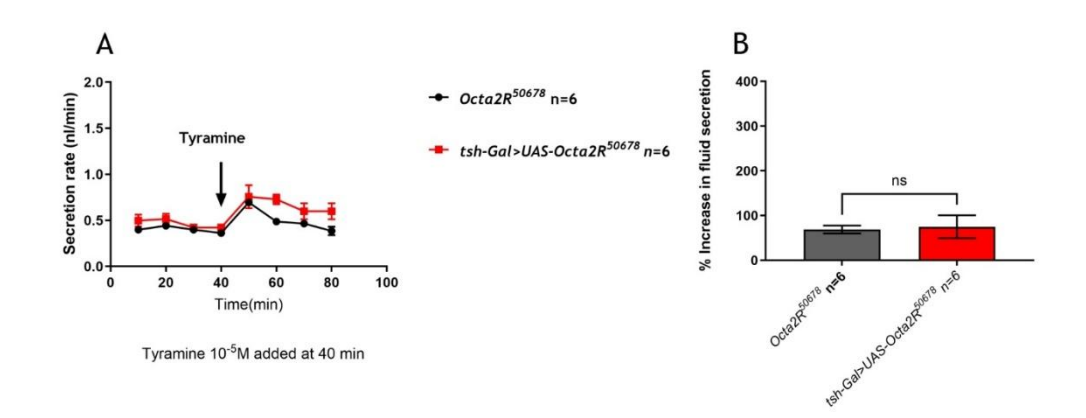


Figure 4.21 Effect of tyramine on the fluid secretion rate of Octa2R knockdown tubules. Secretion rates ($nL \cdot min^{-1}$) were measured in tsh-Gal4>UAS-Oct $\alpha 2R^{50678}$ (red) and the parental $Octa2R^{50678}$ control (black). Tyramine (10^{-5} M) was added at 40 min (arrow). (A) Time course of secretion rates recorded every 10 min. (B) Percentage increase in secretion relative to basal values. No significant differences were detected between groups (p>0.05, t-test). Data are mean \pm SEM, n=6. Y-axis scaling was matched to Figures 4.17-4.20 to allow direct comparison across amines.

In contrast to the results with tyramine stimulation, the knockdown of the octopamine receptor affects the fluid secretion rate under octopamine stimulation. As shown in Figure 4.22, the basal rate was affected by the knockdown of Octa2R in stellate cells, and octopamine stimulated the secretion rate was significantly impaired in ths-Gal4>UAS-Oct α 2R⁵⁰⁶⁷⁸ flies at all four measurement points (p<0.05). The y-axes in Figure 4.22 were adjusted to allow clear visualisation of secretion changes and to enable comparison with previous

figures. A percentage increase with octopamine stimulation relative to basal secretion for each tubule was measured and calculated, and the experimental group and control groups were compared using a t-test. The secretion rate of tubules from *Octa2R* RNAi lines following stimulation with octopamine was calculated to be 105% of the basal secretion rate. The secretion rate of tubules from *ths*-Gal4>UAS-Octα2R⁵⁰⁶⁷⁸ flies was 89% of basal secretion, suggesting that knockdown of *Octa2R* from *Drosophila* leads to a reduced sensitivity of the Malpighian tubules to octopamine. These results identify a previously unreported role of Octα2R in mediating octopamine-stimulated fluid secretion in Malpighian tubules. Previously, no articles had described that octopamine could stimulate fluid secretion in tubules.

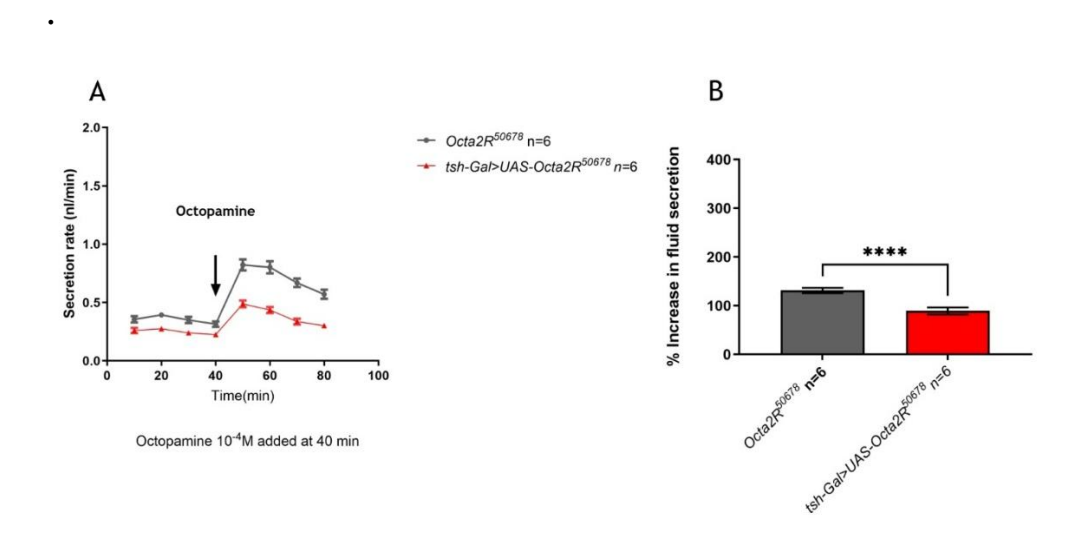


Figure 4.22 Secretion assay for tsh-Gal4>UAS-Oct α 2R⁵⁰⁶⁷⁸ compared with the parental RNAi line. (A) Basal secretion rate from control (black) and *Octa2R* knockdown (red) tubules before and after stimulation with 10⁻⁴ M octopamine. (B) Percentage increase in secretion following octopamine stimulation. Data are mean \pm SEM, n = 6. Statistical analysis was performed using a t-test. p < 0.05, p < 0.0001. The y-axes were standardised to match earlier figures for direct comparison of secretion responses.

Overall, these data indicate that the knockdown of the Octa2R gene in the $Octa2R^{50678}$ RNAi line reduces tubule performance in fluid homeostasis. This is specifically shown as a reduction in the fluid secretion rate. In the fluid secretion assay of $Octa2R^{50678}$, octopamine can affect the secretion rate of the experimental line (tsh-Gal4>UAS-Octa2R), suggesting that tubules respond to octopamine. This chapter shows that the Octa2R is specifically expressed in the

stellate cells of *Drosophila* Malpighian tubules. One of the UAS lines effectively knocked down *Octa2R* expression in these tubules when driven by *tsh*-Gal4. This study also indicates that tubule secretion is particularly sensitive to octopamine than other biogenic amines, suggesting the unique responsiveness of Malpighian tubules to octopamine signalling. The knockdown of *Octa2R* in stellate cells further decreased the secretion rate, indicating its sensitivity to octopamine. These findings suggest a previously undocumented functional role for octopamine in *Drosophila* tubules. Within the timeframe of this project, additional experiments testing dopamine and tryptamine responses in *Octa2R* knockdown tubules were not performed. These could be addressed in future studies to assess whether the observed effect is specific to octopamine or shared with other biogenic amines.

4.4 Discussion

The experiments detailed in this chapter were designed to investigate whether octopamine affects *Drosophila* Malpighian tubules when *Octa2R* is knocked down. This question was investigated from multiple angles, with the three primary steps involved being to identify *Octa2R* in stellate cells, knockdown of *Octa2R* from tubules using the tsh-*Gal4* line and assess the effect of octopamine on tubule secretion after the knockdown of *Octa2R* in tubules. Although the main question has been resolved, the three steps have been completed, and the hypothesis validated, the results have also raised new questions.

I tested all four biogenic amines at different concentrations to determine the best concentration for each amine. The results for each concentration are shown in Figures 4.16 through 4.19. All data were analysed statistically; detailed information is provided in the appendix. By comparing the p-values for each concentration, the selected concentration for each biogenic amine was presented in Figure 4.20.

In my investigative experiment, it was found that octopamine clearly stimulated the tubules, whereas the responses to other amines were weaker and more variable. Dopamine and tyramine produced stimulatory effects only at certain concentrations, while tryptamine showed no consistent effect. These findings indicate that, although octopamine is a more effective stimulator, some degree of stimulation from other biogenic amines can also occur in a concentration-dependent manner. My results are in line with earlier observations by Kerr et al. (2004), showing that one of the biogenic amines, serotonin, does not stimulate the tubules (Kerr et al., 2004). Their experiments demonstrated that serotonin manipulates intracellular second messengers such as cGMP and cAMP, and serotonin receptor expression responses to secrete fluid. Although serotonin is not tryptamine, tryptamine is a precursor for serotonin biosynthesis, and both serotonin and tryptamine are synthesised from tryptophan (Ruaud and Thummel, 2008).

My study describes pharmacologically characterising the effects of manipulating different biogenic amine concentrations on stimulating fluid secretion in Drosophila tubules and determining the optimal octopamine concentrations. Compared with my pharmacologically characterising study on amine, Kerr et al. focus on pharmacologically characterising the effects of manipulating intracellular second messengers (cGMP, cAMP, and serotonin receptor) expression to regulate fluid secretion in the *Drosophila* Malpighian tubules. Specifically, their result shows that ectopic expression of the rat GC-A receptor in *Drosophila* principal and stellate cells of the Malpighian tubules stimulates cGMP signalling and increases fluid transport. It also demonstrates that 5HT acts through the 5HT7Dro receptor to stimulate cAMP production and fluid secretion in the Malpighian tubules. Furthermore, previous studies have mentioned that Oct2R responds to both serotonin and octopamine (Nakagawa et al., 2022), but this was not shown in my results. Due to time constraints, I did not complete fluid secretion measurements under serotonin stimulation in tubules with Oct2R knockdown.

Interestingly, Nakagawa et al.'s research showed that stimulating Octα2R inhibits cAMP. However, I found that octopamine stimulation increases secretion, which is consistent with increased cAMP. There could be several possible reasons. One possible is the different isoforms of the receptor, each isoform with distinct ligand-binding affinities and signalling properties. Another is that stellate cells may have unique signalling pathways or coupling mechanisms to convert receptors to second messengers.

Regarding the first step of identifying the Octa2R expression in tubules, the overall result indicates that Octa2R are expressed in the stellate cells and can be knocked down with the tsh-Gal4 line. Comparing the $Octa2R^{50678}$ RNAi line expression level with those obtained by knocking down Octa2R in the tubules, the expression of Octa2R in tsh-GAL4>UAS-Oct α 2R dramatically decreased in stellate cells compared with the parental control line (UAS-Oct α 2R and tsh-Gal4) (Figure 4.13). p<0.05. To more clearly observe the specific effect of the knockdown Octa2R, the data for the RNAi line and knockdown line were listed

and compared in Figure 4.14. An 87% decrease in Octα2R expression was observed (Figure 4.14). This suggests that *Octa2R* can be knocked down in tubules. The *tsh-Gal4* line is a specific stellate cell line, indicating that *Octa2R* are in a stellate cell. The results could support the previous description in Figure 4.10 from FlyAtlas, which demonstrated the expression of *Octa2R* in renal tubules. However, this raises an important question: is the effect of Octα2R specific to octopamine, or could this receptor also respond to other biogenic amines, such as serotonin. Previous studies have suggested that Octα2R may be activated by both octopamine and serotonin (Nakagawa et al., 2022), but this was not confirmed in my experiments. In particular, serotonin and tryptamine were not tested under *Octa2R* knockdown conditions, leaving open the possibility that *Octa2R* might contribute to a broader amine sensitivity in Malpighian tubule.

The result exists when the $Octa2R^{50678}$ were used. Before using the $Octa2R^{50678}$ line, $Octa2R^{10214}$ and $Octa2R^{10215}$ were first crossed with the specific stellate cell tsh-Gal4 line and the specific principal cell line CapaR-Gal4, respectively, to test whether Octa2R could be knocked down in the tubules. The results are shown in Figure 4.12. Figures 4.12 A and B do not show a decrease in the expression levels of Octa2R in the experiment group compared to the controls. This result indicates that although all three fly lines ($Octa2R^{10214}$, $Octa2R^{10215}$ and $Octa2R^{50678}$) are UAS-Oct α 2R RNAi lines, the $Octa2R^{10214}$ and $Octa2R^{10215}$ fly line exhibit different results in the knockdown line (tsh-Gal4>UAS-Oct α 2R) compared to the $Octa2R^{50678}$ line. Octa2R could not be knocked down in the tubules in $Octa2R^{10214}$ and $Octa2R^{10215}$ fly lines.

The difference in knockdown efficiency between *Octa2R*¹⁰²¹⁴, *Octa2R*¹⁰²¹⁵, and *Octa2R*⁵⁰⁶⁷⁸ likely has several factors. First, it could be due to factors related to the design of the RNAi constructs. The *Octa2R*¹⁰²¹⁴ line and *Octa2R*¹⁰²¹⁵ line are GD line, but *Octa2R*⁵⁰⁶⁷⁸ is the TRiP line. The RNAi construct in the TRiP line may target a different region of the *Octa2R* gene that is more effective at reducing *Octa2R* expression in Malpighian tubules. Perkins *et al.* (2015) demonstrated that TRiP lines generally provide more efficient vectors for RNAi (Perkins *et al.*,

2015). Secondly, it could be due to the effects of different insertion sites. The TRiP line is typically inserted at the attP2 and attP40 docking sites for LexA drivers and Gal4-driven TRiP insertions (van der Graaf *et al.*, 2022). GD line has their insertions at different sites with random insertion sites. This randomness may result in less effective gene knockdown. Moreover, Nakagawa *et al.* (2022) also successfully knocked down the *Oct2R* gene in the *Octa2R*⁵⁰⁶⁷⁸ line.

Regarding the final step of identifying the effect of octopamine on the *Octa2R* knockdown tubule compared with the parental, the overall result indicates that the knockdown of *Octa2R* in tubules reduces fluid secretion rate and is sensitive to octopamine. This step was measured and calculated through fluid secretion assays. To assess whether *Octa2R* knockdown influences responses to kinin, secretion assays were performed using the *Octa2R*¹⁰²¹⁴ and *Octa2R*¹⁰²¹⁵ RNAi lines. However, neither line produced a measurable reduction in *Octa2R* expression (see Section 4.3.2); consequently, the kinin data from these lines cannot be interpreted as evidence of knockdown-dependent effects. The secretion rates observed under kinin stimulation therefore do not inform the role of *Octa2R*, and these datasets were not used for further conclusions (full traces are provided in Appendix 6 and Appendix 7).

Next, the fluid secretion assay was conducted using the *Octa2R*¹⁰²¹⁵ to identify whether *Octa2R* knockdown in *Octa2R*¹⁰²¹⁵ reduces tubules' secretion performance. Unlike the secretion assay of *Octa2R*¹⁰²¹⁴, the *Octa2R*¹⁰²¹⁵ line secretion assay used two peptides stimulate, capa and kinin peptides. In insects, capa peptides control fluid secretion and diuresis to maintain water balance. These activities are accomplished by raising nitric oxide, cyclic GMP (cGMP), and calcium levels in the principal cells of MTs (Davies *et al.*, 2013). This elevation in these molecules increases the capacity of tubules to excrete water. Thus, capa peptide was used to identify whether the knockdown of *Oct2R* would affect fluid homeostasis under stimulated conditions for this tissue. The statistical results showed no significant difference between the *Oct2R* knockdown and control tubules (Appendix 7 A and C) p>0.05. Whether under-stimulated or non-stimulated conditions, the knockdown of *Oct2R* did not affect fluid homeostasis

in *Octa2R*¹⁰²¹⁴ and *Octa2R*¹⁰²¹⁵ line tubules. Interestingly, the results showed a statistically significant difference when the kinin peptide and capa peptide were used to stimulate the experimental and control groups at the 30-minute and 60-minute, respectively. P<0.05. However, because the *Octa2R*¹⁰²¹⁴ and *Octa2R*¹⁰²¹⁵ lines did not produce an effective knockdown of *Octa2R* expression (see Section 4.3.2), these findings cannot be interpreted as evidence for a functional role of *Octa2R* in peptide-mediated secretion. Instead, they likely reflect variability unrelated to *Octa2R* knockdown, and so these data were not considered further in drawing conclusions.

The previous data were insufficient to clarify the impact of gene knockdown on fluid secretion in tubules. TRiP line $Octa2R^{50678}$ was used for fluid secretion assays to enable a more effective comparison. I used the same method to measure their fluid secretion rates and then calculated the percentage change in secretion rate. In the result of this assay, the basal secretion rate was affected by the knockdown of Octa2R in the stellate cells of the Malpighian tubules, and the kinin-stimulated secretion rate was significantly impaired in tsh-Gal4>UAS-Oct α 2R. Knockdown of Octa2R could affect fluid homeostasis under non-stimulated and stimulated conditions, interfering with tubules' ability to respond to kinin.

Combining the knockdown experiment results shown in Figure 4.14, the fluid secretion assay results following octopamine stimulation further indicate that an 87% knockdown of *Octa2R* in the tubules can disrupt the tubules' response to octopamine (Figure 4.22). However, the results from another group of fluid secretion assay of Octa2R knockdown experiment with tyramine stimulation indicate that 87% knockdown of *Octa2R* in the tubules cannot disrupt the tubules' response to tyramine (Figure 4.21). Thus, octopamine affects *Octa2R* knockdown tubules compared with parental flies' tubules.

The results show that the Octα2R receptor is expressed specifically in the stellate cells of *Drosophila* Malpighian tubules, and that knockdown of *Octa2R* by RNAi line leads to a marked reduction in fluid secretion after octopamine stimulation. This response was specific, as other biogenic amines (tyramine) did not show similar effects, highlighting the unique role of octopamine signalling in this system. Earlier studies have shown that octopamine receptors in *Drosophila* regulate behaviour and metabolic responses (Maqueira et al., 2005; Farooqui, 2012), but their role in renal physiology remains unclear. The present study extends this understanding by suggesting that *Octa2R* may play an important role in the regulation of tubule secretion under stress or stimulatory conditions.

These findings are novel in showing that octopamine signalling through Octα2R contributes directly to renal fluid homeostasis and identify the Malpighian tubule as an octopamine-sensitive tissue. Given the tubule's central role in insect osmoregulation and detoxification, Octα2R-mediated signalling likely provides a mechanism for integrating systemic stress responses with tubule fluid secretion. This sensitivity may allow insects to rapidly adjust water and ion balance in response to environmental or metabolic cues, a function that is not observed with other tested amines. Thus, the results of this chapter provide the first direct evidence of a previously undocumented functional role of octopamine in *Drosophila* tubules, emphasising its significance in renal physiology and identifying a new functional role for octopamine in *Drosophila* Malpighian tubules.

Chapter 5 Characterisation of the *Drosophila* Novel Gene CG6602

5.1 Summary

CG6602 is an uncharacterised gene in *Drosophila*. Bioinformatic prediction suggests that it encodes a small conserved protein with no clearly defined functional domains, and there are currently no mammalian orthologs. Limited information is available, but initial studies by Musselman et al. (2019) confirmed that it exhibits a unique expression pattern under varying metabolic conditions. Their studies demonstrated the sensitivity of CG6602 expression to dietary modes and supported a possible role for CG6602 in glucose metabolism, potentially interacting with insulin signalling pathways. However, apart from its correlation with diet patterns, the functional role of CG6602 remains largely uncharacterised, making it a suitable candidate for functional study. In this chapter, I focused on the strong, tubule-specific expression and cell-type specificity of CG6602 in stellate cells of the Malpighian tubules. Knockdown experiments indicated enrichment in stellate cells, consistent with single-cell sequencing data. To assess its functional relevance, fluid secretion assays were performed using independent RNAi lines from the GD and KK collections. These two RNAi resources are widely used in *Drosophila* genetics because they provide independent constructs for the same target, thereby helping to confirm that phenotypes are not due to off-target effects. Interestingly, the GD and KK lines produced different results: knockdown in stellate cells with the GD line led to a significant reduction in stimulated secretion, whereas the KK line showed no detectable effect. Based on this, further analyses were concentrated on the GD line. Finally, to address whether CG6602 contributes to systemic physiology, we asked whether its knockdown alters weight gain under temperature stress. Comparisons between GD knockdown flies and parental controls showed no significant difference in wet-to-dry weight ratios, suggesting that CG6602 does not play a major role in whole-body weight regulation under these conditions.

5.2 Introduction

The FlyAtlas2 data show that *CG6602* is highly enriched in the Malpighian tubules of *Drosophila* melanogaster (Krause et al., 2022; Figure 5.1). Single-cell transcriptomic data from the Fly Cell Atlas further indicate that expression of the *CG6602* transcript is localised to stellate cells of the main segment (Li and Janssens et al., 2022; Figure 5.2). Together, these datasets provide evidence that *CG6602* may have a role in tubule physiology. Nevertheless, almost nothing is currently known about the gene. To date, the only substantial experimental investigation remains that of Musselman et al. (2019).

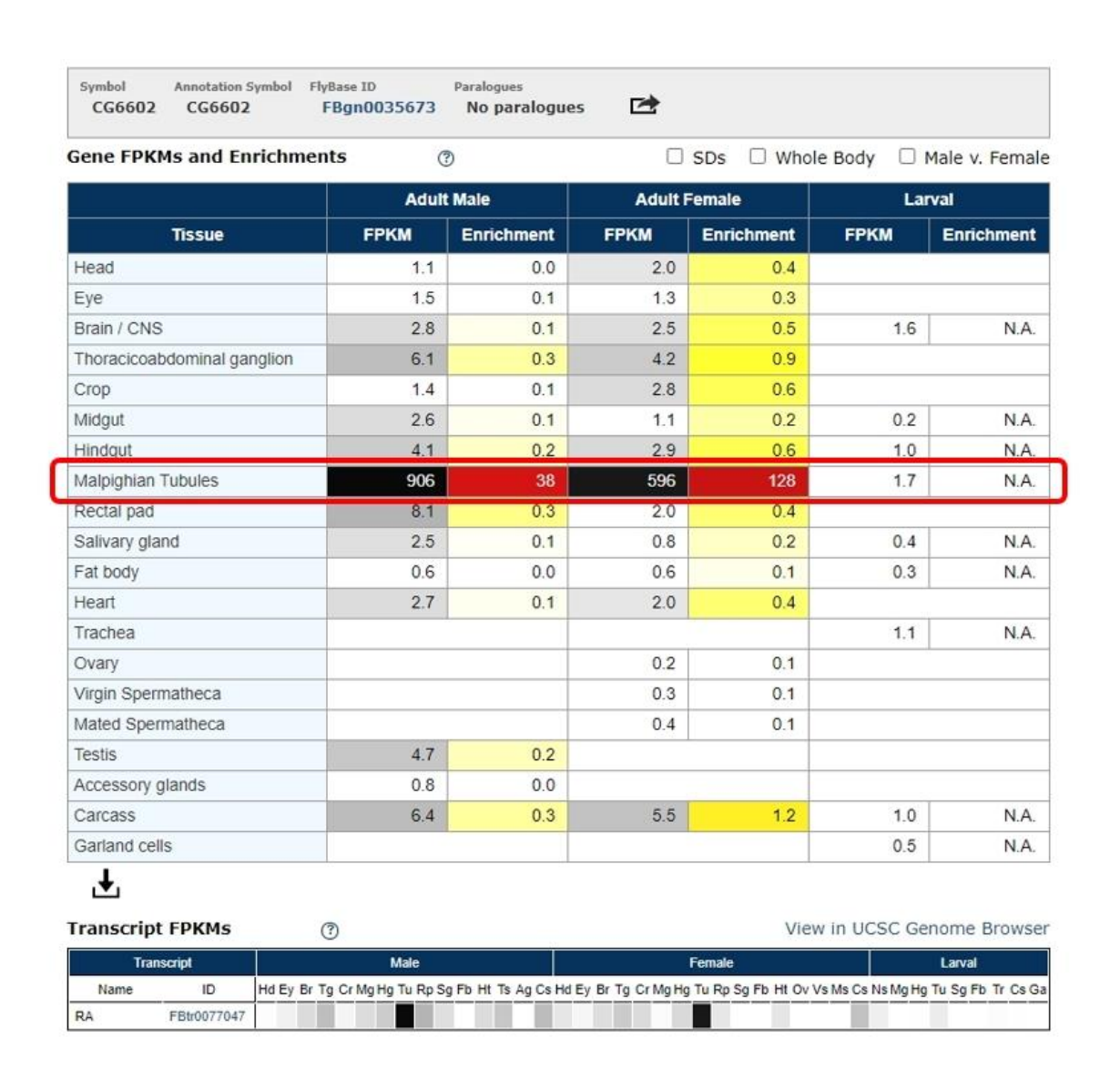


Figure 5.1 Tissue expression of CG6602 in *Drosophila***.** Expression levels across tissues extracted from FlyAtlas2, showing strong enrichment in the Malpighian tubules (highlighted in red box) compared with other tissues (Krause *et al.*, 2022).

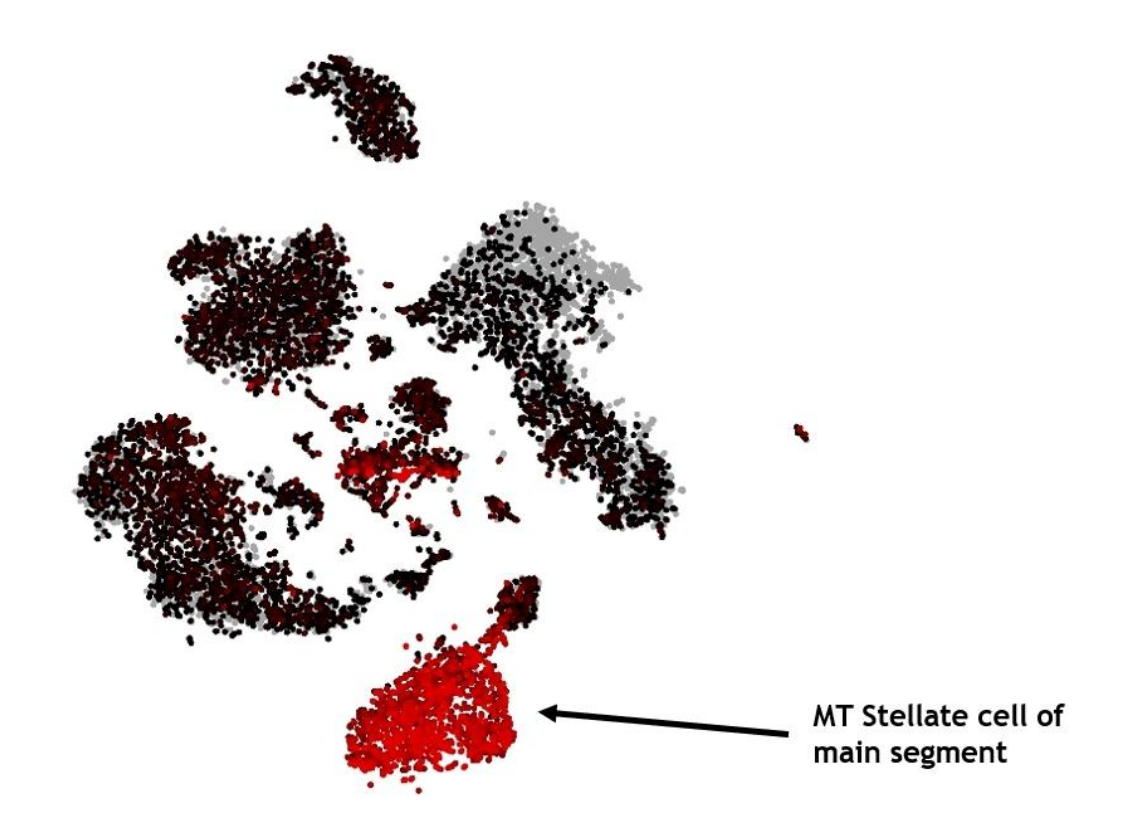


Figure 5.2 Single-cell expression profile of CG6602 in adult Malpighian tubules. Data from the Fly Cell Atlas demonstrate specific localisation to stellate cells of the main segment (Li and Janssens et al., 2022).

Previous work has shown that *CG6602* expression is influenced by dietary conditions. Musselman et al. (2019) reported that larvae fed a high-glucose diet had higher levels of *CG6602* mRNA in the fat body compared with those on a high-fructose diet, while expression under a normal diet was unaffected. Data from FlyAtlas2 indicate that CG6602 expression in the fat body is very low compared with the Malpighian tubules (Krause *et al.*, 2022; Figure 5.1). This contrast emphasises the tubule as the primary tissue of interest for investigating the role of *CG6602* and suggests that the diet-dependent changes observed in larvae may be relevant to understanding its broader physiological function.

The mechanisms and pathways through which *CG6602* acts remain unresolved, highlighting the need for further investigation. To address this, I combined transcriptomic evidence with functional genetic analysis as a framework to explore its potential role in tubule function.

5.3 Result

The expression analysis for the *Drosophila melanogaster CG6602* gene was designed to measure its expression level in Malpighian tubules and confirm if this is expressed on stellate cells or principal cells in Malpighian tubules. Therefore, I explore the tissue and cell expression data of *CG6602* from FlyAtlas 2 to confirm this hypothesis. These data showed that *CG6602* is highly expressed in tubules (Figure 5.1), suggesting the potential involvement of *CG6602* in renal functions. Additionally, Fly Cell Atlas analyses indicated the Malpighian tubule specific expression of *CG6602* with enrichment in stellate cells (Figure 5.2). *CG6602* is found in similar cell clusters in the tubule data from FlyCellAtlas as *tsh. CG6602* is mainly expressed in the stellate cell of main segment. These results suggest that *CG6602* may function in one or more aspects of stellate cell function, including ion transport and modulating osmotic conditions within the tubule.

5.3.1 *CG6602* is mainly expressed in the stellate cells of the tubule.

As the *CG6602* gene is expressed in the fat bodies and tubules, I conducted gene knockdown experiments to investigate its function. Two publicly available *CG6602* (GD and KK) lines were used to reduce the mRNA levels in the tubules. The primary aim of this experiment was to determine the impact of *CG6602* knockdown in these tissues by crossing the target lines with specific GAL4 drivers. I measured the levels of *CG6602*, with the parental *CG6602* lines and specific GAL4 driver lines serving as controls. The tsh-GAL4 driver line was crossed with the *CG6602* target lines for targeted gene knockdown in the tubules. The levels of *CG6602* mRNA were then measured in the tubules of both control and knockdown flies. Following the methodology described in Chapter 3, *RPL32* was used as a control gene to validate the gene expression analysis.

CG6602 GD (GD18900) and CG6602 KK (KK 106152) were initially selected for this experiment, with the results in Figures 5.3 A and B. The expression level of the CG6602 gene in the parental CG6602 lines was set to a baseline value of 1. The relative expression in the knockdown flies was then compared to this control

tsh-GAL4 line and other parental control lines. In the Malpighian tubules (highlighted by the green box in Figure 5.3), when crossed with the tsh-GAL4 line, there was a significant reduction in *CG6602* mRNA expression levels observed in the *CG6602* GD knockdown line (tsh4-GAL4>CG6602) (Figure 5.3 A), indicating successful knockdown. Similarly, the knockdown of *CG6602* using the *CG6602* KK line also resulted in a marked reduction in expression levels compared to the parental control lines (Figure 5.3 B). The expression of *CG6602* was not knocked down in the principal cells of tubules using CapaR-Gal4 in both GD and KK lines. These results suggest effective knockdown of *CG6602* in the stellate cell of tubules, confirming that *CG6602* is expressed in the stellate cell of tubules. In these two UAS lines, the *CG6602* GD line provided the most efficient knockdown and was therefore used in subsequent experiments.

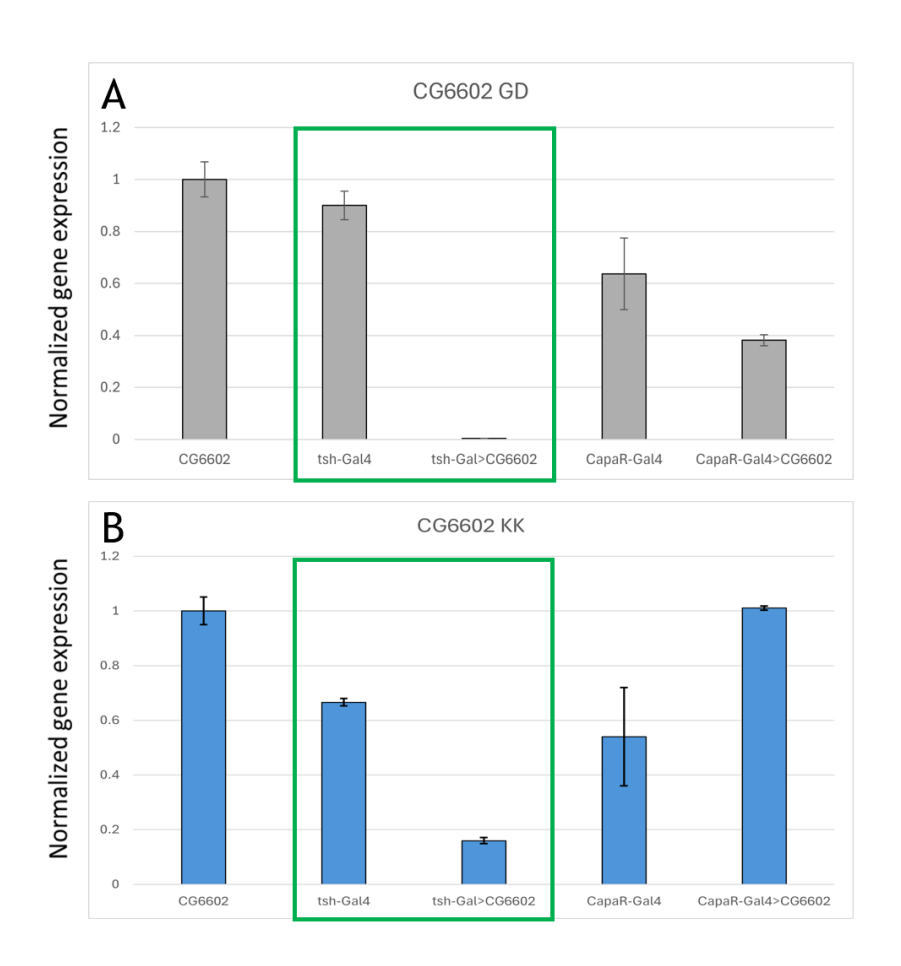


Figure 5.3 Validation of knockdown of CG6602 GD and CG6602 KK expression in MTs. The green box represents a specific knockdown of the CG6602 gene in stellate cells. A: There are three parent lines: CG6602 (GD), tsh-Gal4, and CapaR-Gal4. CG6602 was crossed with the tsh-Gal4 and CapaR-Gal4 lines. tsh-Gal>CG6602 and CapaR-Gal4>CG6602. B: Similarly, CG6602 (KK) was also crossed with the tsh-Gal4 and CapaR-Gal4 lines. p<0.05.

5.3.2 Knockdown of *CG6602*i¹⁸⁹⁰⁰ does affect the fluid secretion of the tubules

To assess the function of the CG6602 gene in fluid secretion within tubules, I used targeted RNAi knockdown in combination with the GAL4/UAS system and established fluid secretion assays. The objective was to determine the effect of CG6602 knockdown on basal and stimulated secretion rates. In these experiments, the tsh-GAL4 driver was used due to the high expression of CG6602 in stellate cells. Secretion rates were measured over time, and stimulation was induced using kinin peptides and CAPA peptides to assess any changes in secretion responses.

I compared the $CG6602i^{18900}$ (GD 18900) and tsh-Gal4>UAS-CG6602i groups at different intervals. The results shown in Figure 5.4(A) indicate that basal secretion rates were not affected compared to control MTs. Similarly, the capastimulated secretion rate in tsh-Gal4>UAS-CG6602i MTs also did not change compared to controls (p>0.05). After kinin stimulation, however, there was a significant reduction in secretion rates in the tsh-Gal4>UAS-CG6602i group compared with the $CG6602i^{18900}$ parental controls (p<0.05). This indicates that knockdown of CG6602 in stellate cells specifically reduced the kinin-stimulated secretion response between 70 and 90 minutes.

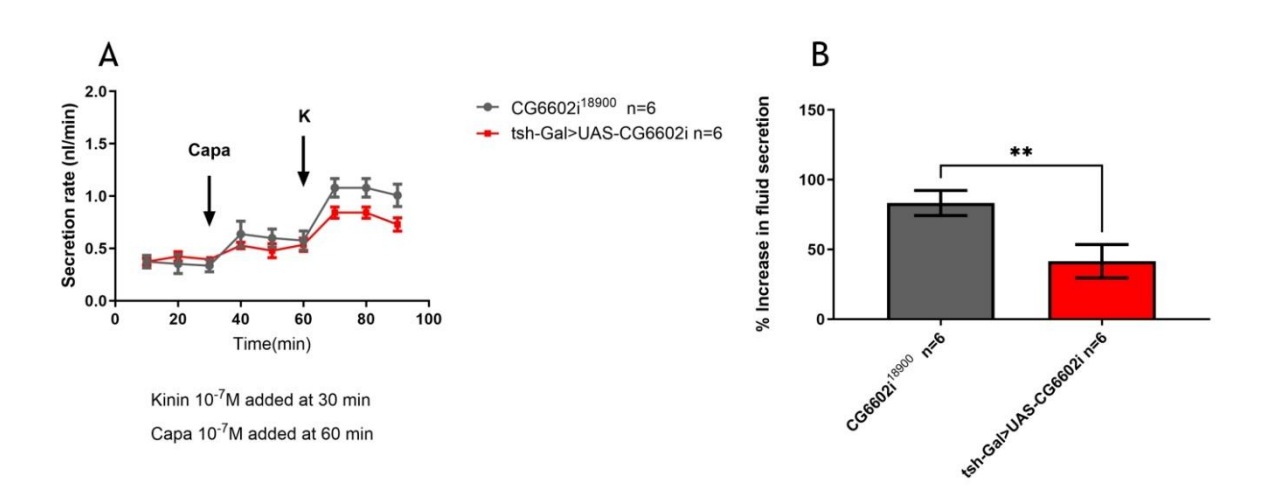


Figure 5.4 Secretion assay for tsh-Gal4>UAS-CG6602i compared with parental line CG6602i¹⁸⁹⁰⁰ (GD 18900). A: The fluid secretion rate (nL·min⁻¹) was measured in tsh-Gal4>UAS-CG6602i (red squares) and UAS-CG6602i¹⁸⁹⁰⁰ (GD 18900) (dark grey circles) in the Malpighian tubules. The data is shown at 10 min intervals up to 90 min. Capa was added at 30 mins, and Kinin (K) was added at 60 mins (shown by arrows). B. The percentage increase in fluid secretion after stimulation by capa and kinin in CG6602 knockdown flies. The mean percentage change from the three biological replicates of the fluid secretion assay is shown and calculated. Formulas are described in the previous chapter. * Indicates a statistically significant difference (p<0.01). All graphs show mean ± SEM. N=6.

In the control group, stimulation with capa or kinin produced higher secretion rates compared with basal levels. A similar pattern was observed in the tsh-Gal4>UAS-CG6602i knockdown group, where secretion also rose after capa or kinin stimulation. These findings confirm that both peptides act as strong stimulators of secretion in the tubules. However, when comparing the extent of

the increase between groups, the kinin-stimulated rise was clearly reduced in the knockdown flies relative to controls, while the capa-stimulated increase did not differ significantly between the two groups. This indicates that *CG6602* knockdown reduces the kinin-driven component of fluid secretion, whereas the effect of capa was not altered.

Figure 5.4(B) provides a summary of the percentage increase in secretion relative to basal levels *for CG6602i*¹⁸⁹⁰⁰ (GD 18900) and tsh-Gal4>UAS-CG6602i flies. The bar chart shows a significant reduction in the knockdown group compared with parental controls (p<0.01). In the parental line, the percentage increase ranged from approximately 62.45 to 119.46, whereas in the knockdown line, the increase ranged from 22.05 to 55.63. Together, these results indicate that *CG6602* expression in stellate cells is required for a full kinin-stimulated secretory response and contributes specifically to signalling pathways that mediate kinin-dependent, but not capa-dependent, fluid secretion.

5.3.3 $CG6602i^{106152}$ (KK 106152) does not affect the fluid secretion of the tubules

Further fluid secretion assay shows another UAS-dependent RNAi line, *CG6602i*¹⁰⁶¹⁵² (KK 106152), that was examined for its secretion rate in decreasing CG6602 mRNA level in Figure 5.5. The RNAi line was used as the control. For the *CG6602i*¹⁰⁶¹⁵² (KK 106152) line, comparing the basal rate to the kinin-stimulated secretion rate showed a highly significant increase, confirming that kinin can affect the secretion rate in this group. p-value>0.05. The tsh-Gal4>UAS-CG6602i group showed a similar pattern. There is a significant increase comparing basal and kinin-stimulated rates within this group. p-value>0.05. This finding indicates that kinin effectively stimulates fluid secretion in tsh-Gal4>UAS-CG6602i flies, and the knockdown of *CG6602* does not alter the group's physiological response to kinin.

When comparing the *CG6602i*¹⁰⁶¹⁵² (KK 106152) and tsh-Gal4>UAS-CG6602i groups, there was no significant difference between the RNAi and experimental groups at basal levels. This indicates that the fluid secretory rates of the RNAi line and the tsh-Gal4>UAS-CG6602i line are similar without stimulation. After kinin stimulation, the p-value is also higher than 0.05. It shows that kinin stimulation increased secretion in both groups but that the secretion rate of tsh-Gal4>UAS-CG6602i MTs did not differ from the control.

Figure 5.5 (B) shows a bar chart summary of the percentage delta increase in fluid secretion over basal level for $CG6602i^{106152}$ (KK 106152) and tsh-Gal4>UAS-CG6602i. Raw data show that $CG6602i^{106152}$ (KK 106152) values are between 101.7 to 127 in this group, while the tsh-Gal4>UAS-CG6602i group ranges from approximately 93.4 to 120.5. Together, this suggests that both groups exhibit an increase in secretion following kinin stimulation. Although the $CG6602i^{106152}$ (KK 106152) group (grey bar) shows a higher percentage increase compared to the tsh-Gal4>UAS-CG6602i group (red bar), the statistical annotation "ns" indicates no statistically significant difference between the two groups' percentage increases in secretion. Moreover, wet and dry weight measurements were conducted to assess whether knockdown of CG6602 produced any broader

effects on whole-animal physiology, such as changes in overall growth or water balance. These measurements did not reveal consistent differences between experimental and control flies, and the full data are provided in Appendix 8.

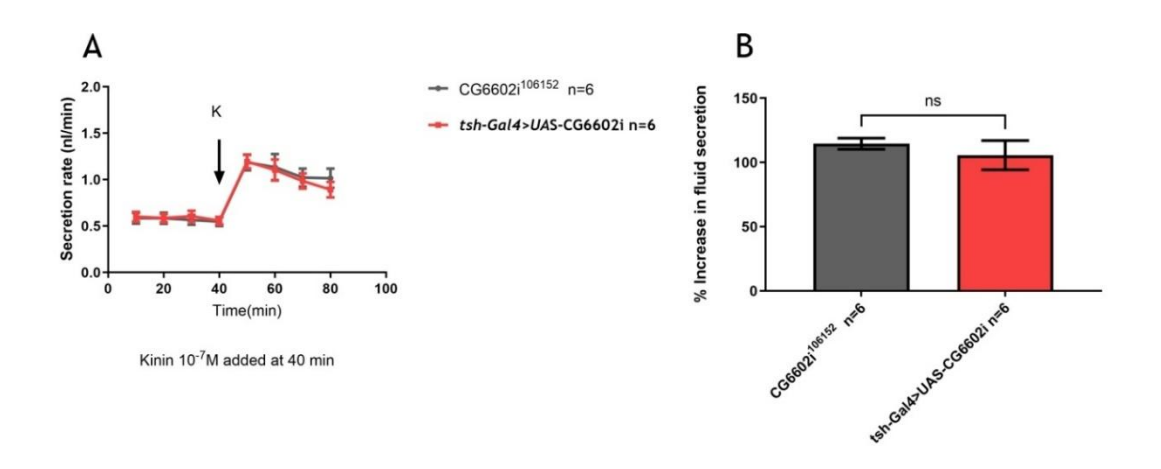


Figure 5.5 Secretion assay for tsh-Gal4>UAS-CG6602i compared with parental line $CG6602i^{106152}$ (KK 106152). (A) Changes in secretion rates (nL·min⁻¹) in Malpighian tubules from knockdown flies (tsh-Gal4>UAS-CG6602i, red squares) and the corresponding parental control (UAS-CG6602i¹⁰⁶¹⁵², dark grey circles). Measurements were taken every 10 min up to 80 min. Kinin (10^{-7} M) was added at 40 min (arrow). (B) Quantification of the percentage increase in secretion after kinin stimulation. Values represent the mean percentage change from three independent biological replicates. Data are presented as mean \pm SEM (N=6). No significant difference was detected between knockdown and control groups (p>0.05).

Overall, these results show that knockdown of *CG6602* with the KK line does not alter basal or kinin-stimulated secretion rates. In contrast, a clear difference was observed in the GD line, where kinin stimulation significantly changed secretion in the experimental group (tsh-Gal4>UAS-*CG6602*) compared with controls. This indicates that the effect of *CG6602* on tubule secretion is context-dependent, being evident in the GD RNAi line but absent in the KK line.

5.4 Discussion

As seen for basal secretion rates of both groups in Figure 5.3, these data indicate that the knockdown of *CG6602* in stellate cells did not affect secretion before capa stimulation. Although, after capa stimulation, secretion rates were not statistically significant in the experimental and control groups, if we compare the p-value for this set of data with the p-value for previous basal rate data, I can find that a potential trend of difference in fluid secretion rates between these two group as the p-value is 0.072, which is approaching the threshold for significance. Additionally, the within-group comparisons for control and experimental group analysis results demonstrate that capa and kinin stimulation increases fluid secretion rates. Both capa and kinin stimulation can affect the changes in the fluid secretion rate of *CG6602i*¹⁸⁹⁰⁰ (GD 18900). Similarly, the tsh-Gal4>CG6602 group also showed significant differences.

The difference in delta values between the knockdown and RNAi groups was only seen after kinin stimulation. In the $CG6602i^{18900}$ (GD 18900) line, knocking down CG6602 led to a lower secretion rate compared with the RNAi control group. This result suggests that CG6602 is involved in the kinin-stimulated fluid secretion of the tubules, and that reducing its expression in the $CG6602i^{18900}$ (GD 18900) line weakens the fluid secretion rate.

This study analyses fluid secretion levels from two groups, *CG6602* RNAi line and tsh-Gal4>UAS-CG6602i, to determine whether the knockdown of *CG6602* from *CG6602* RNAi line affects their baseline and stimulated secretion levels. I started by comparing the basal rates, measured from 10 to 40 minutes. Based on statistical testing, there seemed to be no difference in basal secretion rates between CG6602i and tsh-Gal4>UAS-CG6602i group. In both groups, secretion increased after kinin stimulation compared to before kinin stimulation. However, the experimental group and RNAi line had similar trends, and no statistical significance was observed between the two groups. Although *CG6602* was knocked down from RNAi KK line flies, the tsh-Gal4>UAS-CG6602i group retains a secretion rate comparable to the *CG6602i* group when stimulated by kinin.

The small percentage increase in secretion rate is stimulated by kinin, and there is no statistical difference between the two groups (Figure 5.5 B). This result suggests that the knockdown of *CG6602* in tsh-Gal4>UAS-CG6602i (KK 106152) has no detectable effect on the fluid secretion rate when compared with its parental control, UAS-CG6602i¹⁰⁶¹⁵² (KK 106152). Under kinin stimulation, the knockdown of *CG6602* in this KK line did not change the secretion rate, which suggests two possible explanations: a limited role for *CG6602* in this setting, or compensation by other pathways that maintain fluid transport. By contrast, in the GD line, the knockdown of *CG6602* in tsh-Gal4>UAS-CG6602i (GD 18900) reduced the kinin-stimulated secretion rate compared with its parental line, UAS-CG6602i¹⁸⁹⁰⁰ (GD 18900).

Interestingly, the *CG6602* KK and GD lines showed different experimental results in the secretion assays. This indicates that each line responds to kinin stimulation in a different way. One explanation is that the two RNAi constructs differ in their ability to reduce *CG6602* expression. qPCR validation confirmed that the GD line achieved a greater reduction of *CG6602* mRNA levels in the tubules than the KK line, reflecting higher knockdown efficiency (Figure 5.3). This difference in knockdown levels is consistent with the observation that only the GD line showed a decrease in kinin-stimulated secretion. Another factor may be differences in chromosomal insertion sites. According to the VDRC, GD insertions can occur on chromosomes 1, 2, or 3, whereas KK insertions are restricted to chromosome 2. Taken together, both knockdown efficiency and positional effects may explain why the GD line, but not the KK line, displayed a functional phenotype.

Another possibility is variable RNAi efficiency. Due to differences in RNAi targeting, the knockdown efficiency of different RNAi lines can also vary. GD lines may show stronger knockdown than KK lines (Xia *et al.*, 2021), leading to detectable physiological effects under kinin stimulation. In addition, the efficiency of knockdown may differ between tissues, as the GAL4/UAS system can drive expression in a tissue-specific manner (Heigwer *et al.*, 2018). This means that *CG6602* knockdown could be more effective in the tubules of GD

lines than in KK lines. Furthermore, the chromosomal location of the RNAi construct could influence efficiency. If the $CG6602i^{18900}$ (GD line) has its RNAi insertion in a genomic region with higher transcriptional activity, it may achieve a stronger reduction of CG6602 expression than the $CG6602i^{106152}$ (KK line).

The specificity of the kinin response may also explain this difference. The kinin response in the *CG6602* line may depend on the interaction between *CG6602* and another signalling pathway. However, because each RNAi line was analysed against its own parental stock, baseline kinin sensitivity is controlled within each pair; therefore, a general higher sensitivity of tsh-Gal4>UAS-CG6602i (GD 18900) to kinin is unlikely to account for the data. Instead, the reduction in kinin-stimulated secretion was observed only for tsh-Gal4>UAS-CG6602i (GD 18900) relative to UAS-CG6602i¹⁸⁹⁰⁰ (GD 18900), whereas tsh-Gal4>UAS-CG6602i (KK 106152) and UAS-CG6602i¹⁰⁶¹⁵² (KK 106152) showed no change. This pattern is consistent with the qPCR results showing a marked reduction of *CG6602* mRNA in tsh-Gal4>UAS-CG6602i (GD 18900) compared with UAS-CG6602i¹⁸⁹⁰⁰ (GD 18900) (Figure 5.3) and may also reflect insertion-site effects. This difference is most likely attributable to the efficiency of *CG6602* knockdown in stellate cells, rather than to differences in kinin sensitivity between the pairs.

As discussed earlier in this chapter, *CG6602* is related to insulin signalling. The *CG6602* GD and KK lines show different results in fluid secretion assays, which may be related to variable interactions with the insulin signalling pathway. Given that *CG6602* expression responds to dietary sugar and insulin receptor activity, the knockdown of the *CG6602* gene in each KK line and GD line may have different effects on insulin signalling. This could alter the intracellular environment to affect fluid secretion responses, especially under conditions of kinin stimulation, which might amplify metabolic and signalling differences.

Second, if *CG6602* has a role in insulin signalling or metabolic homeostasis, which impacts fluid secretion rates and other behaviours, the knockdown of this gene might affect fluid secretion rates by modulating how cells respond to

signalling molecules. Under experimental conditions, the knockdown of *CG6602* might enhance sensitivity to insulin-related pathways. This specific sensitivity might affect the physiological response to kinin in the Malpighian tubules, resulting in differences in secretion assays. In contrast, the KK line may not present the same metabolic or signalling pathway due to differences in the knockdown RNAi efficiency, resulting in different effects on fluid secretion in response to kinin. This variation between GD and KK lines could indicate that specific RNAi constructs interact differently with the insulin signalling pathway.

The reduction in kinin-stimulated secretion observed only in tsh-Gal4>UAS-CG6602i (GD 18900) compared with its parental control, UAS-CG6602i¹⁸⁹⁰⁰ (GD 18900), highlights a potential role of CG6602 in stellate cell function. Stellate cells are central to regulating chloride and water movement in the Malpighian tubules and are the main target for peptide hormones such as kinins. The loss of kinin responsiveness in the GD knockdown therefore suggests that CG6602 may contribute to the mechanisms that allow stellate cells to drive fluid secretion. CG6602 could influence the activity or availability of chloride channels that mediate kinin-stimulated secretion, or it may affect intracellular signalling downstream of the kinin receptor, such as calcium mobilisation or protein kinase activation, which are both known to regulate fluid secretion. qPCR analysis showed that tsh-Gal4>UAS-CG6602i (GD 18900) produced a clear reduction in CG6602 mRNA levels in the tubules compared with UAS-CG6602i¹⁸⁹⁰⁰ (GD 18900), which matches the observed phenotype, while tsh-Gal4>UAS-CG6602i (KK 106152) and UAS-CG6602i¹⁰⁶¹⁵² (KK 106152) did not. These findings suggest that CG6602 may act in stellate cells to connect metabolic status with hormonal control of tubule secretion, although technical factors such as RNAi construct design and insertion site effects cannot be ignored.

In conclusion, the different results obtained with the two RNAi lines may be due to differences in construct design, insertion site, genetic background, and knockdown efficiency. These technical considerations underline the need for caution when interpreting RNAi-based studies. The consistent finding across assays is that knockdown with tsh-Gal4>UAS-CG6602i (GD 18900) reduces kinin-

stimulated fluid secretion, whereas knockdown with tsh-Gal4>UAS-CG6602i (KK 106152) does not. This chapter therefore shows that knockdown of *CG6602* in stellate cells alters tubule function under kinin stimulation, and it provides a foundation for the transcriptomic and metabolomic analyses presented in the following chapter.

Chapter 6 Transcriptomics of CG6602

6.1 Summary

This chapter describes the RNA-seq transcriptomic analysis of *CG6602* knockdown in the Malpighian tubule of *Drosophila melanogaster*. RNA-seq identified both up- and down-regulated genes across the cellular stress response, xenobiotic detoxification, metabolism, and transport. The expression pattern is consistent with activation of stress-response programmes together with altered expression of ion-transport and metabolic genes, indicating efforts by the tubule to stabilise function under challenge. Genes related to detoxification and ion transport were clear in these data. In addition, reduced expression of genes involved in lipid metabolism and clearance, together with lower expression of regulators such as *mat* (which encodes the Mob-family protein Mats that activates Wts in the Hippo pathway), suggests that *CG6602* knockdown can increase cellular stress and affect lipid balance. Overall, the results support a role for *CG6602* in tubule homeostasis by maintaining detoxification and redox capacity, preserving ion and water transport, and limiting stress-induced changes in metabolic gene expression.

6.2 Introduction

Transcriptomic approaches are a powerful tool to analyse all RNA transcripts in a cell, tissue, or organism under specific conditions or at various developmental stages (Wang et al., 2009). These techniques provide information about gene expression, regulation, and how the genome is transcribed in many biological conditions (Samuels et al., 2021). Transcriptomics does not only identify expressed genes but also helps in functional annotation of the genome and explanation of gene structures (Lowe et al., 2017; Rosato et al., 2021; Dong et al., 2014). A major use of transcriptomics is to compare gene expression across different experimental conditions, identifying differentially expressed genes and understanding how cells respond to internal and external stimulation (Golubnitschaja and Costigliola, 2018). RNA-seq is one method in transcriptomics used to measure RNA and discover novel transcripts (Conesa et al., 2016). It provides a detailed and quantitative view of gene expression at different developmental stages and environmental conditions by sequencing RNA and mapping the reads to a reference genome (Kukurba and Montgomery, 2015; Dobin and Gingeras, 2015; Conesa et al., 2016). Additionally, transcriptomics can identify co-expressed genes and gene networks, providing insights into the interactions of genes regulating biological processes (Yin et al., 2021).

Reverse genetics is a useful approach to explaining gene function within the framework of transcriptomics. It starts with a known gene sequence and examines its function by disrupting or altering that gene to see the resultant phenotype. This technique is particularly helpful in transcriptome research. It allows scientists to modulate the expression of specific genes, including novel or uncharacterised genes, to explain their functions in development or physiology mechanisms. RNA interference (RNAi) can be used to downregulate target genes, facilitating the assessment of transcriptomic alterations resulting from gene disruption.

In *Drosophila*, reverse genetics can be combined with transcriptomics to investigate the function of uncharacterised genes such as *CG6602*. By knocking down *CG6602*, I can observe how its changed expression affects overall gene

expression patterns. Integrating reverse genetics and transcriptomics is helpful when examining uncharacterised gene functions. It helps researchers understand the roles of individual genes in complex cellular processes and how they lead to phenotype changes.

In *Drosophila* tubules, the transcriptomics technique can help identify co-expressed genes and pathways that may interact with *CG6602*. By comparing the transcriptomic data of wild-type and *CG6602* knockdown, the impact of *CG6602* knockdown on gene networks and cellular pathways can be detected. It helps to understand *CG6602*'s features within the tubule's regulatory system. This co-expression analysis could also highlight previously unknown connections between *CG6602* and established regulatory pathways in the Malpighian tubules, thereby helping to understand the molecular networks that support tubule function.

In characterising *CG6602*, transcriptomic analyses can show genes that may be trying to compensate or be controlled by *CG6602*. When *CG6602* is knocked down, other genes may alter their expression levels to maintain cellular function, indicating a compensatory response. This compensation mechanism may be because biological systems have overlapping pathways to ensure stability, particularly in tubules' essential functions such as osmoregulation and ion transport. By analysing these genes, I can explore the alternative pathways activated by the cell when *CG6602* expression is knocked down.

Furthermore, transcriptomics can identify specific genes under the direct or indirect control of *CG6602*. Knockdown of *CG6602* can lead to modified expression levels of genes that are co-regulated with CG6602 if it functions as a regulator of specific pathways. If *CG6602* is involved in a signalling pathway that controls ion transport, knocking down *CG6602* could lead to increased or decreased expression of genes encoding transporters or channel proteins to maintain homeostasis. The changes in expression of these genes indicate that *CG6602* has some regulatory control of them either due to being in a common pathway or related by direct regulatory interactions.

To identify genes with altered expression when *CG6602* is knocked down, I used reverse genetics to knock down the expression of the *CG6602* in *Drosophila*. I identified known and novel genes by analysing transcriptomic data from both control and knockdown lines. Additionally, the data suggest the presence of potential compensatory mechanisms at the transcriptomic level. Detailed experimental analyses and data are presented in the following chapter.

6.3 Results

6.3.1 Up-regulated gene in the CG6602

This study's transcriptomics analysis discovered 36 genes (Figure 6.1) that were significantly up-regulated and 58 genes that were significantly down-regulated following the knockdown of *CG6602* in *Drosophila* tubules (Figure 6.7). The up-regulation was detected using criteria that included a log₂ fold change of 1 or more and an adjusted p-value threshold, so it was statistically significant in identifying differentially expressed genes. These genes show different base mean expression levels, indicating the average strength of the signal.

Several up-regulated genes showed strong increases in expression, with log₂ fold change values exceeding 5; for example, *CG13871*, *TpnC4*, and *CG9555*. These data indicate a significant reaction to knockdown of *CG6602*. The up-regulation may indicate activation of compensatory or adaptive mechanisms within the tubule to stabilise cellular function under stress, or it may reflect that the normal role of *CG6602* is to negatively regulate these genes, so that their expression increases when *CG6602* expression is reduced.

The list of up-regulated genes contains many with established roles in cellular stress responses, metabolism, and transport, as well as others whose functions remain poorly characterised. These data suggest the presence of a compensatory mechanism by which the tubules attempt to maintain homeostasis following *CG6602* knockdown. The subsequent analysis focuses on 36 genes that are highly expressed in the tubules.

Gene	BaseMean	Log2FoldChange	padj
CG13871	43.79	5.53	1.07E-13
TpnC4	3.86	5.50	2.95E-02
CG9555	7.56	5.48	6.20E-03
Ugt50B3	222.90	4.71	2.36E-46
Irc	169.74	3.92	9.62E-44
lncRNA:CR44642	9.98	3.92	2.89E-03
CG42329	111.88	3.11	9.84E-21
stan	10.40	2.68	4.69E-02
phr	24.57	2.56	6.72E-05
MtnD	13.17	2.47	1.23E-02
alpha-Est4aPsi	654.89	2.24	7.33E-30
CG13313	232.59	2.19	2.26E-18
Ugt35C1	962.63	1.89	6.56E-25
CG4467	45.53	1.82	7.23E-05
CG16898	266.32	1.73	3.25E-12
CG30371	968.08	1.58	3.15E-18
lncRNA:CR46472	48.65	1.58	7.08E-04
Fst	165.21	1.56	3.55E-04
Cyp6a8	4736.97	1.45	3.56E-18
Ugt36E1	59.29	1.44	5.99E-04
Gadd45	120.54	1.41	2.90E-04
Slc45-1	920.53	1.35	4.67E-08
Damm	121.03	1.35	4.53E-06
CG12780	45.22	1.31	1.63E-02
Socs36E	85.27	1.30	1.15E-02
CG33346	60.79	1.22	2.68E-02
Ziz	1904.39	1.15	1.34E-10
asRNA:CR45140	52.79	1.11	4.24E-02
CG6908	338.80	1.09	2.36E-05
CG32107	173.07	1.08	1.61E-03
Cyp6d5	262.62	1.05	2.17E-03
CG7142	174.50	1.00	2.05E-03
CG7900	189.23	0.98	5.31E-04
Cyp4e1	308.79	0.98	2.82E-05
Pdk	570.06	0.98	7.83E-06
MFS12	771.17	0.97	1.06E-02

Figure 6.1 Significantly up-regulated genes in the CG6602. Each gene listed shows significant expression changes through three main columns: BaseMean, Log₂FoldChange, and padj. The BaseMean represents the average strength of the signal of each gene across all samples. The Log₂FoldChange column indicates the magnitude of expression change for each gene, with positive values showing up-regulation in response to CG6602 knockdown. padj column is for adjusted p-value. It is a statistically significant feature for changes in gene expression and multiple testing corrections and is related to multiple comparisons.

The eight genes listed in Figure 6.2 are up-regulated upon *CG6602* knockdown and highly expressed in *Drosophila* tubules (FlyAtlas 2 data, Krause *et al.*, 2022). This list shows the high transcription level of these genes in tubule tissues, indicating their probable involvement in tubule function or response to *CG6602* knockdown. These base mean values are from ~173 to 4737, representing a high level of expression variation between genes and, in some cases, genes with strong transcription signals.

Gene	BaseMean	Log2FoldChange	padj
CG13313	233	2.19	2.3E-18
Ugt35C1	963	1.89	6.6E-25
CG30371	968	1.58	3.1E-18
Cyp6a8	4737	1.45	3.6E-18
Slc45-1	921	1.35	4.7E-08
CG32107	173	1.08	1.6E-03
CG7142	174	1.00	2.0E-03
MFS12	771	0.97	1.1E-02

Figure 6.2 These are the up-regulated genes in the *CG6602***.** Eight genes were selected because they show significant up-regulation in the knockdown condition and strong expression in Malpighian tubules as reported in FlyAtlas2.

Ugt35C1

Among the high-expression, up-regulated genes, *Ugt35C1*, *Cyp6a8*, *Slc45-1*, and *MFS12* have been previously described, which helps to interpret their roles in the tubule. *Ugt35C1* encodes a UDP-glucuronosyltransferase and shows high expression in Malpighian tubules (Figure 6.3A). UGT enzymes catalyse glucuronidation (Guillemette, 2003), contribute to stress adaptation (Zhang *et al.*, 2021), and their increased expression has been linked to antioxidant and xenobiotic defence (Mourikis *et al.*, 2006). The up-regulation of *Ugt35C1* in the *CG6602* knockdown is therefore consistent with activation of detoxification pathways in the tubule.

In the STRING network (Figure 6.3B), *Ugt35C1* connects to enzymes involved in small-molecule metabolism (e.g. *Adh*, *Est-6*, *betaGlu*, *CG15117*). These associations indicate shared functional contexts rather than physical binding. The co-expression heatmap (Figure 6.3C) summarises pairwise co-expression across *Drosophila* datasets: each square shows the strength of correlated expression between two genes (darker = stronger). *Ugt35C1* shows co-expression signals with *Adh*, *Est-6*, *betaGlu* and *CG15117*, suggesting that these genes may participate in related metabolic processes in the tubule.

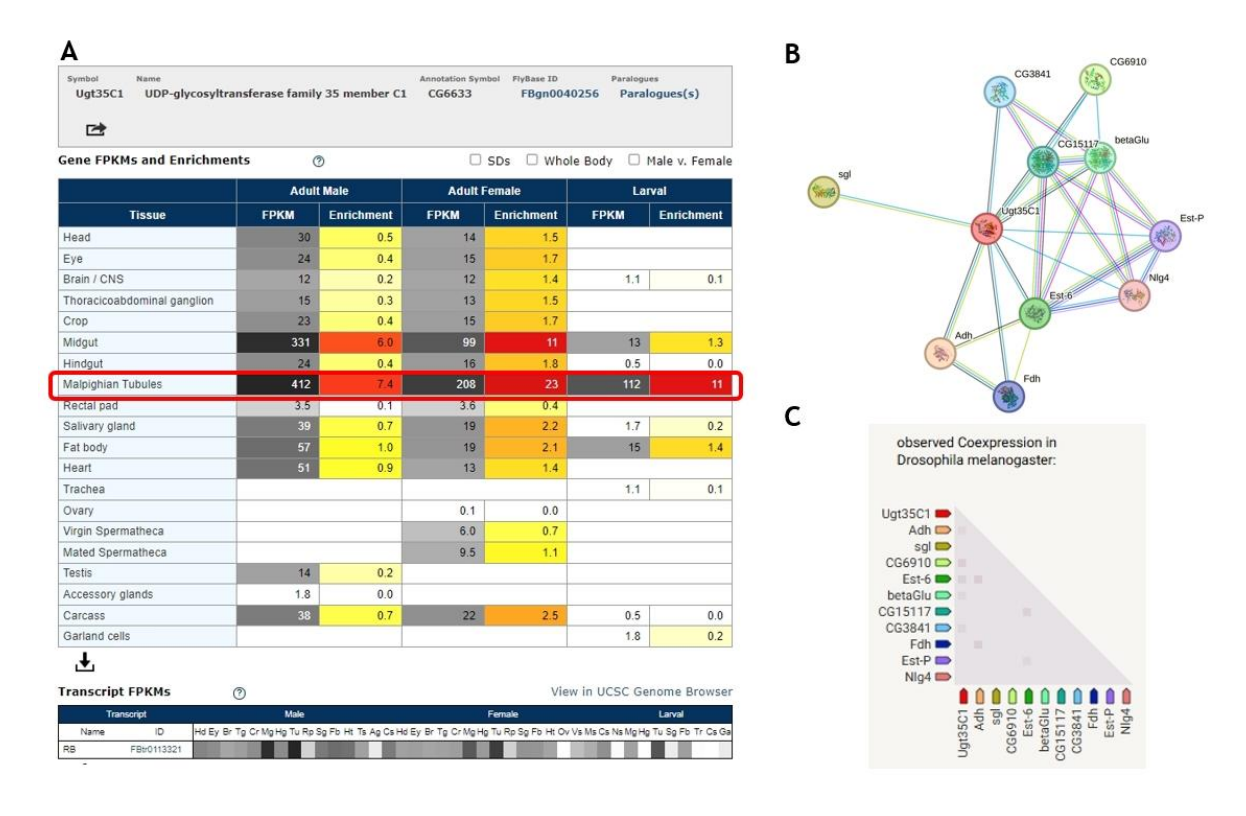


Figure 6.3 Expression and interaction context of *Ugt35C1*. (A) FlyAtlas2 tissue expression for *Ugt35C1* in *Drosophila*; the red box highlights Malpighian tubules (Krause *et al.*, 2022). (B) STRING network for *Ugt35C1*. The central node (*Ugt35C1*) is connected to enzymes involved in small-molecule metabolism. Node colours distinguish the query from its partners. Edge colours indicate the source of supporting evidence: green = gene neighbourhood, red = gene fusion, blue = curated databases, purple = experimentally determined, light blue = gene co-occurrence, yellow = text mining, black = co-expression, and grey = protein homology (Szklarczyk *et al.*, 2023). These links represent functional associations and do not necessarily imply direct physical interactions. (C) STRING co-expression matrix for *Drosophila melanogaster*. Each square shows the correlation in expression between two genes across public datasets (darker shading = stronger correlation). *Ugt35C1* shows co-expression with *Adh*, *Est-6*, *betaGlu* and *CG15117*, suggesting related metabolic functions in the tubule (Szklarczyk *et al.*, 2023).

Cyp6a8

The expression and interaction context of *Cyp6a8* is shown in Figure 6.4. *Cyp6a8* is highly expressed in Malpighian tubules and encodes a cytochrome P450 enzyme. The Cyp6a8 protein catalyses oxidative reactions of exogenous and endogenous compounds (Lee *et al.*, 2023). Two other P450 family members, *Cyp6d5* and *Cyp4e1*, also appear among the up-regulated genes (Figure 6.1), but they are less abundant in tubules than *Cyp6a8* (Supplementary Figure). Cytochrome P450 enzymes contribute to protection against environmental stressors, including toxins and pesticides; increased *Cyp6a8* expression may therefore enhance detoxification capacity in *Drosophila* tubules.

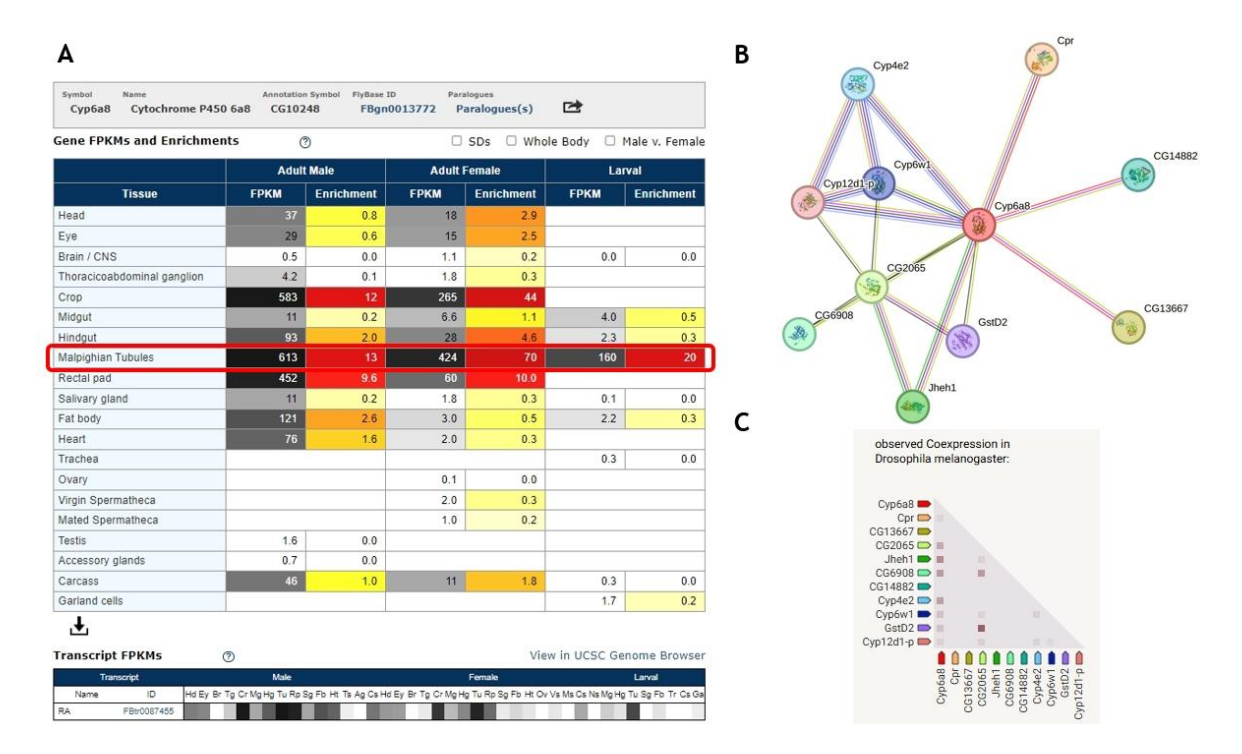


Figure 6.4 Expression and interaction information of *Cyp6a8*. (A) FlyAtlas2 tissue expression showing high levels of *Cyp6a8* in Malpighian tubules (Krause *et al.*, 2022). (B) STRING network for *Cyp6a8*. The central node (*Cyp6a8*) is connected to predicted interaction partners involved in oxidative metabolism. Edges are coloured according to different sources of supporting evidence (for example, curated databases, experimental data, co-expression). These links denote functional associations rather than direct physical binding (Szklarczyk *et al.*, 2023). (C) STRING co-expression matrix for *Drosophila melanogaster*. Each square represents the degree of co-expression between two genes across public datasets, with darker shading indicating stronger correlation. *Cyp6a8* shows co-expression with partners such as *Cpr*, *CG13667* and *CG2065*, supporting its role in detoxification pathways in the tubule. (Szklarczyk *et al.*, 2023).

Slc45-1

Slc45-1 belongs to the solute carrier (SLC45) family of membrane transporters (He et al., 2009). Proteins in this family transport small solutes, typically proton-coupled carriers for small metabolites such as sugars, across cellular membranes. Its high expression in the Malpighian tubule suggests a role in handling osmolytes and nutrient-derived metabolites (Figure 6.5A). In our RNA-seq data, Slc45-1 is up-regulated in the CG6602 knockdown, which may reflect a compensatory adjustment of solute transport to help stabilise tubule function under knockdown conditions.

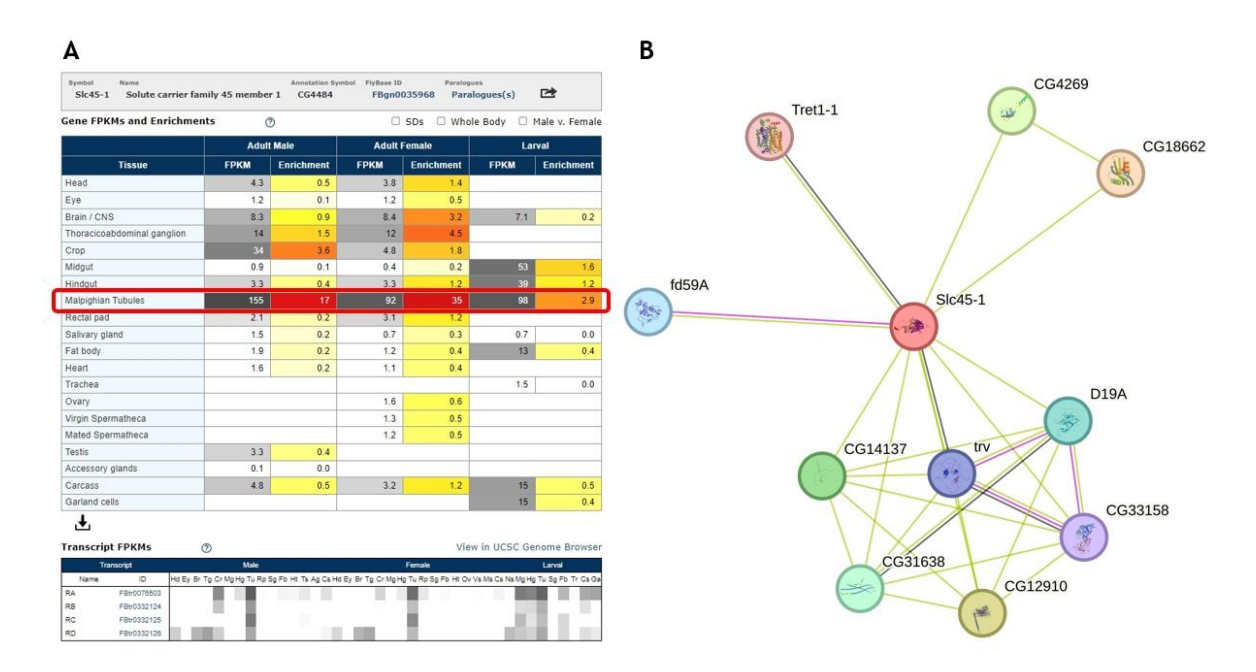


Figure 6.5 Expression and interaction context of *Slc45-1***.** (A) FlyAtlas2 tissue expression showing enrichment of *Slc45-1* in Malpighian tubules (Krause *et al.*, 2022). (B) STRING network for *Slc45-1* with predicted interaction partners. Node colours indicate the query protein and its partners. Edges are coloured according to different evidence channels (see Figure 6.3 for the full key, for example curated databases, experimental data, co-expression). These links denote functional associations and do not necessarily imply direct physical interactions (Szklarczyk *et al.*, 2023).

MFS12

The last gene on the up-regulated list (Figure 6.1) is MFS12. Its log_2FC value is the smallest on the list, which means that the change in its expression level on the up-regulated genes list is also the smallest. MFS12 is a member of the major facilitator superfamily, contributing to the transmembrane movement of small solutes and various substrates across cellular membranes (Wang $et\ al.$, 2020). Its higher expression in the tubules suggests a potential involvement in the metabolic modifications important for maintaining the tubule's stability and function (Figure 6.6 A). MFS12 up-regulation after CG6602 reduction could indicate the need to adjust the transport routes within the tubules to restore the cellular balance.

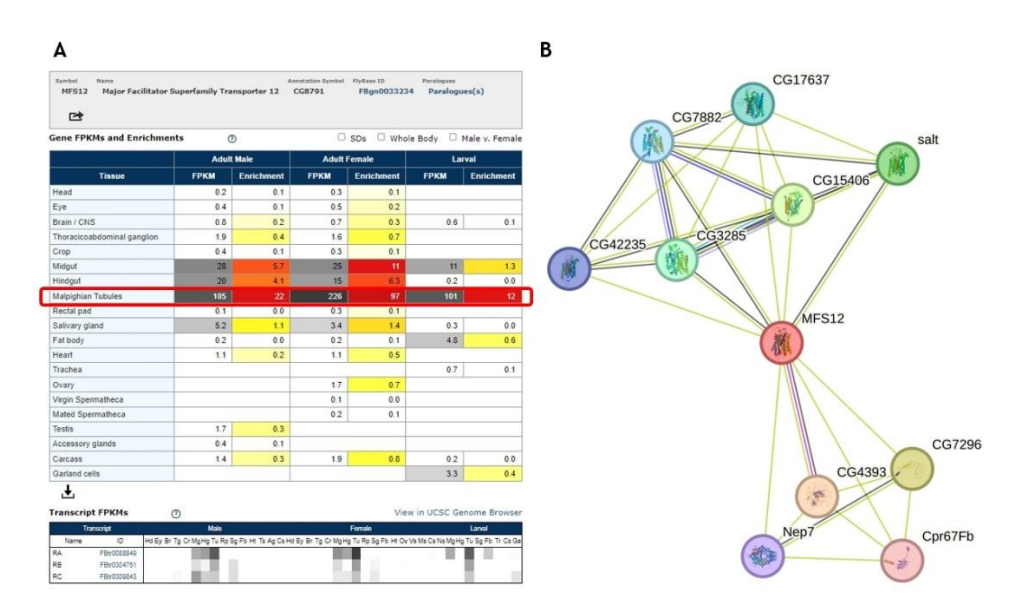


Figure 6.6 Expression and interaction information of MFS12. (A) FlyAtlas2 tissue expression showing enrichment of MFS12 in Malpighian tubules (Drosophila; Krause et al., 2022). (B) STRING network for MFS12 and its predicted partners. Node colours distinguish the query protein from its partners. Edge colours follow the evidence channels defined by STRING; see Figure 6.3 for the full colour key. These associations indicate functional relationships and do not necessarily imply direct physical interactions (Szklarczyk et al., 2023).

Together, these genes show high expression levels in tubules, and their upregulation following *CG6602* knockdown suggests a role in compensatory responses. All of them contribute to the tubule's basal excretory, detoxification, and transport functions that are essential for maintaining homeostasis, particularly under physiological stress caused by *CG6602* knockdown.

6.3.2 Down-regulated gene in tubules

As shown in Figure 6.7, several genes were significantly down-regulated in Drosophila tubules with CG6602 knockdown during transcriptomic analysis. In particular, the expression levels of these genes (log_2 fold change < 0) decreased markedly. This down-regulation indicates that in the knockdown of CG6602, the expression levels of a subset of genes are reduced.

In particular, the strongly down-regulated genes include *tbc*, *Cyp4p2* and *CG1695*, each with a log² fold change of -6 or more. The gene *tbc* shows a large negative log² fold change despite very low basal expression in tubules reported by public datasets. In our RNA-seq, low but detectable counts in controls fell further in the *CG6602* knockdown, producing a large fold change. Because this pattern arises near the detection limit, the biological interpretation of *tbc* should be made with caution, and emphasis is placed on down-regulated genes with clearer tubule expression profiles (Figure 6.7; Supplementary Figure). Unlike *Cyp4e1*, which appears in the up-regulated list (Figure 6.1), another member of the Cyp4 subfamily, *Cyp4p2*, is represented in the down-regulated list.

The down-regulated gene set spans several biological processes, including detoxification, cellular transport, and structural maintenance, which are reduced or altered under *CG6602* knockdown. Suppression of specific genes may therefore reflect a broader adjustment mechanism in which tubules down-regulate multiple pathways to compensate for changes caused by genetic knockdown.

Gene	BaseMean	Log2FoldChange	padj
tbc	248	-8.87	3.9E-22
Cyp4p2	61	-7.41	1.5E-09
CG1695	37	-6.69	2.1E-07
snoRNA:Psi18S-1389b	15	-6.28	2.6E-04
CG8560	7	-6.26	1.7E-03
CG33109	26	-5.57	1.2E-06
CG44142	4	-5.31	4.0E-02
Muc68E	14	-5.30	1.3E-03
yip7	61	-5.22	2.3E-13
CG17633	35	-4.98	3.5E-09
CG8562	6	-4.88	4.8E-02
LysD	9	-4.59	2.5E-02
LysP	20	-4.46	1.2E-05
CG10477	9	-4.01	1.3E-02
CG45080	136	-3.94	1.2E-22
CG18180	8	-3.88	2.7E-02
CG43680	18	-3.75	3.6E-05
CG3868	13	-3.52	2.2E-03
lcs	85	-3.50	6.2E-15
CG43366	15	-3.44	1.6E-03
Jon65Aiii	12	-3.30	5.5E-02
lncRNA:flam	111	-2.99	1.8E-18
Syn1	10	-2.77	5.3E-02
snoRNA:Psi28S-3316c	9	-2.72	5.3E-02
CG13397	146	-2.70	6.0E-20
CG33307	30	-2.68	9.8E-06
CG16826	976	-2.48	8.0E-24
IntS12	21	-2.38	2.1E-03
PGRP-SC2	16	-2.31	1.5E-02
whe	116	-2.21	1.4E-10
Cyp28a5	57	-2.10	1.2E-05
COX4L	17	-1.99	4.3E-02
snoRNA:Psi28S-3316d	20	-1.98	2.4E-02
CG8539	112	-1.94	2.2E-11
snoRNA:Psi28S-3316a	21	-1.93	2.2E-02
CG17751	5418	-1.77	2.0E-17
CG4781	103	-1.76	1.2E-03
CG10175	60	-1.75	1.1E-05
Adh	40	-1.68	1.0E-03
CG34212	47	-1.68	5.3E-04
Cht10	32	-1.61	6.0E-03
Ance	23	-1.59	4.6E-02
CG17224	184	-1.51	1.2E-05
ASPP	30	-1.45	4.1E-02
CG13160	95	-1.41	3.1E-04
snoRNA:Psi28S-1180	366	-1.34	1.1E-08
CG42673	98	-1.30	1.4E-04
CG8768	55	-1.23	1.5E-02
mat	1906	-1.21	1.7E-07
CG16935	272	-1.08	3.6E-06
		1100	

Figure 6.7 Down-regulated genes in *Drosophila* tubules following *CG6602* knockdown. Genes with significantly reduced expression are shown with their average expression level (BaseMean), log₂ fold change, and adjusted p-value (padj). BaseMean values are rounded to integers, log₂ fold changes are given to two decimal places, and padj values are shown in scientific notation with two significant figures. padj<0.05.

The data in Figure 6.8 are extracted from Figure 6.7. CG17224, CG17751, and mat are three downregulated genes, but they are highly expressed in tubules. The list shows a decrease in *CG17751* gene expression to about 29.2% of the original level, a reduction in *CG17224* gene expression to about 35.3% of the original level, and a decrease in mat gene expression to about 43.5% of the original level. It indicates their probable involvement in tubule function or response to *CG6602* knockdown.

Gene	BaseMean	Log2FoldChange	padj
CG17751	5418	-1.77	2.0E-17
CG17224	184	-1.51	1.2E-05
mat	1906	-1.21	1.7E-07

Figure 6.8 Highly expressed tubule genes with reduced expression after *CG6602* knockdown. These are the down-regulated genes in the CG6602 with a log 2-fold change of -1 or less and high expression in tubules. padj<0.05.

mat

Among these genes, only mat was previously characterised (Figure 6.9 A). This figure column shows that the mat gene is not expressed in many *Drosophila* tissues but is highly expressed in adult males, adult females and larval tubules. Figure 6.9 B from STRING shows the protein-protein interaction network for mat. Mat is in the central position, and it may have potential interaction with nine proteins. Given these predicted links, mat shows associations with ten proteins in the STRING network (Figure 6.9B). These associations indicate functional relationships rather than direct physical binding, and no specific pathways are defined from this analysis.

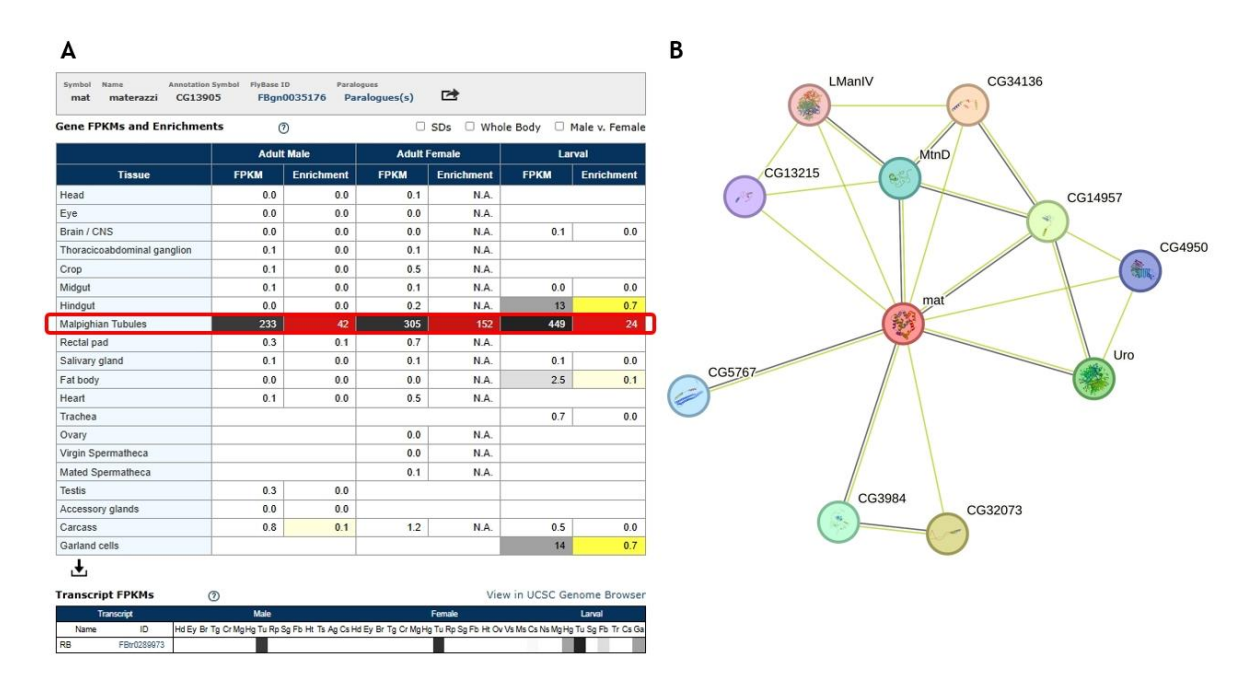


Figure 6.9 Expression and interaction information of *Mat*. (A) FlyAtlas2 tissue expression for *mat* in *Drosophila*; the red box marks Malpighian tubules (Krause *et al.*, 2022). (B) STRING network for *mat*. Node colours distinguish the query and its predicted partners. Edges are coloured according to STRING evidence channels; see Figure 6.3 for the full colour key. The network illustrates predicted associations with ten proteins but does not imply direct physical interactions (Szklarczyk *et al.*, 2023)..

6.4 Discussion

On the up-regulated list (Figure 6.1), *Ugt35C1*, *Ugt36E1*, and *Ugt50B3* are members of the Ugt family. They exhibit differential responses to *CG6602* knockdown. This may be due to differences in their expression levels across tissues and the specific enzymatic roles of each gene within the family. As important enzymes in insects, Ugt proteins play a significant role in detoxification and homeostasis by catalysing the conjugation of sugars with small lipophilic compounds (Ahn and Marygold, 2021). The differential responses to *CG6602* knockdown among the *Ugt* genes may reflect an adaptation of each gene to the physiological requirements of its primary tissue of expression.

Ugt50B3 shows the most significant change in expression in three Ugt genes in Figure 6.1 after the knockdown of CG6602, with a Log2 fold change (Log2FC) of 4.71, but it is not detected in the tubules according to FlyAtlas2 data (Supplementary Figure). It suggests that this gene may play a role in other tissues. The up-regulation of Ugt50B3 in response to CG6602 knockdown might have a compensatory mechanism. It may be metabolised in different tissues to compensate for the knockdown of CG6602 in tubules. This could indicate a compensatory response to maintain homeostasis. For example, when tubule detoxification is impaired, other tissues such as the fat body or midgut may increase their metabolic activity, with Ugt50B3 contributing to xenobiotic clearance outside the tubules.

Although the expression level of *Ugt35C1* also shows significant changes (padj<0.05) following *CG6602* knockdown, comparing their Log₂FC values that the up-regulated of *Ugt35C1* expression is less than that of *Ugt50B3* (Figure 6.1). However, FlyAtlas2 shows that *Ugt35C1* is highly expressed in the tubules. It may play a direct role in the tubule-specific detoxification process. The moderate upregulation of *Ugt35C1* upon *CG6602* knockdown (Log₂FC of 1.89) might indicate that this gene contributes directly to the tubules' response to stress or metabolic imbalance or maybe a specific response to enhance detoxification functions in the tubules when *CG6602* is knocked down. Although the reaction is

less than *Ugt50B3*, it is likely due to its already high baseline expression in this tissue.

Expression levels of UGT36E1 could be detected at lower levels than Ugt35C1 in the tubules (FlyAtlas 2, supplementary Figure). Among the three Ugt genes in the up-regulated list (Figure 6.1) following CG6602 knockdown, UGT36E1 shows the weakest upregulation ($Log_2FC = 1.44$). This may be because the lower baseline expression may indicate an accessory role in tubule detoxification, but its low expression under normal conditions suggests that it is unlikely to be a main detoxification enzyme in tubules.

In String interaction data, the ugt35C1 protein interaction network shows the connections between Ugt35C1 and potentially other metabolic and detoxification genes (Figure 6.3 B). Adh (alcohol dehydrogenase), Fdh (formate dehydrogenase), Est-6 (esterase-6) and betaGlu (beta-glucosidase) are all important interacting partners of Ugt35C1. Adh is an enzyme catalyst for the oxidation and reduction reactions of alcohols (de Miranda et al., 2022). Fdh is involved in formate metabolism (Genath et al., 2020). Their cooperation with ugt35c1 suggests the existence of a coordinated network working together to manage metabolites.

Est-6 is involved in the degradation of larger compounds, specifically the male pheromone cVA (carbon dioxide) in *Drosophila*. It cleaves or hydrolyses esters (Chertemps et al., 2012). BetaGlu, as a lysosomal hydrolase enzyme, is also involved in the degradation of complex compounds. It is responsible for the degradation of complex polysaccharides and glycosaminoglycans (Bar et al., 2018). The interaction of Ugt35C1, Est-6, and betaGlu implies a cooperative role in degrading various substances *Drosophila* may experience in nature. Finally, two uncharacterised genes, CG6910 and CG3841, possibly have a similar metabolic route with Ugt35C1. Ugt35C1 is in a complicated regulatory network. These interactions indicate the complex nature of Ugt35C1 in tubule maintenance.

Although *Ugt35C1*, *Ugt36E1*, and *Ugt50B3* are part of the same gene family, their expression patterns and differential responses to *CG6602* knockdown display functional specialisation. *Ugt35C1*'s high expression in the tubules may suggest a direct role in supporting tubule detoxification. At the same time, *Ugt50B3* is not expressed in the tubules, but significant upregulation indicates a compensatory mechanism in non-tubule tissues. *Ugt36E1*'s response suggests a supporting role, potentially involved in more metabolic functions. This differential regulation presents the complexity of detoxification pathways and the tissue-specific adaptations that allow *Drosophila* to maintain metabolic stability.

Furthermore, Figure 6.1 shows that the two *Cyp* family members on the list are *Cyp6d5* and *Cyp4e1*. *Cyp6d5* belongs to the same *Cyp6* subfamily as *Cyp6a8* and is generally associated with insect xenobiotic metabolism, indicating a role in detoxifying xenobiotics. Because they are members of the same subfamily, *Cyp6d5* and *Cyp6a8* may share overlapping functions, although their substrate specificities could differ. Another *Cyp* family gene in the up-regulated list that is not highly expressed in tubules is *Cyp4e1*. However, it belongs to the *Cyp4* family, which is distinct from *Cyp6*. Enzymes in the *Cyp4* family frequently participate in fatty acid metabolism and detoxification (Edson and Rettie, 2013), and they may target different substrates compared with *Cyp6* family enzymes..

In Figure 6.4 B, Cyp6a8 is known to have multiple interacting partners. These interactions show that Cyp6a8 works with a suite of other cytochrome P450 and detoxification genes that help the tubules' metabolism. For example, Cyp6w1 and Cyp4e2 have similar functions with Cyp6a8, as they are members of the cytochrome P450 family and may have a cooperative relationship. This collaboration could enhance the tubules' detoxification capacity, especially when CG6602 knockdown may compromise normal detoxification pathways. Cpr (Cytochrome P450 reductase) is another key partner of Cyp6a8 since a functional P450 needs this electron-transfer protein for its activity (Zhu *et al.*, 2012; lijima *et al.*, 2019). It interacts with Cyp6a8, indicating that P450 enzymes rely on electron transfer protein for detoxifying functions.

The other two interactions are between *CG14882* with Cyp6a8 and *Jheh1* with Cyp6a8, respectively. Although *CG14882* is an uncharacterised gene, the association with Cyp6a8 suggests that it may function to participate in detoxification pathways. Another hormone metabolism-related gene, *Jheh1*, is important for juvenile hormone degradation in *Drosophila* (Borovsky et al., 2022). The predicted association between the Jheh1 protein and Cyp6a8 suggests a possible link between hormone turnover and detoxification, but no mechanism is concluded from these data.

P450 and UGT are phase I and phase II metabolism enzymes. They play an important role in detoxification (Hu *et al.*, 2019; Miyauchi *et al.*, 2021) and may be collaborators in detoxification. Specifically, when a compound is absorbed in the body, it can be oxidised by Cyp enzymes to a reactive or intermediate compound. Subsequently, this product can be conjugated by UGTs after a glucuronic acid molecule is linked, which increases solubility and helps to excrete in the body. So, in *Drosophila*, this collaboration between CYP and UGT enzymes is important for protecting cells from external stress and ensuring effective clearance of potentially harmful substances.

Cyp6 and Cyp4 gene families contribute to the detoxification and metabolic roles of the Malpighian tubules in Drosophila. The up-regulation of Cyp6a8, Cyp6d5 and Cyp4e1 following CG6602 knockdown suggests that these genes may be involved in compensatory responses that help maintain detoxification capacity when tubule function is challenged.

Slc45-1 also showed up-regulation after the knockdown of CG6602. This could suggest a compensatory mechanism within the Malpighian tubules for maintaining homeostasis. As a member of the solute carrier family, the high expression level of Slc45-1 in tubules indicates that it may participate in the regulation of ion and solute transport. This response highlights the adaptability of the tubules in managing intracellular changes. By upregulating Slc45-1 expression, the insect may enhance the tubules' ability to modulate cellular

metabolism and excretion, suggesting a possible functional relationship between *CG6602* and *Slc45-1*. *CG6602* could therefore influence the transport processes supported by Slc45-1.

STRING interaction data for Slc45-1 shows associations with multiple other transporters and maintenance-related genes, indicating that Slc45-1 is part of an interconnected network (Figure 6.5 B). Some transporter proteins are connected to carbohydrate transport or the vesicle-mediated transport process. These gene interactions indicate that Slc45-1 may collaborate with these genes to facilitate a functionally coordinated role for ion, nutrient or metabolic waste transport in the tubules.

This suggests that up-regulated *Slc45-1* following *CG6602* knockdown could show activities to use other members of the transport network to stabilise tubule function. The tubules could also enhance their transport and excretory capacity by enhancing *Slc45-1* and activating its associations with genes in compensation for the disruption that the knockdown of *CG6602* causes. This interaction network indicates that transport pathways do not act independently; they are coordinated responses involving multiple transport proteins. Altogether, this upregulation of *Slc45-1* suggests adaptive regulation in response to the loss of *CG6602* function within the tubules. The activity of transporters or cooperation is likely to compensate for the loss of ionic and metabolic homeostasis to maintain the intracellular environment.

The last gene on the list is MFS12. Salt is a key interacting partner of MFS12, as salt is also highly expressed in tubules similar to MFS12. The salt gene is involved in Drosophila dietary salt stress response and is highly expressed in tubules. This interaction suggests a possible cooperation between these genes in maintaining tubule ion homeostasis when tubule function is compromised by CG6602 knockdown. This cooperation further suggests that MFS12 may be involved in helping salt in ion or small molecule transport to support salt regulation. Moreover, MFS12 appears to interact with some uncharacterised

genes, raising the possibility that this protein is connected to cellular transport or regulatory processes. Although the functions of these genes have yet to be confirmed, they have potential interactions with *MFS12*.

In the down-regulated gene list, the *mat* gene is particularly interesting because it shows a minor decrease among the down-regulated genes and is also the only highly expressed gene in the tubules among the characterised genes. Although research on the *mat* gene is very limited, we can still identify some of its characteristics from the available articles. Li *et al.* (2020) named *CG13905* materazzi (*mat*) because mutants succumbed to stressful conditions. The *mat* gene encodes the Mat protein, a lipid-binding protein that contributes to the clearance of lipids from the haemolymph and plays an important role in managing oxidative stress. Induction of *mat* expression during pathogenic infection, injury, or exposure to oxidative stress promotes lipid excretion via the Malpighian tubules and protects *Drosophila* against otherwise exacerbated tissue damage.

In the down-regulated transcriptomic data, I found that *mat* expression is about 43.5% of the control (Figure 6.8). The Mat protein is important for lipid clearance: it promotes removal of haemolymph lipids via the tubules and helps prevent oxidative stress and lipid peroxidation **in** haemocytes (Li *et al.*, 2020). When *mat* expression is reduced, the tubules clear lipids less efficiently, leading to lipid accumulation and cellular stress.

The knockdown of *CG6602* reduces the levels of the *mat*, supporting a possible role for *CG6602* in stress response pathways appearing within tubules. Therefore, the downregulation of mat expression in *CG6602* knockdown flies likely indicates disruption to cellular homeostasis, making tubules less efficient at re-processing reactive oxygen species and metabolising lipid-associated stress. This interaction suggests that *CG6602* may have a role in maintaining tubule function by regulating genes like *mat*. Collectively, the knockdown of *CG6602* leads to decreased mat levels, may help explain the downstream physiological

changes in flies lacking this enzyme, and suggests an intimate relationship between these factors related to regulated protective function within tubules.

A key interacting partner of *mat* is *Uro* (Figure 6.9). Urate is important in maintaining oxidative balance in the Malpighian tubules of *Drosophila* melanogaster (Hilliker *et al.*, 1992). As a product of purine metabolism, it acts as a potent antioxidant to protect tubule cells from oxidative damage (Kamleh *et al.*, 2008; Bratty *et al.*, 2011). The importance of urate is shown in *rosy* (*ry*) mutants, which lack xanthine dehydrogenase and cannot synthesise urate, rendering them hypersensitive to oxidative stressors. These details will be described in the next metabolomics chapter.

More than 30 genes were identified in this analysis, but the discussion here focused on those with strong expression in the tubules, where their contribution is most likely to matter. These genes are candidates for follow-up work, and reverse genetic approaches such as RNAi knockdowns could be used to test their specific roles. The changes in gene expression also match the secretion phenotypes described in the previous chapter. This links the molecular responses after CG6602 knockdown with the functional changes seen in tubule fluid regulation. These shifts are not isolated outcomes but part of a broader adjustment of the tubule to maintain homeostasis under stress. From these data, CG6602 appears to be involved in stress-related and transport pathways, influencing both metabolic and excretory functions of the tubule. Future work can test the role of individual candidate genes in these processes and give a clearer picture of how CG6602 works with other genes to maintain tubule physiology and homeostasis.

Chapter 7 Metabolomics Analysis in CG6602

7.1 summary

This chapter presents a metabolomics analysis of the novel *Drosophila* Malpighian tubule gene CG6602. Although the function of CG6602 is unknown, evidence from Chapter 6 points to a role in stress responses. Here, knockdown of CG6602 produces clear shifts across multiple pathways, notably glutathione metabolism, D-amino acid metabolism, and nitrogen and polyamine metabolism. Metabolites including L-ornithine, L-glutamate, L-arginine, L-glutamine, and Lmethionine are enriched in the CG6602 knockdown tubules, consistent with enhanced antioxidant defence and altered nitrogen handling. Taken together, these data support a model in which CG6602 helps regulate oxidative stress protection and nitrogen homeostasis in the tubule. Importantly, these metabolite shifts occur without broad or consistent changes in the enzymeencoding genes detected in the CG6602 knockdown transcriptome (see Chapter 6). This suggests that CG6602 affects pathway activity indirectly, for example through regulation after transcription, through changes in enzyme activity, or through changes in transport, rather than by directly changing the transcription of metabolic enzymes.

7.2 Introduction

Metabolomics is a highly quantitative analytical technique that analyses the small molecules present in a biological system (Muthubharathi *et al.*, 2021). The metabolic profile of cells, tissue or organisms in specific conditions is investigated (Manickam *et al.*, 2023). Unlike transcriptomics, metabolomics targets the end products of those genes and metabolic pathways (Yan *et al.*, 2024). This enables researchers to measure small molecules or metabolites, such as amino acids, sugars, lipids and nucleotides, allowing information collection about cellular processes, physiological states and disease mechanisms (Tounta *et al.*, 2021). Each metabolite can be a functional biomarker. It responds to alterations in enzyme function, gene expression, diet, environment and circadian rhythms (Dyar *et al.*, 2018; Qiu *et al.*, 2023).

Modern metabolomic studies use high-throughput techniques, nuclear magnetic resonance (NMR), gas chromatography-mass spectrometry (GC-MS) and liquid chromatography-mass spectrometry (LC-MS) (Emwas *et al.*, 2019). These have advantages for certain classes of metabolites that can be separated based on their size, polarity, and concentration. NMR is a non-destructive technique (Viola *et al.*, 2006). GC-MS and LC-MS enable sensitive measurement of up to hundreds or thousands of metabolites/parametric signals from single-run detection (Tautenhahn *et al.*, 2008). They can be directed to target specific known metabolites or used in untargeted metabolic profiling studies surveying the total metabolome of an organism.

Similar to the reverse approach in the transcriptomics technique, RNAi knocks down the gene to decrease its expression. The main objective would be to identify the metabolites in flies with knockdown of *CG6602* and compare them with the wild type. Using this approach, metabolic change or pathway disruption is observed as caused by the knockdown of *CG6602* (Barreto *et al.*, 2015; Porokhin *et al.*, 2021). Using metabolomic data associated with *CG6602*, the results indicate which metabolites or pathways influenced by the gene of interest can be identified (Maan *et al.*, 2023).

In the case of *CG6602*, metabolomics could explain its involvement in metabolic processes within specific tissues, such as the Malpighian tubules. Targeted metabolome analysis of *CG6602* knockdown flies may indicate a metabolic signature, such as altered energy metabolism, amino acid or lipid pathway, that suggests the cellular role played by the gene. Metabolomics also enable us to explore whether *CG6602* knockdown leads to possible compensatory mechanisms, which may be activated in the organism and are not possible with traditional functional genomics approaches.

Integrating metabolomic changes with reverse genetics contributes to building a metabolic map of novel genes, such as *CG6602*, to the phenotype in *Drosophila*. This gives functional relevance and explores the functional role of the gene within the context of metabolic regulation and homeostasis, understanding the metabolites of novel genes. The following section presents detailed metabolic changes from metabolomics analyses, showing the specific pathways and biochemical responses of *CG6602* in tubule tissue.

7.3 Results

Metabolomic profiling was performed using LC-MS on tubule extracts from CG6602 knockdown and control flies, followed by pathway enrichment analysis to identify altered metabolic processes. Metabolomics analysis of Drosophila tubules targeting the novel gene CG6602 revealed several metabolic pathways: those that support the tubules' fundamental functions and those that are adaptive and important for stress response. As Malpighian tubules are involved in excretion, osmoregulation, and detoxification, analysis into these pathways can thus explore tubule function and the effect of CG6602, particularly in stress response. Figure 7.1 shows that pathway enrichment methods identified metabolic pathways significantly overrepresented in the data. Three of these were selected for further study. It summarises pathways to show metabolites identified or fragments linked with CG6602 in tubules and focuses on those related to adaptation during stress.

Figure 7.1 provides a bar representation of the metabolic pathways with the number of metabolites identified in *Drosophila* tubules, as revealed by the metabolomics analysis of *CG6602*. The pathways are shown as vertical bars, and the horizontal lines show the number of identified metabolites in each pathway. The bars represent pathway coverage. The extended bar means more metabolite presence in that pathway, suggesting metabolic complexity.

Purine metabolism, D-amino acid metabolism, and glutathione metabolism display a higher number of metabolites, as shown in Figure 7.1, which is marked by red circles. These pathways were selected not only because of the number of metabolites detected, but also because of their known relevance to stress response and tubule physiology. For example, glutathione and purine metabolism are closely related to cell stress response mechanisms (Li *et al.*, 2023; Perl *et al.*, 2011; Zeng *et al.*, 2022; Southey *et al.*, 2023). Moreover, glycerophospholipid metabolism, cysteine and methionine metabolism, pyrimidine metabolism, and starch and sucrose metabolism also show a high metabolite count in Figure 7.1, but their KEGG maps are listed in the appendices.

Number of Metabolites in a Pathway

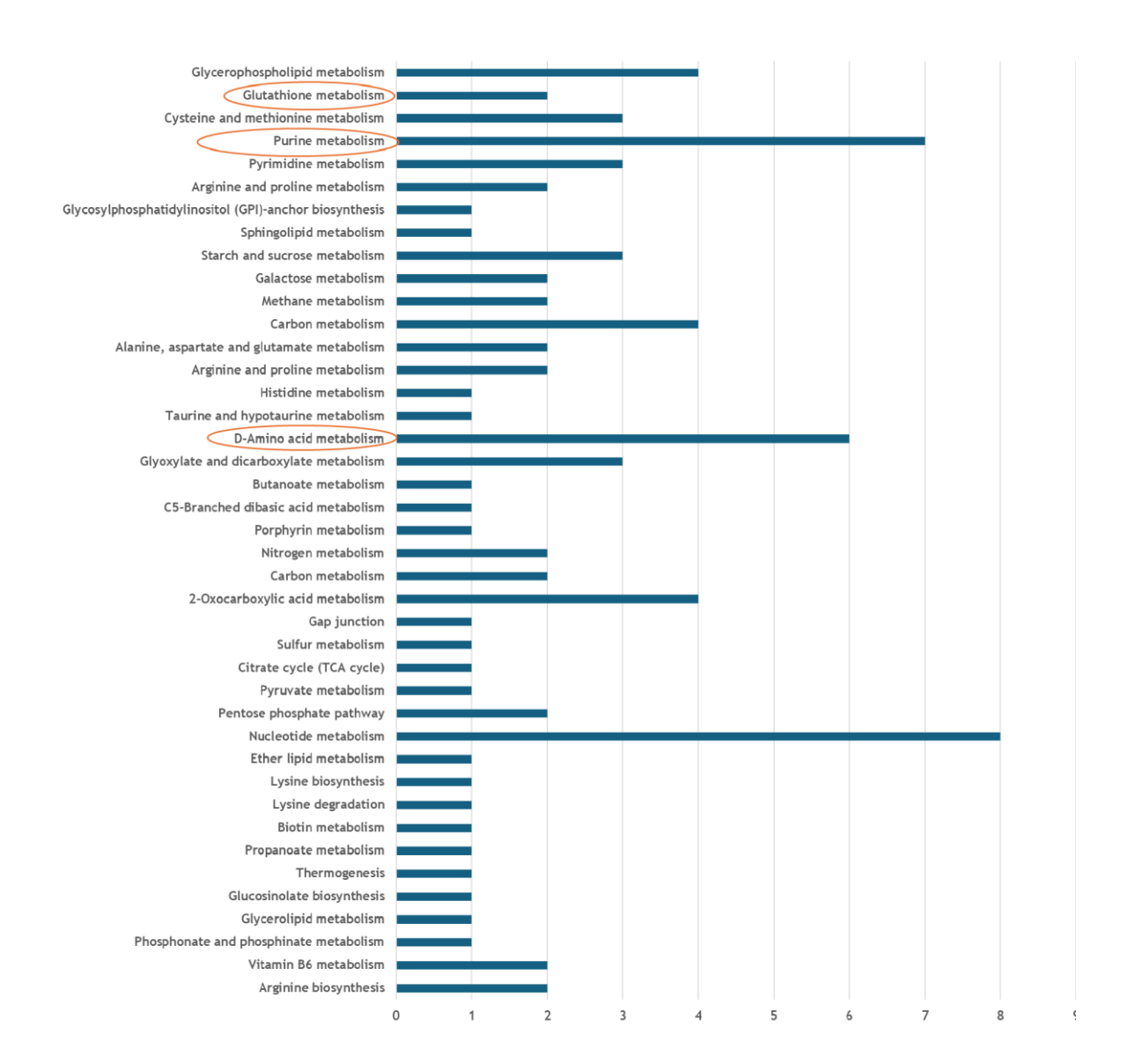


Figure 7.1 *Drosophila* tubules metabolomics analysis of *CG6602*. Bar chart showing the number of significantly altered metabolites in *CG6602* knockdown tubules compared with controls, grouped by KEGG metabolic pathways. The horizontal axis indicates the number of metabolites identified in each pathway, and the vertical axis lists the pathways. Longer bars represent pathways with higher metabolite counts, suggesting greater metabolic involvement. Key stress-related pathways, including glutathione metabolism, purine metabolism, D-amino acid metabolism, and cysteine and methionine metabolism, are highlighted in the figure.

7.3.1 Glutathione metabolism

One of the significantly changed pathways in Figure 7.1 is glutathione metabolism. Glutathione is a key molecule in detoxification and antioxidant defence (Pizzorno, 2014). A KEGG map of glutathione metabolism in *Drosophila* is shown in Figure 7.2, with pathways highlighted in green to indicate the presence of detected metabolites. Red circles mark two metabolites, L-glutamate and L-ornithine, which were selected from the metabolomic dataset as the peaks showing the highest log₂ fold change in tubules between *CG6602* knockdown and control. Only metabolites that were confidently identified or supported by fragment data were included. This map illustrates the role of glutathione metabolism and its connections with other pathways related to stress adaptation, including cysteine, methionine, taurine, and proline metabolism.

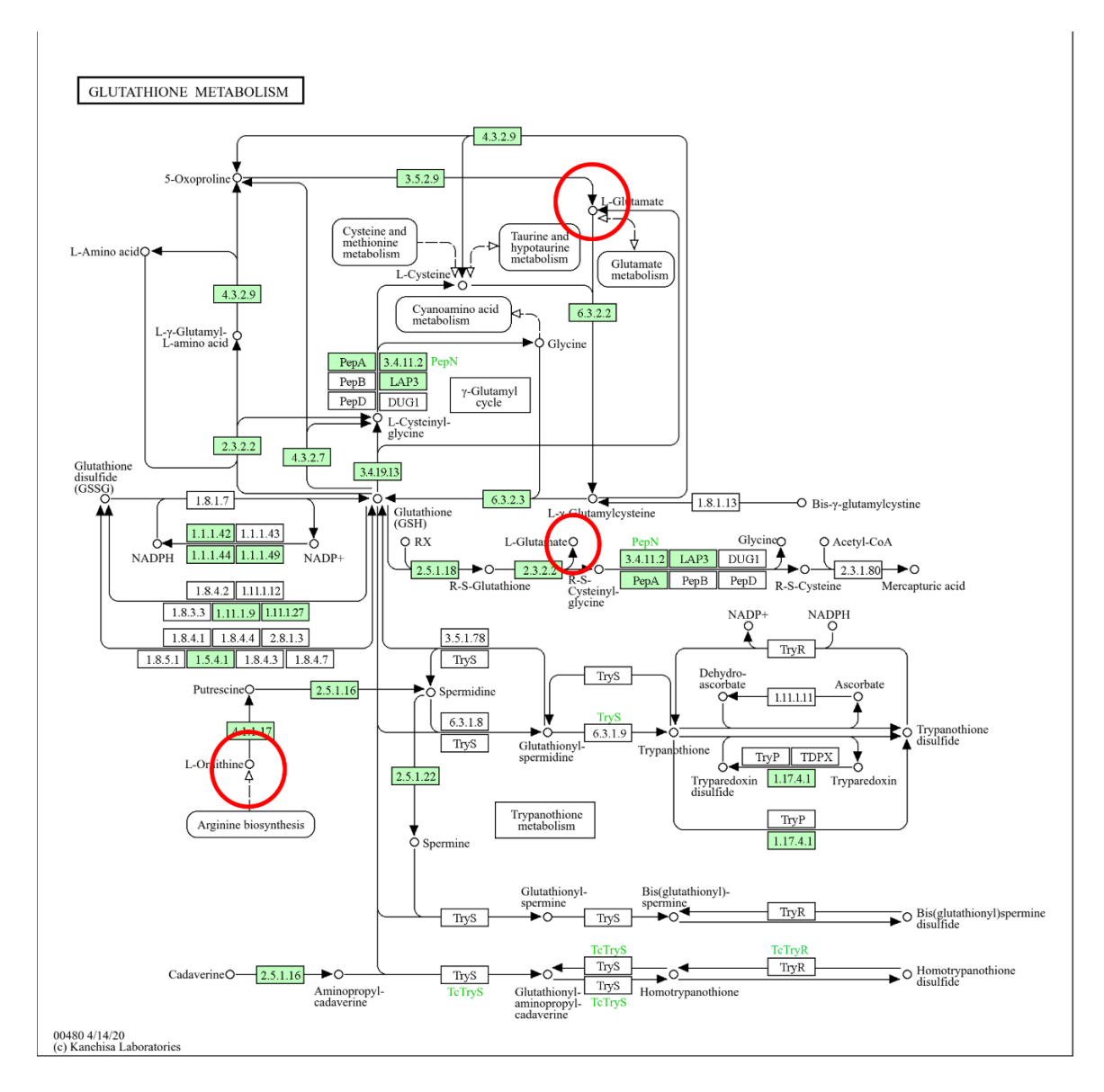
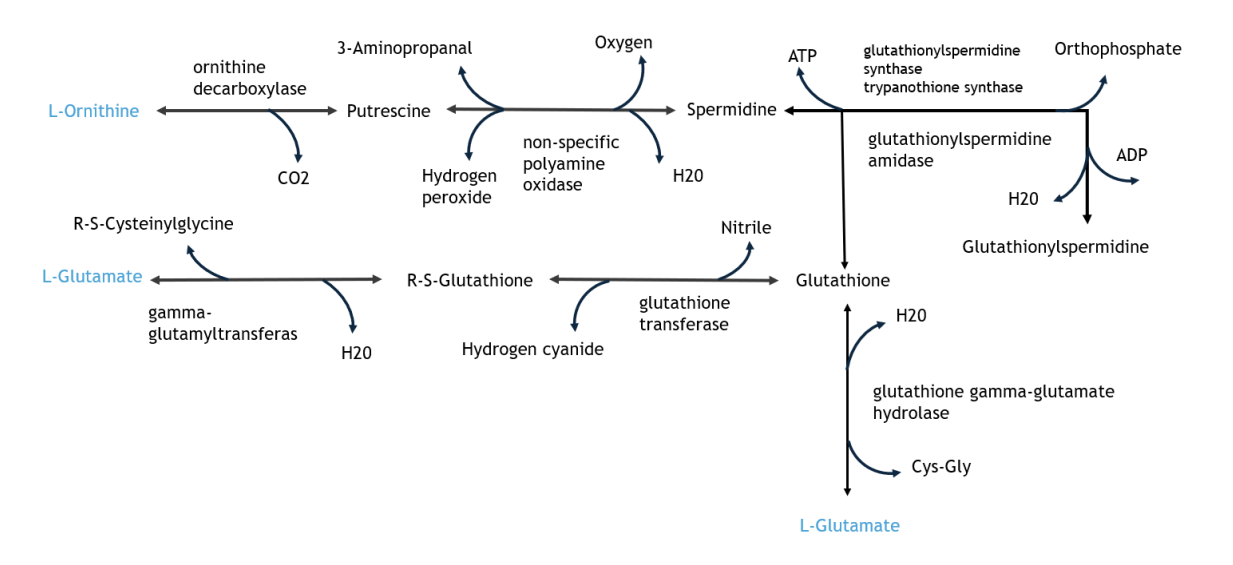


Figure 7.2 Changes in glutathione metabolism in *Drosophila* tubules caused by the knockdown of *CG6602*. KEGG map for *Drosophila melanogaster* glutathione metabolism. Green boxes represent metabolites identified in *Drosophila* by LC-MS analysis. Red circles highlight L-glutamate and L-ornithine, which showed the highest log₂ fold change between *CG6602* knockdown and control (Kanehisa *et al.*, 2025).

Figure 7.3 shows a biochemical pathway constructed based on the reactions associated with L-glutamate and L-ornithine. Metabolites highlighted in blue, including L-ornithine and L-glutamate, show more levels in *CG6602*, indicating a potential increase in flux through these pathways. The figure also includes a table summarising enzyme information for glutathione gamma-glutamate hydrolase, with several key enzymes identified in tubule tissues. However, because ornithine decarboxylase is related to over 100 genes, it is not specified in the table, indicating the complexity of this enzyme's role across multiple reactions and pathways.



glutathione gamma-glutamate hydrolase				
Gene	Found in Tubule	Differential expressed in		
		CG6602		
CG17636	Yes	No		
Ggt-1	Yes	No		
CG1492	No	No		
CG4829	Yes	No		
CG4752	Yes	No		
gamma-glutamyltransferas				
No genes identified in FlyBase with this name				

Figure 7.3 Biochemical pathway of glutathione metabolism in *Drosophila* following knockdown of *CG6602*. Blue labels mark two metabolites, L glutamate and L ornithine, which showed the largest log₂ fold change in glutathione metabolism between *CG6602* knockdown and control. These were included only if identified or supported by fragment data. The table summarises the enzymes shown and the corresponding *Drosophila* genes, indicating presence in tubules and differential expression in the *CG6602* knockdown.

7.3.2 Amino acid metabolism

The KEGG map of *Drosophila* D-amino acid metabolism is shown in Figure 7.4. L-glutamine, L-arginine, L-methionine, L-glutamate, and ornithine, indicated with red circles, are five metabolites enriched in *CG6602* compared with the control (RNAi line). This metabolite map links identified metabolites to other pathways such as arginine and proline metabolism, methionine metabolism, and citrate cycle.

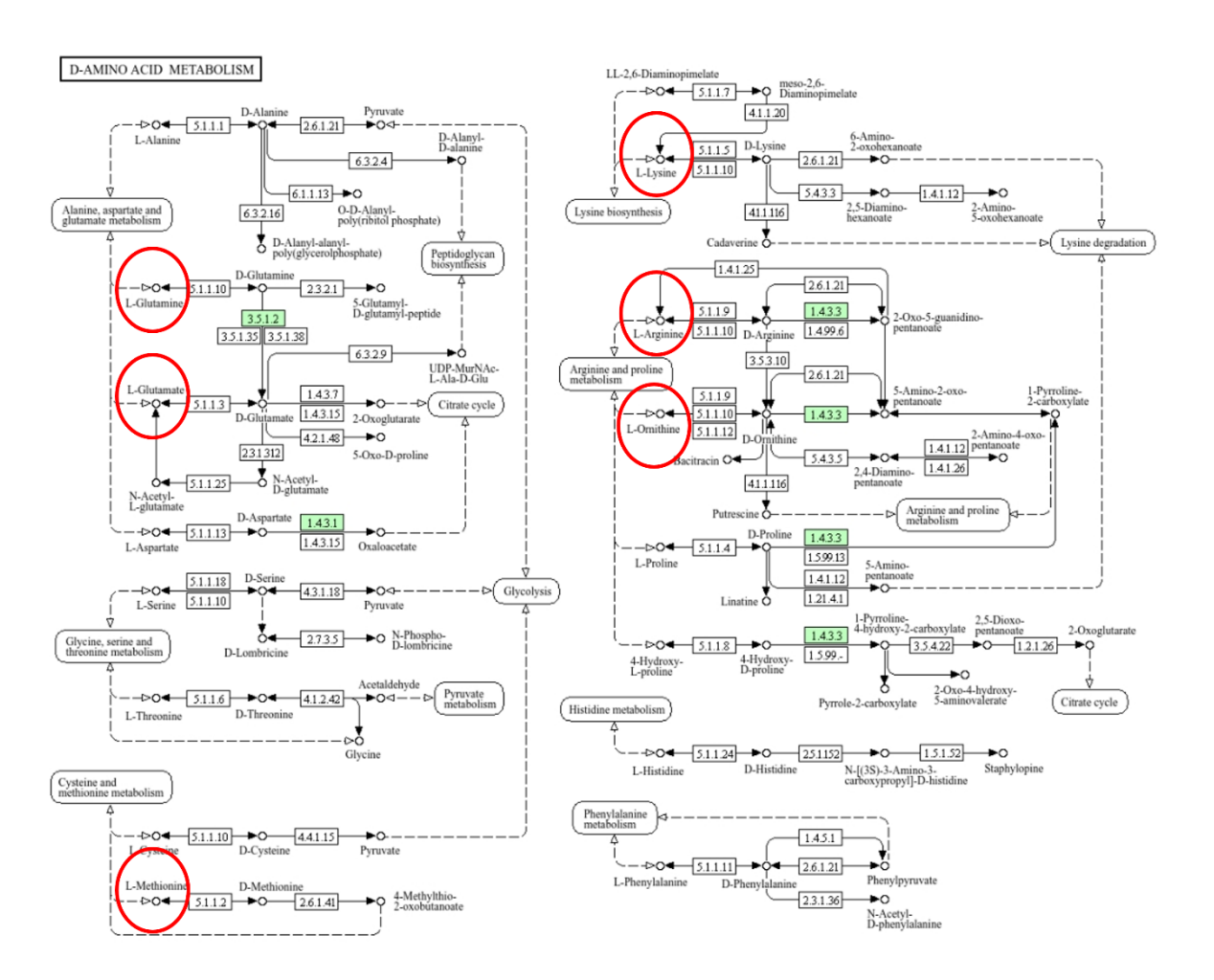
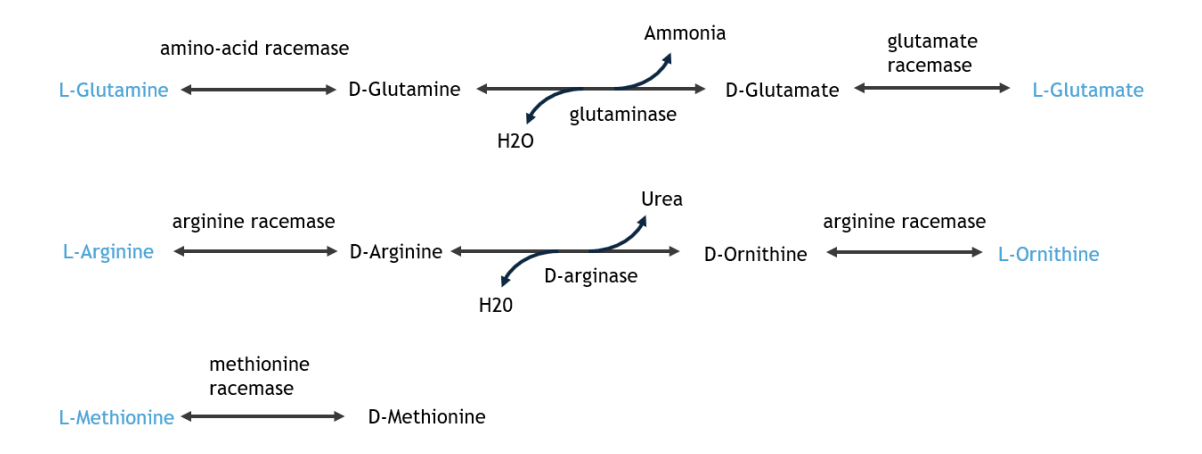


Figure 7.4 Changes in D-amino acid metabolism in the tubules caused by the knockdown of *CG6602*. KEGG map of *Drosophila melanogaster* D-amino acid metabolism; green block represents metabolites identified in *Drosophila* by the LC-MS analysis. Red circles show metabolite changes in D-amino acid metabolism caused by the knockdown of *CG6602* (Kanehisa *et al.*, 2025).

Figure 7.5 expands on D amino acid metabolism by listing the biochemical reactions involving the identified metabolites and their enzymes. The metabolites shown in blue (L glutamate, L ornithine, L arginine, L glutamine and L methionine) are enriched in *CG6602* knockdown. These were chosen from the metabolomic dataset because, within this pathway, they showed the highest log₂ fold change in tubules between *CG6602* knockdown and control, and only metabolites with confident identification or fragment support were included. The table in Figure 7.5 summarises the enzymes for these reactions and the *Drosophila* genes that encode them, indicating whether the genes are found in the tubules and whether they are differentially expressed in the *CG6602* knockdown.



amino-acid racemase		D-arginase			
Gene	Found in Tubule	Differential expressed in CG6602	Gene	Found in Tubule	Differential expressed in CG6602
Srr	Yes	No	Arg	Yes	No
	glutaminase		CG12516	No	No
Gene	Found in Tubule	Differential expressed in CG6602	CG11634	No	No
Gls	Yes	Yes	CG2336	No	No
glissade	No	No	CG31076	Yes	No
CG8526	No	No	CG6661	No	No
CG6428	Yes	No	P5CDh2	No	No
Nadsyn	Yes	No	CG8665	Yes	No
Gfat2	Yes	No	CG31274	No	No
m	ethionine racema	ase	Aldh7A1	Yes	No
Gene	Found in Tubule	Differential expressed in CG6602	MESK4	No	No
Srr	Yes	No	CG15717	Yes	No
			CG31075	Yes	No
			P5cr-2	Yes	No
			P5CDh1	Yes	No
			Ssadh	Yes	No
			Aldh-III	Yes	No
			CG17896	Yes	No
			P5cr	Yes	No
			Oat	Yes	No
			Aldh	Yes	No
			CG11241	Yes	No
			CG8745	Yes	No
			Gabat	Yes	No

Figure 7.5 Biochemical reactions of identified metabolites in D amino acid metabolism following knockdown of CG6602. Blue labels indicate five metabolites (L glutamine, L arginine, L methionine, L glutamate and L ornithine) that showed the highest \log_2 fold change between CG6602 knockdown and control and were included only if identified or supported by fragment data. The table summarises the associated enzymes and the corresponding Drosophila genes, noting their presence in tubules and whether they are differentially expressed in the CG6602 knockdown.

7.3.3 Purine metabolism

A KEGG map of purine metabolism is shown in Figure 7.6. Green boxes indicate pathways present in *Drosophila*. Red circles around seven metabolites: D-ribose 5-phosphate, L-glutamate, adenosine, isoxanthine, AMP and GMP show a higher metabolite level in CG6602 knockdown than controls. These important metabolites contribute to nucleotide biosynthesis, energy transfer, and cellular signalling.

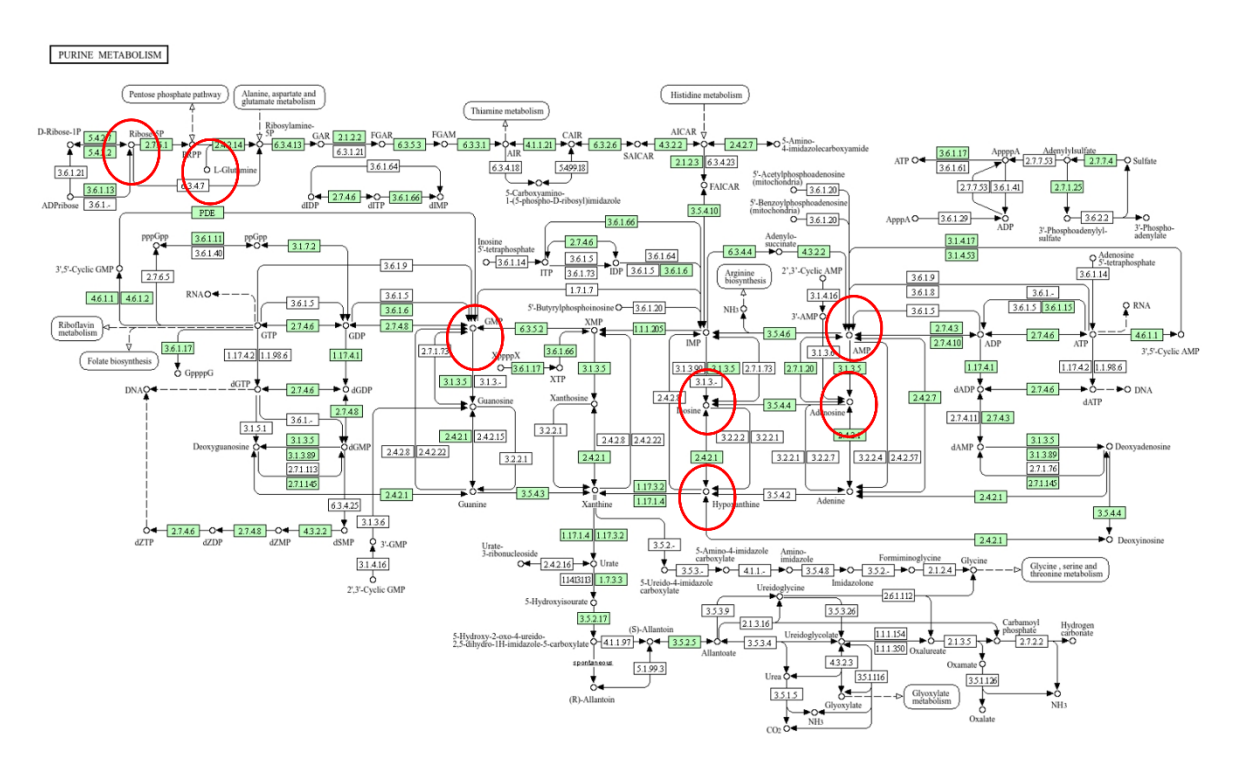


Figure 7.6 Changes in purine metabolism in the tubules caused by the knockdown of *CG6602*. KEGG map of *Drosophila melanogaster* purine metabolism; green block represents metabolites identified in *Drosophila* by the LC-MS analysis. Red circles show metabolites increased in purine metabolism caused by the knockdown of *CG6602*.

The key metabolites with relevant reactions are shown in simplified diagrams, including only metabolites and enzymes (Figure 7.7). Blue-highlighted (D-ribose 5-phosphate, L-glutamate, Adenosine, Inosine, AMP, GMP, and Hypoxanthine) metabolites are enriched in *CG6602*. Although the metabolite xanthine is not marked in blue, its related metabolite hypoxanthine is found in higher amounts in *CG6602* (marked in blue). Hypoxanthine is converted to xanthine and then on to urate, and the enzyme noticed that it is rosy in *Drosophila*. The rosy is an antioxidant that converts xanthine into urate. It is also important for tubules as its product urates (Dow and Romero, 2010).

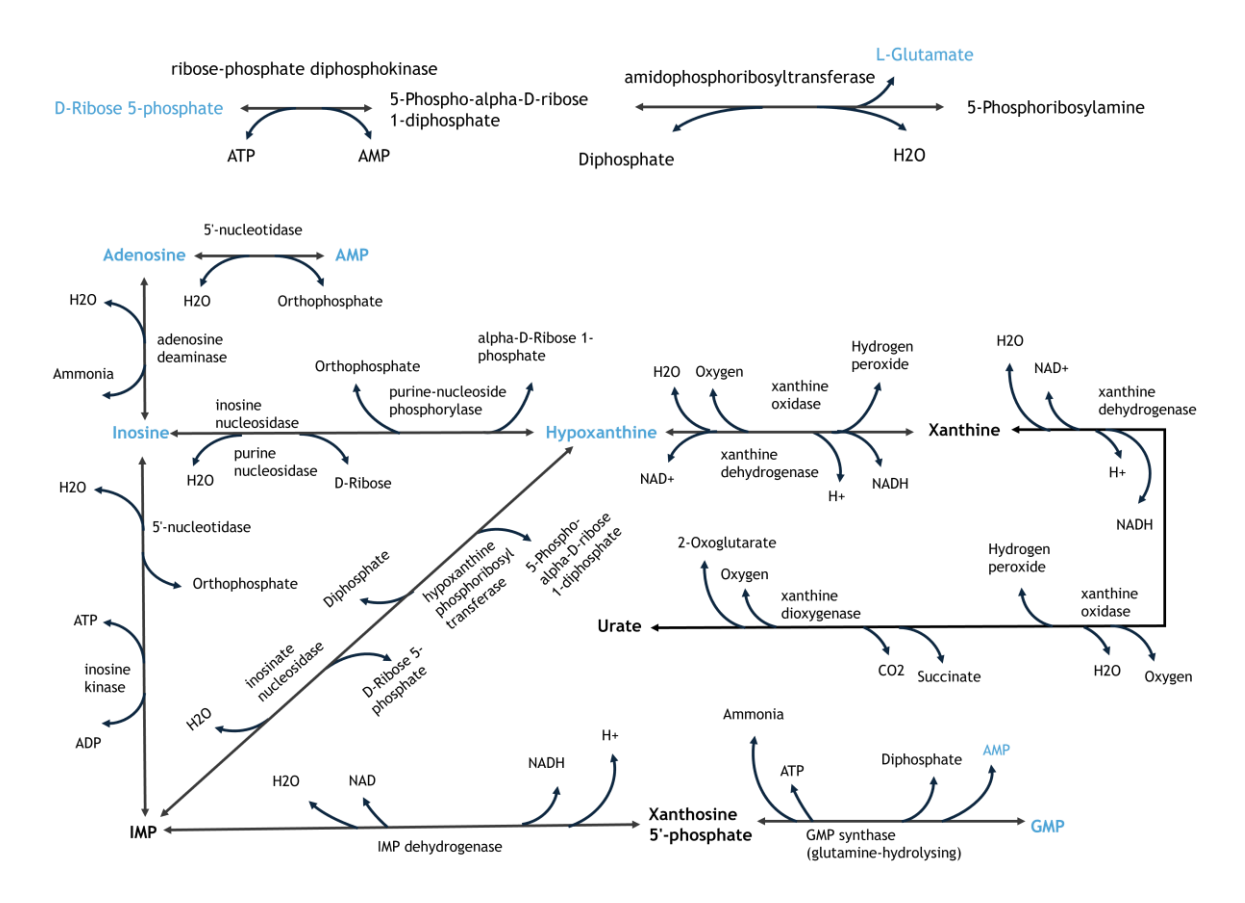


Figure 7.7 Biochemical reactions of identified metabolites in purine metabolism. This schematic diagram illustrates the purine metabolism pathway in *Drosophila* melanogaster, focusing on the interconversion of key metabolites. These eight metabolites in blue are found more in *CG6602* than in the control (RNAi line). Arrows indicate the direction of metabolic reactions, with reversible reactions marked where applicable.

Table of genes related to enzymes participating in purine metabolism in *Drosophila*, showing tubule expression and differential expressions in *CG6602* (Table 7.8). Each enzyme category is listed along with its related genes. No genes are shown in the differential expressed column in *CG6602*. This was discovered by analysing the padj values of each gene in the metabolomics data.

ribose-phosphate diphosphokinase			purine-nucleoside phosphorylase			
Gene	Found in Tubule	Differential expressed in CG6602	Gene	Found in Tubule	Differential expressed in CG6602	
Prop	Yes	No	CG18128	No	No	
amidopl	hosphoribosylti	ansferase	CG16758	No	No	
amidophosphoribosyltransferase		CG31115	No	No		
	Found in Tubule	Differential	Mtap	Yes	No	
Gene		expressed in CG6602	IMP dehydrogenase			
Prat2	No	No			Differential	
Prat	Yes	No	Gene	Found in Tubule	expressed in	
	5'-nucleotidas	e			CG6602	
		Differential	Ldh	Yes	No	
Gene	Found in Tubule	expressed in	ras	Yes	No	
Cene	Tourid III Tubule	CG6602		GMP synthase		
cN-IIIB	Yes	No			Differential	
Nt5c	Yes	No	Gene	Found in Tubule	expressed in	
Nt5a	Yes	No			CG6602	
Nt5b	Yes	No	Nos	No	No	
NT5E-2	Yes	No	bur	Yes	No	
veil	Yes	No	Nadsyn	Yes	No	
CG30103	No	No	cGlr1	No	No	
CG42249	Yes	No	Sting	No	No	
CG11883	Yes	No	cGlr2	Yes	No	
CG7789			CG7194	Yes	No	
	Yes	No	CG4766	No	No	
Acph-1 CG15743	Yes	No	CG15865	No	No	
CG15/43	Yes	No	mab-21	No	No	
ad	lenosine deami	nase	Rel	Yes	No	
		Differential	IKKB	Yes	No	
Gene	Found in Tubule	expressed in	IKKε	Yes	No	
		CG6602	xanthine oxidase			
Ada	Yes	No			Differential	
Adar	Yes	No	Gene	Found in Tubule	expressed in	
Adat1	Yes	No	Jane	Tourid in Tubule	CG6602	
Adgf-E	No	No	AOX1	Yes	No	
Adgf-B	No	No	AOX2	No	No	
Adgf-A	Yes	No	AOX3	Yes	No	
Adgf-D	No	No	AOX4	No	No	
Adgf-C	Yes	No	shop	Yes	No	
Adgf-A2	No	No		Yes	No	
AMPdeam	Yes	No	Mocs1	Yes	No	
CG10927	No	No	mal	Yes	No	
CG5292	Yes	No	cin	Yes	No	
Sas10	No	No	Mocs2B	Yes	No	
inosine kinase			Mocs3 (CG13090		No	
Gene	Found in Tubule	Differential expressed in CG6602				
SNF4Ay	No	No	1			

Table 7.8 Table of known genes for each enzyme. The table summarises the genes associated with key enzymes in purine metabolism in *Drosophila melanogaster*. They are organised into different categories: Ribose-Phosphate Diphosphokinase, Amidophosphoribosyltransferase, 5'-nucleotidase, Adenosine Deaminase, Inosine Kinase, Purine-Nucleoside Phosphorylase, IMP Dehydrogenase, GMP Synthase, and Xanthine Oxidase. Each enzyme is listed with three columns indicating the gene name, found in the tubule, and differentially expressed in CG6602. Found in Tubule: whether each gene is expressed in the tubules (Yes/No). Differentially Expressed in CG6602: Indicates if the gene shows differential expression in CG6602 or wild type (Yes/No). The red arrow indicates the rosy gene.

7.4 Discussion

Previous studies suggested that the three pathways shown in Figure 7.1 (Purine metabolism, D-amino acid metabolism, and glutathione metabolism) relate to tubule metabolic adjustment to stress. The number of metabolites observed within each pathway also suggests a function in cellular stress response and keeping the tubules stable during stress conditions. Thus, each of these pathways has an important but different role.

Glutathione metabolism plays an important role in antioxidant defence in the tubule (Enayati *et al.*, 2005). In our data, the metabolites that increased within the glutathione pathway after *CG6602* knockdown were L-glutamate and L-ornithine. This pattern does not necessarily mean that glutathione synthesis capacity is higher. Two possible explanations can be considered. The first is a compensatory change: when *CG6602* is reduced, oxidative stress rises, and the tubule may respond by raising levels of building blocks or increasing activity in related pathways to help maintain redox balance. The second is that one step in the pathway is less efficient, leading to accumulation of upstream metabolites while downstream products remain lower, a pattern consistent with the role of glutathione-s-transferases in detoxification (Sheehan *et al.*, 2001). In support of either explanation, no broad transcriptional changes were detected in the genes encoding glutathione enzymes in Chapter 6, suggesting that regulation is more likely to occur after transcription, through enzyme activity or transport processes, rather than through direct changes in transcription.

The enrichment of L-glutamate is important because it is the precursor of glutathione, one of the main antioxidants against reactive oxygen species and for maintaining redox balance (Wu et al., 2004). Higher L-glutamate in CG6602 knockdown tubules may therefore help support glutathione production and allow the tubules to cope with oxidative stress. This is particularly relevant because tubules are under constant oxidative challenge as they process and remove waste. The increase in L-ornithine suggests a shift towards polyamine metabolism, which can stabilise intracellular structures and add further protection against oxidative stress. These findings may reflect a compensatory

response to stress or an imbalance that causes metabolite build-up, both pointing to a role for *CG6602* in maintaining tubule function under stress.

L-glutamate enrichment also affects glutathione metabolism and antioxidant defence (Wu et al., 2004). L-glutamate is the precursor of glutathione, an important antioxidant against reactive oxygen species and for maintaining cellular redox homeostasis. Under CG6602 knockdown conditions, higher L-glutamate may reflect a general adjustment to support glutathione production and help the tubules cope with oxidative stress. This would be significant for the tubules, which are constantly exposed to oxidative challenge because of their role in processing and detoxifying waste.

Since *CG6602* knockdown tubules also show enrichment of L ornithine together with L glutamate, it is reasonable to propose that *CG6602* contributes to the control of glutathione related metabolism so that essential metabolites are maintained for stress resistance. The pattern suggests that loss of *CG6602* may trigger changes in one or more steps of the pathway, with a compensatory response that supports antioxidant defence. These adjustments would help preserve tubule function when *CG6602* is reduced.

A major change reported by PiMP (Polyomics Integrated Metabolomics Pipeline), the LC-MS data processing pipeline used in this study, was enrichment of the D-amino acid metabolism pathway. This call was based on changes in the L-amino acids circled in Figure 7.4 and summarised in Figure 7.5. Because D-amino acids are rarely found in insects, it is unlikely that this result reflects genuine changes in D-amino acid metabolism. Instead, it is more likely that PiMP misannotated this pathway, with the signal driven by changes in L-amino acids. The literature on D-amino acids in *Drosophila* is very limited: an early study reported that larvae can substitute some essential amino acids with their D-isomers for growth (Geer, 1966), and a more recent study showed that D-amino acids can affect sleep and activity (Nakagawa *et al.*, 2021). Although these examples indicate that D-amino acids can have biological roles, they are exceptional cases. In the

present context, the simplest interpretation is that the pathway assignment arises from database overlap, and that *CG6602* knockdown altered levels of Lamino acids rather than D-amino acids.

Purine metabolism in *Drosophila* primarily presents to recycle purine bases, maintaining energy by recovering bases for re-use (Petitgas *et al.*, 2024). It is an essential step of cellular metabolism. The knockdown of *CG6602* has resulted in the enrichment of several key metabolites, suggesting that *CG6602* may have a potential role in purine metabolism within the tubules. By modulating purine metabolism, adenine nucleotide biosynthesis and salvage pathways, *CG6602* may contribute to cellular homeostasis, enabling the tubules to handle metabolic demands and stress efficiently.

The enrichment of D-Ribose 5-phosphate and L-Glutamate after *CG6602* knockdown also indicates a compensatory metabolic adjustment in the tubules to deal with oxidative stress. D-ribose 5-phosphate is an important pentose phosphate pathway (PPP) intermediate and contributes to NADPH production. As mentioned by Wang *et al.* (2011), increased PPP activity contributes to antioxidant defences. The enrichment of D-Ribose 5-phosphate could suggest an adaptive response to oxidative stress in tubules after *CG6602* knockdown. Similarly, the enrichment of L-glutamate -a central metabolite for amino acid metabolism and intracellular signalling—may support metabolic and stress-adaptive functions. Moreover, L-glutamate is an obligatory inhibitory neurotransmitter in *Drosophila* (Liu and Wilson, 2013); its enrichment may also affect the stress response at the cellular level.

Enrichment of adenosine, AMP, and GMP has many functions in *CG6602*. They play a specific role in the purine metabolism pathway related to *Drosophila's* energy regulation, stress response, and homeostasis (Marsac *et al.*, 2019). In particular, adenosine acts as an anti-stress molecule when metabolism is not balanced and accumulates upon oxidative stress. In *Drosophila*, adenosine

contributes to the immune response during periods of oxidative stress (Zemanová *et al.*, 2016).

The hypoxanthine plays an important role in *Drosophila's* response to oxidative stress via its biochemical reaction products (Figure 7.7). In this pathway, hypoxanthine is converted to xanthine and then urate by the enzyme xanthine dehydrogenase. The rosy (ry) is a known gene for the enzyme, and urate is a strong antioxidant in *Drosophila* (Hilliker *et al.*, 1992; Dow *et al.*, 2010). This activity protects tissues from oxidative damage.

Urate acts as an oxidative defence in *Drosophila*; previous studies (Hilliker et al., 1992) on rosy mutants generate no urate because of the absence of xanthine dehydrogenase. These mutants are considerably more sensitive to oxygen stress than wild-type ones because they no longer metabolise ROS. The reactions to the urate deficiency reveal the critical protective role of urate against oxidative damage in vivo and highlight the contribution of the hypoxanthine pathway to cellular homeostasis.

Urate is especially important to *Drosophila* since the tubules are central to excretion, osmoregulation and detoxification. Our lab has shown that rosy, urate oxidase, is expressed exclusively in tubules (Kamleh et al., 2008; Bratty et al., 2011). This suggests that tubules play a central role in managing urate levels in the body, emphasising their importance more than other tissues. These processes produce numerous oxidative products, making the tubules significantly affected by oxidative stress. By accumulating urate, the tubules store urate. This localised antioxidant activity is critical because it contributes to tubule survival in reactions as oxidative stress peaks.

These data indicate that CG6602 knockdown affects the hypoxanthine urate pathway and changes the oxidative balance in the tubules. In our results, hypoxanthine related metabolites were enriched in the knockdown condition, which could be part of a compensatory adjustment helping the tubules to cope

with oxidative stress. This also points to a possible normal role for CG6602, since under wild type conditions it may help to keep metabolite levels balanced, preventing excess hypoxanthine and supporting conversion to urate. In this way, CG6602 is likely to contribute to routine oxidative defence in the tubules, and its loss leads to secondary changes that try to restore stability. These findings suggest that CG6602 plays a part in *Drosophila*'s resistance to oxidative stress.

In conclusion, the enrichment of L ornithine and L glutamate following CG6602 knockdown may suggest the importance of CG6602 in supporting metabolic balance and stress management in the tubules. CG6602 seems to help the tubules cope with oxidative stress and maintain homeostasis by influencing pathways involved in glutathione metabolism and other related processes. The current data do not demonstrate direct regulation of these pathways by CG6602 but rather indicate that loss of CG6602 leads to increased metabolite levels. consistent with a negative regulatory role under normal conditions. Increased L glutamate reflects an adaptable transition to maintain redox balance and stress management. In contrast, higher adenosine, AMP, and GMP show the contribution of purine metabolism to energy homeostasis and cellular signalling. The enrichment of hypoxanthine related metabolites and their link to urate production suggest that CG6602 may also affect the modulation of oxidative stress, with urate acting as an antioxidant within the tubules. CG6602 knockdown appears to be offset by increases in metabolite levels that support stress tolerance, nitrogen management, and the cellular environment. This may indicate that CG6602 normally acts to limit these pathways, and that its reduction triggers compensatory responses to restore homeostasis. Future studies could directly test whether CG6602 plays a negative regulatory role in these metabolic pathways and assess how this contributes to antioxidant control and resistance to oxidative stress in Drosophila tubules.

Chapter 8 Conclusion and Future Work

8.1 Summary

This chapter summarises the results described in each chapter, collecting the key contributions this thesis makes. This includes a summary of results across the several experimental chapters, an overview of challenges faced during the research process and a discussion on potential future directions. This thesis, titled "Investigating the Role of Gap Junction Protein and Novel Genes in Renal Function," aims to understand the functions of several proteins in the gap junction, a bioamine receptor ($Oct\alpha 2R$), and the novel gene CG6602, which I found highly expressed in tubules. Further, this study validates the use of Drosophila melanogaster combined with standard reverse genetics methods for tubule gene studies. By summarising experimental results and analysing the data, this study complements previous work and outlines the potential role of the novel gene in the tubules.

8.2 Introduction

In this thesis, I start with a historical overview of *Drosophila* melanogaster as a model organism. Its unique advantages make it suitable for genetic, developmental, physiological, and many other types of biological studies. By detailing the Malpighian tubules of *Drosophila*, with the specific functions of principal and stellate cells, this chapter explains why *Drosoph*ila is a suitable system for renal physiology and why gap junctions are important for tubule function. In addition, literature on cell-cell junctions describes how gap junctions formed by innexin proteins are key to intercellular communication that maintains tubule function and homeostasis. Finally, the introduction chapter discussed biogenic amines and their receptors, which regulate many physiological functions in *Drosophila*. This thesis focuses on determining how gap junction proteins and novel genes affect renal function, thus providing a theoretical foundation for the experimental investigations presented in later chapters. The detailed experimental methodologies, including fluid secretion assays, RNA sequencing, and metabolomics, have already been fully described in the earlier chapters and are therefore not repeated in this chapter.

8.3 Results

8.3.1 Gap junction

Gap junctions are thought to be very important in epithelia. This study is a direct experimental test of that theory. I have characterised the expression and localisation of two gap junction genes, Innexin 2 (Inx2) and Innexin 7 (Inx7), in Drosophila Malpighian tubules and their functional requirement for fluid secretion. These two Innexin genes were knocked down using RNAi lines and the GAL4/UAS system. The expression levels of the genes were quantified using qPCR, and the fluid secretion rate was measured to assess the impact of their knockdown on the tubule. Both Inx2 and Inx7 are expressed in the principal cells of tubules, as shown by RNAi line knockdown experiments. Although these innexins constitute the gap junctions required for intercellular communication, the knockdown of Inx2 or Inx7 did not result in marked differences in basal or kinin-stimulated fluid secretion rates. It may reflect compensatory mechanisms within tubules to maintain secretory function after the knockdown of the innexin gene from gap junctions. However, this study had limitations. One key issue is that the experiments could not clearly demonstrate whether Inx2 and Inx7 play a direct role in fluid secretion. The neutral results may reflect several challenges, such as incomplete knockdown or limited sensitivity of the assays to detect small changes in secretion rate. In addition, the Gal4/UAS system is temperaturesensitive, and differences in activity at 21-22 °C versus 25 °C could have influenced the strength of knockdown or the expression of other genes. These factors may have reduced the consistency of the results and limit how firmly the role of Inx2 and Inx7 in secretion can be defined.

8.3.2 Drosophila a2-adrenergic-like octopamine receptor

This chapter has investigated the role of Octα2R in tubules to understand its expression, function, and physiological relevance. This study used the *tsh* promoter-specific Gal4 line crossed with the Octα2R RNAi line for *Octa2R* knockdown in the stellate cells and combined with a fluid secretion assay to assess the receptor's role. I also have shown that some biogenic amines impact fluid secretion in *Drosophila* and that *Octa2R* senses the octopamine signal.

This result shows a previously undocumented role for octopamine in *Drosophila* tubule function and highlights the importance of *Octa2R* in fluid secretion. Reducing *Octa2R* expression in stellate cells decreases the secretion rate and reduces sensitivity to octopamine. Although several lines were tested, only the *Octa2R*⁵⁰⁶⁷⁸ line showed clear knockdown effects, while others did not. The interaction of *Octa2R* with other amines such as dopamine, tyramine, and tryptamine was not fully resolved, leaving open questions about its broader role in tubule signalling.

Drosophila Malpighian tubules are known to be regulated by multiple neuroendocrine inputs, including CAPA, kinin, DH31, and DH44, each contributing a distinct role in secretion. Octopamine also acts on the tubules, and the findings of this study suggest a specific physiological role for this signal. A reasonable hypothesis is that octopamine, acting through Octa2R in stellate cells, enables the tubules to adjust secretion rapidly during periods of increased activity or stress. By enhancing fluid transport under such conditions, octopamine signalling could complement the actions of peptide hormones, which regulate secretion over longer timescales. In this way, octopamine provides a fast modulatory input that links systemic arousal states to renal fluid balance, ensuring that water and ion homeostasis is maintained when metabolic demand changes.

8.3.3 Characterisation of the *Drosophila* Novel Gene *CG6602*

This chapter focused on the novel *Drosophila* gene *CG6602* and its expression and function in the Malpighian tubules. The main purpose was to test how reducing *CG6602* in these tissues affects tubule activity. To achieve this, RNAi lines were combined with the stellate cell driver tsh-Gal4, which restricts knockdown to the cell type where *CG6602* is expressed most strongly. This approach allowed us to ask whether the gene contributes to basal secretion under unstimulated conditions or to the changes in secretion that occur following hormonal input. Two independent RNAi lines, GD and KK, were used so that any observed effects could be compared between different constructs. By testing both basal and kinin-stimulated rates, the experiments provided a framework for linking *CG6602* expression in stellate cells with its possible role in regulating fluid secretion.

The results showed that CG6602 is specifically expressed in stellate cells of the Malpighian tubules. Functional tests demonstrated that knockdown with tsh-Gal4>UAS-CG6602i (GD 18900) led to a clear reduction in fluid secretion after kinin stimulation, whereas knockdown with tsh-Gal4>UAS-CG6602i (KK 106152) did not produce any detectable change. These findings are supported by the qPCR analysis, which confirmed a strong reduction in CG6602 transcript levels in the GD knockdown but not in the KK knockdown. This indicates that CG6602 is required for a full kinin-stimulated secretory response in stellate cells, at least under conditions where the gene is efficiently reduced by the GD construct. Although the function of CG6602 is not yet fully characterised, the results suggest that it may contribute to the signalling or transport processes that enable stellate cells to regulate chloride and water movement in response to hormonal input. These data provide important new insight, but also highlight limitations, particularly the differing effects seen between RNAi lines, which emphasise the need for caution when interpreting RNAi-based studies. Furthermore, based on earlier reports, CG6602 has been linked to insulin signalling (Musselman et al., 2019), suggesting that its role in tubules may extend to the integration of metabolic status with fluid balance.

8.3.4 Transcriptomic Analysis of CG6602

This chapter examined transcriptomic changes in the Malpighian tubules after knockdown of *CG6602*. Both up-regulated and down-regulated genes were identified, showing that loss of *CG6602* affects multiple pathways. The altered expression patterns may reflect compensatory responses within the tubules, but other explanations, such as indirect systemic effects or pathway-specific feedback cannot be ignored.

Several up-regulated genes, including *Ugt35C1*, *Cyp6a8*, *Slc45-1* and *MFS12*, are linked to stress responses, detoxification and ion transport. Their expression changes suggest that *CG6602* influences pathways important for maintaining metabolic balance and solute handling in the tubules.

Among the down-regulated genes, mat is notable because it is highly expressed in tubules and has been linked to lipid clearance and oxidative stress protection. Its reduced expression in *CG6602* knockdown flies suggests a connection between *CG6602* and stress-related pathways. However, interpretation is limited by the use of RNAi knockdown and reliance on transcriptomic data, which cannot provide information on protein interactions or confirm functional pathways. Future studies using complementary genetic and biochemical approaches will be required to test the roles of these candidate genes and to clarify how *CG6602* contributes to tubule physiology and stress regulation.

8.3.5 Metabolomics analysis in CG6602

In this chapter, I have used metabolomic data of the novel gene *CG6602* to analyse its potential roles in metabolic pathways in the Malpighian tubules. Glasgow Polyomics also generated these metabolomics data. In the previous chapter, the transcriptomic data suggested a possible role in stress response, specifically oxidative stress. The metabolomics analysis of this chapter thus focused on identifying changes in metabolites and pathways associated with stress responses and antioxidant defence.

The results revealed significant enrichment of multiple metabolites in *CG6602* knockdown tubules. Pathway enrichment of the significantly varied metabolites showed changes in several pathways related to glutathione and purine metabolism. This indicated that the oxidative stress defence system supports homeostasis and cellular balance by *CG6602*. The enrichment of metabolites, such as L-ornithine, L-glutamate, and hypoxanthine, induce antioxidant and stress responses that potentially imply the gene could be involved in these pathways (Terhzaz *et al.*, 2010; Bratty *et al.*, 2011; Dow and Romero, 2010). These results suggest a possible regulatory function for *CG6602* in metabolic changes necessary to control tubule stability.

One major limitation of the study is that it is limited to analysing metabolomics data by one method. I used these data to build biochemical reactions and metabolic pathways considering *CG6602*. Although these methods show changes to key metabolites, they do not provide the depth of analysis possible through complementary approaches. Additional strategies such as chiral LC-MS, isotope tracing, or targeted metabolite validation could provide more precise insights and strengthen the interpretation of the metabolic shifts observed in *CG6602* knockdown tubules.

8.4 Future Work

8.4.1 Gap junction

Future studies need to address the unresolved question of whether Inx2 and Inx7 have essential and non-redundant roles in Malpighian tubule secretion and cellcell communication. The results in this study did not provide a consistent functional requirement, so future work should aim to clarify whether the neutral outcomes reflect true biology or technical limitations of the current approach. To strengthen the conclusions, future studies could include larger sample sizes and replicate experiments using additional independent RNAi lines. Testing the simultaneous knockdown of both innexins would further address whether redundancy between Inx2 and Inx7 masks their individual contributions to tubule function. In addition, applying a broader range of kinin and CAPA peptide concentrations in secretion assays may yield more precise results, helping to define more clearly the role of gap junction proteins in renal function. Further characterisation of possible protein-protein interactions between Inx2 and Inx7 may also provide a mechanistic understanding of how these innexins promote renal physiology and homeostasis in *Drosophila*. Finally, dye coupling assays can be used to observe the function of Inx2 and Inx7 in the gap junction (Keven et al., 2002). A fluorescent dye is injected into a tubule cell with a glass microelectrode. If the dye spread between cells is observed in the tubule cell, the dye could be injected into Inx2 and Inx7 mutants, enabling a direct assessment of the role of these proteins in the gap junction. These approaches may help us understand the role of gap junction proteins in tubules.

8.4.2 Drosophila a2-adrenergic-like octopamine receptor

Future work could target different RNAi lines to address these limitations and generate more consistent knockdown of *Octa2R*. Investigation of the receptor response to other biogenic amines, such as serotonin, would provide deeper insight into the potential role of *Octa2R* in tubules. Moreover, simultaneous knockdown of *Octa2R* and other related receptors might clarify whether compensatory pathways maintain tubule function, pointing to possible redundancy in biogenic amine signalling. It will also be important to establish when and where octopamine is released in vivo, and under what physiological conditions it acts on the tubules. These approaches would extend our understanding of octopamine receptor function in the renal physiology of *Drosophila*.

8.4.3 Characterisation of the *Drosophila* Novel Gene *CG6602*

Using other RNAi lines or another UAS-Gal4 driver system could help to validate these results further, particularly since *CG6602* knockdown effects seem inconsistent across experimental lines. Moreover, as the previous paper describes (Musselman *et al.*, 2019), *CG6602* functions are related to the context of insulin signalling; one possible experiment that could be designed is modulating systemically acting insulin (or feeding animals high-sugar diets) to determine whether the expression of *CG6602* changes in a manner consistent with its predicted role within Malpighian tubules. Downstream signalling molecules related to insulin and kinin pathways could be analysed by biochemical assays, including Western blotting or qPCR, to determine the position of *CG6602* in these networks. Further co-immunoprecipitation research on potential protein interactions with *CG6602* could also help further characterise its functional partners in the renal system of *Drosophila*.

8.4.4 Transcriptomic Analysis of CG6602

Future experimentation could design targeted protein interaction assays or specific biochemical tests, such as enzyme activity measurements or metabolite assays, to verify whether *CG6602* interacts with stress response genes. To clarify the role of *CG6602* in stress pathways, experiments under different dietary conditions or environmental stresses (e.g., oxidative stress) may help explain how *CG6602* influences these responses. Further investigation using genetic approaches to up- or down-regulate related pathways could reveal compensatory mechanisms that maintain homeostasis following *CG6602* knockdown, improving our understanding of how this novel gene contributes to renal function in *Drosophila*.

8.4.5 Metabolomics analysis in CG6602

Future work could address these limitations by targeting biochemical assays to explore protein interactions within these metabolic pathways. More metabolomics-focused approaches on *CG6602* can complement this study in the future as it works through various metabolic pathways. More methods can be used to complete advanced metabolomic analysis. Metabolite enrichment and pathway analysis may indicate the metabolic routes most impacted by *CG6602* knockdown. Using different approaches may be able to detect more patterns of metabolites associated with stress response pathways or the connection between metabolites and their downstream. Moreover, exploring the response of *CG6602* under stress conditions such as oxidative stress could help to understand the possible functions of *CG6602* in tubules. Finally, the decreased metabolite riboflavin in *CG6602* will be analysed.

8.5 General Discussion

The main results of this thesis can be brought together to describe a layered model of Malpighian tubule regulation.

First, the knockdown of *Inx2* and *Inx7* showed that the loss of individual innexins does not alter basal or kinin-stimulated secretion. This suggests that coupling between principal cells is robust, most likely buffered by redundancy among innexins. Similar redundancy has been reported in other epithelial systems where multiple gap junction proteins provide overlapping roles (Stebbings et al., 2002; Liu et al., 2011). In the context of *Drosophila*, innexins are essential during embryonic development (Stebbings et al., 2002), yet their loss in adult epithelia often produces subtle or no phenotypes, consistent with the idea that adult epithelia rely on redundant mechanisms to maintain homeostasis.

Second, the identification of Octα2R as a functional octopamine receptor in stellate cells highlights a new layer of regulation. Octopamine acting through Octα2R allows rapid modulation of secretion, complementing the slower actions of peptide hormones such as CAPA, kinin, DH31 and DH44 (Dow and Romero, 2010; Terhzaz *et al.*, 2012; Cabrero *et al.*, 2002). This supports the broader model that insect tubules integrate inputs across different timescales, with peptide hormones acting to sustain steady-state osmoregulation and octopamine providing rapid adjustment of renal output during acute stress or arousal. Comparable dual-modulation systems have been described in other insect tissues, where bioamines rapidly modify activity while peptide hormones sustain longer-term changes (Nässel and Winther, 2010).

Third, *CG6602* emerges as a novel gene that links renal function to stress and metabolic pathways. Its expression in stellate cells, secretion phenotype after knockdown, and transcriptomic and metabolomic profiles suggest a role in integrating metabolic state with tubule output. Prior studies linked *CG6602* to insulin signalling (Musselman et al., 2019), and the data here extend this by implicating stress- and detoxification-related genes (Davies et al., 2014; Terhzaz

et al., 2010) and metabolites involved in glutathione and purine metabolism. The combination of transcriptomic and metabolomic findings therefore supports a role for *CG6602* in tuning tubule physiology during metabolic or oxidative stress, linking renal homeostasis with systemic energy balance.

Taken together, these findings show that tubule regulation involves three layers: baseline stability maintained by redundant coupling, fast modulation through octopamine signalling, and metabolic integration via novel genes such as *CG6602*. This layered framework illustrates how renal tissues achieve robust control of water and ion balance under variable physiological conditions and places the Malpighian tubule as a useful model for understanding general principles of epithelial regulation. Redundancy, rapid modulation and metabolic integration are not specific to *Drosophila* and can also be seen in epithelial tissues of other organisms that need to maintain function under variable conditions (Beyenbach and Piermarini, 2011).

8.6 Final conclusion

This thesis has tested the idea that genes with strong tissue-specific expression are important for function, and by using reverse genetic analysis several new insights were obtained. Knockdown of *Inx2* and *Inx7* showed that gap junction coupling in tubules is robust and resilient. Reduction of Octα2R revealed a fast bioamine pathway that complements peptide hormone regulation of secretion. Functional assays, transcriptomics, and metabolomics point to a role for *CG6602* in linking secretion with stress and metabolism. Taken together, these findings establish a framework in which robust epithelial coupling, rapid neuromodulation, and metabolic tuning jointly maintain renal physiology in *Drosophila*.

Appendices

Appendix 1: The composition of Schneider's medium

	· ·	
3.33 mM glycine,	2.76 mM L-tyrosine,	
2.3 mM L-arginine,	2.56 mM Lvaline,	
3.01 mM Laspartic acid,	5.62 mM β-alanine,	
0.496 mM L-cysteine,	5.41 mM CaCl2,	
0.417 mM L-cysteine,	15.06 mM MgSO4,	
5.44 mM L-glutamic acid,	21.33 mM KCl,	
12.33 mM L-glutamine,	3.31 mM KH2PO4,	
2.58 mM Lhistidine,	4.76 mM NaHCO3,	
1.15 mM L-isoleucine,	36.21 mM NaCl,	
1.15 mM L-leucine,	4.94 mMNa2HPO4,	
9.02 mM Llysine hydrochloride,	1.37 mM α-ketoglutari acid,	
5.37mML-methionine,	11.11 mM D-glucose,	
0.909mML-phenylalanine,	0.862 mM fumaric acid,	
14.78 mM L-proline,	0.746 mM malic acid,	
2.38 mM L-serine,	0.847 mM succinic acid,	
2.94 mM L-threonine,	5.85 mM trehalose,	
0.49 mM L-tryptophan,	2000 mg/L yeast plate	

Appendix 2: Calculation formula of fluid secretion rate

The general formula for measuring the volume of the secretion:

 $V=4/3\pi r^{3}$

 $V=4/3\pi (D/2)^3$

 $V=4/3\pi (D/2 \times GCF)^3$

The result to nanoliters:

V= $4/3\pi$ (D/2 x GCF)³ x 1000 (1 mm³ =1 μ L)

Then secreted fluid in nL/min= V=4/3 π (D/2 x GCF)³ x 1000 /(T₁-T₀)

Appendix 3 List of additional primers Octα2R

Primer	Forward	Reverse	
Octa2R	ATTGCCACGGAGAAGTCGTT	TAGCTCATTGGCCAGCGAAA	
Octa2R	TGCGAGGCACTTGTAACCAT	TGAAAGTTCCAGCGCTGCTA	

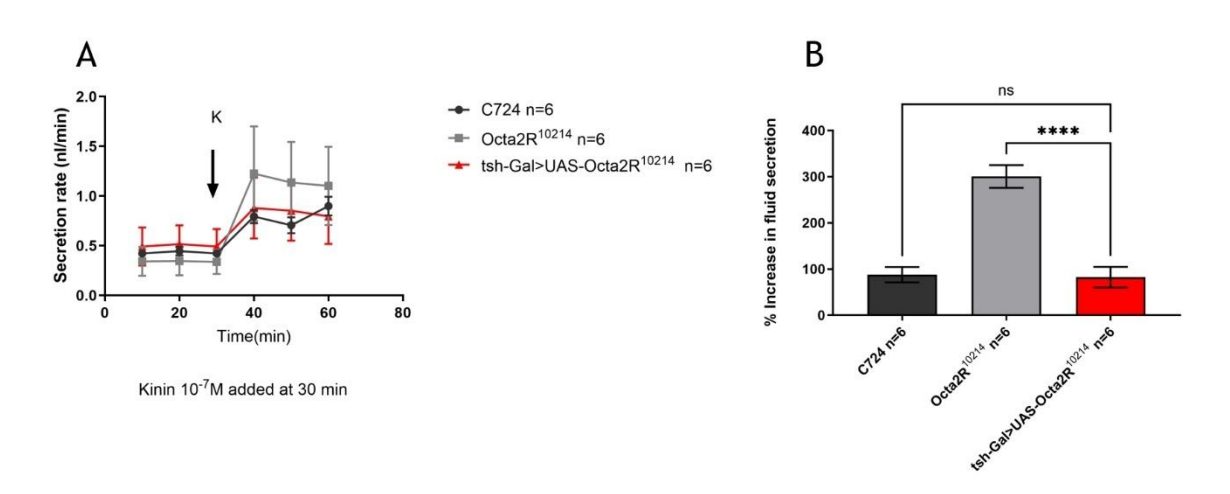
Appendix 4 5X TBE buffer recipe

Compound	Quantity		
Tris base	54g/l		
Boric acid	27.5g/l		
EDTA pH8	20ml/l		
Make up to 1L with ddH2O and			
then dilute 1/10 for 0.5X solution			

Appendix 5 10X PBS Buffer

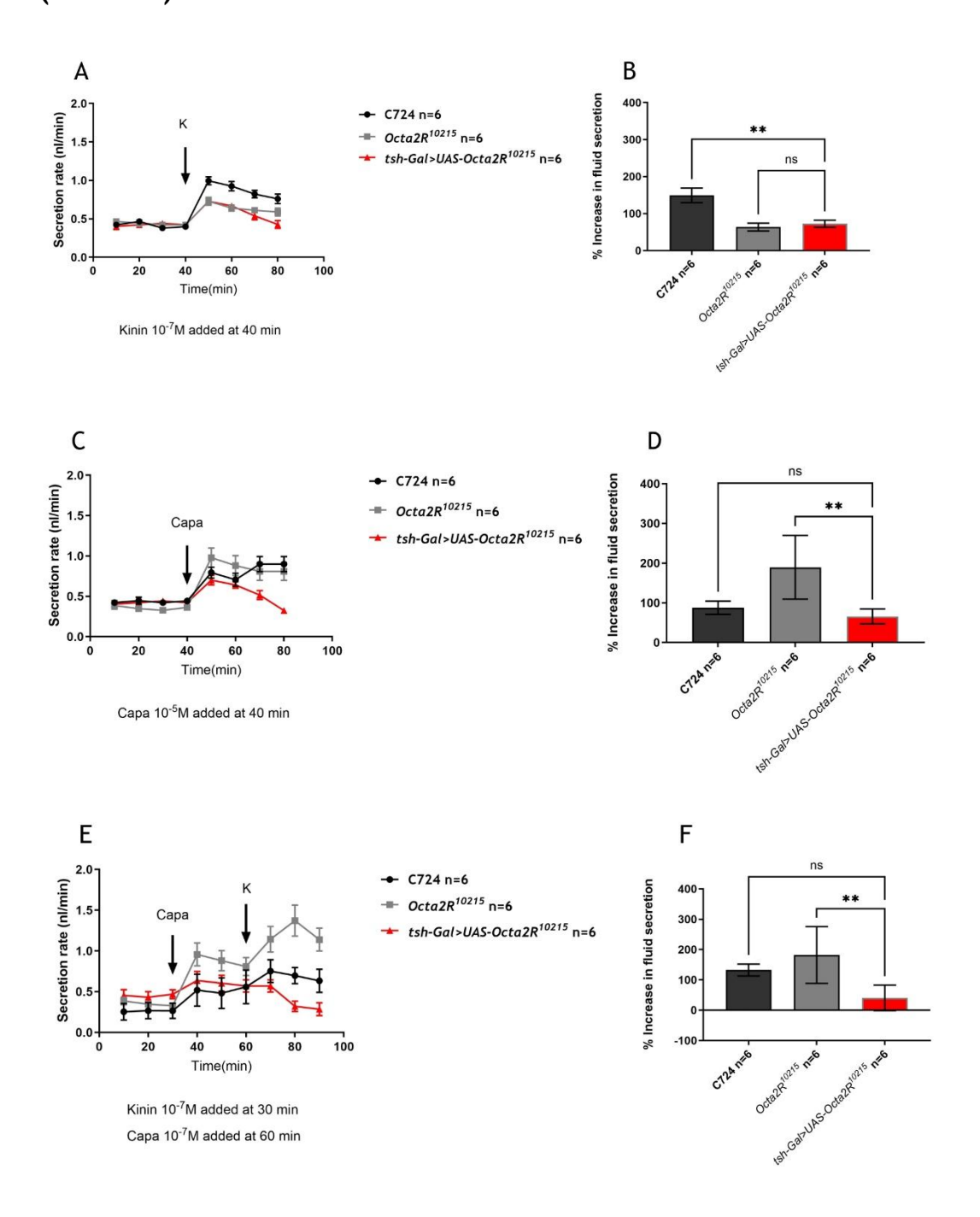
Compound	Quantity			
NaCl	80g/l			
KCL	2g/l			
Na₂HPO₄	14.4g/l			
KH₂PO₄	2.4g/l			
Make up to 1L with ddH2O and				
adjust pH to7.4				

Appendix 6 Fluid secretion assay using the UAS-Octα2R RNAi (#10214) line.



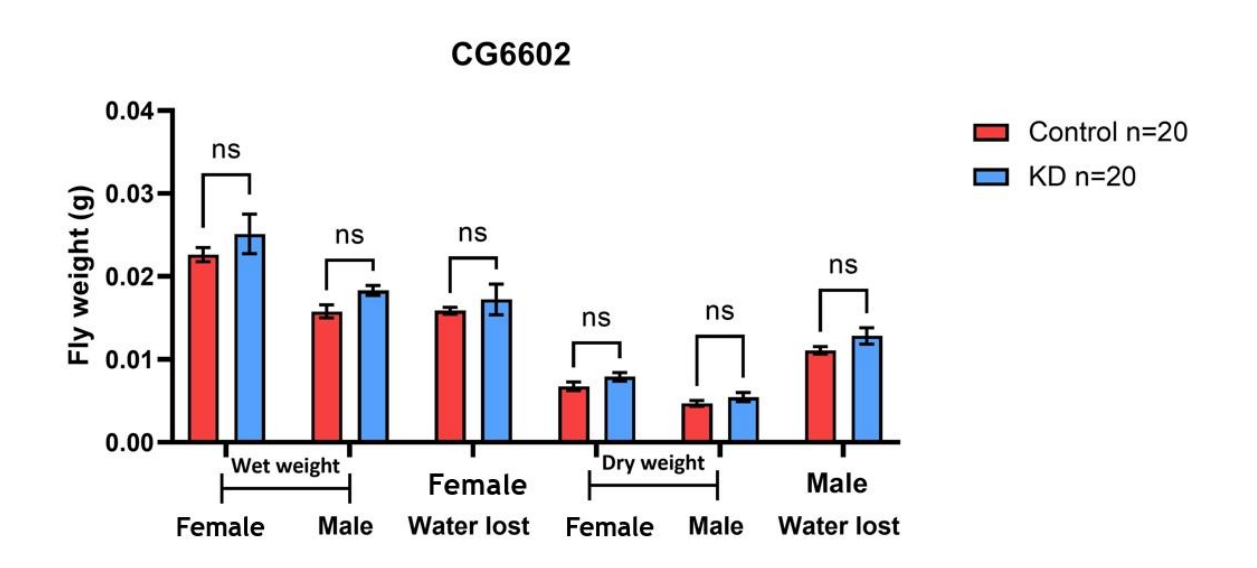
The Ramsay assay was performed on $Octa2R^{10214}$ knockdown flies (tsh-GAL4>UAS- $Oct\alpha2R^{10214}$) and controls (tsh-GAL4 and parental RNAi line). (A) Basal and kininstimulated secretion rate over time. (B) Percentage increase in secretion following kinin stimulation. Knockdown flies did not show a consistent or significant reduction in secretion compared with controls. Data are mean \pm SEM, n = 6, one-way ANOVA.

Appendix 7 Fluid secretion assay using the UAS-Octα2R RNAi (#10215) line.



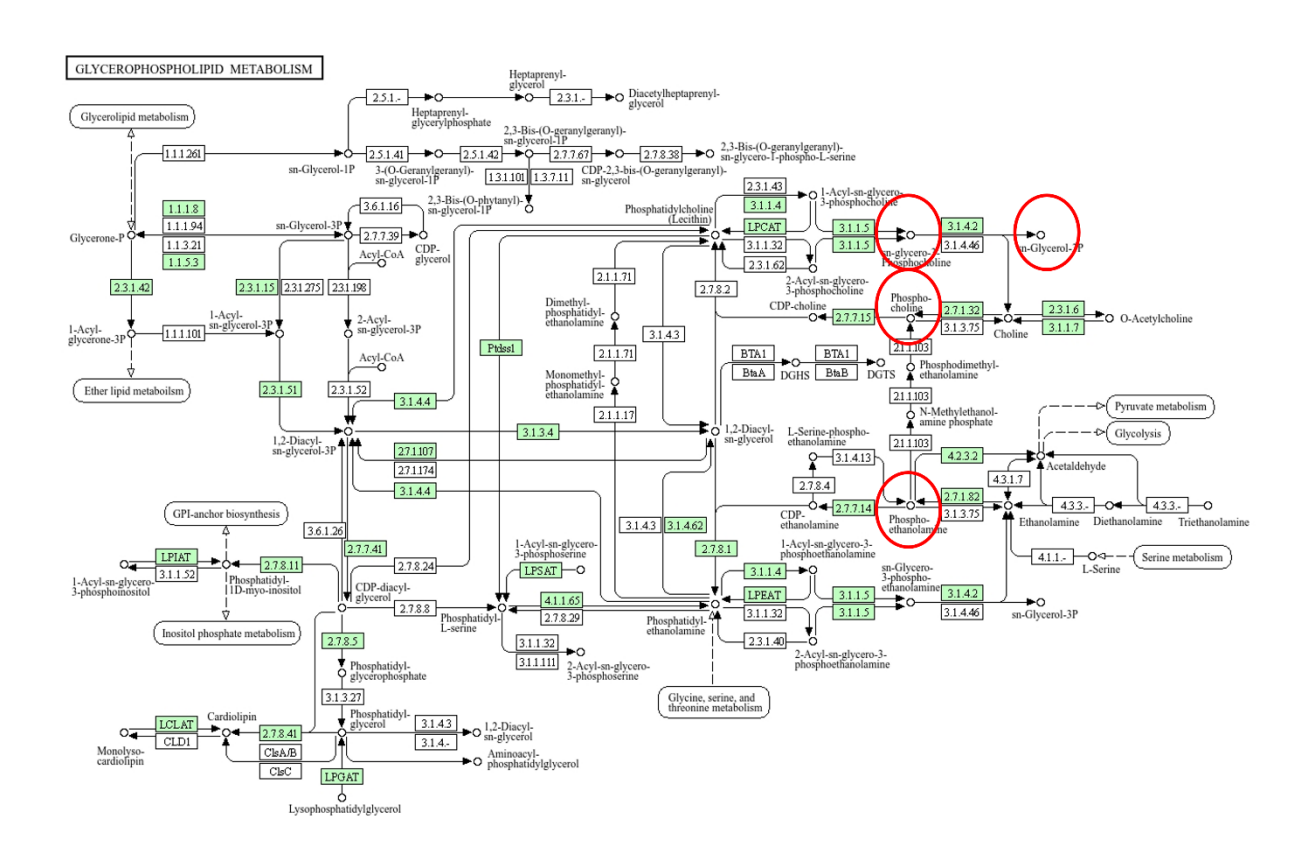
The Ramsay assay was performed on $Octa2R^{10215}$ knockdown flies (tsh-GAL4>UAS-Oct α 2R¹⁰²¹⁵) and controls (tsh-GAL4 and parental RNAi line). (A, C, E) Basal and peptide-stimulated secretion rates were recorded following addition of kinin (10^{-7} M) or capa (10^{-5} M). (B, D, F) Percentage increase in secretion was calculated after stimulation. Knockdown flies did not show a consistent reduction in secretion compared with controls. Data are mean \pm SEM, n = 6, one-way ANOVA.

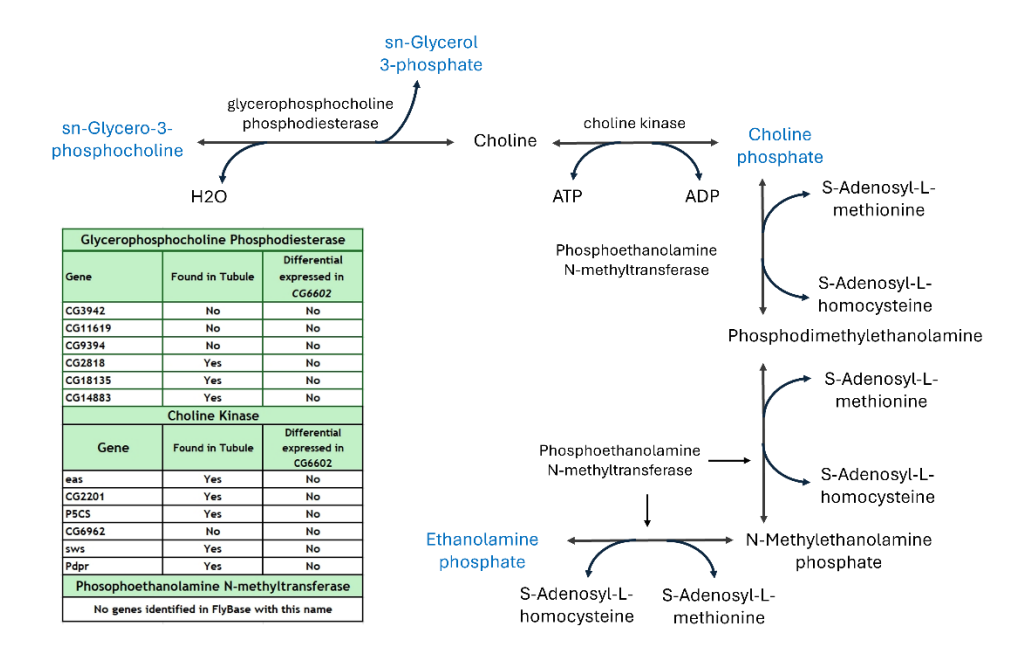
Appendix 8 Wet and Dry Weight of CG6602 line



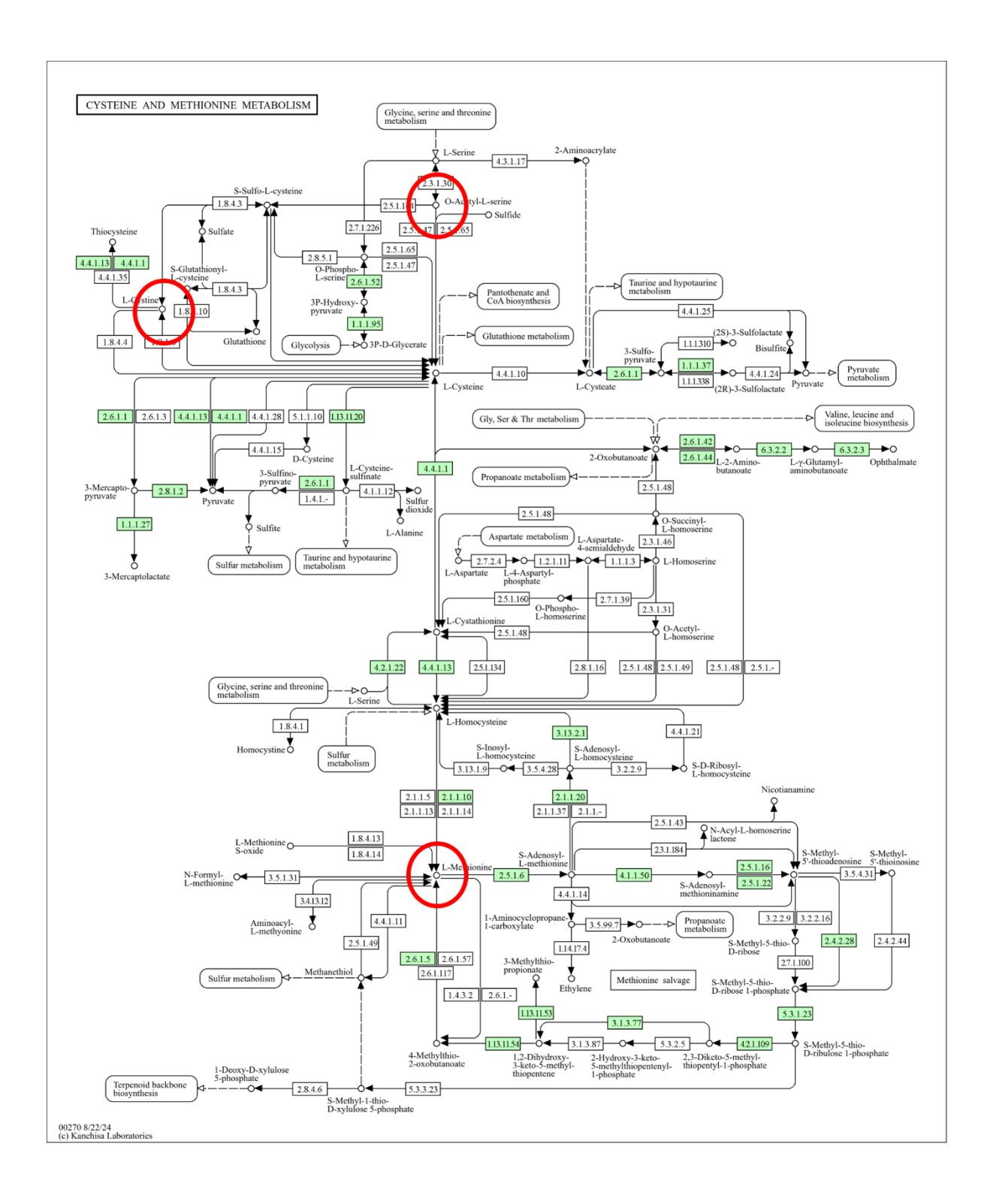
Knockdown of CG6602 and RNAi line Wet and Dry Weight measurement

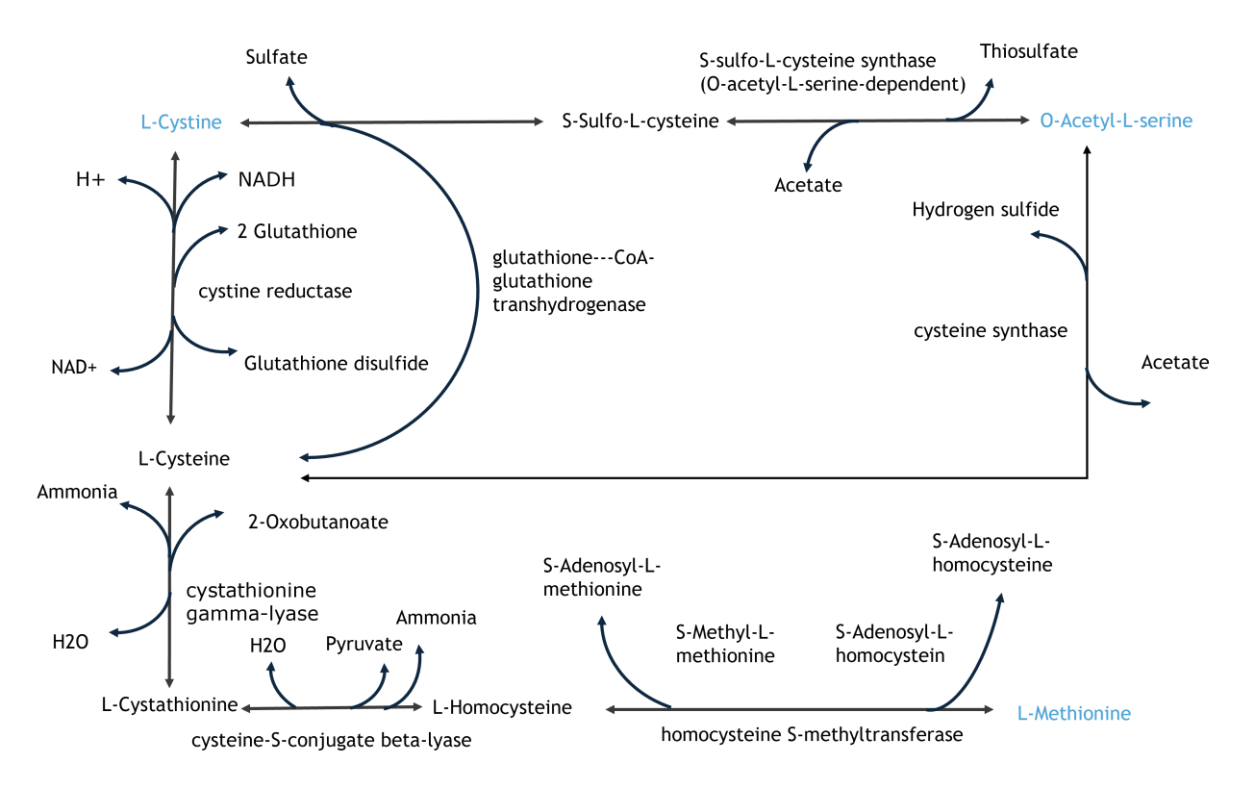
Appendix 9: KEGG map of *Drosophila melanogaster* and biochemical reactions of identified metabolites in Glycerophospholipid metabolism





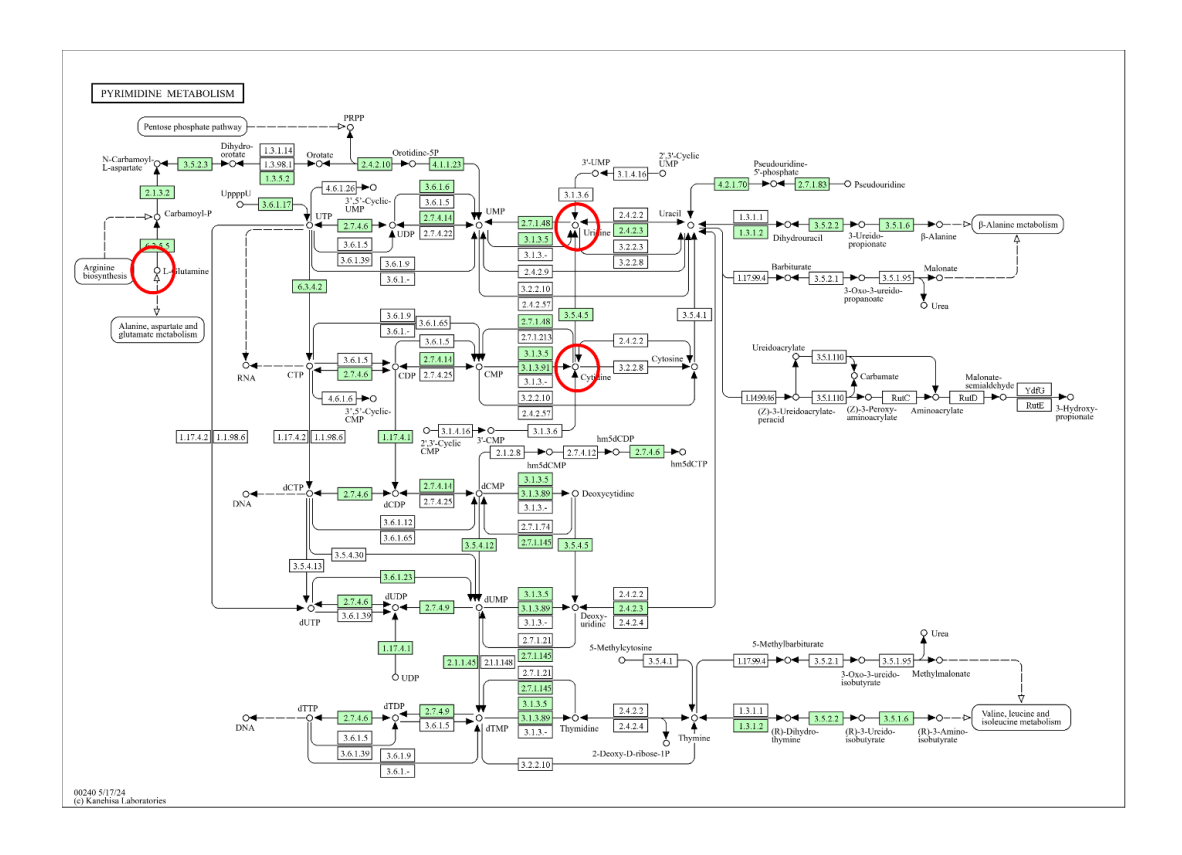
Appendix 10: KEGG map of *Drosophila melanogaster* and biochemical reactions of identified metabolites in Cysteine and methionine metabolism.

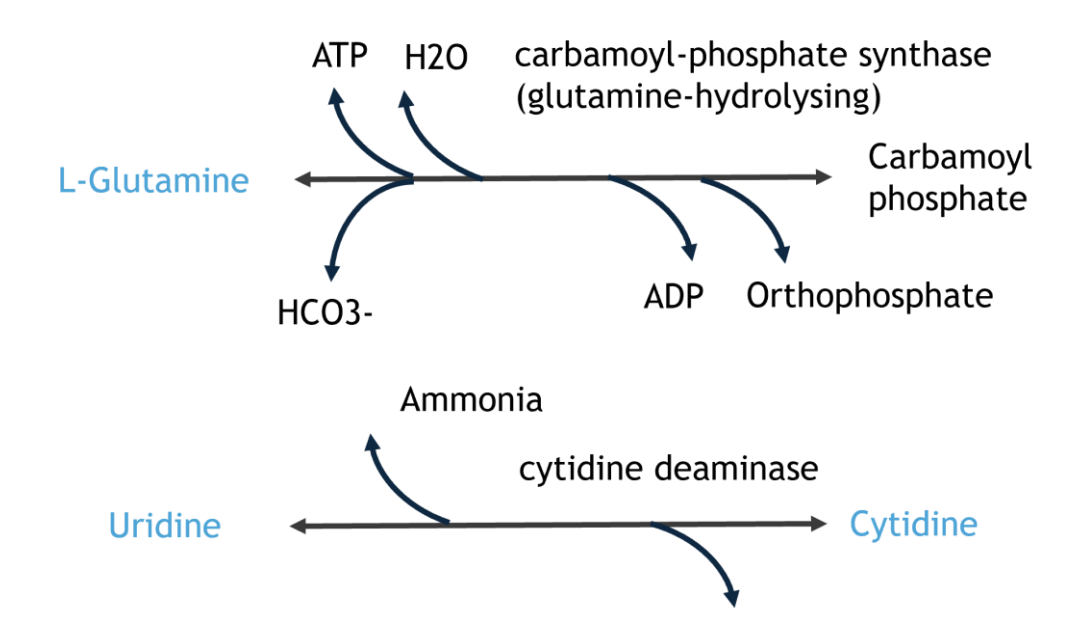




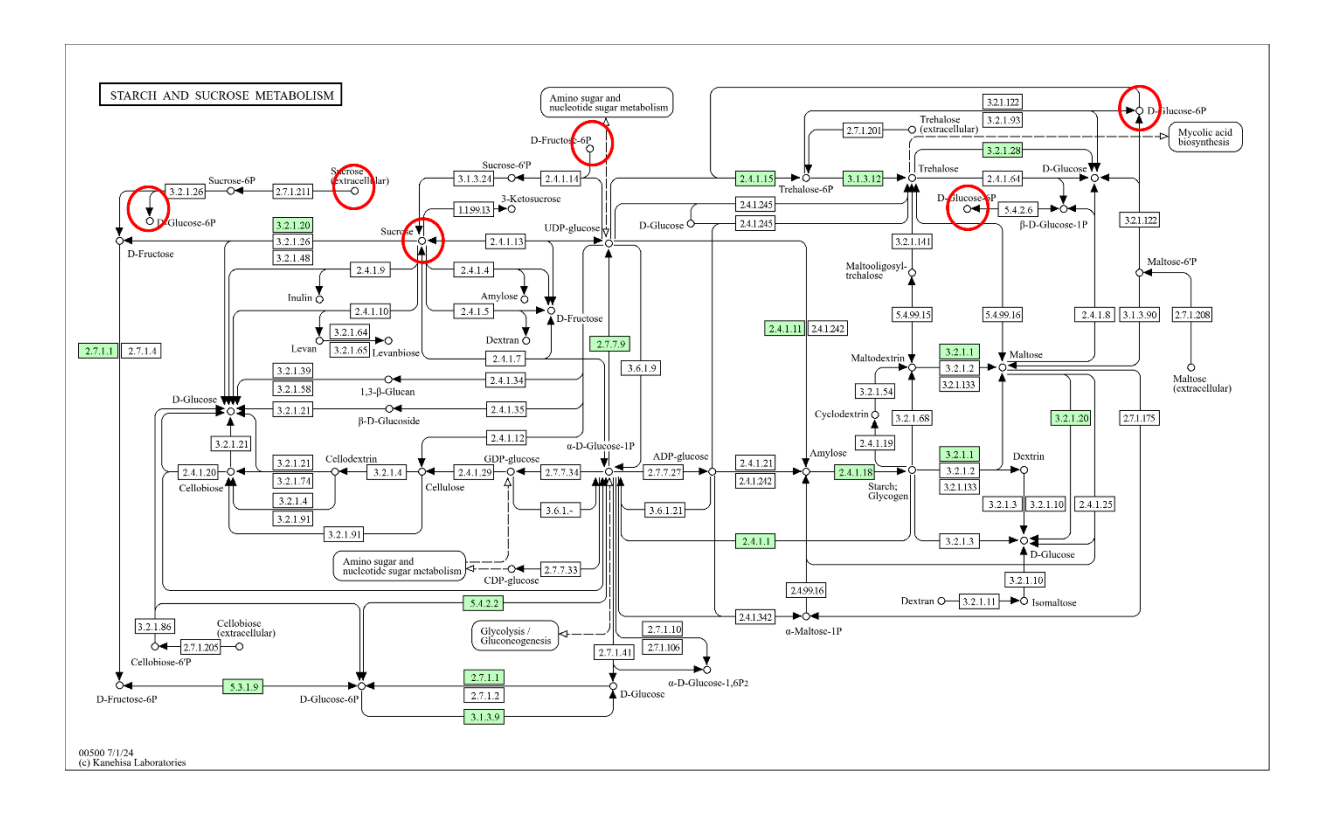
cystathionine gamma-lyase				
Gene	Found in Tubule	Differential expressed in CG6602		
Cth	No	No		
cysteine-S-conjugate beta-lyase				
Gene	Found in Tubule	Differential expressed in CG6602		
Kyat	Yes	No		
(ysteine synthase	9		
Gene	Found in Tubule	Differential expressed in CG6602		
Sms	Yes	No		
SpdS	Yes	No		
Cbs	No	No		
amd	No	No		
Gss1	No	No		
Sam-s	Yes	No		
Gss2	No	No		
Srr	Yes	No		
Enoph	Yes	No		
Dph1	Yes	No		
Dph2	Yes	No		
CG12173	Yes	No		
ScsBA	Yes	No		
Ctu1	Yes	No		
nanos	No	No		

Appendix 11: KEGG map of *Drosophila melanogaster* and biochemical reactions of identified Cysteine and Pyrimidine metabolism metabolites.





Appendix 12: KEGG map of *Drosophila melanogaster* and biochemical reactions of identified in Starch and sucrose metabolism.



List of references:

Abascal, F. and Zardoya, R., 2013. Evolutionary analyses of gap junction protein families. Biochimica et Biophysica Acta (BBA)-Biomembranes, 1828(1), pp.4-14.

Abdulbagi, M., Wang, L., Siddig, O., Di, B. and Li, B., 2021. D-amino acids and D-amino acid-containing peptides: potential disease biomarkers and therapeutic targets?. Biomolecules, 11(11), p.1716.

Ables, E.T., 2015. Drosophila oocytes as a model for understanding meiosis: an educational primer to accompany "corolla is a novel protein that contributes to the architecture of the synaptonemal complex of Drosophila". Genetics, 199(1), pp.17-23.

Abraham, A.D., Neve, K.A. and Lattal, K.M., 2014. Dopamine and extinction: a convergence of theory with fear and reward circuitry. Neurobiology of learning and memory, 108, pp.65-77.

Adams, M.D., Celniker, S.E., Holt, R.A., Evans, C.A., Gocayne, J.D., Amanatides, P.G., Scherer, S.E., Li, P.W., Hoskins, R.A., Galle, R.F. and George, R.A., 2000. The genome sequence of Drosophila melanogaster. Science, 287(5461), pp.2185-2195.

Ahn, S.J. and Marygold, S.J., 2021. The UDP-glycosyltransferase family in Drosophila melanogaster: Nomenclature update, gene expression and phylogenetic analysis. Frontiers in physiology, 12, p.648481.

Alberts, B., Johnson, A., Lewis, J., Raff, M., Roberts, K. and Walter, P., 2002. Studying gene expression and function. In Molecular Biology of the Cell. 4th edition. Garland Science.

Amberg, A., Riefke, B., Schlotterbeck, G., Ross, A., Senn, H., Dieterle, F. and Keck, M., 2017. NMR and MS Methods for Metabolomics. Drug safety evaluation: methods and protocols, pp.229-258.

Angelotti, T., Daunt, D., Shcherbakova, O.G., Kobilka, B. and Hurt, C.M., 2010. Regulation of G-Protein Coupled Receptor Traffic by an Evolutionary Conserved Hydrophobic Signal. Traffic, 11(4), pp.560-578.

Anglada-Girotto, M., Handschin, G., Ortmayr, K., Campos, A.I., Gillet, L., Manfredi, P., Mulholland, C.V., Berney, M., Jenal, U., Picotti, P. and Zampieri, M., 2022. Combining CRISPRi and metabolomics for functional annotation of compound libraries. Nature chemical biology, 18(5), pp.482-491.

Arbeitman, M.N., Furlong, E.E., Imam, F., Johnson, E., Null, B.H., Baker, B.S., Krasnow, M.A., Scott, M.P., Davis, R.W. and White, K.P., 2002. Gene expression during the life cycle of Drosophila melanogaster. Science, 297(5590), pp.2270-2275.

Ashburner, M. and J. J. C. S. H. P. Roote (2007). "Maintenance of a Drosophila laboratory: general procedures." 2007(3): pdb. ip35.

Asmamaw, M. and Zawdie, B., 2021. Mechanism and applications of CRISPR/Cas-9-mediated genome editing. Biologics: Targets and Therapy, pp.353-361.

Aso, Y., Hattori, D., Yu, Y., Johnston, R.M., Iyer, N.A., Ngo, T.T., Dionne, H., Abbott, L.F., Axel, R., Tanimoto, H. and Rubin, G.M., 2014. The neuronal architecture of the mushroom body provides a logic for associative learning. elife, 3, p.e04577.

Bacqué-Cazenave, J., Bharatiya, R., Barrière, G., Delbecque, J.P., Bouguiyoud, N., Di Giovanni, G., Cattaert, D. and De Deurwaerdère, P., 2020. Serotonin in animal cognition and behavior. International journal of molecular sciences, 21(5), p.1649.

Balfanz, S., Strünker, T., Frings, S. and Baumann, A., 2005. A family of octapamine receptors that specifically induce cyclic AMP production or Ca2+ release in Drosophila melanogaster. Journal of neurochemistry, 93(2), pp.440-451.

Banerjee, S., Benji, S., Liberow, S. and Steinhauer, J., 2020. Using Drosophila melanogaster to discover human disease genes: an educational primer for use with "amyotrophic lateral sclerosis modifiers in Drosophila reveal the phospholipase D pathway as a potential therapeutic target". Genetics, 216(3), pp.633-641.

Banerjee, S., Sousa, A.D. and Bhat, M.A., 2006. Organization and function of septate junctions: an evolutionary perspective. Cell biochemistry and biophysics, 46, pp.65-77.

Bar, S., Prasad, M. and Datta, R., 2018. Neuromuscular degeneration and locomotor deficit in a Drosophila model of mucopolysaccharidosis VII is attenuated by treatment with resveratrol. Disease Models & Mechanisms, 11(11), p.dmm036954.

Barbero, F., Mannino, G. and Casacci, L.P., 2023. The role of biogenic amines in social insects: with a special focus on ants. Insects, 14(4), p.386.

Barmore, W., Azad, F. and Stone, W.L., 2018. Physiology, urea cycle.

Barnard, A.R. and Nolan, P.M., 2008. When clocks go bad: neurobehavioural consequences of disrupted circadian timing. PLoS genetics, 4(5), p.e1000040.

Barreto, F.S., Schoville, S.D. and Burton, R.S., 2015. Reverse genetics in the tide pool: knock-down of target gene expression via RNA interference in the copepod T igriopus californicus. Molecular Ecology Resources, 15(4), pp.868-879.

Bassett, A.R. and Liu, J.L., 2014. CRISPR/Cas9 and genome editing in Drosophila. Journal of genetics and genomics, 41(1), pp.7-19.

Baumann, A., Blenau, W. and Erber, J., 2009. Biogenic amines. In Encyclopedia of insects (pp. 80-82). Academic Press.

Bauer, R., Lehmann, C., Martini, J., Eckardt, F. and Hoch, M., 2004. Gap junction channel protein innexin 2 is essential for epithelial morphogenesis in the Drosophila embryo. *Molecular biology of the cell*, 15(6), pp.2992-3004.

Bayliss, A., Roselli, G. and Evans, P.D., 2013. A comparison of the signalling properties of two tyramine receptors from Drosophila. Journal of neurochemistry, 125(1), pp.37-48.

Becnel, J., Johnson, O., Luo, J., Nässel, D.R. and Nichols, C.D., 2011. The serotonin 5-HT7Dro receptor is expressed in the brain of Drosophila, and is essential for normal courtship and mating. PloS one, 6(6), p.e20800.

Belgacem, Y.H. and Martin, J.R., 2002. Neuroendocrine control of a sexually dimorphic behavior by a few neurons of the pars intercerebralis in Drosophila. Proceedings of the National Academy of Sciences, 99(23), pp.15154-15158.

Bergman, P., Esfahani, S.S. and Engström, Y., 2017. Drosophila as a model for human diseases—focus on innate immunity in barrier epithelia. Current topics in developmental biology, 121, pp.29-81.

Berry, J.A., Cervantes-Sandoval, I., Nicholas, E.P. and Davis, R.L., 2012. Dopamine is required for learning and forgetting in Drosophila. Neuron, 74(3), pp.530-542.

Bertaud, A., Cens, T., Rousset, M., Thibaud, J.B., Ménard, C., Guiramand, J., Vignes, M., Vivaudou, M. and Charnet, P., 2022, September. Identification of signaling pathways of octopamine receptors in Apis mellifera and Varroa destructor. In 31th Ion Channel meeting.

Beyenbach, K.W., Skaer, H. and Dow, J.A., 2010. The developmental, molecular, and transport biology of Malpighian tubules. *Annual review of entomology*, 55(1), pp.351-374.

Beyenbach, K.W. and Piermarini, P.M., 2011. Transcellular and paracellular pathways of transepithelial fluid secretion in Malpighian (renal) tubules of the yellow fever mosquito Aedes aegypti. *Acta Physiologica*, 202(3), pp.387-407.

Bhatia, S.K., Kumar, V., Kumar, V., Bhatia, R.K. and Yang, Y.H., 2023. Microbial activity and productivity enhancement strategies. In Basic Biotechniques for Bioprocess and Bioentrepreneurship (pp. 85-104). Academic Press.

Blenau, W. and Baumann, A., 2001. Molecular and pharmacological properties of insect biogenic amine receptors: lessons from Drosophila melanogaster and Apis mellifera. Archives of Insect Biochemistry and Physiology: Published in Collaboration with the Entomological Society of America, 48(1), pp.13-38.

Blenau, W., Bremer, A.S., Schwietz, Y., Friedrich, D., Ragionieri, L., Predel, R., Balfanz, S. and Baumann, A., 2022. PaOctB2R: Identification and functional characterization of an octopamine receptor activating adenylyl cyclase activity in the American cockroach Periplaneta americana. International journal of molecular sciences, 23(3), p.1677.

Blenau, W., Wilms, J.A., Balfanz, S. and Baumann, A., 2020. AmOctα2R: Functional characterization of a honeybee octopamine receptor inhibiting adenylyl cyclase activity. International journal of molecular sciences, 21(24), p.9334.

Blumenthal, E.M., 2003. Regulation of chloride permeability by endogenously produced tyramine in the Drosophila Malpighian tubule. American Journal of Physiology-Cell Physiology, 284(3), pp.C718-C728.

Bohrmann, J. and Zimmermann, J., 2008. Gap junctions in the ovary of Drosophila melanogaster: localization of innexins 1, 2, 3 and 4 and evidence for intercellular communication via innexin-2 containing channels. *BMC developmental biology*, 8(1), p.111.

Bond, S.R. and Naus, C.C., 2014. The pannexins: past and present. Frontiers in physiology, 5, p.58.

Bonner, J.J. and Pardue, M.L., 1976. The effect of heat shock on RNA synthesis in Drosophila tissues. Cell, 8(1), pp.43-50.

Bonner, J.J. and Pardue, M.L., 1977. Polytene chromosome puffing and in situ hybridization measure different aspects of RNA metabolism. Cell, 12(1), pp.227-234.

Borovsky, D., Breyssens, H., Buytaert, E., Peeter, T., Laroye, C. and Stoffels, K., 2022. Cloning and characterization of Drosophila melanogaster juvenile hormone epoxide hydrolases (JHEH) and their promoters. Biomolecules, 12, 991

Bratty, M.A., Hobani, Y., Dow, J.A. and Watson, D.G., 2011. Metabolomic profiling of the effects of allopurinol on Drosophila melanogaster. Metabolomics, 7, pp.542-548.

Brede, M., Philipp, M., Knaus, A., Muthig, V. and Hein, L., 2004. α2-Adrenergic Receptor Subtypes—Novel Functions Uncovered in Gene-Targeted Mouse Models. Biology of the Cell, 96(5), pp.343-348.

Brown, J.A., Petersen, N., Centanni, S.W., Jin, A.Y., Yoon, H.J., Cajigas, S.A., Bedenbaugh, M.N., Luchsinger, J.R., Patel, S., Calipari, E.S. and Simerly, R.B., 2023. An ensemble recruited by α2a-adrenergic receptors is engaged in a stressor-specific manner in mice. Neuropsychopharmacology, 48(8), pp.1133-1143.

Buchon, N., Silverman, N. and Cherry, S., 2014. Immunity in Drosophila melanogaster—from microbial recognition to whole-organism physiology. Nature reviews immunology, 14(12), pp.796-810.

Busch, S., Selcho, M., Ito, K. and Tanimoto, H., 2009. A map of octopaminergic neurons in the Drosophila brain. Journal of Comparative Neurology, 513(6), pp.643-667.

Cabrero, P., Richmond, L., Nitabach, M., Davies, S.A. and Dow, J.A., 2013. A biogenic amine and a neuropeptide act identically: tyramine signals through calcium in Drosophila tubule stellate cells. Proceedings of the Royal Society B: Biological Sciences, 280(1757), p.20122943.

Cabrero, P., Radford, J.C., Broderick, K.E., Costes, L., Veenstra, J.A., Spana, E.P., Davies, S.A. and Dow, J.A., 2002. The Dh gene of Drosophila melanogaster encodes a diuretic peptide that acts through cyclic AMP. *Journal of Experimental Biology*, 205(24), pp.3799-3807.

Cabrero, P., Terhzaz, S., Romero, M.F., Davies, S.A., Blumenthal, E.M. and Dow, J.A., 2014. Chloride channels in stellate cells are essential for uniquely high secretion rates in neuropeptide-stimulated Drosophila diuresis. Proceedings of the National Academy of Sciences, 111(39), pp.14301-14306.

Carlson, E.A., 2013. HJ Muller's contributions to mutation research. Mutation Research/Reviews in Mutation Research, 752(1), pp.1-5.

Carroll, S.B., 1995. Homeotic genes and the evolution of arthropods and chordates. *Nature*, *376*(6540), pp.479-485.

Carson, H.L., 1970. Chromosome Tracers of the Origin of Species: Some Hawaiian Drosophila species have arisen from single founder individuals in less than a million years. Science, 168(3938), pp.1414-1418.

Cattabriga, G., Giordani, G., Gargiulo, G. and Cavaliere, V., 2023. Effect of aminergic signaling on the humoral innate immunity response of Drosophila. Frontiers in Physiology, 14, p.1249205.

Caygill, E.E. and Brand, A.H., 2016. The GAL4 system: a versatile system for the manipulation and analysis of gene expression. Drosophila, pp.33-52.

Chen, S., 2014. Function of the insect olfactory receptor co-receptor subunit and its interactions with odorant binding subunits (Doctoral dissertation, University of Miami).

Chen, X., Ohta, H., Ozoe, F., Miyazawa, K., Huang, J. and Ozoe, Y., 2010. Functional and pharmacological characterization of a B-adrenergic-like octopamine receptor from the silkworm Bombyx mori. Insect biochemistry and molecular biology, 40(6), pp.476-486.

Chen, Y., Li, E.M. and Xu, L.Y., 2022. Guide to metabolomics analysis: a bioinformatics workflow. Metabolites, 12 (4), 357

Chentsova, N.A., Gruntenko, N., Bogomolova, E., Adonyeva, N., Karpova, E. and Rauschenbach, I., 2002. Stress response in Drosophila melanogaster strain inactive with decreased tyramine and octopamine contents. Journal of Comparative Physiology B, 172, pp.643-650.

Chertemps, T., François, A., Durand, N., Rosell, G., Dekker, T., Lucas, P. and Maïbèche-Coisne, M., 2012. A carboxylesterase, Esterase-6, modulates sensory physiological and behavioral response dynamics to pheromone in Drosophila. BMC biology, 10, pp.1-12.

Chien, S., Reiter, L.T., Bier, E. and Gribskov, M., 2002. Homophila: human disease gene cognates in Drosophila. Nucleic acids research, 30(1), pp.149-151.

Chintapalli, V.R., Wang, J. and Dow, J.A., 2007. Using FlyAtlas to identify better Drosophila melanogaster models of human disease. Nature genetics, 39(6), pp.715-720.

Cho, K.S., Bang, S.M. and Toh, A., 2014. Lipids and lipid signaling in Drosophila models of neurodegenerative diseases. In Omega-3 fatty acids in brain and neurological health (pp. 327-336). Academic Press.

Christie, A.E., Hull, J.J. and Dickinson, P.S., 2020. Assessment and comparison of putative amine receptor complement/diversity in the brain and eyestalk ganglia of the lobster, Homarus americanus. Invertebrate Neuroscience, 20, pp.1-14.

Cingolani, P., Patel, V.M., Coon, M., Nguyen, T., Land, S.J., Ruden, D.M. and Lu, X., 2012. Using Drosophila melanogaster as a model for genotoxic chemical mutational studies with a new program, SnpSift. Frontiers in genetics, 3, p.35.

Clish, C.B., 2015. Metabolomics: an emerging but powerful tool for precision medicine. Molecular Case Studies, 1(1), p.a000588.

Cohen, E., Sawyer, J.K., Peterson, N.G., Dow, J.A. and Fox, D.T., 2020. Physiology, development, and disease modeling in the Drosophila excretory system. Genetics, 214(2), pp.235-264.

Cole, S.H., Carney, G.E., McClung, C.A., Willard, S.S., Taylor, B.J. and Hirsh, J., 2005. Two functional but noncomplementing Drosophila tyrosine decarboxylase genes: distinct roles for neural tyramine and octopamine in female fertility. Journal of Biological Chemistry, 280(15), pp.14948-14955.

Conesa, A., Madrigal, P., Tarazona, S., Gomez-Cabrero, D., Cervera, A., McPherson, A., Szcześniak, M.W., Gaffney, D.J., Elo, L.L., Zhang, X. and Mortazavi, A., 2016. A survey of best practices for RNA-seq data analysis. Genome biology, 17, pp.1-19.

Curtin, K.D., Zhang, Z. and Wyman, R.J., 1999. Drosophila has several genes for gap junction proteins. Gene, 232(2), pp.191-201.

D'Aniello, E., Paganos, P., Anishchenko, E., D'Aniello, S. and Arnone, M.I., 2020. Comparative neurobiology of biogenic amines in animal models in deuterostomes. Frontiers in Ecology and Evolution, 8, p.587036.

Daines, B., Wang, H., Wang, L., Li, Y., Han, Y., Emmert, D., Gelbart, W., Wang, X., Li, W., Gibbs, R. and Chen, R., 2011. The Drosophila melanogaster transcriptome by paired-end RNA sequencing. Genome research, 21(2), pp.315-324.

Daniel, E., Daude, M., Kolotuev, I., Charish, K., Auld, V. and Le Borgne, R., 2018. Coordination of septate junctions assembly and completion of cytokinesis in proliferative epithelial tissues. Current Biology, 28(9), pp.1380-1391.

Das, M., Cheng, D., Matzat, T. and Auld, V.J., 2023. Innexin-mediated adhesion between glia is required for axon ensheathment in the peripheral nervous system. Journal of Neuroscience, 43(13), pp.2260-2276.

Daubner, S.C., Le, T. and Wang, S., 2011. Tyrosine hydroxylase and regulation of dopamine synthesis. Archives of biochemistry and biophysics, 508(1), pp.1-12.

Davenport, C.B., 1941. The early history of research with Drosophila. Science, 93(2413), pp.305-306.

Davie, K., Janssens, J., Koldere, D., De Waegeneer, M., Pech, U., Kreft, Ł., Aibar, S., Makhzami, S., Christiaens, V., González-Blas, C.B. and Poovathingal, S., 2018. A single-cell transcriptome atlas of the aging Drosophila brain. Cell, 174(4), pp.982-998.

Davies, S.A. and Dow, J.A., 2009. Modulation of epithelial innate immunity by autocrine production of nitric oxide. General and comparative endocrinology, 162(1), pp.113-121.

Davies, S.A. and Terhzaz, S., 2009. Organellar calcium signalling mechanisms in Drosophila epithelial function. Journal of Experimental Biology, 212(3), pp.387-400.

Davies, S.A., Cabrero, P., Marley, R., Corrales, G.M., Ghimire, S., Dornan, A.J. and Dow, J.A., 2019. Epithelial function in the Drosophila malpighian tubule: an in vivo renal model. Kidney Organogenesis: Methods and Protocols, pp.203-221.

Davies, S.A., Cabrero, P., Overend, G., Aitchison, L., Sebastian, S., Terhzaz, S. and Dow, J.A., 2014. Cell signalling mechanisms for insect stress tolerance. Journal of Experimental Biology, 217(1), pp.119-128.

De Maio, A., Santoro, M.G., Tanguay, R.M. and Hightower, L.E., 2012. Ferruccio Ritossa's scientific legacy 50 years after his discovery of the heat shock response: a new view of biology, a new society, and a new journal. Cell stress and chaperones, 17, pp.139-143.

de Miranda, A.S., Milagre, C.D. and Hollmann, F., 2022. Alcohol dehydrogenases as catalysts in organic synthesis. Frontiers in Catalysis, 2, p.900554.

Deng, B., Li, Q., Liu, X., Cao, Y., Li, B., Qian, Y., Xu, R., Mao, R., Zhou, E., Zhang, W. and Huang, J., 2019. Chemoconnectomics: mapping chemical transmission in Drosophila. Neuron, 101(5), pp.876-893.

Denholm, B., 2013. Shaping up for action: the path to physiological maturation in the renal tubules of Drosophila. Organogenesis, 9(1), pp.40-54.

Denholm, B., Sudarsan, V., Pasalodos-Sanchez, S., Artero, R., Lawrence, P., Maddrell, S., Baylies, M. and Skaer, H., 2003. Dual origin of the renal tubules in Drosophila: mesodermal cells integrate and polarize to establish secretory function. Current Biology, 13(12), pp.1052-1057.

Dieterle, F., Riefke, B., Schlotterbeck, G., Ross, A., Senn, H. and Amberg, A., 2011. NMR and MS methods for metabonomics. Drug Safety Evaluation: Methods and Protocols, pp.385-415.

Dietzl, G., Chen, D., Schnorrer, F., Su, K.C., Barinova, Y., Fellner, M., Gasser, B., Kinsey, K., Oppel, S., Scheiblauer, S. and Couto, A., 2007. A genome-wide transgenic RNAi library for conditional gene inactivation in Drosophila. Nature, 448(7150), pp.151-156.

Dobin, A. and Gingeras, T.R., 2015. Mapping RNA-seq reads with STAR. Current protocols in bioinformatics, 51(1), pp.11-14.

Dong, Z. and Chen, Y., 2013. Transcriptomics: advances and approaches. Science China Life Sciences, 56, pp.960-967.

Dow, J.A. and Davies, S.A., 2001. The Drosophila melanogaster malpighian tubule.

Dow, J.A. and Davies, S.A., 2003. Integrative physiology and functional genomics of epithelial function in a genetic model organism. Physiological reviews, 83(3), pp.687-729.

Dow, J.A. and Davies, S.A., 2006. The Malpighian tubule: rapid insights from post-genomic biology. *Journal of Insect Physiology*, *52*(4), pp.365-378.

Dow, J.A. and Romero, M.F., 2010. Drosophila provides rapid modeling of renal development, function, and disease. American Journal of Physiology-Renal Physiology, 299(6), pp.F1237-F1244.

Dow, J.A., 2007. Integrative physiology, functional genomics and the phenotype gap: a guide for comparative physiologists. Journal of Experimental Biology, 210(9), pp.1632-1640.

Dow, J.A., 2007. Model organisms and molecular genetics for endocrinology. General and comparative endocrinology, 153(1-3), pp.3-12.

Dow, J.A., Davies, S.A. and SOÖZEN, M.A., 1998. Fluid secretion by the Drosophila Malpighian tubule. American zoologist, 38(3), pp.450-460.

Dow, J.A., Krause, S.A. and Herzyk, P., 2021. Updates on ion and water transport by the Malpighian tubule. Current Opinion in Insect Science, 47, pp.31-37.

Drew, D., North, R.A., Nagarathinam, K. and Tanabe, M., 2021. Structures and general transport mechanisms by the major facilitator superfamily (MFS). Chemical reviews, 121(9), pp.5289-5335.

Drysdale, R. and FlyBase Consortium, 2008. FlyBase: a database for the Drosophila research community. Drosophila: Methods and Protocols, pp.45-59.

Drysdale, R.A., FlyBase Consortium, Crosby, M.A. and FlyBase Consortium, 2005. FlyBase: genes and gene models. Nucleic acids research, 33(suppl_1), pp.D390-D395.

Duffy, J.B., 2002. GAL4 system in Drosophila: a fly geneticist's Swiss army knife. genesis, 34(1-2), pp.1-15.

Dyar, K.A., Lutter, D., Artati, A., Ceglia, N.J., Liu, Y., Armenta, D., Jastroch, M., Schneider, S., de Mateo, S., Cervantes, M. and Abbondante, S., 2018. Atlas of circadian metabolism reveals system-wide coordination and communication between clocks. Cell, 174(6), pp.1571-1585.

Edgar, B.A. and Orr-Weaver, T.L., 2001. Endoreplication cell cycles: more for less. Cell, 105(3), pp.297-306.

Edson, K.Z. and Rettie, A.E., 2013. CYP4 enzymes as potential drug targets: focus on enzyme multiplicity, inducers and inhibitors, and therapeutic modulation of 20-hydroxyeicosatetraenoic acid (20-HETE) synthase and fatty acid ω -hydroxylase activities. Current topics in medicinal chemistry, 13(12), pp.1429-1440.

Elias, M., Fraqueza, M.J. and Laranjo, M., 2018. Biogenic amines in food: presence and control measures.

El-Kholy, S., Stephano, F., Li, Y., Bhandari, A., Fink, C. and Roeder, T., 2015. Expression analysis of octopamine and tyramine receptors in Drosophila. Cell and tissue research, 361, pp.669-684.

El-Kholy, S.E., Afifi, B., El-Husseiny, I. and Seif, A., 2022. Octopamine signaling via OctαR is essential for a well-orchestrated climbing performance of adult Drosophila melanogaster. Scientific Reports, 12(1), p.14024.

Elliott, D.A. and Brand, A.H., 2008. The GAL4 system: a versatile system for the expression of genes. Drosophila: methods and protocols, pp.79-95.

Emwas, A.H., Roy, R., McKay, R.T., Tenori, L., Saccenti, E., Gowda, G.N., Raftery, D., Alahmari, F., Jaremko, L., Jaremko, M. and Wishart, D.S., 2019. NMR spectroscopy for metabolomics research. Metabolites, 9(7), p.123.

Emwas, A.H.M., 2015. The strengths and weaknesses of NMR spectroscopy and mass spectrometry with particular focus on metabolomics research. Metabonomics: Methods and protocols, pp.161-193.

Enayati, A.A., Ranson, H. and Hemingway, J., 2005. Insect glutathione transferases and insecticide resistance. Insect molecular biology, 14(1), pp.3-8.

Ercan, S.S., Bozkurt, H. and Soysal, Ç., 2013. Significance of biogenic amines in foods and their reduction methods. Journal of Food Science and Engineering, 3(8).

Erdag, D., Merhan, O. and Yildiz, B., 2018. Biochemical and pharmacological properties of biogenic amines. Biogenic amines, 8, pp.1-14.

Eriksson, A., Raczkowska, M., Navawongse, R., Choudhury, D., Stewart, J.C., Tang, Y.L., Wang, Z. and Claridge-Chang, A., 2017. Neuromodulatory circuit effects on Drosophila feeding behaviour and metabolism. Scientific reports, 7(1), p.8839.

Evans, P.D., 1981. Multiple receptor types for octopamine in the locust. The Journal of physiology, 318(1), pp.99-122.

Farooqui, T., 2007. Octopamine-mediated neuromodulation of insect senses. Neurochemical research, 32, pp.1511-1529.

Farooqui, T., 2012. Review of octopamine in insect nervous systems. Open access insect physiology, pp.1-17.

Fernandez, A.I., 2017. Octopamine in Sexual Behavior. The University of Texas at El Paso.

Fernández-Ayala, D.J., Jiménez-Gancedo, S., Guerra, I. and Navas, P., 2014. Invertebrate models for coenzyme q10 deficiency. Molecular syndromology, 5(3-4), pp.170-179.

Fernández-Moreno, M.A., Farr, C.L., Kaguni, L.S. and Garesse, R., 2007. Drosophila melanogaster as a model system to study mitochondrial biology. Mitochondria: Practical Protocols, pp.33-49.

Fiore, V.G., Kottler, B., Gu, X. and Hirth, F., 2017. In silico interrogation of insect central complex suggests computational roles for the ellipsoid body in spatial navigation. Frontiers in behavioral neuroscience, 11, p.142.

Freeman, M.R., 2015. Drosophila central nervous system glia. Cold Spring Harbor perspectives in biology, 7(11), p.a020552.

Friggi-Grelin, F., Coulom, H., Meller, M., Gomez, D., Hirsh, J. and Birman, S., 2003. Targeted gene expression in Drosophila dopaminergic cells using regulatory sequences from tyrosine hydroxylase. Journal of neurobiology, 54(4), pp.618-627.

Fuchs, S., Rende, E., Crisanti, A. and Nolan, T., 2014. Disruption of aminergic signalling reveals novel compounds with distinct inhibitory effects on mosquito reproduction, locomotor function and survival. Scientific reports, 4(1), p.5526.

Gainetdinov, R.R., Hoener, M.C. and Berry, M.D., 2018. Trace amines and their receptors. Pharmacological reviews, 70(3), pp.549-620.

Gajardo-Gómez, R., Labra, V.C. and Orellana, J.A., 2016. Connexins and pannexins: new insights into microglial functions and dysfunctions. Frontiers in molecular neuroscience, 9, p.86.

Gannett, L. and Griesemer, J.R., 2004. 4 Classical genetics and the geography of genes. In Classical genetic research and its legacy (pp. 57-87). Routledge.

Gautam, N.K., Verma, P. and Tapadia, M.G., 2017. Drosophila Malpighian tubules: a model for understanding kidney development, function, and disease. Kidney Development and Disease, pp.3-25.

Gebrie, A., 2023. Transposable elements as essential elements in the control of gene expression. Mobile DNA, 14(1), p.9.

Geer, B.W., 1966. Utilization of D-amino acids for growth by Drosophila melanogaster larvae. The Journal of Nutrition, 90(1), pp.31-39.

Genath, A., Sharbati, S., Buer, B., Nauen, R. and Einspanier, R., 2020. Comparative transcriptomics indicates endogenous differences in detoxification capacity after formic acid treatment between honey bees and varroa mites. Scientific reports, 10(1), p.21943.

Georgiades, M., Alampounti, A., Somers, J., Su, M.P., Ellis, D.A., Bagi, J., Terrazas-Duque, D., Tytheridge, S., Ntabaliba, W., Moore, S. and Albert, J.T., 2023. Hearing of malaria mosquitoes is modulated by a beta-adrenergic-like octopamine receptor which serves as insecticide target. Nature Communications, 14(1), p.4338.

Ghosh, S.K. and Kumar, A., 2018. Marcello Malpighi (1628-1694): Pioneer of microscopic anatomy and exponent of the scientific revolution of the 17 th Century. European Journal of Anatomy, 22(5), pp.433-439.

Gillmor, C.S. and Lukowitz, W., 2020. EMS mutagenesis of Arabidopsis seeds. Plant Embryogenesis: Methods and Protocols, pp.15-23.

Giuliani, F., Giuliani, G., Bauer, R. and Rabouille, C., 2013. Innexin 3, a new gene required for dorsal closure in Drosophila embryo. PloS one, 8(7), p.e69212.

Gleason, K.M., 2017. Hermann Joseph Muller's Study of X-rays as a Mutagen, (1926-1927). Arizona State University. School of Life Sciences. Center for Biology and Society. Embryo Project Encyclopedia. | Arizona Board of Regents.

Gloaguen, Y., Morton, F., Daly, R., Gurden, R., Rogers, S., Wandy, J., Wilson, D., Barrett, M. and Burgess, K., 2017. PiMP my metabolome: an integrated, webbased tool for LC-MS metabolomics data. Bioinformatics, 33(24), pp.4007-4009.

Golubnitschaja, O. and Costigliola, V., 2017. Predictive, preventive and personalised medicine as the medicine of the future: anticipatory scientific innovation and advanced medical services. Anticipation and medicine, pp.69-85.

Green, M.M., 2010. 2010: A century of Drosophila genetics through the prism of the white gene. Genetics, 184(1), pp.3-7.

Gu, G.G. and Singh, S., 1997. Modulation of the dihydropyridine-sensitive calcium channels in Drosophila by a phospholipase C-mediated pathway. Journal of neurobiology, 33(3), pp.265-275.

Güiza, J., Barría, I., Sáez, J.C. and Vega, J.L., 2018. Innexins: expression, regulation, and functions. *Frontiers in physiology*, 9, p.1414.

Guillemette, C., 2003. Pharmacogenomics of human UDP-glucuronosyltransferase enzymes. The pharmacogenomics journal, 3(3), pp.136-158.

Gullan, P.J. and Cranston, P.S., 2014. The insects: an outline of entomology. John Wiley & Sons.

Gurevich, V.V. and Gurevich, E.V., 2019. GPCR signaling regulation: the role of GRKs and arrestins. Frontiers in pharmacology, 10, p.125.

Hamasaka, Y. and Nässel, D.R., 2006. Mapping of serotonin, dopamine, and histamine in relation to different clock neurons in the brain of Drosophila. Journal of Comparative Neurology, 494(2), pp.314-330.

Halberg, K.A., Terhzaz, S., Cabrero, P., Davies, S.A. and Dow, J.A., 2015. Tracing the evolutionary origins of insect renal function. *Nature* communications, 6(1), p.6800.

Han, K.A., Millar, N.S. and Davis, R.L., 1998. A Novel Octopamine Receptor with Preferential Expression inDrosophila Mushroom Bodies. Journal of Neuroscience, 18(10), pp.3650-3658.

Hardin, P.E., Hall, J.C. and Rosbash, M., 1990. Feedback of the Drosophila period gene product on circadian cycling of its messenger RNA levels. *Nature*, *343*(6258), pp.536-540.

Harbola, A., Negi, D., Manchanda, M. and Kesharwani, R.K., 2022. Bioinformatics and biological data mining. In Bioinformatics (pp. 457-471). Academic Press.

Harrison, B.R., Wang, L., Gajda, E., Hoffman, E.V., Chung, B.Y., Pletcher, S.D., Raftery, D. and Promislow, D.E., 2020. The metabolome as a link in the genotype-phenotype map for peroxide resistance in the fruit fly, Drosophila melanogaster. BMC genomics, 21, pp.1-22.

Hasebe, M. and Shiga, S., 2021. Oviposition-promoting pars intercerebralis neurons show period-dependent photoperiodic changes in their firing activity in the bean bug. Proceedings of the National Academy of Sciences, 118(9), p.e2018823118.

Hay, A.E., Deborde, C., Dussarrat, T., Moing, A., Millery, A., Hoang, T.P.T., Touboul, D., Rey, M., Ledru, L., Ibanez, S. and Pétriacq, P., 2024. Comparative metabolomics reveals how the severity of predation by the invasive insect Cydalima perspectalis modulates the metabolism re-orchestration of native Buxus sempervirens. Plant Biology.

Hayashi, T., Katoh, L., Ozoe, F. and Ozoe, Y., 2021. Structure-dependent receptor subtype selectivity and G protein subtype preference of heterocyclic agonists in heterologously expressed silkworm octopamine receptors. Pesticide Biochemistry and Physiology, 177, p.104895.

He, L., Vasiliou, K. and Nebert, D.W., 2009. Analysis and update of the human solute carrier (SLC) gene superfamily. Human genomics, 3, pp.1-12.

Heigwer, F., Port, F. and Boutros, M., 2018. RNA interference (RNAi) screening in Drosophila. Genetics, 208(3), pp.853-874.

Hein, L., Altman, J.D. and Kobilka, B.K., 1999. Two functionally distinct α2-adrenergic receptors regulate sympathetic neurotransmission. Nature, 402(6758), pp.181-184.

Heinze, S., 2017. Unraveling the neural basis of insect navigation. Current opinion in insect science, 24, pp.58-67.

Heisenberg, M., 1998. What do the mushroom bodies do for the insect brain? An introduction. Learning & memory, 5(1), pp.1-10.

Helvig, C., Tijet, N., Feyereisen, R., Walker, F.A. and Restifo, L.L., 2004. Drosophila melanogaster CYP6A8, an insect P450 that catalyzes lauric acid (ω -1)-hydroxylation. Biochemical and biophysical research communications, 325(4), pp.1495-1502.

Hering, L., Rahman, M., Potthoff, S.A., Rump, L.C. and Stegbauer, J., 2020. Role of α 2-adrenoceptors in hypertension: focus on renal sympathetic

neurotransmitter release, inflammation, and sodium homeostasis. Frontiers in Physiology, 11, p.566871.

Hilliker, A.J., Duyf, B., Evans, D. and Phillips, J.P., 1992. Urate-null rosy mutants of Drosophila melanogaster are hypersensitive to oxygen stress. Proceedings of the National Academy of Sciences, 89(10), pp.4343-4347.

Hodgetts, R.B. and O'Keefe, S.L., 2006. Dopa decarboxylase: a model geneenzyme system for studying development, behavior, and systematics. Annual review of entomology, 51(1), pp.259-284.

Holcroft, C.E., Jackson, W.D., Lin, W.H., Bassiri, K., Baines, R.A. and Phelan, P., 2013. Innexins Ogre and Inx2 are required in glial cells for normal postembryonic development of the Drosophila central nervous system. Journal of cell science, 126(17), pp.3823-3834.

Hoffmann, J.A., 2003. The immune response of Drosophila. *Nature*, 426(6962), pp.33-38.

Hu, B., Zhang, S.H., Ren, M.M., Tian, X.R., Wei, Q., Mburu, D.K. and Su, J.Y., 2019. The expression of Spodoptera exigua P450 and UGT genes: tissue specificity and response to insecticides. Insect Science, 26(2), pp.199-216.

Huang, J., Liu, W., Qi, Y.X., Luo, J. and Montell, C., 2016. Neuromodulation of courtship drive through tyramine-responsive neurons in the Drosophila brain. Current Biology, 26(17), pp.2246-2256.

Huang, R.C., 2018. The discoveries of molecular mechanisms for the circadian rhythm: The 2017 Nobel Prize in Physiology or Medicine. *Biomedical journal*, 41(1), pp.5-8.

Hughes, A.L., 2014. Evolutionary diversification of insect innexins. Journal of Insect Science, 14(1), p.221.

lijima, M., Ohnuki, J., Sato, T., Sugishima, M. and Takano, M., 2019. Coupling of redox and structural states in cytochrome P450 reductase studied by molecular dynamics simulation. Scientific reports, 9(1), p.9341.

Ingham, P.W. and McMahon, A.P., 2001. Hedgehog signaling in animal development: paradigms and principles. *Genes & development*, *15*(23), pp.3059-3087.

Jack, J. and Myette, G., 1999. Mutations that alter the morphology of the malpighian tubules in Drosophila. Development genes and evolution, 209, pp.546-554.

Jiang, Y. and Reichert, H., 2013. Analysis of neural stem cell self-renewal and differentiation by transgenic RNAi in Drosophila. Archives of biochemistry and biophysics, 534(1-2), pp.38-43.

Johnson, O., Becnel, J. and Nichols, C.D., 2009. Serotonin 5-HT2 and 5-HT1A-like receptors differentially modulate aggressive behaviors in Drosophila melanogaster. Neuroscience, 158(4), pp.1292-1300.

Juárez Olguín, H., Calderón Guzmán, D., Hernández García, E. and Barragán Mejía, G., 2016. The role of dopamine and its dysfunction as a consequence of oxidative stress. Oxidative medicine and cellular longevity, 2016(1), p.9730467.

Kaminker, J.S., Bergman, C.M., Kronmiller, B., Carlson, J., Svirskas, R., Patel, S., Frise, E., Wheeler, D.A., Lewis, S.E., Rubin, G.M. and Ashburner, M., 2002. The transposable elements of the Drosophila melanogaster euchromatin: a genomics perspective. Genome biology, 3, pp.1-20.

Kamleh, M.A., Dow, J.A. and Watson, D.G., 2009. Applications of mass spectrometry in metabolomic studies of animal model and invertebrate systems. Briefings in Functional Genomics and Proteomics, 8(1), pp.28-48.

Kamleh, M.A., Hobani, Y., Dow, J.A.T. and Watson, D.G., 2008. Metabolomic profiling of Drosophila using liquid chromatography Fourier transform mass spectrometry. FEBS letters, 582(19), pp.2916-2922.

Kanehisa, M., Furumichi, M., Sato, Y., Matsuura, Y. and Ishiguro-Watanabe, M., 2025. KEGG: biological systems database as a model of the real world. *Nucleic acids research*, *53*(D1), pp.D672-D677.

Kapoor, D., Khan, A., O'Donnell, M.J. and Kolosov, D., 2021. Novel mechanisms of epithelial ion transport: insights from the cryptonephridial system of lepidopteran larvae. Current Opinion in Insect Science, 47, pp.53-61.

Kaufman, T.C., 2017. A short history and description of Drosophila melanogaster classical genetics: Chromosome aberrations, forward genetic screens, and the nature of mutations. Genetics, 206(2), pp.665-689.

Kaushik, P., Gorin, F. and Vali, S., 2007. Dynamics of tyrosine hydroxylase mediated regulation of dopamine synthesis. Journal of computational neuroscience, 22, pp.147-160.

Keven Williams, K. and Watsky, M.A., 2002. Gap junctional communication in the human corneal endothelium and epithelium. Current eye research, 25(1), pp.29-36.

Koehler, S. and Huber, T.B., 2023. Insights into human kidney function from the study of Drosophila. Pediatric Nephrology, pp.1-13.

Komel, S., 2023. Technology in scientific practice: how HJ Muller used the fruit fly to investigate the X-ray machine. History and philosophy of the life sciences, 45(2), p.22.

Koval, M., Isakson, B.E. and Gourdie, R.G., 2014. Connexins, pannexins and innexins: protein cousins with overlapping functions. *FEBS letters*, *588*(8), p.1185.

Krause, S.A., Overend, G., Dow, J.A. and Leader, D.P., 2022. FlyAtlas 2 in 2022: enhancements to the Drosophila melanogaster expression atlas. Nucleic Acids Research, 50(D1), pp.D1010-D1015.

Kukurba, K.R. and Montgomery, S.B., 2015. RNA sequencing and analysis. Cold Spring Harbor Protocols, 2015(11), pp.pdb-top084970.

Kyriacou, C.P. and Tauber, E., 2010. Genes and Genomic Searches. in-Chief, Encyclopedia of Animal Behavior, 1, pp.12-20.

Lange, A.B., 2009. Tyramine: from octopamine precursor to neuroactive chemical in insects. General and comparative endocrinology, 162(1), pp.18-26.

Láruson, Á.J., Yeaman, S. and Lotterhos, K.E., 2020. The importance of genetic redundancy in evolution. Trends in ecology & evolution, 35(9), pp.809-822.

Lawrence, P.A., 1992. The making of a fly: the genetics of animal design. Blackwell Scientific Publications Ltd.

Leader, D.P., Krause, S.A., Pandit, A., Davies, S.A. and Dow, J.A.T., 2018. FlyAtlas 2: a new version of the Drosophila melanogaster expression atlas with

RNA-Seq, miRNA-Seq and sex-specific data. Nucleic acids research, 46(D1), pp.D809-D815.

Lechner, H., Josten, F., Fuss, B., Bauer, R. and Hoch, M., 2007. Cross regulation of intercellular gap junction communication and paracrine signaling pathways during organogenesis in Drosophila. *Developmental biology*, 310(1), pp.23-34.

Lee, T., Lee, A. and Luo, L., 1999. Development of the Drosophila mushroom bodies: sequential generation of three distinct types of neurons from a neuroblast. Development, 126(18), pp.4065-4076.

Lee, G., Jang, H. and Oh, Y., 2023. The role of diuretic hormones (DHs) and their receptors in Drosophila. BMB reports, 56(4), p.209.

Lee, H.G., Rohila, S. and Han, K.A., 2009. The octopamine receptor OAMB mediates ovulation via Ca2+/calmodulin-dependent protein kinase II in the Drosophila oviduct epithelium. PloS one, 4(3), p.e4716.

Lee, H.G., Seong, C.S., Kim, Y.C., Davis, R.L. and Han, K.A., 2003. Octopamine receptor OAMB is required for ovulation in Drosophila melanogaster. Developmental biology, 264(1), pp.179-190.

Lee, J.L. and Streuli, C.H., 2014. Integrins and epithelial cell polarity. Journal of cell science, 127(15), pp.3217-3225.

Lee, P.T., Zirin, J., Kanca, O., Lin, W.W., Schulze, K.L., Li-Kroeger, D., Tao, R., Devereaux, C., Hu, Y., Chung, V. and Fang, Y., 2018. A gene-specific T2A-GAL4 library for Drosophila. elife, 7, p.e35574.

Lee, S.A., Kim, V., Choi, B., Lee, H., Chun, Y.J., Cho, K.S. and Kim, D., 2023. Functional characterization of drosophila melanogaster CYP6A8 fatty acid hydroxylase. Biomolecules & Therapeutics, 31(1), p.82.

Lehmann, C., Lechner, H., Loer, B., Knieps, M., Herrmann, S., Famulok, M., Bauer, R. and Hoch, M., 2006. Heteromerization of innexin gap junction proteins regulates epithelial tissue organization in Drosophila. Molecular biology of the cell, 17(4), pp.1676-1685.

Lemaitre, B., Nicolas, E., Michaut, L., Reichhart, J.M. and Hoffmann, J.A., 1996. The dorsoventral regulatory gene cassette spätzle/Toll/cactus controls the potent antifungal response in Drosophila adults. *Cell*, 86(6), pp.973-983.

Lemaitre, B. and Hoffmann, J., 2007. The host defense of Drosophila melanogaster. *Annu. Rev. Immunol.*, 25(1), pp.697-743.

Lewis, E.B., 1978. A gene complex controlling segmentation in Drosophila. *Nature*, 276(5688), pp.565-570.

Li, H., Janssens, J., De Waegeneer, M., Kolluru, S.S., Davie, K., Gardeux, V., Saelens, W., David, F.P., Brbić, M., Spanier, K. and Leskovec, J., 2022. Fly Cell Atlas: A single-nucleus transcriptomic atlas of the adult fruit fly. Science, 375(6584), p.eabk2432.

Li, J., Liu, X., Xu, L., Li, W., Yao, Q., Yin, X., Wang, Q., Tan, W., Xing, W. and Liu, D., 2023. Low nitrogen stress-induced transcriptome changes revealed the molecular response and tolerance characteristics in maintaining the C/N balance of sugar beet (Beta vulgaris L.). Frontiers in Plant Science, 14, p.1164151.

Li, X., Rommelaere, S., Kondo, S. and Lemaitre, B., 2020. Renal purge of hemolymphatic lipids prevents the accumulation of ROS-induced inflammatory oxidized lipids and protects Drosophila from tissue damage. Immunity, 52(2), pp.374-387.

Li, Y., Ding, Y. and Pan, L., 2022. Effects of increasing temperature and aestivation on biogenic amines, signal transduction pathways and metabolic enzyme activities in the sea cucumber (Apostichopus japonicus). Marine Biology, 169, pp.1-16.

Li, Y., Li, L., Stephens, M.J., Zenner, D., Murray, K.C., Winship, I.R., Vavrek, R., Baker, G.B., Fouad, K. and Bennett, D.J., 2014. Synthesis, transport, and metabolism of serotonin formed from exogenously applied 5-HTP after spinal cord injury in rats. Journal of Neurophysiology, 111(1), pp.145-163.

Lim, J., Sabandal, P.R., Fernandez, A., Sabandal, J.M., Lee, H.G., Evans, P. and Han, K.A., 2014. The octopamine receptor OctB2R regulates ovulation in Drosophila melanogaster. PloS one, 9(8), p.e104441.

Link, N. and Bellen, H.J., 2020. Using Drosophila to drive the diagnosis and understand the mechanisms of rare human diseases. Development, 147(21), p.dev191411.

Linton, S.M. and O'Donnell, M.J., 1999. Contributions of K+: Cl- cotransport and Na+/K+-ATPase to basolateral ion transport in malpighian tubules of Drosophila melanogaster. Journal of Experimental Biology, 202(11), pp.1561-1570.

Liu, C., Meng, Z., Wiggin, T.D., Yu, J., Reed, M.L., Guo, F., Zhang, Y., Rosbash, M. and Griffith, L.C., 2019. A serotonin-modulated circuit controls sleep architecture to regulate cognitive function independent of total sleep in Drosophila. Current Biology, 29(21), pp.3635-3646.

Liu, H., Bebu, I. and Li, X., 2010. Microarray probes and probe sets. Frontiers in bioscience (Elite edition), 2, p.325.

Liu, W.W. and Wilson, R.I., 2013. Glutamate is an inhibitory neurotransmitter in the Drosophila olfactory system. Proceedings of the National Academy of Sciences, 110(25), pp.10294-10299.

Lowe, R., Shirley, N., Bleackley, M., Dolan, S. and Shafee, T., 2017. Transcriptomics technologies. PLoS computational biology, 13(5), p.e1005457.

Luo, J., Lushchak, O.V., Goergen, P., Williams, M.J. and Nässel, D.R., 2014. Drosophila insulin-producing cells are differentially modulated by serotonin and octopamine receptors and affect social behavior. PloS one, 9(6), p.e99732.

Lv, H., 2013. Mass spectrometry-based metabolomics towards understanding of gene functions with a diversity of biological contexts. Mass Spectrometry Reviews, 32(2), pp.118-128.

Maan, K., Baghel, R., Dhariwal, S., Sharma, A., Bakhshi, R. and Rana, P., 2023. Metabolomics and transcriptomics based multi-omics integration reveals radiation-induced altered pathway networking and underlying mechanism. NPJ Systems Biology and Applications, 9(1), p.42.

Machado Almeida, P., Lago Solis, B., Stickley, L., Feidler, A. and Nagoshi, E., 2021. Neurofibromin 1 in mushroom body neurons mediates circadian wake drive through activating cAMP-PKA signaling. Nature Communications, 12(1), p.5758.

MacPherson, M.R., Pollock, V.P., Kean, L., Southall, T.D., Giannakou, M.E., Broderick, K.E., Dow, J.A., Hardie, R.C. and Davies, S.A., 2005. Transient receptor potential-like channels are essential for calcium signaling and fluid transport in a Drosophila epithelium. Genetics, 169(3), pp.1541-1552.

Malakoff, D., 2000. The rise of the mouse, biomedicine's model mammal. Science, 288(5464), pp.248-253.

Malenka, R. ed., 2010. Intercellular communication in the nervous system. Academic Press.

Maloy, S. and Hughes, K., 2001. Brenner's Encyclopedia of Genetics. Utah.: Academic Press.

Malpighi, M., 1666. De viscerum structura exercitatio anatomica. Accedit dissertatio ejusdem de polypo cordis. Bologna: Giacomo Monti

Malpighi, M., Marcelli Malpighii philosophi & medici Bononiensis dissertatio epistolica de bombyce: Societati Regiae, Londini ad Scientiam Naturalem promovendam institutae, dicata. Apud Joannem Martyn & Jacobum Allestry.

Manickam, S., Rajagopalan, V.R., Kambale, R., Rajasekaran, R., Kanagarajan, S. and Muthurajan, R., 2023. Plant metabolomics: current initiatives and future prospects. Current Issues in Molecular Biology, 45(11), pp.8894-8906.

Maqueira, B., Chatwin, H. and Evans, P.D., 2005. Identification and characterization of a novel family of Drosophilaß-adrenergic-like octopamine G-protein coupled receptors. Journal of neurochemistry, 94(2), pp.547-560.

Marcobal, A., De Las Rivas, B., Landete, J.M., Tabera, L. and Muñoz, R., 2012. Tyramine and phenylethylamine biosynthesis by food bacteria. Critical reviews in food science and nutrition, 52(5), pp.448-467.

Markow, T.A., 2015. The secret lives of Drosophila flies. elife, 4, p.e06793.

Marsac, R., Pinson, B., Saint-Marc, C., Olmedo, M., Artal-Sanz, M., Daignan-Fornier, B. and Gomes, J.E., 2019. Purine homeostasis is necessary for developmental timing, germline maintenance and muscle integrity in Caenorhabditis elegans. Genetics, 211(4), pp.1297-1313.

Marsh, J.L. and Thompson, L.M., 2006. Drosophila in the study of neurodegenerative disease. Neuron, 52(1), pp.169-178.

Matter, K. and Balda, M.S., 2003. Signalling to and from tight junctions. Nature reviews Molecular cell biology, 4(3), pp.225-237.

McCullers, T.J. and Steiniger, M., 2017. Transposable elements in Drosophila. Mobile genetic elements, 7(3), pp.1-18.

McEwen, B.S., 1987. Glucocorticoid-biogenic amine interactions in relation to mood and behavior. Biochemical pharmacology, 36(11), pp.1755-1763.

McGuire, S.E., Roman, G. and Davis, R.L., 2004. Gene expression systems in Drosophila: a synthesis of time and space. TRENDS in Genetics, 20(8), pp.384-391.

McGinnis, W. and Krumlauf, R., 1992. Homeobox genes and axial patterning. *Cell*, *68*(2), pp.283-302.

Mège, R.M. and Ishiyama, N., 2017. Integration of cadherin adhesion and cytoskeleton at adherens junctions. Cold Spring Harbor perspectives in biology, 9(5), p.a028738.

Millburn, G.H., Crosby, M.A., Gramates, L.S., Tweedie, S. and FlyBase Consortium, 2016. FlyBase portals to human disease research using Drosophila models. Disease Models & Mechanisms, 9(3), pp.245-252.

Miller, D.E., Cook, K.R., Yeganeh Kazemi, N., Smith, C.B., Cockrell, A.J., Hawley, R.S. and Bergman, C.M., 2016. Rare recombination events generate sequence diversity among balancer chromosomes in Drosophila melanogaster. Proceedings of the National Academy of Sciences, 113(10), pp.E1352-E1361.

Miller, J., Chi, T., Kapahi, P., Kahn, A.J., Kim, M.S., Hirata, T., Romero, M.F., Dow, J.A. and Stoller, M.L., 2013. Drosophila melanogaster as an emerging translational model of human nephrolithiasis. The Journal of urology, 190(5), pp.1648-1656.

Miyauchi, Y., Takechi, S. and Ishii, Y., 2021. Functional interaction between cytochrome P450 and UDP-glucuronosyltransferase on the endoplasmic reticulum membrane: one of post-translational factors which possibly contributes to their

inter-individual differences. Biological and Pharmaceutical Bulletin, 44(11), pp.1635-1644.

Monastirioti, M., 1999. Biogenic amine systems in the fruit fly Drosophila melanogaster. Microscopy research and technique, 45(2), pp.106-121.

Monastirioti, M., Gorczyca, M., Rapus, J., Eckert, M., White, K. and Budnik, V., 1995. Octopamine immunoreactivity in the fruit fly Drosophila melanogaster. Journal of Comparative Neurology, 356(2), pp.275-287.

Morgan, T.H., 1910. Sex limited inheritance in Drosophila. Science, 32(812), pp.120-122.

Musselman, L.P., Fink, J.L. and Baranski, T.J., 2019. Similar effects of high-fructose and high-glucose feeding in a Drosophila model of obesity and diabetes. *PLoS One*, *14*(5), p.e0217096.

Mourikis, P., Hurlbut, G.D. and Artavanis-Tsakonas, S., 2006. Enigma, a mitochondrial protein affecting lifespan and oxidative stress response in Drosophila. Proceedings of the National Academy of Sciences, 103(5), pp.1307-1312.

Muñoz-López, M. and García-Pérez, J.L., 2010. DNA transposons: nature and applications in genomics. Current genomics, 11(2), pp.115-128.

Murtazina, R.Z., Kuvarzin, S.R. and Gainetdinov, R.R., 2021. TAARs and Neurodegenerative and Psychiatric Disorders. In Handbook of Neurotoxicity (pp. 1-18). Cham: Springer International Publishing.

Mustard, J.A., Beggs, K.T. and Mercer, A.R., 2005. Molecular biology of the invertebrate dopamine receptors. Archives of Insect Biochemistry and Physiology: Published in Collaboration with the Entomological Society of America, 59(3), pp.103-117.

Muthubharathi, B.C., Gowripriya, T. and Balamurugan, K., 2021. Metabolomics: small molecules that matter more. Molecular omics, 17(2), pp.210-229.

Nagoshi, E., 2018. Drosophila models of sporadic Parkinson's disease. International journal of molecular sciences, 19(11), p.3343.

Nagy, L. and Hiripi, L., 2002. Role of tyrosine, DOPA and decarboxylase enzymes in the synthesis of monoamines in the brain of the locust. Neurochemistry international, 41(1), pp.9-16.

Nakagawa, H., Maehara, S., Kume, K., Ohta, H. and Tomita, J., 2022. Biological functions of α2-adrenergic-like octopamine receptor in Drosophila melanogaster. Genes, Brain and Behavior, 21(6), p.e12807.

Nakagawa, H., Nakane, S., Ban, G., Tomita, J. and Kume, K., 2022. Effects of Damino acids on sleep in Drosophila. Biochemical and Biophysical Research Communications, 589, pp.180-185.

National Research Council, 2000. Using model animals to assess and understand developmental toxicity. Scientific Frontiers in Developmental Toxicology and Risk Assessment.

Nässel, D.R. and Winther, Å.M., 2010. Drosophila neuropeptides in regulation of physiology and behavior. *Progress in neurobiology*, 92(1), pp.42-104.

Naz, F., Fatima, M., Naseem, S., Khan, W., Mondal, A.C. and Siddique, Y.H., 2020. Ropinirole silver nanocomposite attenuates neurodegeneration in the transgenic Drosophila melanogaster model of Parkinson's disease. Neuropharmacology, 177, p.108216.

Neckameyer, W.S., 2010. A trophic role for serotonin in the development of a simple feeding circuit. Developmental neuroscience, 32(3), pp.217-237.

Nüsslein-Volhard, C. and Wieschaus, E., 1980. Mutations affecting segment number and polarity in Drosophila. *Nature*, 287(5785), pp.795-801.

Obaeda, B.A., 2021. Yeasts as a source of single cell protein production: A review. Plant Archives, 21(1), pp.324-328.

Ocampo, A.B., Cabinta, J.G.Z., Padilla, H.V.J., Yu, E.T. and Nellas, R.B., 2023. Specificity of Monoterpene Interactions with Insect Octopamine and Tyramine Receptors: Insights from in Silico Sequence and Structure Comparison. ACS omega, 8(4), pp.3861-3871.

Ogienko, A.A., Omelina, E.S., Bylino, O.V., Batin, M.A., Georgiev, P.G. and Pindyurin, A.V., 2022. Drosophila as a model organism to study basic mechanisms of longevity. International Journal of Molecular Sciences, 23(19), p.11244.

O'Grady, P.M., Baker, R.H., Durando, C.M., Etges, W.J. and DeSalle, R., 2001. Polytene chromosomes as indicators of phylogeny in several species groups of Drosophila. BMC evolutionary biology, 1(1), pp.1-6.

O'Hare, K. and Rubin, G.M., 1983. Structures of P transposable elements and their sites of insertion and excision in the Drosophila melanogaster genome. Cell, 34(1), pp.25-35.

Ojha, S. and Tapadia, M.G., 2020. Non-apoptotic function of caspase-3 in morphogenesis of epithelial tubes of Drosophila renal system. bioRxiv, pp.2020-08.

Ong, C., Yung, L.Y.L., Cai, Y., Bay, B.H. and Baeg, G.H., 2015. Drosophila melanogaster as a model organism to study nanotoxicity. Nanotoxicology, 9(3), pp.396-403.

Orchard, I., Leyria, J., Al-Dailami, A. and Lange, A.B., 2021. Fluid secretion by Malpighian tubules of Rhodnius prolixus: Neuroendocrine control with new insights from a transcriptome analysis. Frontiers in Endocrinology, 12, p.722487.

Oshima, K. and Fehon, R.G., 2011. Analysis of protein dynamics within the septate junction reveals a highly stable core protein complex that does not include the basolateral polarity protein Discs large. Journal of cell science, 124(16), pp.2861-2871.

Ouyang, Y., Wu, Q., Li, J., Sun, S. and Sun, S., 2020. S-adenosylmethionine: a metabolite critical to the regulation of autophagy. Cell proliferation, 53(11), p.e12891.

Öztürk-Çolak, A., Marygold, S.J., Antonazzo, G., Attrill, H., Goutte-Gattat, D., Jenkins, V.K., Matthews, B.B., Millburn, G., Dos Santos, G. and Tabone, C.J., 2024. FlyBase: updates to the Drosophila genes and genomes database. Genetics, 227(1), p.iyad211.

Pandey, U.B. and Nichols, C.D., 2011. Human disease models in Drosophila melanogaster and the role of the fly in therapeutic drug discovery. Pharmacological reviews, 63(2), pp.411-436.

Parasram, K., Zuccato, A., Shin, M., Willms, R., DeVeale, B., Foley, E. and Karpowicz, P., 2024. The emergence of circadian timekeeping in the intestine. Nature Communications, 15(1), p.1788.

Peel, A.D., Chipman, A.D. and Akam, M., 2005. Arthropod segmentation: beyond the Drosophila paradigm. *Nature Reviews Genetics*, *6*(12), pp.905-916.

Perez, R.E., Basu, A., Nabit, B.P., Harris, N.A., Folkes, O.M., Patel, S., Gilsbach, R., Hein, L. and Winder, D.G., 2020. α2A-adrenergic heteroreceptors are required for stress-induced reinstatement of cocaine conditioned place preference. Neuropsychopharmacology, 45(9), pp.1473-1481.

Perkins, L.A., Holderbaum, L., Tao, R., Hu, Y., Sopko, R., McCall, K., Yang-Zhou, D., Flockhart, I., Binari, R., Shim, H.S. and Miller, A., 2015. The transgenic RNAi project at Harvard Medical School: resources and validation. Genetics, 201(3), pp.843-852.

Perl, A., Hanczko, R., Telarico, T., Oaks, Z. and Landas, S., 2011. Oxidative stress, inflammation and carcinogenesis are controlled through the pentose phosphate pathway by transaldolase. Trends in molecular medicine, 17(7), pp.395-403.

Petitgas, C., Seugnet, L., Dulac, A., Matassi, G., Mteyrek, A., Fima, R., Strehaiano, M., Dagorret, J., Chérif-Zahar, B., Marie, S. and Ceballos-Picot, I., 2024. Metabolic and neurobehavioral disturbances induced by purine recycling deficiency in Drosophila. Elife, 12, p.RP88510.

Pézier, A.P., Jezzini, S.H., Bacon, J.P. and Blagburn, J.M., 2016. Shaking B mediates synaptic coupling between auditory sensory neurons and the giant fiber of Drosophila melanogaster. PLoS One, 11(4), p.e0152211.

Phelan, P., Bacon, J.P., Davies, J.A., Stebbings, L.A. and Todman, M.G., 1998. Innexins: a family of invertebrate gap-junction proteins. Trends in Genetics, 14(9), pp.348-349.

Phelan, P., 2005. Innexins: members of an evolutionarily conserved family of gap-junction proteins. *Biochimica et Biophysica Acta (BBA)-Biomembranes*, 1711(2), pp.225-245.

Philipp, M., Brede, M. and Hein, L., 2002. Physiological significance of α2-adrenergic receptor subtype diversity: one receptor is not enough. American Journal of Physiology-Regulatory, Integrative and Comparative Physiology, 283(2), pp.R287-R295.

Pina, C. and Pignoni, F., 2012. Tubby-RFP balancers for developmental analysis: FM7c 2xTb-RFP, CyO 2xTb-RFP, and TM3 2xTb-RFP. genesis, 50(2), pp.119-123.

Pirri, J.K., McPherson, A.D., Donnelly, J.L., Francis, M.M. and Alkema, M.J., 2009. A tyramine-gated chloride channel coordinates distinct motor programs of a Caenorhabditis elegans escape response. Neuron, 62(4), pp.526-538.

Pisokas, I., Heinze, S. and Webb, B., 2020. The head direction circuit of two insect species. Elife, 9, p.e53985.

Pizzorno, J., 2014. Glutathione!. Integrative Medicine: A Clinician's Journal, 13(1), p.8.

Podda, M.V., Riccardi, E., D'Ascenzo, M., Azzena, G.B. and Grassi, C., 2010. Dopamine D1-like receptor activation depolarizes medium spiny neurons of the mouse nucleus accumbens by inhibiting inwardly rectifying K+ currents through a cAMP-dependent protein kinase A-independent mechanism. Neuroscience, 167(3), pp.678-690.

Porokhin, V., Amin, S.A., Nicks, T.B., Gopinarayanan, V.E., Nair, N.U. and Hassoun, S., 2021. Analysis of metabolic network disruption in engineered microbial hosts due to enzyme promiscuity. Metabolic Engineering Communications, 12, p.e00170.

Port, F. and Boutros, M., 2022. Tissue-specific CRISPR-Cas9 screening in Drosophila. In *Drosophila: Methods and Protocols* (pp. 157-176). New York, NY: Springer US.

Pray, L.A., 2008. Transposons: The jumping genes. Nature education, 1(1), p.204.

Proudman, R.G., Akinaga, J. and Baker, J.G., 2022. The signaling and selectivity of α -adrenoceptor agonists for the human α 2A, α 2B and α 2C-adrenoceptors and comparison with human α 1 and β -adrenoceptors. Pharmacology research & perspectives, 10(5), p.e01003.

Qi, C. and Lee, D., 2014. Pre-and postsynaptic role of dopamine D2 receptor DD2R in Drosophila olfactory associative learning. Biology, 3(4), pp.831-845.

Qi, Y.X., Xu, G., Gu, G.X., Mao, F., Ye, G.Y., Liu, W. and Huang, J., 2017. A new Drosophila octopamine receptor responds to serotonin. Insect biochemistry and molecular biology, 90, pp.61-70.

Qiao, H.H., Wang, F., Xu, R.G., Sun, J., Zhu, R., Mao, D., Ren, X., Wang, X., Jia, Y., Peng, P. and Shen, D., 2018. An efficient and multiple target transgenic RNAi technique with low toxicity in Drosophila. Nature communications, 9(1), p.4160.

Qiu, S., Cai, Y., Yao, H., Lin, C., Xie, Y., Tang, S. and Zhang, A., 2023. Small molecule metabolites: discovery of biomarkers and therapeutic targets. Signal Transduction and Targeted Therapy, 8(1), p.132.

Radford, J.C., Davies, S.A. and Dow, J.A., 2002. Systematic G-protein-coupled receptor analysis inDrosophila melanogaster identifies a leucokinin receptor with novel roles. Journal of Biological Chemistry, 277(41), pp.38810-38817.

Rao, X., Huang, X., Zhou, Z. and Lin, X., 2013. An improvement of the 2^(-delta delta CT) method for quantitative real-time polymerase chain reaction data analysis. Biostatistics, bioinformatics and biomathematics, 3(3), p.71.

Rasmuson-Lestander, A., 1995. The Drosophila Stock Centers and their implications for developmental biology. International Journal of Developmental Biology, 39, pp.765-768.

Reynolds, C.J., Turin, D.R. and Romero, M.F., 2021. Transporters and tubule crystals in the insect Malpighian tubule. Current opinion in insect science, 47, pp.82-89.

Richard, M. and Hoch, M., 2015. Drosophila eye size is determined by Innexin 2-dependent Decapentaplegic signalling. *Developmental biology*, 408(1), pp.26-40.

Richard, M., Bauer, R., Tavosanis, G. and Hoch, M., 2017. The gap junction protein Innexin3 is required for eye disc growth in Drosophila. Developmental biology, 425(2), pp.191-207.

Robinson, S.W., Herzyk, P., Dow, J.A. and Leader, D.P., 2013. FlyAtlas: database of gene expression in the tissues of Drosophila melanogaster. Nucleic acids research, 41(D1), pp.D744-D750.

Roeder, T., 1999. Octopamine in invertebrates. Progress in neurobiology, 59(5), pp.533-561.

Roeder, T., 2005. Tyramine and octopamine: ruling behavior and metabolism. Annu. Rev. Entomol., 50(1), pp.447-477.

Roeder, T., 2020. The control of metabolic traits by octopamine and tyramine in invertebrates. Journal of Experimental Biology, 223(7), p.jeb194282.

Roeder, T., Seifert, M., Kähler, C. and Gewecke, M., 2003. Tyramine and octopamine: antagonistic modulators of behavior and metabolism. Archives of Insect Biochemistry and Physiology: Published in Collaboration with the Entomological Society of America, 54(1), pp.1-13.

Rommelaere, S., Carboni, A., Juarez, J.F.B., Boquete, J.P., Abriata, L.A., Meireles, F.T.P., Rukes, V., Vincent, C., Kondo, S., Dionne, M.S. and Dal Peraro, M., 2024. A humoral stress response protects Drosophila tissues from antimicrobial peptides. Current Biology, 34(7), pp.1426-1437.

Rosato, M., Hoelscher, B., Lin, Z., Agwu, C. and Xu, F., 2021. Transcriptome analysis provides genome annotation and expression profiles in the central nervous system of Lymnaea stagnalis at different ages. BMC genomics, 22, pp.1-16.

Rosikon, K.D., Bone, M.C. and Lawal, H.O., 2023. Regulation and modulation of biogenic amine neurotransmission in Drosophila and Caenorhabditis elegans. Frontiers in Physiology, 14, p.970405.

Rouka, E., Gourgoulianni, N., Lüpold, S., Hatzoglou, C., Gourgoulianis, K., Blanckenhorn, W.U. and Zarogiannis, S.G., 2021. The Drosophila septate junctions beyond barrier function: Review of the literature, prediction of human

orthologs of the SJ-related proteins and identification of protein domain families. Acta Physiologica, 231(1), p.e13527.

Rubin, G.M. and Lewis, E.B., 2000. A brief history of Drosophila's contributions to genome research. Science, 287(5461), pp.2216-2218.

Ruddick, J.P., Evans, A.K., Nutt, D.J., Lightman, S.L., Rook, G.A. and Lowry, C.A., 2006. Tryptophan metabolism in the central nervous system: medical implications. Expert reviews in molecular medicine, 8(20), pp.1-27.

Ryerse, J.S., 1978. Developmental changes in Malpighian tubule fluid transport. Journal of Insect Physiology, 24(4), pp.315-319.

Sahu, A., Ghosh, R., Deshpande, G. and Prasad, M., 2017. A gap junction protein, Inx2, modulates calcium flux to specify border cell fate during Drosophila oogenesis. PLoS genetics, 13(1), p.e1006542.

Sahu, G., Sukumaran, S. and Bera, A.K., 2014. Pannexins form gap junctions with electrophysiological and pharmacological properties distinct from connexins. Scientific reports, 4(1), p.4955.

Saj, A., Arziman, Z., Stempfle, D., Van Belle, W., Sauder, U., Horn, T., Dürrenberger, M., Paro, R., Boutros, M. and Merdes, G., 2010. A combined ex vivo and in vivo RNAi screen for notch regulators in Drosophila reveals an extensive notch interaction network. Developmental cell, 18(5), pp.862-876.

Salzberg, S.L., 2019. Next-generation genome annotation: we still struggle to get it right. Genome biology, 20(1), pp.1-3.

Sampson, M.M., Myers Gschweng, K.M., Hardcastle, B.J., Bonanno, S.L., Sizemore, T.R., Arnold, R.C., Gao, F., Dacks, A.M., Frye, M.A. and Krantz, D.E., 2020. Serotonergic modulation of visual neurons in Drosophila melanogaster. PLoS genetics, 16(8), p.e1009003.

Samuels, D.S., Lybecker, M.C., Yang, X.F., Ouyang, Z., Bourret, T.J., Boyle, W.K., Stevenson, B., Drecktrah, D. and Caimano, M.J., 2021. Gene regulation and transcriptomics. Current issues in molecular biology, 42(1), pp.223-266.

Sayers, E.W., Bolton, E.E., Brister, J.R., Canese, K., Chan, J., Comeau, D.C., Connor, R., Funk, K., Kelly, C., Kim, S. and Madej, T., 2022. Database resources

of the national center for biotechnology information. Nucleic acids research, 50(D1), pp.D20-D26.

Scemes, E., Suadicani, S.O., Dahl, G. and Spray, D.C., 2007. Connexin and pannexin mediated cell-cell communication. Neuron glia biology, 3(3), pp.199-208.

Schaeffer, S.W., Bhutkar, A., McAllister, B.F., Matsuda, M., Matzkin, L.M., O'Grady, P.M., Rohde, C., Valente, V.L., Aguadé, M., Anderson, W.W. and Edwards, K., 2008. Polytene chromosomal maps of 11 Drosophila species: the order of genomic scaffolds inferred from genetic and physical maps. Genetics, 179(3), pp.1601-1655.

Scheiner, R., Baumann, A. and Blenau, W., 2006. Aminergic control and modulation of honeybee behaviour. Current neuropharmacology, 4(4), pp.259-276.

Scheltema, R.A., Jankevics, A., Jansen, R.C., Swertz, M.A. and Breitling, R., 2011. PeakML/mzMatch: a file format, Java library, R library, and tool-chain for mass spectrometry data analysis. Analytical chemistry, 83(7), pp.2786-2793.

Schmittgen, T.D. and Livak, K.J., 2008. Analyzing real-time PCR data by the comparative CT method. Nature protocols, 3(6), pp.1101-1108.

Schulz, D.J., Barron, A.B. and Robinson, G.E., 2002. A role for octopamine in honey bee division of labor. Brain behavior and evolution, 60(6), pp.350-359.

Schützler, N., Girwert, C., Hügli, I., Mohana, G., Roignant, J.Y., Ryglewski, S. and Duch, C., 2019. Tyramine action on motoneuron excitability and adaptable tyramine/octopamine ratios adjust Drosophila locomotion to nutritional state. Proceedings of the National Academy of Sciences, 116(9), pp.3805-3810.

Sehgal, A., Price, J.L., Man, B. and Young, M.W., 1994. Loss of circadian behavioral rhythms and per RNA oscillations in the Drosophila mutant timeless. *Science*, *263*(5153), pp.1603-1606.

Semeshin, V.F., Belyaeva, E.S., Shloma, V.V. and Zhimulev, I.F., 2004. Electron microscopy of polytene chromosomes. Drosophila Cytogenetics Protocols, pp.305-324.

Sharma, G., 2012. The human genome project and its promise. Journal of Indian College of Cardiology, 2(1), pp.1-3.

Sharma, R. and Sharma, R., 2023. Drosophila melanogaster: A Platform to Study Therapeutic Neuromodulating Interventions. Indo Global Journal of Pharmaceutical Sciences, 13, pp.22-29.

Sheehan, D., Meade, G., Foley, V.M. and Dowd, C.A., 2001. Structure, function and evolution of glutathione transferases: implications for classification of non-mammalian members of an ancient enzyme superfamily. Biochemical journal, 360(1), pp.1-16.

Shen, S., Zhan, C., Yang, C., Fernie, A.R. and Luo, J., 2023. Metabolomics-centered mining of plant metabolic diversity and function: Past decade and future perspectives. Molecular Plant, 16(1), pp.43-63.

Shih, M.F. and Wu, C.L., 2017. Gap Junctions Underlying Labile Memory. In Network Functions and Plasticity (pp. 31-50). Academic Press.

Shum, A., Zaichick, S., McElroy, G.S., D'Alessandro, K., Alasady, M.J., Novakovic, M., Peng, W., Grebenik, E.A., Chung, D., Flanagan, M.E. and Smith, R., 2023. Octopamine metabolically reprograms astrocytes to confer neuroprotection against α-synuclein. Proceedings of the National Academy of Sciences, 120(17), p.e2217396120.

Shyu, W.H., Lee, W.P., Chiang, M.H., Chang, C.C., Fu, T.F., Chiang, H.C., Wu, T. and Wu, C.L., 2019. Electrical synapses between mushroom body neurons are critical for consolidated memory retrieval in Drosophila. PLoS genetics, 15(5), p.e1008153.

Siju, K.P., De Backer, J.F. and Grunwald Kadow, I.C., 2021. Dopamine modulation of sensory processing and adaptive behavior in flies. Cell and tissue research, 383, pp.207-225.

Silva, B., Hidalgo, S. and Campusano, J.M., 2020. Dop1R1, a type 1 dopaminergic receptor expressed in Mushroom Bodies, modulates Drosophila larval locomotion. Plos one, 15(2), p.e0229671.

Silver, N., Best, S., Jiang, J. and Thein, S.L., 2006. Selection of housekeeping genes for gene expression studies in human reticulocytes using real-time PCR. BMC molecular biology, 7, pp.1-9.

Sinakevitch, I.T., Wolff, G.H., Pflüger, H.J. and Smith, B.H., 2018. Biogenic amines and neuromodulation of animal behavior. Frontiers in Systems Neuroscience, 12, p.31.

Singh, S.P., Panicker, M.M. and Soman, S., 2016. Multi-Layered Architecture of Serotonin 2A Receptor Signaling. In Serotonin and Melatonin (pp. 545-560). CRC Press.

Skaer, H.L.B., Harrison, J.B. and Maddrell, S.H.P., 1990. Physiological and structural maturation of a polarised epithelium: the Malpighian tubules of a blood-sucking insect, Rhodnius prolixus. Journal of Cell Science, 96(3), pp.537-547.

Skerrett, I.M. and Williams, J.B., 2017. A structural and functional comparison of gap junction channels composed of connexins and innexins. *Developmental neurobiology*, 77(5), pp.522-547.

Slee, R. and Bownes, M., 1990. Sex determination in Drosophila melanogaster. The Quarterly review of biology, 65(2), pp.175-204.

Smith, C.A., Want, E.J., O'Maille, G., Abagyan, R. and Siuzdak, G., 2006. XCMS: processing mass spectrometry data for metabolite profiling using nonlinear peak alignment, matching, and identification. Analytical chemistry, 78(3), pp.779-787.

Snyder, S.H., 2009. Neurotransmitters, receptors, and second messengers galore in 40 years. Journal of Neuroscience, 29(41), pp.12717-12721.

Sosinsky, G.E., Boassa, D., Dermietzel, R., Duffy, H.S., Laird, D.W., MacVicar, B., Naus, C.C., Penuela, S., Scemes, E., Spray, D.C. and Thompson, R.J., 2011. Pannexin channels are not gap junction hemichannels. Channels, 5(3), pp.193-197.

Southey, B.R., Johnson, R.W. and Rodriguez-Zas, S.L., 2023. Influence of Maternal Immune Activation and Stressors on the Hippocampal Metabolome. Metabolites, 13(8), p.881.

Speranza, L., Di Porzio, U., Viggiano, D., de Donato, A. and Volpicelli, F., 2021. Dopamine: the neuromodulator of long-term synaptic plasticity, reward and movement control. Cells, 10(4), p.735.

Stebbings, L.A., Todman, M.G., Phillips, R., Greer, C.E., Tam, J., Phelan, P., Jacobs, K., Bacon, J.P. and Davies, J.A., 2002. Gap junctions in Drosophila: developmental expression of the entire innexin gene family. *Mechanisms of development*, 113(2), pp.197-205.

Stebbings, L.A., Todman, M.G., Phelan, P., Bacon, J.P. and Davies, J.A., 2000. Two Drosophila innexins are expressed in overlapping domains and cooperate to form gap-junction channels. Molecular biology of the cell, 11(7), pp.2459-2470.

Stephenson, R. and Metcalfe, N.H., 2013. Drosophila melanogaster: a fly through its history and current use. The journal of the Royal College of Physicians of Edinburgh, 43(1), pp.70-75.

Strausfeld, N.J. and Sayre, M.E., 2020. Evolution of mushroom body inversion and associated gyriform neuropils parallel the evolved transposition of the mammalian hippocampus. bioRxiv, pp.2020-11.

Sudo, N., 2019. Biogenic amines: signals between commensal microbiota and gut physiology. Frontiers in endocrinology, 10, p.504.

Suver, M.P., Mamiya, A. and Dickinson, M.H., 2012. Octopamine neurons mediate flight-induced modulation of visual processing in Drosophila. Current Biology, 22(24), pp.2294-2302.

Svoboda, P., 2020. Key mechanistic principles and considerations concerning RNA interference. Frontiers in plant science, 11, p.1237.

Swarup, S. and Verheyen, E.M., 2012. Wnt/wingless signaling in Drosophila. *Cold Spring Harbor perspectives in biology*, 4(6), p.a007930.

Szklarczyk, D., Kirsch, R., Koutrouli, M., Nastou, K., Mehryary, F., Hachilif, R., Gable, A.L., Fang, T., Doncheva, N.T., Pyysalo, S. and Bork, P., 2023. The STRING database in 2023: protein-protein association networks and functional enrichment analyses for any sequenced genome of interest. Nucleic acids research, 51(D1), pp.D638-D646.

Taddei, A. and Gasser, S.M., 2012. Structure and function in the budding yeast nucleus. Genetics, 192(1), pp.107-129.

Takaku, Y., Hwang, J.S., Wolf, A., Böttger, A., Shimizu, H., David, C.N. and Gojobori, T., 2014. Innexin gap junctions in nerve cells coordinate spontaneous contractile behavior in Hydra polyps. Scientific reports, 4(1), p.3573.

Taormina, G., Ferrante, F., Vieni, S., Grassi, N., Russo, A. and Mirisola, M.G., 2019. Longevity: lesson from model organisms. Genes, 10(7), p.518.

Tautenhahn, R., Böttcher, C. and Neumann, S., 2008. Highly sensitive feature detection for high resolution LC/MS. BMC bioinformatics, 9, pp.1-16.

Taylor, B.N. and Cassagnol, M., 2023. Alpha-adrenergic receptors. In StatPearls [Internet]. StatPearls Publishing.

Tepass, U. and Hartenstein, V., 1994. The development of cellular junctions in the Drosophila embryo. Developmental biology, 161(2), pp.563-596.

Tepass, U., Gruszynski-DeFeo, E., Haag, T.A., Omatyar, L., Török, T. and Hartenstein, V., 1996. shotgun encodes Drosophila E-cadherin and is preferentially required during cell rearrangement in the neurectoderm and other morphogenetically active epithelia. Genes & development, 10(6), pp.672-685.

Terhzaz, S., Cabrero, P., Chintapalli, V.R., Davies, S.A. and Dow, J.A., 2010. Mislocalization of mitochondria and compromised renal function and oxidative stress resistance in Drosophila SesB mutants. Physiological genomics, 41(1), pp.33-41.

Terhzaz, S., Cabrero, P., Robben, J.H., Radford, J.C., Hudson, B.D., Milligan, G., Dow, J.A. and Davies, S.A., 2012. Mechanism and function of Drosophila capa GPCR: a desiccation stress-responsive receptor with functional homology to human neuromedinU receptor. *PloS one*, *7*(1), p.e29897.

Thomas, J.C., Saleh, E.F., Alammar, N. and Akroush, A.M., 1998. The indole alkaloid tryptamine impairs reproduction in Drosophila melanogaster. Journal of economic entomology, 91(4), pp.841-846.

Tounta, V., Liu, Y., Cheyne, A. and Larrouy-Maumus, G., 2021. Metabolomics in infectious diseases and drug discovery. Molecular omics, 17(3), pp.376-393.

Traven, A., Jelicic, B. and Sopta, M., 2006. Yeast Gal4: a transcriptional paradigm revisited. EMBO reports, 7(5), pp.496-499.

Uçar, A., 2019. Introductory Chapter: Biogenic Amines in Neurotransmission and Human Disease from the Endocrinologist's Perspective. In Biogenic Amines in Neurotransmission and Human Disease. IntechOpen.

Ueno, T., Tomita, J., Tanimoto, H., Endo, K., Ito, K., Kume, S. and Kume, K., 2012. Identification of a dopamine pathway that regulates sleep and arousal in Drosophila. Nature neuroscience, 15(11), pp.1516-1523.

Vallés, A.M. and White, K., 1988. Serotonin-containing neurons in Drosophila melanogaster: Development and distribution. Journal of Comparative Neurology, 268(3), pp.414-428.

van der Graaf, K., Srivastav, S., Singh, P., McNew, J.A. and Stern, M., 2022. The Drosophila melanogaster attP40 docking site and derivatives are insertion mutations of msp-300. PLoS One, 17(12), p.e0278598.

Van Der Zee, M., Benton, M.A., Vazquez-Faci, T., Lamers, G.E., Jacobs, C.G. and Rabouille, C., 2015. Innexin7a forms junctions that stabilize the basal membrane during cellularization of the blastoderm in Tribolium castaneum. Development, 142(12), pp.2173-2183.

Vedelek, V., Bodai, L., Grézal, G., Kovács, B., Boros, I.M., Laurinyecz, B. and Sinka, R., 2018. Analysis of Drosophila melanogaster testis transcriptome. BMC genomics, 19, pp.1-19.

Venken, K.J. and Bellen, H.J., 2007. Transgenesis upgrades for Drosophila melanogaster.

Venken, K.J. and Bellen, H.J., 2014. Chemical mutagens, transposons, and transgenes to interrogate gene function in Drosophila melanogaster. Methods, 68(1), pp.15-28.

Venter, J.C., 2000. The genome sequence of Drosophila melanogaster. Science, 287, p.5461.

Villegas, S.N., 2019. One hundred years of Drosophila cancer research: no longer in solitude. Disease models & mechanisms, 12(4), p.dmm039032.

Viola, R., Tucci, A., Timellini, G. and Fantazzini, P., 2006. NMR techniques: A non-destructive analysis to follow microstructural changes induced in ceramics. Journal of the European Ceramic Society, 26(15), pp.3343-3349.

Vonk, A., Reinart, R. and Rinken, A., 2008. Modulation of adenylyl cyclase activity in rat striatal homogenate by dopaminergic receptors. Journal of pharmacological sciences, 108(1), pp.63-70.

Walther, D.J., Peter, J.U., Bashammakh, S., Hörtnagl, H., Voits, M., Fink, H. and Bader, M., 2003. Synthesis of serotonin by a second tryptophan hydroxylase isoform. Science, 299(5603), pp.76-76.

Wang, C.T., Chen, Y.C., Wang, Y.Y., Huang, M.H., Yen, T.L., Li, H., Liang, C.J., Sang, T.K., Ciou, S.C., Yuh, C.H. and Wang, C.Y., 2012. Reduced neuronal expression of ribose-5-phosphate isomerase enhances tolerance to oxidative stress, extends lifespan, and attenuates polyglutamine toxicity in Drosophila. Aging cell, 11(1), pp.93-103.

Wang, G.H. and Wang, L.M., 2019. Recent advances in the neural regulation of feeding behavior in adult Drosophila. Journal of Zhejiang University-SCIENCE B, 20(7), pp.541-549.

Wang, J., Kean, L., Yang, J., Allan, A.K., Davies, S.A., Herzyk, P. and Dow, J.A., 2004. Function-informed transcriptome analysis of Drosophila renal tubule. Genome biology, 5, pp.1-21.

Wang, L., Zhang, S., Hadjipanteli, S., Saiz, L., Nguyen, L., Silva, E. and Kelleher, E., 2023. P-element invasion fuels molecular adaptation in laboratory populations of Drosophila melanogaster. Evolution, 77(4), pp.980-994.

Wang, P., Jia, Y., Liu, T., Jan, Y.N. and Zhang, W., 2020. Visceral mechanosensing neurons control Drosophila feeding by using Piezo as a sensor. Neuron, 108(4), pp.640-650.

Wang, S.C., Davejan, P., Hendargo, K.J., Javadi-Razaz, I., Chou, A., Yee, D.C., Ghazi, F., Lam, K.J.K., Conn, A.M., Madrigal, A. and Medrano-Soto, A., 2020. Expansion of the Major Facilitator Superfamily (MFS) to include novel transporters as well as transmembrane-acting enzymes. Biochimica et Biophysica Acta (BBA)-Biomembranes, 1862(9), p.183277.

Wang, Y., Chen, Y., Zhang, A., Chen, K. and Ouyang, P., 2023. Advances in the microbial synthesis of the neurotransmitter serotonin. Applied Microbiology and Biotechnology, 107(15), pp.4717-4725.

Wang, Z., Gerstein, M. and Snyder, M., 2009. RNA-Seq: a revolutionary tool for transcriptomics. Nature reviews genetics, 10(1), pp.57-63.

Wangler, M.F., Yamamoto, S. and Bellen, H.J., 2015. Fruit flies in biomedical research. Genetics, 199(3), pp.639-653.

Watanabe, T. and Kankel, D.R., 1992. The l (1) ogre gene of Drosophila melanogaster is expressed in postembryonic neuroblasts. Developmental biology, 152(1), pp.172-183.

Watanabe, T., Sadamoto, H. and Aonuma, H., 2011. Identification and expression analysis of the genes involved in serotonin biosynthesis and transduction in the field cricket Gryllus bimaculatus. Insect molecular biology, 20(5), pp.619-635.

Weigmann, K., Klapper, R., Strasser, T., Rickert, C., Technau, G., Jäckle, H., Janning, W. and Klämbt, C., 2003. FlyMove-a new way to look at development of Drosophila. Trends in Genetics, 19(6), pp.310-311.

Wessing, A. and Eichelberg, D., 1978. Malpighian tubules, rectal papillae and excretion. *The genetics and biology of Drosophila*, 2, pp.1-42.

Wilson, C., Pearson, R.K., Bellen, H.J., O'Kane, C.J., Grossniklaus, U. and Gehring, W.J., 1989. P-element-mediated enhancer detection: an efficient method for isolating and characterizing developmentally regulated genes in Drosophila. Genes & development, 3(9), pp.1301-1313.

Wolf, M.J. and Rockman, H.A., 2008. Drosophila melanogaster as a model system for the genetics of postnatal cardiac function. Drug Discovery Today: Disease Models, 5(3), pp.117-123.

Wong, T.S., Li, G., Li, S., Gao, W., Chen, G., Gan, S., Zhang, M., Li, H., Wu, S. and Du, Y., 2023. G protein-coupled receptors in neurodegenerative diseases and psychiatric disorders. Signal Transduction and Targeted Therapy, 8(1), p.177.

Wu, C.L., Shih, M.F.M., Lai, J.S.Y., Yang, H.T., Turner, G.C., Chen, L. and Chiang, A.S., 2011. Heterotypic gap junctions between two neurons in the Drosophila brain are critical for memory. Current Biology, 21(10), pp.848-854.

Wu, G., Lupton, J.R., Turner, N.D., Fang, Y.Z. and Yang, S., 2004. Glutathione metabolism and its implications for health. The Journal of nutrition, 134(3), pp.489-492.

Wu, S.F., Jv, X.M., Li, J., Xu, G.J., Cai, X.Y. and Gao, C.F., 2017. Pharmacological characterisation and functional roles for egg-laying of a 8-adrenergic-like octopamine receptor in the brown planthopper Nilaparvata lugens. Insect biochemistry and molecular biology, 87, pp.55-64.

Xia, S., VanKuren, N.W., Chen, C., Zhang, L., Kemkemer, C., Shao, Y., Jia, H., Lee, U., Advani, A.S., Gschwend, A. and Vibranovski, M.D., 2021. Genomic analyses of new genes and their phenotypic effects reveal rapid evolution of essential functions in Drosophila development. PLoS genetics, 17(7), p.e1009654.

Xin, J., Fan, T., Guo, P. and Wang, J., 2019. Identification of functional divergence sites in dopamine receptors of vertebrates. Computational biology and chemistry, 83, p.107140.

Xiong, R., Zhao, W., Chen, X., Li, T., Li, H., Li, Y., Shen, W. and Chen, P., 2019. Pharmacological characterization of the 5-HT1A receptor of Bombyx mori and its role in locomotion. Comparative Biochemistry and Physiology Part A: Molecular & Integrative Physiology, 231, pp.56-65.

Xu, G., Zhang, Y.Y., Gu, G.X., Yang, G.Q. and Ye, G.Y., 2022. Molecular and Pharmacological Characterization of B-Adrenergic-like Octopamine Receptors in the Endoparasitoid Cotesia chilonis (Hymenoptera: Braconidae). International Journal of Molecular Sciences, 23(23), p.14513.

Xu, J., Liu, Y., Li, H., Tarashansky, A.J., Kalicki, C.H., Hung, R.J., Hu, Y., Comjean, A., Kolluru, S.S., Wang, B. and Quake, S.R., 2021. A cell atlas of the fly kidney. BioRxiv, pp.2021-09.

Xu, W., Jiang, X. and Huang, L., 2019. RNA interference technology. Comprehensive biotechnology, p.560.

Yamaguchi, M. and Yoshida, H., 2018. Drosophila as a model organism. Drosophila Models for Human Diseases, pp.1-10.

Yan, Q., Zhang, G., Zhang, X. and Huang, L., 2024. A Review of Transcriptomics and Metabolomics in Plant Quality and Environmental Response: From Bibliometric Analysis to Science Mapping and Future Trends. Metabolites, 14(5), p.272.

Yan, W., Lin, H., Yu, J., Wiggin, T.D., Wu, L., Meng, Z., Liu, C. and Griffith, L.C., 2023. Subtype-specific roles of ellipsoid body ring neurons in sleep regulation in Drosophila. Journal of Neuroscience, 43(5), pp.764-786.

Yang, Z., Yu, Y., Zhang, V., Tian, Y., Qi, W. and Wang, L., 2015. Octopamine mediates starvation-induced hyperactivity in adult Drosophila. Proceedings of the National Academy of Sciences, 112(16), pp.5219-5224.

Yin, W., Mendoza, L., Monzon-Sandoval, J., Urrutia, A.O. and Gutierrez, H., 2021. Emergence of co-expression in gene regulatory networks. PloS one, 16(4), p.e0247671.

Youn, H., Kirkhart, C., Chia, J. and Scott, K., 2018. A subset of octopaminergic neurons that promotes feeding initiation in Drosophila melanogaster. PLoS One, 13(6), p.e0198362.

Yuan, Q., Joiner, W.J. and Sehgal, A., 2006. A sleep-promoting role for the Drosophila serotonin receptor 1A. Current Biology, 16(11), pp.1051-1062.

Yuan, Q., Lin, F., Zheng, X. and Sehgal, A., 2005. Serotonin modulates circadian entrainment in Drosophila. Neuron, 47(1), pp.115-127.

Zemanová, M., Stašková, T. and Kodrík, D., 2016. Role of adipokinetic hormone and adenosine in the anti-stress response in Drosophila melanogaster. Journal of insect physiology, 91, pp.39-47.

Zeng, N., Zhang, N., Ma, X., Wang, Y., Zhang, Y., Wang, D., Pu, F. and Li, B., 2022. Transcriptomics integrated with metabolomics: assessing the central metabolism of different cells after cell differentiation in Aureobasidium pullulans NG. Journal of Fungi, 8(8), p.882.

Zhang, Y., Liu, C., Jin, R., Wang, Y., Cai, T., Ren, Z., Ma, K., He, S., Lee, K.S., Jin, B.R. and Li, J., 2021. Dual oxidase-dependent reactive oxygen species are involved in the regulation of UGT overexpression-mediated clothianidin resistance in the brown planthopper, Nilaparvata lugens. Pest Management Science, 77(9), pp.4159-4167.

Zhang, Y., Yu, Y., Qian, M., Gui, W., Shah, A.Z., Xu, G. and Yang, G., 2023. Characterization and functional analysis of an α -adrenergic-like octopamine receptor in the small brown planthopper Laodelphax striatellus. Pesticide Biochemistry and Physiology, 194, p.105509.

Zhang, Z., Curtin, K.D., Sun, Y.A. and Wyman, R.J., 1999. Nested transcripts of gap junction gene have distinct expression patterns. Journal of neurobiology, 40(3), pp.288-301.

Zhao, Y., Zhang, H., Li, Z., Duan, J., Jiang, J., Wang, Y., Zhan, S., Akinkurolere, R.O., Xu, A., Qian, H. and Miao, X., 2012. A major facilitator superfamily protein participates in the reddish brown pigmentation in Bombyx mori. Journal of insect physiology, 58(11), pp.1397-1405.

Zhao, Z., Zhao, X., He, T., Wu, X., Lv, P., Zhu, A.J. and Du, J., 2021. Epigenetic regulator Stuxnet modulates octopamine effect on sleep through a Stuxnet-Polycomb-OctB2R cascade. EMBO reports, 22(2), p.e47910.

Zhou, C., Huang, H., Kim, S.M., Lin, H., Meng, X., Han, K.A., Chiang, A.S., Wang, J.W., Jiao, R. and Rao, Y., 2012. Molecular genetic analysis of sexual rejection: roles of octopamine and its receptor OAMB in Drosophila courtship conditioning. Journal of Neuroscience, 32(41), pp.14281-14287.

Zhou, C., Rao, Y. and Rao, Y., 2008. A subset of octopaminergic neurons are important for Drosophila aggression. Nature neuroscience, 11(9), pp.1059-1067.

Zhu, F., Sams, S., Moural, T., Haynes, K.F., Potter, M.F. and Palli, S.R., 2012. RNA interference of NADPH-cytochrome P450 reductase results in reduced

insecticide resistance in the bed bug, Cimex lectularius. PloS one, 7(2), p.e31037.